

IMPACT OF DRUG-GENE-DISEASE INTERACTIONS  
AND DIURNAL VARIATION ON EXOGENOUS AND  
ENDOGENOUS RENAL TRANSPORTER  
SUBSTRATES

A PHYSIOLOGICALLY BASED PHARMACOKINETIC  
MODELING APPROACH

DISSERTATION

zur Erlangung des Grades des Doktors der Naturwissenschaften  
der Naturwissenschaftlich-Technischen Fakultät  
der Universität des Saarlandes

von

Denise Feick

Diplom-Pharmazeutin/Apothekerin

Saarbrücken

2022

Die vorliegende Arbeit wurde von Dezember 2017 bis November 2021 unter Anleitung von Herrn Professor Dr. Thorsten Lehr in der Fachrichtung Klinische Pharmazie der Naturwissenschaftlich-Technischen Fakultät der Universität des Saarlandes angefertigt.

Tag des Kolloquiums: 14. Dezember 2022

Dekan: Prof. Dr. Ludger Santen

Berichterstatter: Prof. Dr. Thorsten Lehr  
Prof. Dr. Markus R. Meyer

Akad. Mitglied: Dr. Jessica Hoppstädter

Vorsitz: Prof. Dr. Andriy Luzhetskyy

*Probleme kann man niemals mit derselben Denkweise lösen,  
durch die sie entstanden sind*

Albert Einstein



## INCLUDED PUBLICATIONS

---

### PUBLICATIONS INCLUDED IN THIS THESIS

The following papers [1–3] related to projects I–III have been published in scientific journals and are included in this thesis.

- I Hanke N, Türk D, Selzer D, Ishiguro N, Ebner T, Wiebe S, Müller F, Stopfer P, Nock V, and Lehr T. A comprehensive whole-body physiologically based pharmacokinetic drug-drug-gene interaction model of metformin and cimetidine in healthy adults and renally impaired individuals. *Clinical Pharmacokinetics*. 2020;59(11):1419-31. DOI: [10.1007/s40262-020-00896-w](https://doi.org/10.1007/s40262-020-00896-w)
- II Türk D, Hanke N, and Lehr T. A physiologically-based pharmacokinetic model of trimethoprim for MATE<sub>1</sub>, OCT<sub>1</sub>, OCT<sub>2</sub>, and CYP<sub>2C8</sub> drug-drug-gene interaction predictions. *Pharmaceutics*. 2020;12(11):1074. DOI: [10.3390/pharmaceutics12111074](https://doi.org/10.3390/pharmaceutics12111074)
- III Türk D, Müller F, Fromm MF, Selzer D, Dallmann R, and Lehr T. Renal transporter-mediated drug-biomarker interactions of the endogenous substrates creatinine and N<sup>1</sup>-methylnicotinamide: a PBPK modeling approach. *Clinical Pharmacology & Therapeutics*. 2022. Online ahead of print. DOI: [10.1002/cpt.2636](https://doi.org/10.1002/cpt.2636)

### CONTRIBUTION REPORT

The author Denise Feick (née Türk) would like to declare her contributions to the publications related to projects I–III included in this thesis according to the contributor roles taxonomy (CRediT) [4].

- I Formal Analysis, Investigation, Visualization, Writing - Review & Editing
- II Conceptualization, Investigation, Visualization, Writing - Original Draft, Writing - Review & Editing
- III Conceptualization, Formal Analysis, Investigation, Visualization, Writing - Original Draft, Writing - Review & Editing



## ABSTRACT

---

Adverse drug reactions depict one of the leading causes of death in developed countries and can often be attributed to drug-drug, drug-gene and drug-disease interactions. However, due to the very large number of combinations and ethical concerns, coverage of all real-world scenarios in clinical studies is infeasible and therefore, treatment guidelines cannot reflect all patients. Especially regarding the involvement of renal membrane transporters in drug pharmacokinetics and related efficacy and safety, knowledge gaps exist. Whole-body physiologically based pharmacokinetic (PBPK) models are valuable tools to tackle the problem of studying complex drug-gene-disease interaction scenarios and to provide personalized treatment options.

In this thesis, comprehensive PBPK models of the renal transporter inhibitors trimethoprim, pyrimethamine and cimetidine as well as of the clinical substrate metformin and the endogenous substrates creatinine and N<sup>1</sup>-methylnicotinamide have been built and thoroughly evaluated. Models have been successfully applied to describe and predict the effect of drug-gene-disease interactions and diurnal variation on (pharmaco-)kinetics of the exogenous and endogenous renal transporter substrates within an interaction network, also including hypothesis generation and testing. The newly developed models can support future investigations during drug development or calculation of dose adaptations, to facilitate an effective and safe pharmacotherapy for patients.

## ZUSAMMENFASSUNG

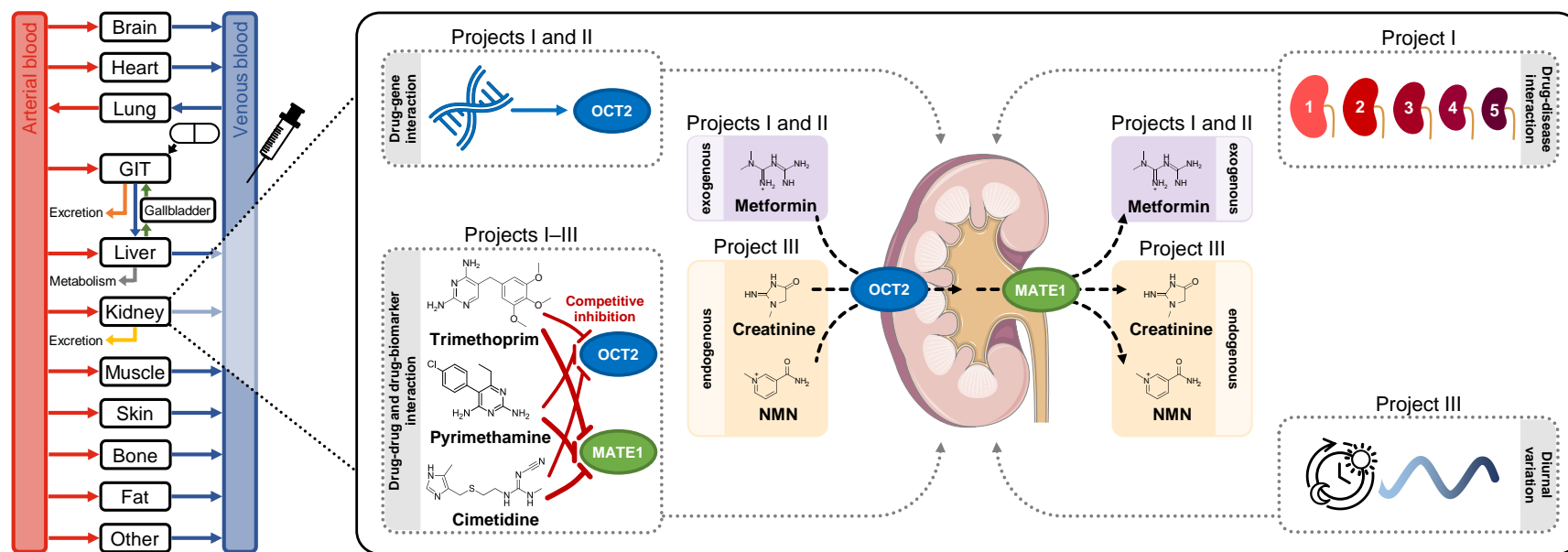
---

Unerwünschte Arzneimittelwirkungen gehören zu den häufigsten Todesursachen in Industriestaaten und lassen sich oft auf unterschiedliche Arzneimittelinteraktionen zurückzuführen. Aufgrund der großen Vielfalt denkbarer Interaktionsszenarien sowie ethischer Bedenken ist es nicht möglich, alle möglichen Fälle in klinischen Studien abzudecken. Therapieleitlinien können daher nicht alle Patienten berücksichtigen. Ein aktuelles Forschungsthema ist die Untersuchung des Einflusses von renalen Membrantransportern auf die Pharmakologie und damit verbundene Wirksamkeit und Sicherheit von Arzneistoffen. Physiologie-basierte Pharmakokinetik Modellierung ist hier ein wertvolles Instrument, um komplexe Arzneimittelinteraktionen abzubilden und personalisierte Therapieoptionen zu ermöglichen.

In dieser Arbeit wurden, mit Fokus auf Nierentransporter, umfassende Physiologie-basierte Pharmakokinetik Modelle der Arzneistoffe Trimethoprim, Pyrimethamin, Cimetidin (jeweils Hemmstoffe) und Metformin (Substrat) sowie der endogenen Substrate Kreatinin und N<sup>1</sup>-Methylnicotinamid entwickelt. Mit Hilfe dieser Modelle konnten Effekte von komplexen Interaktionen als auch von zirkadianer Rhythmik auf die (Pharmako-)Kinetik der exogenen und endogenen Substrate beschrieben und vorhergesagt werden. Die neuen Modelle können zukünftig zur Unterstützung in der Arzneimittelentwicklung sowie zur Berechnung von Dosisanpassungen herangezogen werden, um zu einer wirksamen und sicheren Therapie beizutragen.



## GRAPHICAL ABSTRACT



△

**Graphical abstract.** Illustration of the kidney was taken from Servier [5], licensed under CC BY 3.0 (<https://creativecommons.org/licenses/by/3.0/>). GIT, gastrointestinal tract; MATE, multidrug and toxin extrusion protein; NMN, N<sup>1</sup>-methylnicotinamide; OCT, organic cation transporter.



# CONTENTS

---

INCLUDED PUBLICATIONS	i
Publications included in this thesis	i
Contribution Report	i
ABSTRACT	iii
ZUSAMMENFASSUNG	iv
GRAPHICAL ABSTRACT	v
ABBREVIATIONS	x
1 INTRODUCTION	1
1.1 Motivation	1
1.2 Membrane transporters	2
1.2.1 Overview	2
1.2.2 Renal membrane transporters	3
1.3 Drug-drug and drug-biomarker interactions	5
1.3.1 Interaction mechanisms	5
1.3.2 Transporter-mediated interactions	6
1.3.3 Renal transporter-mediated interactions	7
1.3.4 Biomarker-informed approach to investigate renal transporter-mediated drug-drug interactions	9
1.4 Drug-gene interactions	11
1.4.1 Overview	11
1.4.2 Renal transporter drug-gene interactions	12
1.5 Drug-disease interactions	13
1.5.1 Effect of drug-disease interactions on pharmacology	13
1.5.2 Chronic kidney disease	14
1.6 Diurnal variation	15
1.6.1 Chronopharmacology	15
1.6.2 Diurnal pharmacokinetics	15
1.7 Mechanistic pharmacokinetic modeling analyses	16
1.7.1 Pharmacometrics	16
1.7.2 Physiologically based pharmacokinetic modeling	16
1.7.3 Physiologically based pharmacokinetic model applications	18
1.7.4 Pharmacokinetic modeling to support model-informed drug discovery and development as well as precision dosing	18

<b>2</b>	<b>OBJECTIVES</b>	<b>21</b>
2.1	Project I - Physiologically based pharmacokinetic modeling of metformin and cimetidine	21
2.2	Project II - Physiologically based pharmacokinetic modeling of trimethoprim	21
2.3	Project III - Physiologically based pharmacokinetic modeling of endogenous biomarkers	22
<b>3</b>	<b>METHODS</b>	<b>23</b>
3.1	Physiologically based pharmacokinetic modeling	23
3.1.1	Model building	23
3.1.2	Model evaluation	26
3.1.3	Modeling of drug-drug and drug-biomarker interactions	27
3.1.4	Modeling of drug-gene interactions	28
3.1.5	Modeling of chronic kidney disease	28
3.1.6	Modeling of diurnal variation	28
3.2	Software	29
<b>4</b>	<b>RESULTS</b>	<b>31</b>
4.1	Project I - Physiologically based pharmacokinetic modeling of metformin and cimetidine	31
4.2	Project II - Physiologically based pharmacokinetic modeling of trimethoprim	47
4.3	Project III - Physiologically based pharmacokinetic modeling of endogenous biomarkers	69
<b>5</b>	<b>DISCUSSION AND PERSPECTIVE</b>	<b>83</b>
5.1	Membrane transporters	83
5.2	Renal transporter-mediated drug-drug and drug-biomarker interactions	84
5.3	Drug-(drug-)gene interactions	87
5.4	Drug-disease interactions	88
5.5	Diurnal variation	89
5.6	Mechanistic pharmacokinetic modeling - challenges and opportunities	90
5.6.1	Model development	90
5.6.2	Model-informed drug development and discovery	91
5.6.3	Model-informed precision dosing	92
<b>6</b>	<b>CONCLUSION</b>	<b>93</b>
	<b>BIBLIOGRAPHY</b>	<b>95</b>
<b>A</b>	<b>APPENDIX</b>	<b>121</b>
A.1	Publications	121
A.1.1	Original Publications	121

A.1.2 Review Articles 122  
A.1.3 Conference Abstracts and Posters 122

ACKNOWLEDGMENTS 123

## ABBREVIATIONS

---

2PY	N <sup>1</sup> -methyl-2-pyridone-5-carboxymide
4PY	N <sup>1</sup> -methyl-4-pyridone-5-carboxymide
ABC	ATP-binding cassette
ADME	Absorption, distribution, metabolism, and excretion
ADR	Adverse drug reaction
amp	Amplitude
AOX	Aldehyde oxidase
ATP	Adenosine triphosphate
AUC	Area under the plasma concentration-time curve
AUC <sub>last</sub>	Area under the plasma concentration-time curve calculated from the time of compound administration to the time of the last concentration measurement
BBM	Brush border membrane
BCRP	Breast cancer resistance protein
BLM	Basolateral membrane
CKD	Chronic kidney disease
CL <sub>spec</sub>	Specific enzymatic clearance
C <sub>max</sub>	Maximum plasma concentration
C <sub>max,u</sub>	Unbound maximum plasma concentration
C <sub>obs,i</sub>	i <sup>th</sup> observed concentration
CPI	Coproporphyrin I
CPIC	Clinical Pharmacogenetics Implementation Consortium
C <sub>pred,i</sub>	i <sup>th</sup> predicted concentration
CRediT	Contributor roles taxonomy
C <sub>u</sub>	Unbound plasma concentration
CYP	Cytochrome P450
DBI	Drug-biomarker interaction
DDI	Drug-drug interaction
DDGI	Drug-drug-gene interaction
DGI	Drug-gene interaction
DNA	Deoxyribonucleic acid
DPWG	Dutch Pharmacogenetics Working Group
[E]	Enzyme or transporter concentration

EMA	European Medicines Agency
ENT	Equilibrative nucleoside transporter
FDA	U.S. Food and Drug Administration
GFR	Glomerular filtration rate
GIT	Gastrointestinal tract
GMFE	Geometric mean fold error
[I]	Free inhibitor concentration
IC <sub>50</sub>	Half maximal inhibitory concentration
ITC	International Transporter Consortium
k	Rate constant
k <sub>cat</sub>	Catalytic or transport rate constant
KDIGO	Kidney Disease: Improving Global Outcomes
K <sub>i</sub>	Dissociation constant of the inhibitor-enzyme/-transporter complex
K <sub>M</sub>	Michaelis-Menten constant
K <sub>M,app</sub>	Michaelis-Menten constant in the presence of inhibitor
MATE	Multidrug and toxin extrusion protein
MDR	Multidrug resistance protein
MID <sub>3</sub>	Model-informed drug discovery and development
MIPD	Model-informed precision dosing
MRD	Mean relative deviation
MRP	Multidrug resistance-associated protein
NAD	Nicotinamide adenine dinucleotide
NME	New molecular entity
NMN	N <sup>1</sup> -methylnicotinamide
NNMT	Nicotinamide N-methyltransferase
OAT	Organic anion transporter
OATP	Organic anion transporting polypeptide
OCT	Organic cation transporter
OCTN	Organic cation/carnitine transporter
p	Original parameter value
PBPK	Physiologically based pharmacokinetic
PEPT	Peptide transporter
PET	Positron emission tomography
P-gp	P-glycoprotein
PGx	Pharmacogenetics

PharmGKB	Pharmacogenomics Knowledgebase
$PK_{obs,i}$	$i^{th}$ observed pharmacokinetic parameter
$PK_{pred,i}$	$i^{th}$ predicted pharmacokinetic parameter
PMAT	Plasma membrane monoamine transporter
PopPK	Population pharmacokinetic
RNA	Ribonucleic acid
RPF	Renal plasma flow
$R_{syn}$	Synthesis rate
RT-PCR	Reverse transcription-polymerase chain reaction
[S]	Free substrate concentration
SAH	S-adenosyl homocysteine
SAM	S-adenosyl methionine
shift	Shift in time
SLC	Solute carrier
SNP	Single nucleotide polymorphism
t	Time
THTR	Thiamine transporter
URAT	Urate transporter
U.S.	United States of America
V	Volume
v	Reaction velocity
$v_{max}$	Maximum reaction velocity



## INTRODUCTION

---

### 1.1 MOTIVATION

Adverse drug reactions (ADRs) depict one of the leading causes of death in developed countries, e.g., the United States of America (U.S.) [6], and regularly lead to hospitalization, especially concerning elderly patients [7]. However, about half of outpatient ADRs are assumed to be preventable [8]. In this context, polypharmacy, defined as the concomitant use of five or more medications [9], is a known risk factor, as it is assumed, that in total more than 65% of ADRs are related to drug-drug interactions (DDIs) [10]. For instance, 36% of elderly U.S. citizens take more than five prescribed medications and even 67% use five or more prescribed and over-the-counter medications or dietary supplements at the same time [11]. With increasing number of medications, also the incidence of potential DDIs increases, while 15% of older U.S. citizens may be at risk for an interaction of major or life-threatening severity [11]. Moreover, inadequate prescriptions due to genetic heterogeneity and diseases can affect drug efficacy and safety by increasing the risk and severity of ADRs. For instance, more than 60% of ADRs are related to drug-gene interactions (DGIs), triggered by variants in pharmacogenes [12]. In addition, the kidney plays a special role with regard to pharmacology, highlighted by the fact that about one third of drugs prescribed in the U.S. are excreted renally [13]. Patients with chronic kidney disease (CKD) often experience therapies with inadequate drugs or improper doses [14], resulting in an incidence of 18% for ADRs [15]. Furthermore, CKD depicts a frequent comorbidity in patients with type 2 diabetes [16], a metabolic disease concerning about 6% of the world's population [17].

Contribution of membrane transporters to drug pharmacokinetics and related drug efficacy and safety is a recent research topic in pharmaceutical industry and academia. Inhibition or induction of transporters as well as modulated functionality due to polymorphisms or disease can lead to ADRs [18]. However, quantification of transporter-related ADRs is challenging due to limitation of data and close connection to metabolism, making differentiation of transporter- and metabolism-related ADRs challenging. Especially if transporters are involved, drug interaction risk assessment from *in vitro* tests is impeded. Here, investigations of endogenous transporter substrates, serving as biomarkers, can provide valuable insights into interaction mechanisms [19]. A prime example for organic cation drugs is metformin, depending heavily on active transport to cross membranes

*Adverse drug reactions in polymedicated, genetic heterogenous patients with one or more diseases*

*Role of membrane transporters in pharmacology*

and to be eliminated. It is used as first-line therapy for type 2 diabetes [20] and ranks fourth of the most frequently prescribed outpatient medications in the U.S. with almost 86 million prescriptions in 2019 [21]. A serious but rare adverse effect is lactic acidosis, generally correlated with metformin accumulation [22]. As metformin is not metabolized and mainly excreted renally [23], it is contraindicated in patients with impaired renal function [24, 25].

*Mechanistic  
pharmacokinetic  
models*

To advance drug and biomarker characterization and to support drug development, mechanistic mathematical models are used. Thoroughly built and evaluated mechanistic pharmacokinetic models are established tools to assess underlying processes. Furthermore, investigations of various drug-gene-disease interaction scenarios in clinical studies are only possible to a limited extent owed to the very large number of combinations and ethical concerns due to the risk to which study participants would be exposed. Consequently, significant knowledge gaps exist, and current guidelines are not capable of reflecting all real-world scenarios [26]. Here, physiologically based pharmacokinetic (PBPK) models can be utilized to investigate also complex drug-gene-disease interaction scenarios and to provide personalized treatment options [27]. Especially regarding membrane transporters and related biomarkers, PBPK models supporting drug development and contributing to patient safety are lacking [28, 29] and therefore, new mechanistic models are highly required.

In the following sections, background information about membrane transporters (Section 1.2), DDIs and drug-biomarker interactions (DBIs) (Section 1.3), DGIs (Section 1.4), drug-disease interactions (Section 1.5), diurnal variation (Section 1.6) as well as pharmacokinetic modeling (Section 1.7) will be provided.

## 1.2 MEMBRANE TRANSPORTERS

### 1.2.1 Overview

*Membrane  
transporter  
superfamilies*

Membrane transporters are proteins responsible for transport of endogenous compounds as well as drugs and other xenobiotics across cell membranes, consequently controlling their concentrations at various body sites. More than 400 transporters from two major superfamilies of membrane transporters, ATP-binding cassette (ABC) and solute carrier (SLC) [30], have been described, differing in structure and function. Transporters of the ABC family depend on adenosine triphosphate (ATP) hydrolysis (primary active transport), transporters of the SLC family rely on an electrochemical gradient (secondary active transport) or an antiport of e.g., protons [31]. Furthermore, transporters can act as efflux or uptake transporters. While ABC transporters are generally efflux pumps, SLC transporters mainly mediate uptake but also efflux transport [30].

Transporters affect absorption, distribution, or excretion processes or can be drug targets themselves [32] and hence, contribute to drug efficacy and toxicity. Important membrane transporter sites, as they represent physiological barriers, are the intestinal, blood-brain, hepatic and renal barriers [30, 33], responsible for absorption, distribution into tissues and elimination [34]. A further function includes protection against permeation into vulnerable tissues, especially represented by the prime example blood-brain barrier, due to efflux mechanisms [31]. The focus of this thesis lies on the renal barrier and transporter-mediated drug elimination.

*Important  
transporter sites*

Investigation of transporter effects on drug disposition is a quite new research topic and the number of publications has increased over the last two decades. To support drug development, the International Transporter Consortium (ITC) was established in 2007 [35], involving scientists from academia, industry and regulatory agencies. Members of the ITC regularly evaluate how to investigate the impact of relevant transporters during drug development. Their recommendations and guidances for action are published in established journals and their agreements are summarized in decision trees [36], which are constantly updated and incorporated in recent guidelines of regulatory agencies [37]. Additionally, to serve as informative tool during drug development, the UCSF-FDA Transportal [38] has been established as public transporter database, including details on transporters recommended by the ITC or incorporated in guidelines of regulatory agencies [39]. Transporter-mediated DDIs are described in detail in Section 1.3.2, also specifying the transporters incorporated in current guidelines for DDI investigations.

*International  
Transporter  
Consortium and  
regulatory agencies*

### 1.2.2 Renal membrane transporters

About one third of drugs prescribed in the U.S. show a fraction excreted unchanged in urine greater than or equal to 25% [13]. Urinary excretion is the result of passive glomerular filtration, tubular secretion (active, i.e., transporter-mediated) and tubular reabsorption (active or passive). In the nephron, transporters are expressed on basolateral and apical epithelial membranes of proximal, distal and collecting tubule cells [32], with highest amount of transporters in proximal tubules [40]. An overview of membrane transporters located at the basolateral membrane (BLM) and apical site of proximal tubule epithelial cells (brush border membrane (BBM)) proposed for evaluation during drug development by ITC [41] is shown in Figure 1.1. Of the SLC family, organic anion transporter (OAT) 1 (SLC22A6), OAT3 (SLC22A8), organic cation transporter (OCT) 2 (SLC22A2) and multidrug and toxin extrusion protein (MATE) 1 (SLC247A1) and of the ABC family, P-glycoprotein (P-gp) (also called multidrug resis-

*Active renal drug  
excretion*

tance protein (MDR) 1, *ABCB1*) show the highest expression in human kidney cortex [42].

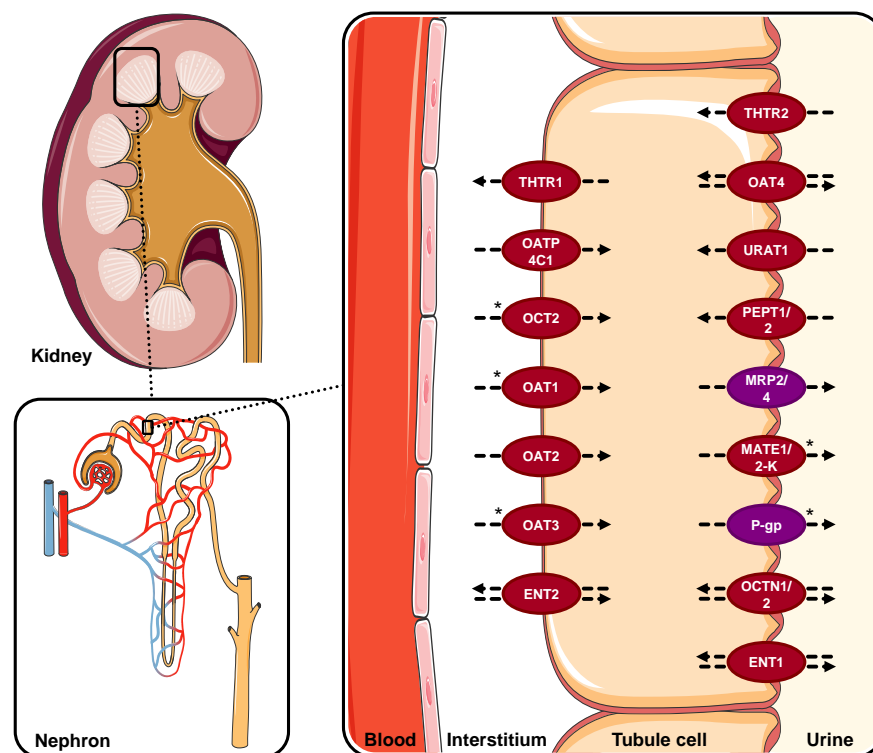


**Figure 1.1.** Overview of membrane transporters located at the basolateral and apical site of proximal tubule epithelial cells adopted from Zamek-Gliszczynski et al. [41]. Transporters belonging to the solute carrier (SLC) and ATP-binding cassette (ABC) superfamilies are shown in red and purple, respectively. The direction of transport is indicated by arrows. Asterisks indicate transporters currently recommended for evaluation during drug development by the International Transporter Consortium (ITC) [41] and incorporated in guidelines of the U.S. Food and Drug Administration (FDA) [37, 43]. Illustrations of kidney, nephron, blood and cells were taken from Servier [5], licensed under CC BY 3.0 (<https://creativecommons.org/licenses/by/3.0/>). ENT, equilibrative nucleoside transporter; MATE, multidrug and toxin extrusion protein; MRP, multidrug resistance-associated protein; OAT, organic anion transporter; OATP, organic anion transporting polypeptide; OCT, organic cation transporter; OCTN, organic cation/carnitine transporter; PEPT, peptide transporter; P-gp, P-glycoprotein, THTR, thiamine transporter; URAT, urate transporter.

About 40% of orally administered drugs as well as many endogenous compounds like choline and  $N^1$ -methylnicotinamide (NMN) are organic cations at physiological pH [31, 44, 45]. As passive diffusion across membranes is limited for these compounds, they rely on active transport via membrane transporters. A subgroup of SLC transporters are OCTs, including OCT<sub>1–3</sub> (*SLC22A1–3*), organic cation/carnitine transporter (OCTN) 1/2 (*SLC22A4/5*), plasma membrane monoamine transporter (PMAT) (*SLC29A4*) and MATE<sub>1/2-K</sub> (*SLC47A1/2*) [46].

For renal excretion of organic cations in proximal tubules, OCT2 and OCT3 are the main contributing transporters at the basolateral membrane while the cation-proton exchanging transporters MATEs are assumed to be the most important contributors at the luminal membrane [46], working in sequential action with OCTs. MATEs depict a special case of SLCs, as their transport direction is pH dependent and at physiological urine pH < 7.4, they act as efflux pumps [32, 40]. However, information about transporter localization and abundance are often controversial. For instance, although existence of MATE2-K, a kidney-specific variant of MATE2, has been reported previously [47, 48], a recent analysis reported MATE2-K levels below the lower limit of quantification in human kidney cortex [42]. Current recommendations by the ITC and guidelines by regulatory agencies include OCT2 and MATEs, to investigate their contribution to pharmacokinetics and associated interaction potential during drug development [37, 41, 43, 49]. Due to their clinical importance, this thesis focuses on OCT2 and MATEs and their related interactions.

*Organic cation transporters*

### 1.3 DRUG-DRUG AND DRUG-BIOMARKER INTERACTIONS

#### 1.3.1 Interaction mechanisms

In general, DDIs can occur during concomitant administration of two or more drugs, one drug acting as the perpetrator and affecting the so-called victim, which can also be an endogenous compound. However, in real-life scenarios, often multiple perpetrators and victims are involved. Major mechanisms of DDIs include pharmacokinetic (effect on absorption, distribution, metabolism, and excretion (ADME) processes) and pharmacodynamic interactions (synergism or antagonism) as well as pharmaceutical incompatibilities (e.g., due to acid-base reactions or altered pH) [50].

*Major interaction mechanisms*

This thesis focuses on pharmacokinetic DDIs, which can lead to increased or decreased area under the plasma concentration-time curve (AUC) or maximum plasma concentration ( $C_{\max}$ ) values of the victim due to altered absorption, biotransformation or clearance, resulting in loss of efficacy or increase of toxicity. Regularly, pharmacokinetic interactions rely on the interaction of a perpetrator with proteins essential for metabolism or transport of the victim and can be divided into the major groups of inhibition or induction mechanisms. Regarding inhibition, reversible and irreversible processes are known. Reversible inhibition can either occur due to binding of an inhibitor (i) to the active site of an enzyme or transporter, competing for binding with the substrate (competitive inhibition); (ii) to an allosteric, from the active site differing binding site of an enzyme or transporter, leading to conformation change of the active site (non-competitive or mixed inhibition) and (iii) to the enzyme- or transporter-substrate complex

*Pharmacokinetic interaction due to inhibition and induction*

(uncompetitive inhibition) [51, 52]. An example of irreversible inhibition is mechanism-based inactivation (also called suicide inhibition), where the inhibitor tightly binds to the enzyme or transporter, leading to inactivation of the protein and requiring *de novo* synthesis to restore activity [53]. Induction is characterized by increase of protein biosynthesis due to interaction with transcription factors.

*Investigation of drug-drug interactions during drug development*

Investigation of DDIs is an essential part of drug development to ensure drug efficacy and safety [30], assessed by a combination of *in vitro* tests, *in vivo* studies in preclinical animal species and humans with proven, so-called index perpetrators and substrates [54] and *in silico* techniques [28]. To support in this process, guidelines have been published by regulatory agencies [37, 43, 49], proposing strong inhibitors and sensitive substrates for the use in clinical studies.

### 1.3.2 Transporter-mediated interactions

*Transporter-mediated drug-drug interactions in drug development*

Transporter-mediated DDIs are a research topic of increasing interest over the last decades due to importance of transporters in drug disposition and response [55]. Recommendations on transporter-mediated DDIs were first included in guidelines by the FDA in 2006 [33]. It is assumed that cytochrome P450 (CYP)-mediated DDIs are generally better understood than transporter-mediated DDIs [56], emphasizing the need of further research in this area. Regarding transporter-mediated DDIs, recent guidelines on DDI investigations focus on the efflux transporters P-gp, breast cancer resistance protein (BCRP) (*ABCG2*) and MATEs and the uptake transporters organic anion transporting polypeptide (OATP) 1B1/3 (*SLCO1B1/3*), OAT1/3 and OCT2 [28, 37, 43].

*Challenges in investigations of transporter-mediated drug-drug interactions*

During drug development, investigations of transporter-mediated DDIs include the determination of elimination routes of new drugs and their related transporters as well as the interaction potential of new drugs with transporters [33] based on *in vitro* and *in vivo* tests. For inhibitors, the FDA and the European Medicines Agency (EMA) recommend *in vivo* studies based on *in vitro* results if the quotient of unbound maximum plasma concentration ( $C_{\max,u}$ ) of the perpetrator drug and the half maximal inhibitory concentration ( $IC_{50}$ ) equals or exceeds 0.1 and 0.02, respectively [37, 49]. If the investigational drug is assumed to be a substrate of a specific transporter, clinical DDI studies are indicated if 25% or more of the systemic clearance can be attributed to this process [37, 43]. Effects of transporter-mediated DDIs can be versatile, including changes in systemic exposure and clearance. However, investigations of transporter-mediated DDI are impeded by different factors. For instance, *in vitro* to *in vivo* correlation and estimation of clinical significance is often challenging, e.g., due to false positive (leading to unnecessary studies in humans) or false negative results (possible oversight of potential interactions) [57, 58]. Late-stage failures might occur, e.g., if information about DDI

mechanisms were lacking earlier [59]. Furthermore, substrate dependency of transporter inhibitors has been described [60], complicating extrapolation of results from one to another perpetrator-victim combination [19, 55]. Additionally, there is a lack of recommended clinical index transporter inhibitors and substrates with predictable exposure change due to transporter inhibition [28, 54].

To support investigations of transporter-mediated DDIs, the ITC has published decision trees [36], which have been adapted by the FDA [61–67]. Furthermore, a biomarker-informed approach (Section 1.3.4) or *in silico* techniques, which are already established in drug development (Section 1.7), depict promising ways to improve investigations of transporter-mediated DDIs and are further highlighted in this thesis.

*Assessment of transporter-mediated drug-drug interactions*

### 1.3.3 Renal transporter-mediated interactions

According to recommendations by the ITC [41] and guideline documents on DDI investigations by the FDA [37, 43], renal transporters that should be considered during DDI assessment are P-gp, MATEs, OAT1/3 and OCT2 (Figure 1.1). This thesis focuses on the renal secretion axis of organic cations, which is represented by consecutive action of OCT2 and MATEs [40], and their related DDIs. Trimethoprim, pyrimethamine and cimetidine are recommended OCT2 and MATE inhibitors and metformin the only recommended OCT2 and MATE substrate for the use in clinical DDI studies by the FDA [43, 54]. Generally, interactions with renal transporters can affect the clearance of their substrates and consequently their efficacy and toxicity. Inhibition of OCT2, expressed at the basolateral site of tubule epithelial cells, can lead to decreased clearance and increased exposure, while inhibition of MATE1, expressed at the apical site, can lead to decreased clearance but also to accumulation in renal cells [34]. Although inhibition of both OCTs and MATEs by trimethoprim, pyrimethamine and cimetidine has been described, comparison of  $IC_{50}$  values with therapeutic  $C_{max}$  values as well as unbound concentrations in plasma and kidney cells reveals that MATE inhibition is the main contributor to these interactions [46].

*Renal transporter-mediated drug-drug interactions in the scope of this thesis*

The effect of trimethoprim, pyrimethamine and cimetidine on systemic exposure and renal clearance of metformin as observed by several studies is illustrated in Figure 1.2. Trimethoprim co-administration results in 28% higher metformin AUC and 26% lower renal clearance compared to metformin alone [68]. Combining therapeutic doses of pyrimethamine and metformin leads to an increase of metformin AUC up to 158% [58, 69, 70] and decrease of renal clearance up to 72% [58, 70]. During co-administration of cimetidine, a mean increase in AUC of 58% [71, 72] and a 45% decrease of metformin renal clearance [71] have been reported.

*Metformin drug-drug interactions*

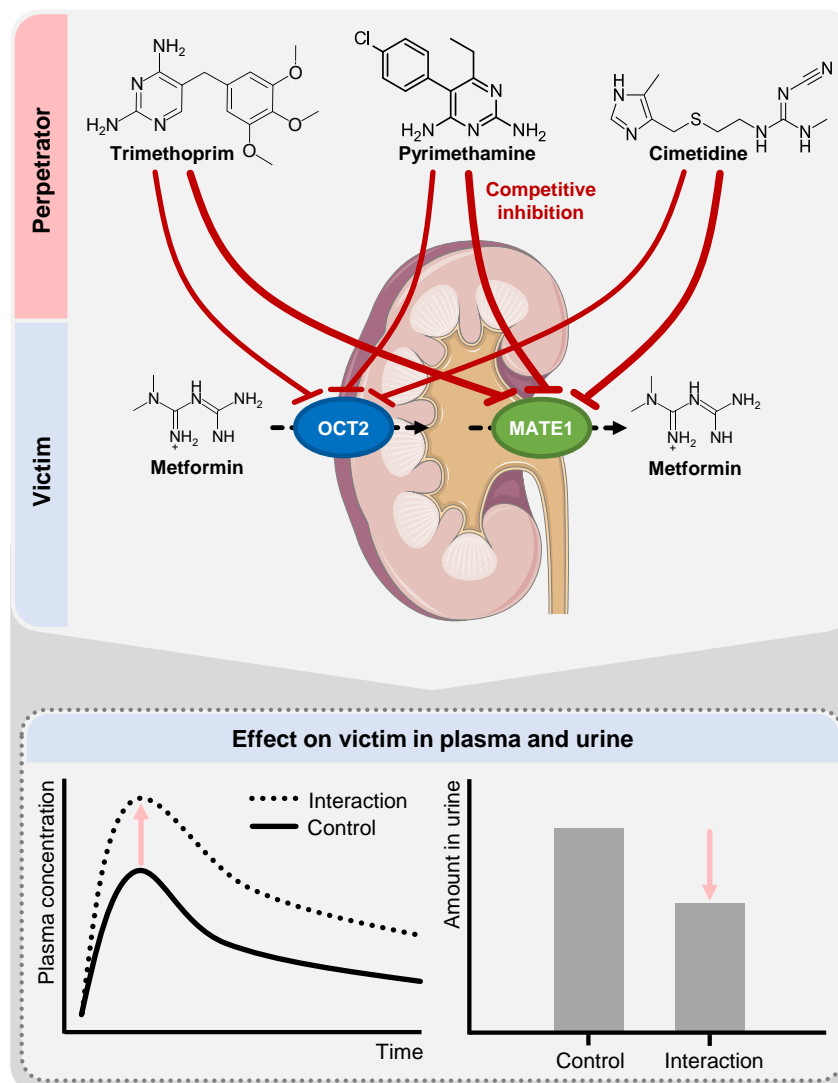


**Figure 1.2.** Renal transporter-mediated drug-drug interactions (DDIs) of trimethoprim, pyrimethamine and cimetidine with metformin. Metformin is actively secreted into urine via consecutive action of organic cation transporter (OCT) 2, an influx transporter located at the basolateral site, and multidrug and toxin extrusion protein (MATE) 1, an efflux transporter located at the apical site of tubule epithelial cells. Trimethoprim, pyrimethamine and cimetidine are competitive inhibitors of OCT2 and MATE1, demonstrated by red lines. Bold lines indicate that MATE1 inhibition is the main contributor to DDIs due to magnitude of interaction constants. Chemical structures show the predominant form at physiological pH. Illustration of the kidney was taken from Servier [5], licensed under CC BY 3.0 (<https://creativecommons.org/licenses/by/3.0/>).



#### 1.3.4 Biomarker-informed approach to investigate renal transporter-mediated drug-drug interactions

Endogenous compounds quantified in blood or urine can serve as biomarkers by shedding light on physiological and pharmacological processes. Differences in biomarker levels can indicate pathophysiological changes or interaction of a perpetrator drug with absorption, synthesis, distribution, metabolism or excretion of the biomarker, referred to as DBI. Observations of endogenous biomarkers can complement recent DDI investigation techniques, as they can support in understanding interaction mechanisms, evaluating DDI risks in early stage *in vivo* studies as well as study planning and prioritization [59, 73, 74]. Various factors need to be considered to identify and select eligible biomarkers for DDI assessment, like sensitivity, specificity, predictivity, robustness and ease of accessibility [59, 75, 76]. Here, investigations with mechanistic pharmacokinetic modeling can provide helpful insights. With respect to OCT2- and MATE-mediated DDIs, the endogenous biomarkers creatinine and NMN have been identified as suitable OCT2 and MATE substrates [77–80]. Recently, a further biomarker for renal SLC transporter-mediated DDIs has been proposed, N<sup>1</sup>-methyladenosine, a nucleotide from transfer ribonucleic acid (RNA), as plasma concentrations and renal clearance are affected by pyrimethamine administration [58, 81]. However, studies in humans are rarely available, to assess its potential applicability for transporter-mediated DDI investigations.

Creatinine, an endogenous breakdown product from muscle and protein metabolism, is formed non-enzymatically during ATP-dependent conversion of creatine and phosphocreatine via creatine kinase in muscle cells. Creatine precursors are the amino acids arginine and glycine, converted to guanidinoacetate in the kidney, which is further methylated in the liver [82]. Creatinine is excreted renally mainly by passive filtration but also active tubular secretion (10–40% of renal clearance [83]), predominantly via OCT2 and MATEs, but also contribution of other renal transporters, e.g., OAT2, has been described [84, 85]. Tubular reabsorption of creatinine is controversial [83]. Creatinine plasma concentration time profiles exhibit diurnal variation, showing highest levels during the night and greatest clearance in the afternoon [86]. Endogenous creatinine levels are increased during administration of trimethoprim, pyrimethamine and cimetidine by 29% [87–93], 15% [58, 69, 94] and 22% [95, 96], respectively. Simultaneously, decreased renal clearance by 23% [68, 89–93], 19% [58, 69] and 15% [96] could be observed. Interestingly, creatinine clearance becomes similar to glomerular filtration rate (GFR), if tubular secretion is inhibited, e.g., shown for cimetidine [97].

NMN is a molecule formed during metabolism of tryptophan and vitamin B<sub>3</sub> (consisting of nicotinic acid and nicotinamide) (Figure 1.3).

*Endogenous biomarkers as supportive tool for conventional drug-drug interaction investigations*

*Creatinine*

*N*<sup>1</sup>-  
methylnicotinamide

It is excreted unchanged into urine as well as in form of its carboxamide metabolites, while passive filtration, tubular secretion mainly via OCT2 and MATEs as well as concentration-dependent tubular reabsorption [98] of NMN have been described. NMN plasma levels exhibit a pronounced diurnal variation, which could be attributed to nicotinamide adenine dinucleotide (NAD) degradation [99]. A possible pitfall concerning NMN is inconsistent nomenclature, as NMN is also abbreviated with "MNA", "meNAM" or "MNAM" in literature reports. Renal clearance is decreased by 27% [68] and up to 70% [58, 77] during administration of trimethoprim and pyrimethamine, respectively. However, plasma concentrations are not increased (as expected from other renal transporter substrates) but decreased during trimethoprim and pyrimethamine administration [58, 68, 77]. An inhibition of synthesis has been proposed [74], but the underlying mechanisms have not been identified yet.

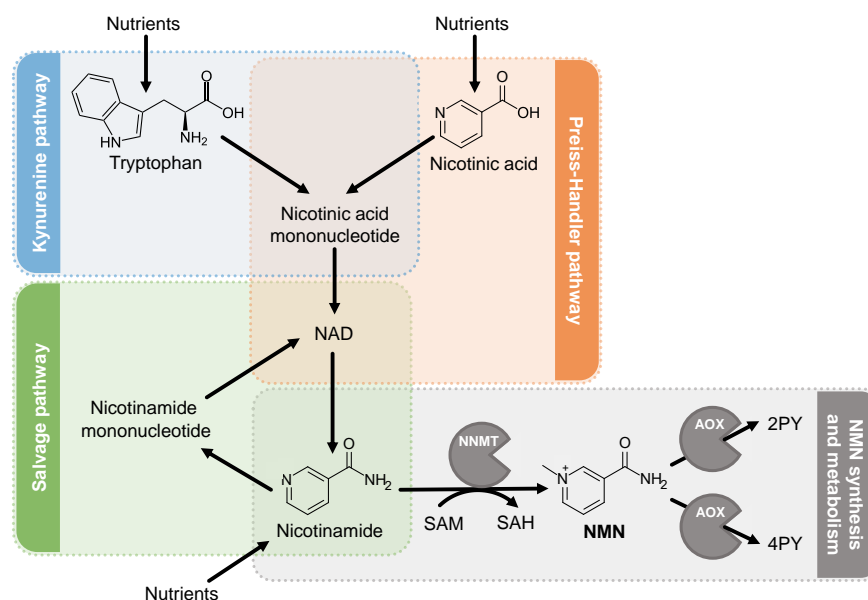


**Figure 1.3.** N<sup>1</sup>-methylnicotinamide (NMN) synthesis involving tryptophan, nicotinic acid and nicotinamide from nutrient sources [100, 101]. As last step, nicotinamide is methylated by nicotinamide N-methyltransferase (NNMT) with S-adenosyl methionine (SAM) as methyl donor. NMN is metabolized via aldehyde oxidase (AOX) to N<sup>1</sup>-methyl-2-pyridone-5-carboxamide (2PY) and N<sup>1</sup>-methyl-4-pyridone-5-carboxamide (4PY) [102]. NAD, nicotinamide adenine dinucleotide; SAH, S-adenosyl homocysteine.

*Clinical risk  
assessment for renal  
OCT2 and MATE  
drug-drug  
interactions using a  
biomarker-informed  
strategy*

Mathialagan et al. [19] described challenges of *in vitro* to *in vivo* translation for OCT2- and MATE-mediated DDIs and pointed out the advantages of a biomarker-informed approach to support DDI risk assessment by studying the impact of the drug of interest on the renal clearance of the biomarkers in phase I studies prior to performing a dedicated DDI study (Figure 1.4). In comparison, recent DDI risk assessment is performed by calculating the ratio of known or projected

$C_{\max,u}/IC_{50}$  of the drug of interest, e.g., a new molecular entity (NME), with no requirement for a clinical DDI study for values below 0.1 and 0.02 according to FDA and EMA [37, 49], respectively.

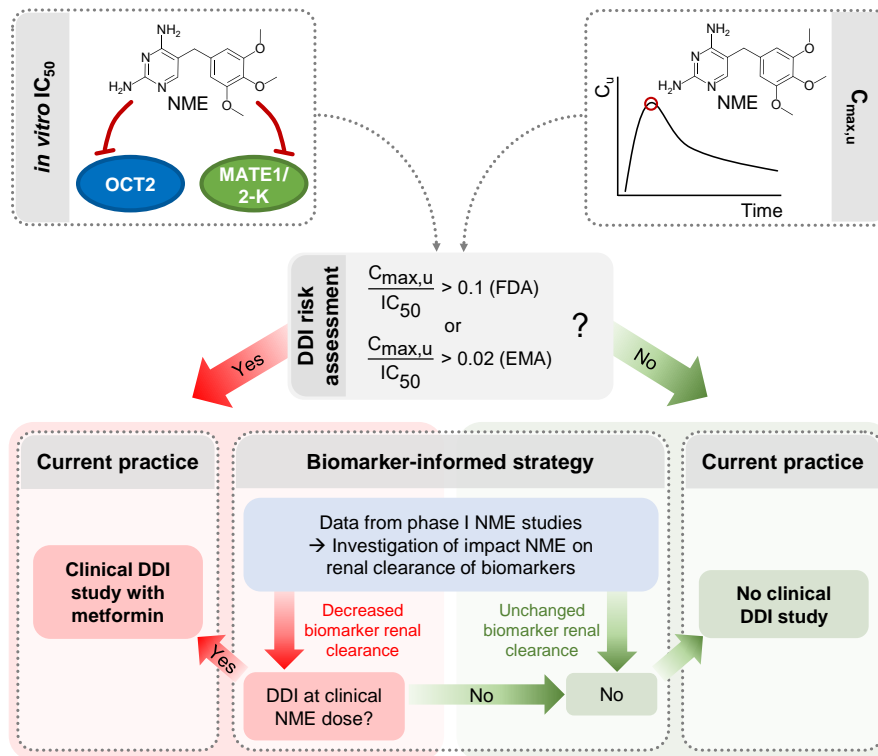


**Figure 1.4.** Drug-drug interaction (DDI) risk assessment workflow incorporating a biomarker-informed strategy adopted from Mathialagan et al. [19].  $C_{\max,u}$ , unbound maximum plasma concentration;  $C_u$ , unbound plasma concentration; EMA, European Medicines Agency; FDA, U.S. Food and Drug Administration;  $IC_{50}$ , half maximal inhibitory concentration; MATE, multidrug and toxin extrusion protein; NME, new molecular entity; OCT, organic cation transporter.

## 1.4 DRUG-GENE INTERACTIONS

### 1.4.1 Overview

DGIs can occur when a drug's pharmacology is affected by one or multiple variations in pharmacogenes coding for metabolizing enzymes, transporters or other target structures [103]. Variations in pharmacogenes can lead to different phenotypes compared to the so-called wild-type due to alteration of protein expression, enzyme or transporter activity or inducibility [104, 105]. Various causes of genetic variations are known, but difference in one single position in the deoxyribonucleic acid (DNA) sequence, single nucleotide polymorphisms (SNPs), depict the most common type of genetic variations

Variants in  
pharmacogenes

[106]. Genotypes can be determined with a variety of biological assays [107]. From these, translation into the respective phenotype is possible for many relevant pharmacogenes, e.g., by making use of an activity score-based system. Phenotyping without genotyping can be performed by administering a probe drug and determining the urinary excretion ratio of unchanged compound to its metabolite. The Clinical Pharmacogenetics Implementation Consortium (CPIC) provides an overview of definitions, contributing to a uniform nomenclature of phenotypes [108]. DGIs are closely connected with interethnic variability, e.g., the dominant CYP3A5 allele in Caucasians is the CYP3A5\*3 (no-function) allele, while the functional CYP3A5\*1 allele occurs only with low frequency. In contrast, other ethnicities like African Americans or Asians exhibit higher frequencies of the functional allele [109, 110].

Guidelines  
providing  
information on  
drug-gene  
interactions

The labels of more than 350 drugs approved by the FDA include information on pharmacogenetics [111], to improve effectiveness and safety of pharmacotherapies. Furthermore, dosing guidelines, e.g., by the CPIC or the Dutch Pharmacogenetics Working Group (DPWG), are constantly developed as well as other information resources like the Pharmacogenomics Knowledgebase (PharmGKB), providing an overview of 68 important pharmacogenes significantly affecting ADME of one or several drugs (“Very Important Pharmacogenes” [112–114]).

Drug-gene  
interactions  
affecting drug-drug  
interactions

Pharmacokinetic and also pharmacodynamic interactions may be genetically modulated [50] and so-called drug-drug-gene interactions (DDGIs) can result in further changes in the victim drug’s pharmacokinetics or pharmacodynamics compared to the DGI or DDI alone. DDGIs can be categorized, if a perpetrator drug either (i) inhibits or induces the same enzyme or transporter as influenced by a genetic variant; (ii) affects an enzyme or transporter divergent from the enzyme or transporter influenced by a genetic variant or (iii) is affected by a genetic variant in an enzyme or transporter gene not directly interfering with the victim drug’s pharmacokinetics or pharmacodynamics but indirectly leading to a more or less pronounced interaction effect [27].

#### 1.4.2 Renal transporter drug-gene interactions

Several genetic polymorphisms of renal transporters affecting drug pharmacokinetics have been reported. As this thesis focuses on OCT2 and MATE1 interactions, common variants and their effect on drug pharmacokinetics are discussed below.

OCT2 (SLC22A2) c.808G>T (p.270Ala>Ser, rs316019) [115] depicts the most frequent variant with 15% over different ethnicities [22]. Reports on the consequences for transporter activity are controversial, as decreased [116], equal [117] or increased [118] transport velocity for the variant OCT2 protein compared to wild-type has been observed during *in vitro* studies. The same applies for *in vivo*, where

either decreased [71, 116] or increased [118, 119] renal clearance of the important substrate metformin are reported. Regarding pharmacodynamics, no data investigating the polymorphism effect on metformin glucose-lowering effect are currently available [22]. Interestingly, the variant protein seems to be less sensitive to the effect of known OCT2 inhibitors, as varying  $IC_{50}$  values in wild-type and variant OCT2 have been determined for several inhibitors [117]. Another important OCT2 substrate depicts the chemotherapeutic cisplatin and, due to basolateral uptake into tubule epithelial cells, OCT2 is related to the extent of nephrotoxicity [120]. Also here, conflicting effects of *SLC22A2* polymorphisms in terms of this serious adverse event have been observed and studies based on cell lines, animals or humans report either lower nephrotoxicity [120–122] or no association of this variant with nephrotoxicity [123].

*SLC22A2*  
polymorphisms

For *MATE1* (*SLC47A1*), a polymorphism located in the promoter region, *SLC47A1* g.-66T>C (rs2252281) [124], shows a frequency between 23% (Asians) and 45% (Africans) [125]. Here, a reduced transcriptional activity can be suggested from *in vitro* experiments [125]. Another variant located in an intronic area, *SLC47A1* rs2289669 G>A, shows a global frequency around 40% [126]. For this variant, a positive influence on the glucose-lowering effect of metformin has been found in diabetes patients [127].

*SLC47A1*  
polymorphisms

To assess the influence of genetic polymorphisms involved in metformin pharmacokinetics, determination of variants in genes of both OCT2 and *MATE1* seems to be important. For instance, a study on the effect of the *SLC22A2* c.808G>T variant reported an increased metformin clearance in subjects carrying the reference *SLC47A1* g.-66T>C variant compared to a reduced clearance in carriers of both variants [119]. This importance is further underlined by two DDGI studies. During the DDI with the OCT2 and *MATE1* inhibitor cimetidine, a lower effect of the inhibitor has been determined in *SLC22A2* c.808G>T variant carriers [71]. However, the *SLC47A1* genotype was not reported in this study. In contrast, during DDI with the OCT2 and *MATE1* inhibitor trimethoprim, presence of both *SLC22A2* (rs316019) and *SLC47A1* (rs2289669) variants leads to a reduced DDI effect compared to *SLC22A2* wild-type or single polymorphism carriers [91].

Combination of  
*SLC22A2* and  
*SLC47A1*  
polymorphisms

## 1.5 DRUG-DISEASE INTERACTIONS

### 1.5.1 Effect of drug-disease interactions on pharmacology

The disease state of a patient can have a strong impact on the medication, while it can be distinguished between acute and chronic diseases [128]. For instance, inflammation has been shown to negatively affect the activity of metabolizing enzymes and transporters [128]. Chronic diseases like hepatic or renal impairment can also influence

drug metabolism and excretion, leading to an increased risk of adverse drug events or safety issues when neglected. The following section takes a closer look at CKD.

### 1.5.2 Chronic kidney disease

#### Classification of chronic kidney disease

The progressive reduction of renal function, CKD, is one of the leading public health problems worldwide with a global prevalence of about 13% [129]. CKD can be classified into 5 stages based on GFR as surrogate for renal function [130] (Figure 1.5).

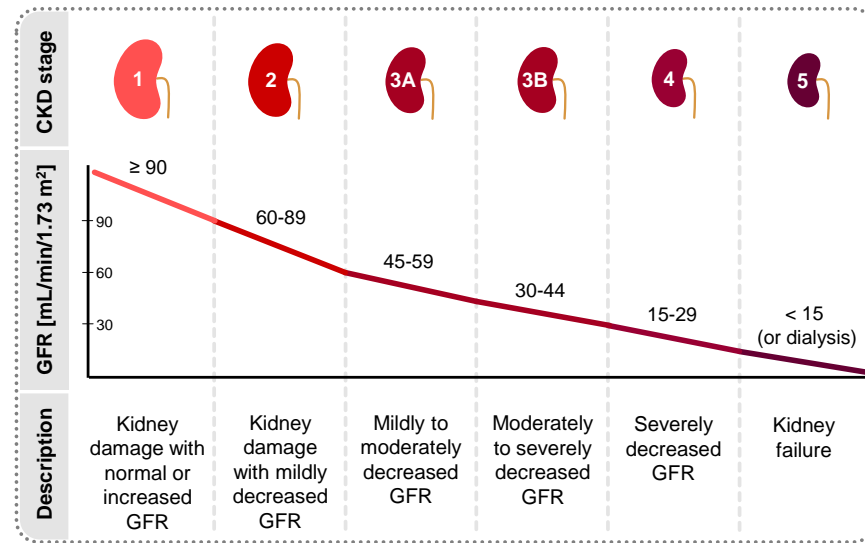


**Figure 1.5.** Classification of chronic kidney disease (CKD) according to Levey et al. [130] and the CKD evaluation and management guideline by the Kidney Disease: Improving Global Outcomes (KDIGO) [131]. GFR, glomerular filtration rate.

Administration of appropriate drugs and adequate doses is crucial in CKD patients, to avoid overdosing or safety issues. Therefore, an essential part during drug development is to evaluate the influence of decreased renal function on drug pharmacokinetics. It has been observed that CKD not only affects renal excretion but also other pharmacokinetic processes due to accumulation of uremic toxins, inflammatory cytokines and parathyroid hormones [132–134] and therefore, also influences pharmacokinetics of non-renally excreted drugs. For instance, renal impairment can lead to modulated function of CYP enzymes [132] and changes in albumin concentration [135], emphasizing that also effects on hepatic metabolism, active transport and protein binding need to be considered. For the OCT2-mediated secretory clearance, a decrease in parallel with GFR from CKD stage 2 to 4 has been reported [136], being in contrast to findings for OAT1 and OAT3, where a faster deterioration than for GFR has been observed [137]. For MATE1, decreased levels in rats with CKD have been described [138].

#### Effect of chronic kidney disease on pharmacokinetics

However, a recent analysis in hyperuricemic rats showed an induction of rOCT2 and rMATE1 [139], but equivalent studies in humans are lacking.

Several guidelines of regulatory agencies are available to support drug development with respect to the impact of CKD [140, 141]. To assess the need to conduct dedicated studies in renally impaired individuals, a “totality of evidence” approach has been proposed [142, 143], including knowledge from (pre-)clinical studies, information on mass balance, bioavailability and DDIs, as well as *in silico* approaches like exposure-response analyses, population pharmacokinetic (PopPK) and PBPK modeling [143]. The FDA guideline on investigations of pharmacokinetics in patients with impaired renal function also recommends to apply modeling and simulation strategies like PBPK modeling during consideration of renal impairment studies [140].

*Investigation of decreased renal function during drug development*

## 1.6 DIURNAL VARIATION

### 1.6.1 Chronopharmacology

Many physiological processes exhibit an intraday variation. This can be attributed to hierarchical organized endogenous clocks [144], while the suprachiasmatic nuclei of the hypothalamus represent the superordinate clock with subsequent peripheral clocks in the organs [145]. Chronopharmacology plays an important role, as different drugs show varying pharmacokinetics and pharmacodynamics when applied at different daytimes. For instance, the extent of nephrotoxicity due to cisplatin therapy is differently pronounced comparing morning or evening drug administration [146–148]. In different fields (e.g., cancer treatment), personalized chronotherapy has been emphasized as advantageous treatment option [149]. However, for most drugs, no dedicated studies have been performed on investigating chronopharmacology, although results might contribute to more effective and safe therapies.

### 1.6.2 Diurnal pharmacokinetics

Circadian clocks influencing ADME-relevant processes can lead to diurnal variation in pharmacokinetics [144] and thus to changes in drug exposure and correlated efficacy or toxicity. Drug absorption can be influenced by varying gastric pH [150], gastric emptying [151] or gut motility [152]. In the liver, daytime-dependent activity of drug transporters, metabolizing enzyme and hepatobiliary elimination has been determined [144] as well as changes in hepatic blood flow [153]. In the kidney, renal blood flow, GFR as well as urine pH show diurnal variation [86, 97, 154, 155]. Variability of GFR cannot be explained solely by fluctuation of renal blood flow [86], as the oscillation phases

are not completely synchronized for GFR and renal plasma flow (RPF). Furthermore, it has been shown in mice, that the intrinsic clock in podocytes contributes to diurnal rhythmicity of the GFR [156], but the involvement of the kidney clock is not completely understood, yet [157]. Regarding renal transporters, especially OCTs, diurnal variation has not been shown in humans yet, but OCT2 messenger RNA and protein exhibit diurnal variation while this does not apply to MATE1 in mice kidney [158].

## 1.7 MECHANISTIC PHARMACOKINETIC MODELING ANALYSES

### 1.7.1 Pharmacometrics

Pharmacometrics is defined as a “branch of science concerned with mathematical models of biology, pharmacology, disease, and physiology used to describe and quantify interactions between xenobiotics and patients, including beneficial effects and side effects resultant from such interfaces” [159] and “the science of developing and applying mathematical and statistical methods to characterize, understand, and predict a drug’s pharmacokinetic, pharmacodynamic, and biomarker-outcomes behavior” [160]. Pharmacometric approaches include pharmacokinetic and pharmacodynamic modeling techniques as well as disease progression models [161].

### 1.7.2 Physiologically based pharmacokinetic modeling

Pharmacokinetic models aim to describe and predict ADME-related processes and resulting concentration-time profiles of a compound of interest. An overview of different compartmental pharmacokinetic model structures is illustrated in [Figure 1.6](#).

Whole-body PBPK modeling is a compartmental modeling approach where each compartment represents a different organ, mimicking the (human) body. These compartments are further divided into sub-compartments, e.g., cellular space, interstitium, blood plasma and red blood cells ([Figure 1.6](#)). Compartments are connected by blood flow and distribution between (sub-)compartments is accomplished passively or by implementing directed transport. The change of compound concentration over time in (sub-)compartments is described by differential equations [162].

PBPK models are usually developed by a “bottom up” approach, implementing anatomy- and physiology-related parameters as well as compound-related information and subsequently, optimizing unknown model parameters [162]. Model building is usually supported by data derived from clinical studies, mostly concentration measurements in easily accessible body fluids like blood and urine. Tissue concentrations measured by e.g., positron emission tomography (PET)

*Physiologically  
based  
pharmacokinetic  
model structure*



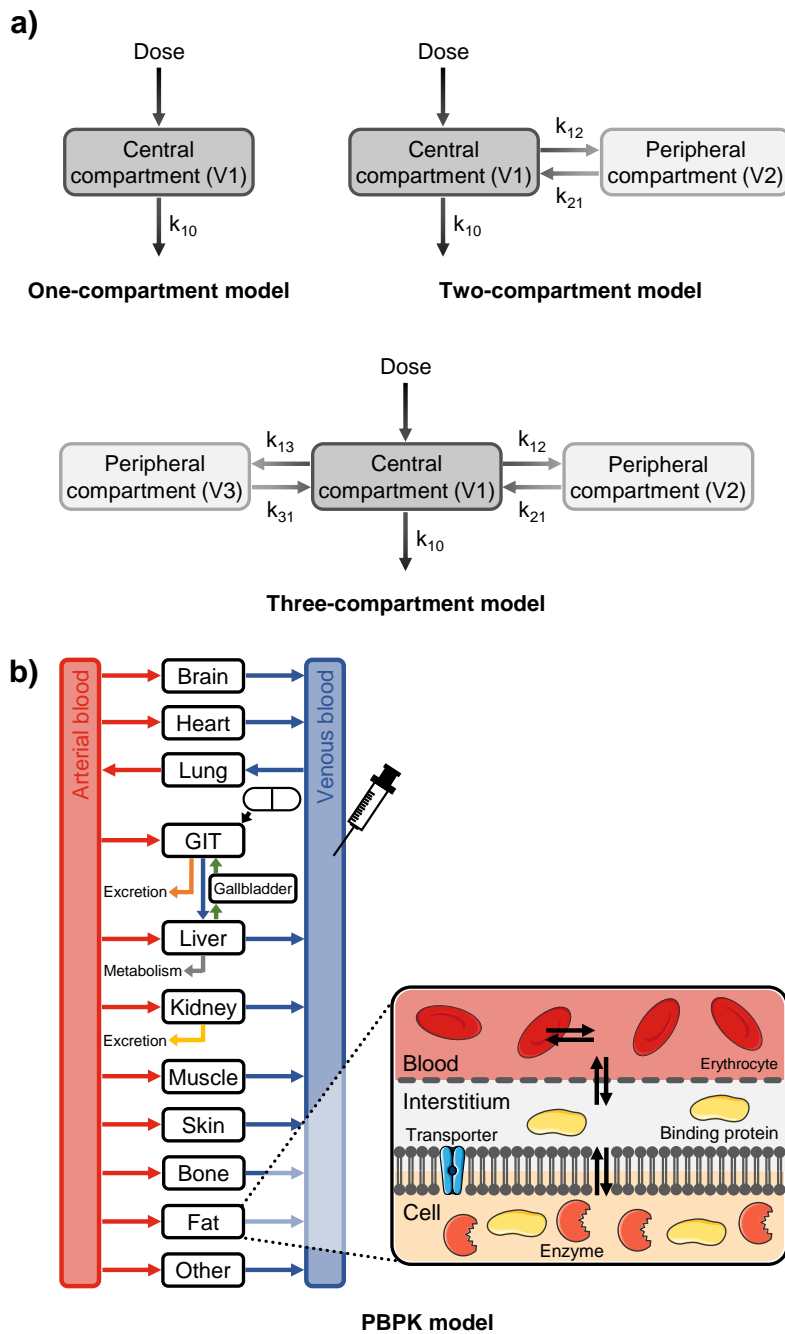


**Figure 1.6.** Compartmental pharmacokinetic models. a) Schematic illustration of one-, two- and three-compartment models. Compartments, described by compartment volume ( $v$ ), are connected via rate constant ( $k$ ) values. b) Schema of a whole-body physiologically based pharmacokinetic (PBPK) model. Organs are represented by compartments connected via arterial (red arrows) and venous blood flow (blue arrows) and divided into sub-compartments. Illustrations of blood and cell components were taken from Servier [5], licensed under CC BY 3.0 (<https://creativecommons.org/licenses/by/3.0/>). GIT, gastrointestinal tract.

are helpful, especially during development of transporter-based PBPK models, but only rarely available [163]. PBPK models can predict compound concentrations in all integrated tissues, however, comparison against clinical data is often difficult. A further shortcoming of PBPK models might be that they require a large number of model input parameters to mechanistically portray complex physiological and ADME-related processes, which is often associated with assumptions. However, PBPK modeling depicts a mechanistic approach among pharmacometrics, allowing investigation of underlying processes affecting compound ADME including hypothesis testing.

### 1.7.3 *Physiologically based pharmacokinetic model applications*

An increasing interest in PBPK modeling, measured by the number of publications including PBPK analyses, has been shown over the last two decades [164]. The same trend has been observed for PBPK model submissions to the FDA, where application areas include enzyme-based DDIs (60% of submissions), pediatrics (15%), transporter-based DDIs (7%), hepatic impairment (6%), renal impairment (4%), absorption/food effect (4%) and pharmacogenetics (2%) [165]. Next to the mentioned application areas, PBPK models are further valuable tools to perform cross-species extrapolation, e.g., from preclinical animals to humans [166] or to extrapolate from healthy individuals to special populations like patients by taking their pathophysiological background, polymedication and (genetic) heterogeneity into account [166]. Models can be further extended, e.g., to investigate drug pharmacodynamics [166]. Another interesting application area is assessing the effect of chronopharmacology. The comprehensive models can finally be utilized to guide personalized treatment by calculating dose adaptations with the aim to achieve the same drug exposure in patients as in a typical healthy individual without co-medication and genetic polymorphisms [1, 26, 167].

### 1.7.4 *Pharmacokinetic modeling to support model-informed drug discovery and development as well as precision dosing*

Applications of pharmacokinetic models for model-informed drug discovery and development (MID<sub>3</sub>) are versatile, comprising support during different stages of drug development. Selection of the appropriate modeling technique depends on the research question, e.g., information of trial design, dose calculations or extrapolation to special populations [168]. For instance, pharmacokinetic models alone or in combination with pharmacodynamic models are suitable in discovery phase, preclinical and clinical development and lifecycle management [169]. During discovery, preclinical and clinical phases, also more specialized models, like systems pharmacology models and allometric

scaling techniques as well as PBPK and PopPK models are required [169]. Pharmacometrics is represented in several guidances provided by regulatory agencies to support MID<sub>3</sub> [170–174]. Next to their usefulness in drug development, models can be utilized to improve patient therapies by treatment personalization (model-informed precision dosing (MIPD)), requiring not only reliable models but also access via decision-support systems to make models available for non-pharmacometricians [27].



## OBJECTIVES

---

The overall objective of this thesis was to apply mechanistic pharmacokinetic modeling techniques to investigate the effect of transporter-mediated DDIs, DBIs, DGIs as well as of CKD and diurnal variation on the pharmacokinetics of exogenous and endogenous renal transporter substrates, to demonstrate their potential suitability in supporting drug development or individualization of pharmacotherapy by dose adaptations. The thesis' objective was realized within the scope of the following three projects:

### 2.1 PROJECT I - PHYSIOLOGICALLY BASED PHARMACOKINETIC MODELING OF METFORMIN AND CIMETIDINE

The objectives of project I were (i) to develop whole-body PBPK models of the renal transporter substrate metformin and the renal transporter substrate and inhibitor cimetidine, metformin recommended by the FDA as OCT2 and MATE substrate and cimetidine as MATE inhibitor to use in clinical drug interaction studies; (ii) to extend the metformin PBPK model with metformin-*SLC22A2* 808G>T DGI predictions; (iii) to predict the cimetidine-metformin DDI and DDGI; (iv) to investigate metformin exposure in subjects with different stages of CKD and (v) to provide model-based dose adaptations in patients with CKD and to compare them to existing dosing guidelines.

### 2.2 PROJECT II - PHYSIOLOGICALLY BASED PHARMACOKINETIC MODELING OF TRIMETHOPRIM

The objectives of project II were (i) to develop a whole-body PBPK model of trimethoprim, recommended by the FDA as CYP2C8 and MATE inhibitor to use in clinical drug interaction studies; (ii) to model the rifampicin-trimethoprim DDI, to gain insights into unidentified trimethoprim metabolism and transport processes; (iii) to predict DDIs and DDGIs of trimethoprim with the OCT and MATE victim drug metformin in *SLC22A2* wild-type and 808G>T polymorphic subjects and (iv) to further challenge the DDI performance of the trimethoprim model as CYP2C8 inhibitor during DDIs with repaglinide and pioglitazone, including DDGI predictions of pioglitazone in *CYP2C8*\*3 allele carriers.

### 2.3 PROJECT III - PHYSIOLOGICALLY BASED PHARMACOKINETIC MODELING OF ENDOGENOUS BIOMARKERS

The objectives of project III were (i) to develop whole-body PBPK models of the endogenous OCT2 and MATE substrates and proposed biomarkers creatinine and NMN, mechanistically describing their absorption, synthesis, biotransformation and transporter-mediated excretion, also generating hypotheses for underlying causes of observed diurnal variation, to contribute to biomarker characterization and (ii) to predict biomarker kinetics during DBIs by linking the new models with previously evaluated perpetrator models of the potent OCT and MATE inhibitors trimethoprim, pyrimethamine and cimetidine, establishing a comprehensive PBPK DDI/DBI network, underlining the ability of the biomarker models to support transporter-mediated interaction predictions.

## METHODS

## 3.1 PHYSIOLOGICALLY BASED PHARMACOKINETIC MODELING

The whole-body PBPK modeling workflow applied in projects I–III is illustrated in Figure 3.1 and described in detail below.

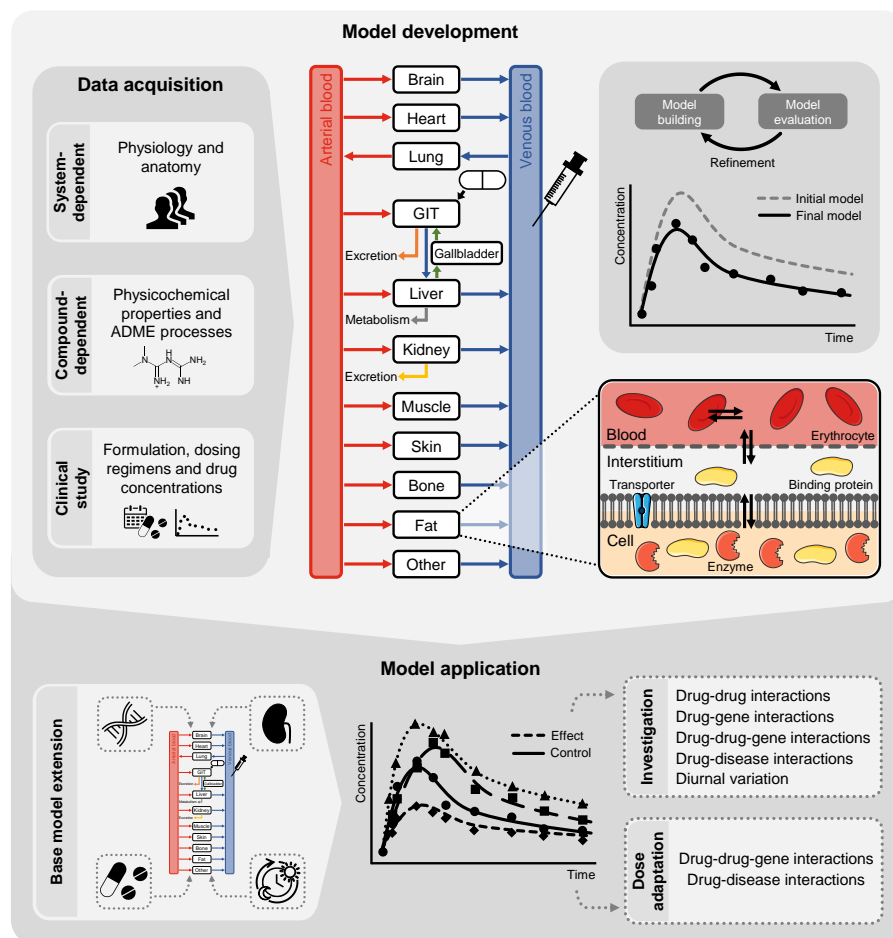


**Figure 3.1.** Whole-body physiologically based pharmacokinetic (PBPK) modeling workflow adopted from Türk et al. [27]. Illustrations of cell components were taken from Servier [5], licensed under CC BY 3.0 (<https://creativecommons.org/licenses/by/3.0/>). ADME, absorption, distribution, metabolism, and excretion; GIT, gastrointestinal tract.

## 3.1.1 Model building

Model building was initiated with acquisition of system-dependent (i.e., physiological and anatomical information) and compound-de-

*Data acquisition*

pendent parameters for the compounds of interest (i.e., physicochemical properties and information about ADME processes). Additionally, studies reporting concentrations in whole blood, plasma and serum (in the following referred to as “plasma”) and relevant organs and tissues as well as studies quantifying compound excretion, e.g., by providing amount in urine, urinary excretion rate or renal clearance, were collected. Furthermore, information from clinical studies about drug formulation and dosing regimen were extracted. Data were divided into a training dataset for model building and a test dataset for model evaluation. For model building, studies were preferably selected to include (pharmaco-)kinetic profiles of frequent data sampling as well as measurements after administrations of various routes and doses. To simulate compound concentrations in the different compartments, virtual twins of study individuals were created according to the demographics reported by the respective clinical studies, namely ethnicity, sex, age, body weight, and height. Information on renal function (i.e., GFR) was incorporated whenever available.

*Protein expression and localization*

Subsequently, protein expression data, and metabolism, transport and binding rates of relevant enzymes, transporters and targets were implemented in the model according to current literature. Detailed information about expression and localization of relevant enzymes and transporters is provided in [Table 3.1](#).

*Implementation of ADME processes*

Metabolism and transport processes were implemented with first-order kinetics ([Equation 3.1](#)) or, if saturable, Michaelis-Menten kinetics ([Equation 3.2](#)). For endogenous compounds, a synthesis rate ( $R_{\text{syn}}$ ) was implemented as synthesized amount per time in relevant organs in accordance with literature reports.

$$v = \text{CL}_{\text{spec}} \cdot [\text{E}] \cdot [\text{S}] \quad (3.1)$$

with  $v$  = reaction velocity,  $\text{CL}_{\text{spec}}$  = specific enzymatic clearance,  $[\text{E}]$  = enzyme concentration and  $[\text{S}]$  = free substrate concentration.

$$v = \frac{v_{\text{max}} \cdot [\text{S}]}{K_{\text{M}} + [\text{S}]} = \frac{k_{\text{cat}} \cdot [\text{E}] \cdot [\text{S}]}{K_{\text{M}} + [\text{S}]} \quad (3.2)$$

with  $v$  = reaction velocity,  $v_{\text{max}}$  = maximum reaction velocity,  $[\text{S}]$  = free substrate concentration,  $K_{\text{M}}$  = Michaelis-Menten constant,  $k_{\text{cat}}$  = catalytic or transport rate constant and  $[\text{E}]$  = enzyme or transporter concentration.



**Table 3.1.** Expression and localization of relevant enzymes and transporters.

Enzyme/transporter	Reference concentration <sup>a</sup>	Relative expression <sup>b</sup>	Localization	Direction	Half-life [h]
AOX1	1.00 <sup>c</sup> [175]	RT-PCR [176]	Intracellular	-	36 (liver), 23 (intestine)
CYP3A4	4.32 [177]	RT-PCR [178]	Intracellular	-	36 (liver), 23 (intestine) [179, 180]
MATE1	0.13 <sup>d</sup> [42, 181]	Kidney only [48, 182]	Apical	Efflux	-
OAT3	0.09 <sup>d</sup> [42, 181]	RT-PCR [183]	Basolateral	Influx	36 (liver)
OCT1	0.16 <sup>e</sup> [184, 185]	ArrayExpress [186] <sup>f</sup>	Basolateral <sup>g</sup>	Influx	36 (liver), 23 (intestine)
OCT2	0.19 <sup>d</sup> [42, 181]	Expressed Sequence Tag [187]	Basolateral	Influx	-
P-gp	1.41 [188]	RT-PCR [183] <sup>h</sup>	Apical	Efflux	36 (liver), 23 (intestine)
PMAT	1.00 <sup>c</sup> [175]	RT-PCR [183] <sup>f</sup>	Basolateral <sup>g</sup>	Influx	36 (liver), 23 (intestine)
Tubular reabsorption	1.00 <sup>c</sup> [175]	Kidney only	Basolateral	Efflux	-

-, not applicable; AOX, aldehyde oxidase; CYP, cytochrome P450; MATE, multidrug and toxin extrusion protein; OAT, organic anion transporter; OCT, organic cation transporter; P-gp, P-glycoprotein; PMAT, plasma membrane monoamine transporter; RT-PCR, reverse transcription-polymerase chain reaction; <sup>a</sup>  $\mu\text{mol protein/L}$  in tissue of highest expression; <sup>b</sup> relative expression in different organs (PK-Sim<sup>®</sup> expression database); <sup>c</sup> if no information was available, mean reference concentration was set to 1.00  $\mu\text{mol/L}$  and catalytic or transport rate constant ( $k_{\text{cat}}$ ) was optimized according to Meyer et al. [175]; <sup>d</sup> calculated from transporter per mg membrane protein  $\cdot$  26.2 mg human kidney microsomal protein per g kidney [181]; <sup>e</sup> calculated from transporter per mg membrane protein  $\cdot$  37.0 mg membrane protein per g liver [184]; <sup>f</sup> large intestinal mucosa  $\rightarrow$  0; <sup>g</sup> in enterocytes apical [189–191]; <sup>h</sup> intestinal mucosa  $\rightarrow$  factor 3.57 [188].

## 3.1.2 Model evaluation

Graphical model  
evaluation

PBPK models were evaluated by comparison of (i) predicted and observed plasma and urine profiles over time, (ii) all plasma and urine predictions to their corresponding observed values in goodness-of-fit plots and (iii) predicted and observed AUC and  $C_{\max}$  values, where AUC was calculated from the time of compound administration to the time of the last concentration measurement ( $AUC_{\text{last}}$ ) for predicted and observed plasma concentration-time profiles.

Quantitative  
measures of model  
performance

As quantitative measures of model performances, mean relative deviations (MRDs, Equation 3.3) of all plasma predictions and geometric mean fold errors (GMFEs, Equation 3.4) of all  $AUC_{\text{last}}$ ,  $C_{\max}$  and urine predictions were calculated, assuming an adequate model performance for MRD and GMFE values  $\leq 2$ .

$$\text{MRD} = 10^x; \quad x = \sqrt{\frac{1}{k} \sum_{i=1}^k (\log_{10} C_{\text{pred},i} - \log_{10} C_{\text{obs},i})^2} \quad (3.3)$$

with  $C_{\text{pred},i}$  =  $i^{\text{th}}$  predicted concentration,  $C_{\text{obs},i}$  =  $i^{\text{th}}$  observed concentration and  $k$  = number of observed values.

$$\text{GMFE} = 10^x; \quad x = \frac{1}{m} \sum_{i=1}^m \left| \log_{10} \left( \frac{\text{PK}_{\text{pred},i}}{\text{PK}_{\text{obs},i}} \right) \right| \quad (3.4)$$

with  $\text{PK}_{\text{pred},i}$  =  $i^{\text{th}}$  predicted pharmacokinetic parameter,  $\text{PK}_{\text{obs},i}$  =  $i^{\text{th}}$  observed pharmacokinetic parameter and  $m$  = number of studies.

Sensitivity analysis

Local sensitivity analyses were performed to investigate the effect of model parameters on the predicted  $AUC_{\text{last}}$ . Parameters were considered during analyses if they have been optimized during parameter identifications, if they were associated with optimized parameters or if they might have a strong impact on model predictions, e.g., as they are included in equations to calculate permeabilities or partition coefficients. Sensitivity analyses were performed using the highest recommended or reported compound doses and a relative parameter perturbation of 1000%. The threshold value for sensitivity was set to 0.5, implying that a 100% change of the investigated parameter value causes a 50% change of the predicted  $AUC_{\text{last}}$ . Sensitivity was calculated according to Equation 3.5.

$$S = \frac{\Delta AUC_{\text{last}}}{AUC_{\text{last}}} \cdot \frac{p}{\Delta p} \quad (3.5)$$

with  $\Delta AUC_{\text{last}}$  = change of the  $AUC_{\text{last}}$ ,  $AUC_{\text{last}}$  = simulated  $AUC_{\text{last}}$  with the original parameter value,  $p$  = original parameter value and  $\Delta p$  = change of the original parameter value.

### 3.1.3 Modeling of drug-drug and drug-biomarker interactions

To describe the impact of the perpetrators on the victims in projects I–III, base PBPK models were extended to mechanistic DDI or DBI models according to the workflow provided by the FDA [192]. Perpetrator models were linked to victim models by including all relevant interaction mechanisms, i.e., competitive inhibition in the scope of this thesis, while competition of substrate and inhibitor for binding to an enzyme or transporter due to reversible binding of the inhibitor to the active site was assumed. During perpetrator (co-)administration, the affinity of the victims to the respective enzyme or transporter, parametrized with Michaelis-Menten constant ( $K_M$ ) values, was decreased, which is described by an apparently increased value for  $K_M$  ( $K_{M,app}$ , Equation 3.6), while maximum reaction velocity ( $v_{max}$ ) remained unchanged. The altered reaction velocity of the victim was modeled according to Equation 3.7.

Competitive inhibition

$$K_{M,app} = K_M \cdot \left( 1 + \frac{[I]}{K_i} \right) \quad (3.6)$$

$$v = \frac{v_{max} \cdot [S]}{K_{M,app} + [S]} = \frac{k_{cat} \cdot [E] \cdot [S]}{K_{M,app} + [S]} \quad (3.7)$$

with  $K_{M,app}$  = Michaelis-Menten constant in the presence of inhibitor,  $K_M$  = Michaelis-Menten constant,  $[I]$  = free inhibitor concentration,  $K_i$  = dissociation constant of the inhibitor-enzyme/-transporter complex,  $v$  = reaction velocity,  $v_{max}$  = maximum reaction velocity,  $[S]$  = free substrate concentration,  $k_{cat}$  = catalytic or transport rate constant and  $[E]$  = enzyme or transporter concentration.

Relevant dissociation constant of the inhibitor-enzyme/-transporter complex ( $K_i$ ) values were extracted from *in vitro* references whenever available and integrated in the perpetrator models of trimethoprim, pyrimethamine and cimetidine, to simulate renal transporter-mediated DDIs and DBIs with metformin, creatinine and NMN. Inhibition of OCT1, the transporter mainly responsible for intestinal and hepatic uptake of metformin, was described for all three modeled perpetrators and was therefore also incorporated in the DDI models with metformin. Models of trimethoprim and cimetidine were further evaluated by DDI predictions with CYP substrates, which is described in detail in the respective publications of projects I and II [1, 2].

Drug-drug and drug-biomarker interaction model building

Resulting DDI and DBI simulations were subsequently evaluated graphically by comparison of (i) victim plasma and urine predictions alone and during perpetrator (co-)administration to observed data and (ii) predicted to observed DDI or DBI ratios, calculated as ratio of the respective DDI or DBI (pharmaco-)kinetic parameter and the related control parameter. As quantitative measures of the DDI or DBI

Drug-drug and drug-biomarker interaction model evaluation

model performance, GMFE values of the predicted DDI or DBI ratios were calculated (Equation 3.4).

### 3.1.4 Modeling of drug-gene interactions

*Drug-gene  
interaction model  
building*

To model the impact of genetic polymorphism on metformin pharmacokinetics in projects I and II, parameters describing the expression or activity of variant *SLC22A2* were taken from literature reports according to Türk et al. [27]. Polymorphic transporters were implemented as two separate proteins with half of the original reference concentration each, to mimic two homologous chromosomal alleles. Homozygous wild-type alleles were modeled with the  $k_{cat}$  value identified during the base model development, variant alleles with adjusted  $k_{cat}$  values identified during parameter optimizations based on information from clinical studies considering homozygous variant allele carriers. Heterozygous variant allele carriers were modeled by combination of one wild-type and one variant allele.

*Drug-gene  
interaction model  
evaluation*

Resulting DGI simulations were subsequently evaluated graphically by comparison of (i) plasma and urine predictions in homozygote wild-type allele carriers and variant allele carriers to observed data and (ii) predicted to observed DGI  $AUC_{last}$  and  $C_{max}$  ratios, calculated as ratio of the respective  $AUC_{last}$  or  $C_{max}$  during DGI and the related wild-type parameter. As quantitative measures of the DGI model performance, GMFE values of the predicted DGI  $AUC_{last}$  ratios and  $C_{max}$  ratios were calculated (Equation 3.4).

### 3.1.5 Modeling of chronic kidney disease

*Drug-disease  
interaction model  
building*

A literature search was performed to identify pathophysiological changes related to renal impairment, also taking their extent at different stages of CKD into account (Section 1.5.2). To subsequently expand the metformin base model to a drug-disease model in project I and to model pharmacokinetics in renally impaired individuals, system-dependent parameters were adapted to cover identified differences in anatomy and physiology.

*Drug-disease  
interaction model  
evaluation*

Drug-disease interaction model performance was evaluated graphically as described in Section 3.1.2 as well as quantitatively, calculating MRDs of all plasma predictions (Equation 3.3) and GMFEs of all predicted  $AUC_{last}$  and  $C_{max}$  values (Equation 3.4).

### 3.1.6 Modeling of diurnal variation

A literature search was performed to identify relevant physiological processes that underlie diurnal variation and therefore possibly affect (pharmaco-)kinetics (Section 1.6.2). To model the impact of diurnal variation on creatinine and NMN in project III, base models

were extended by multiplication of respective model process equations with an oscillation function according to Equation 3.8, assuming a 24 hour-rhythm. Amplitude and acrophase (i.e., clock time of maximal activity) were informed from measurements in humans where available or optimized using observed plasma and urine measurements.

$$f(t) = \text{amp} \cdot \sin\left(\frac{2\pi}{24} \cdot (t + \text{shift})\right) + 1 \quad (3.8)$$

with  $t$  = time,  $\text{amp}$  = amplitude and  $\text{shift}$  = shift in time.

### 3.2 SOFTWARE

PBPK models of cimetidine, creatinine, metformin, NMN, trimethoprim and pyrimethamine were developed in projects I–III using PK-Sim<sup>®</sup> and MoBi<sup>®</sup> modeling software (Open Systems Pharmacology Suite 8.0 (projects I–II) and 9.1 (project III), Open Systems Pharmacology, 2019–2020). Plasma and urine measurements from literature were digitized with GetData Graph Digitizer 2.26.0.20 (project I) (© S. Fedorov, 2013) and Engauge Digitizer 10.12 (projects II–III) (© M. Mitchell [193], 2019) according to best practices [194]. Model parameter optimization and sensitivity analysis were performed within PK-Sim<sup>®</sup> and MoBi<sup>®</sup>. Pharmacokinetic parameter calculation, quantitative model performance assessment and plot generation were accomplished using R 3.6.1 (project I), 3.6.2 (project II) and 4.1.1 (project III) (R Core Team. R: a language and environment for statistical computing. R Foundation for Statistical Computing, Vienna, Austria, 2019–2021) and RStudio 1.1.423 (project I), 1.2.5033 (project II) and 1.4.1717 (project III) (RStudio, Inc., Boston, MA, U.S., 2019–2021).



## RESULTS

#### 4.1 PROJECT I - A COMPREHENSIVE WHOLE-BODY PHYSIOLOGICALLY BASED PHARMACOKINETIC DRUG-DRUG-GENE INTERACTION MODEL OF METFORMIN AND CIMETIDINE IN HEALTHY ADULTS AND RENALLY IMPAIRED INDIVIDUALS

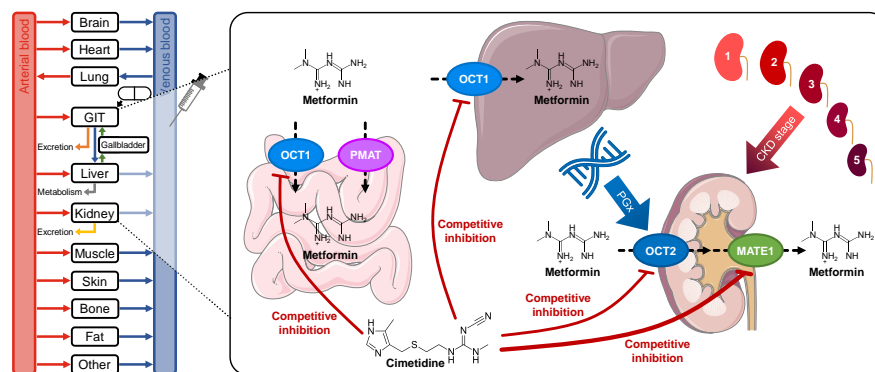


**Figure 4.1.** Whole-body physiologically based pharmacokinetic (PBPK) modeling of metformin and cimetidine for drug-drug-gene-disease interaction predictions. Illustrations of organs were taken from Servier [5], licensed under CC BY 3.0 (<https://creativecommons.org/licenses/by/3.0/>). CKD, chronic kidney disease; GIT, gastrointestinal tract; MATE, multidrug and toxin extrusion protein; OCT, organic cation transporter; PGx, pharmacogenetics; PMAT, plasma membrane monoamine transporter.

#### Publication

Hanke N, Türk D, Selzer D, Ishiguro N, Ebner T, Wiebe S, Müller F, Stopfer P, Nock V, and Lehr T. A comprehensive whole-body physiologically based pharmacokinetic drug-drug-gene interaction model of metformin and cimetidine in healthy adults and renally impaired individuals. *Clinical Pharmacokinetics*. 2020;59(11):1419-31. DOI: [10.1007/s40262-020-00896-w](https://doi.org/10.1007/s40262-020-00896-w)

*Publication I*

#### Supplementary material

The supplementary material to this publication can be found on the accompanying compact disk or can be accessed online via: [https://static-content.springer.com/esm/art%3A10.1007%2Fs40262-020-00896-w/MediaObjects/40262\\_2020\\_896\\_MOESM1\\_ESM.pdf](https://static-content.springer.com/esm/art%3A10.1007%2Fs40262-020-00896-w/MediaObjects/40262_2020_896_MOESM1_ESM.pdf).

## Copyright

This article is licensed under CC BY-NC 4.0 (<https://creativecommons.org/licenses/by-nc/4.0/>), which permits any non-commercial use, sharing, adaptation, distribution and reproduction in any medium or format, as long as you give appropriate credit to the original author(s) and the source, provide a link to the Creative Commons licence, and indicate if changes were made.

© The Author(s) 2020. Reproduced with permission from Springer Nature.

The upper panel of Figure 3 of the manuscript was originally published in Journal of Nuclear Medicine. Gormsen LC, Sundelin EI, Jensen JB, Vendelbo MH, Jakobsen S, Munk OL, Hougaard Christensen MM, Brøsen K, Frøkiær J, and Jessen N. In vivo imaging of human <sup>11</sup>C-metformin in peripheral organs: dosimetry, biodistribution, and kinetic analyses. Journal of Nuclear Medicine. 2016;57(12):1920-6. [195] © SNMMI.

## Author contributions

Declaration of author contributions to the publication related to project I according to CRediT [4]:

Nina Hanke:	Conceptualization, Formal Analysis, Investigation, Visualization, Writing - Original Draft, Writing - Review & Editing
Denise Feick (née Türk):	Formal Analysis, Investigation, Visualization, Writing - Review & Editing
Dominik Selzer:	Formal Analysis, Visualization, Writing - Review & Editing
Naoki Ishiguro:	Conceptualization, Writing - Review & Editing
Thomas Ebner:	Conceptualization, Writing - Review & Editing
Sabrina Wiebe:	Conceptualization, Writing - Review & Editing
Fabian Müller:	Conceptualization, Writing - Review & Editing
Peter Stopfer:	Conceptualization, Writing - Review & Editing
Valerie Nock:	Conceptualization, Writing - Review & Editing
Thorsten Lehr:	Conceptualization, Funding Acquisition, Investigation, Writing - Review & Editing



Clinical Pharmacokinetics (2020) 59:1419–1431  
<https://doi.org/10.1007/s40262-020-00896-w>

ORIGINAL RESEARCH ARTICLE



# A Comprehensive Whole-Body Physiologically Based Pharmacokinetic Drug–Drug–Gene Interaction Model of Metformin and Cimetidine in Healthy Adults and Renally Impaired Individuals

Nina Hanke<sup>1</sup> · Denise Türk<sup>1</sup> · Dominik Selzer<sup>1</sup> · Naoki Ishiguro<sup>2</sup> · Thomas Ebner<sup>3</sup> · Sabrina Wiebe<sup>3,4</sup> · Fabian Müller<sup>3,5</sup> · Peter Stopfer<sup>3</sup> · Valerie Nock<sup>3</sup> · Thorsten Lehr<sup>1</sup>

Published online: 25 May 2020  
 © The Author(s) 2020

## Abstract

**Background** Metformin is a widely prescribed antidiabetic BCS Class III drug (low permeability) that depends on active transport for its absorption and disposition. It is recommended by the US Food and Drug Administration as a clinical substrate of organic cation transporter 2/multidrug and toxin extrusion protein for drug–drug interaction studies. Cimetidine is a potent organic cation transporter 2/multidrug and toxin extrusion protein inhibitor.

**Objective** The objective of this study was to provide mechanistic whole-body physiologically based pharmacokinetic models of metformin and cimetidine, built and evaluated to describe the metformin-*SLC22A2* 808G>T drug–gene interaction, the cimetidine-metformin drug–drug interaction, and the impact of renal impairment on metformin exposure.

**Methods** Physiologically based pharmacokinetic models were developed in PK-Sim<sup>®</sup> (version 8.0). Thirty-nine clinical studies (dosing range 0.001–2550 mg), providing metformin plasma and urine data, positron emission tomography measurements of tissue concentrations, studies in organic cation transporter 2 polymorphic volunteers, drug–drug interaction studies with cimetidine, and data from patients in different stages of chronic kidney disease, were used to develop the metformin model. Twenty-seven clinical studies (dosing range 100–800 mg), reporting cimetidine plasma and urine concentrations, were used for the cimetidine model development.

**Results** The established physiologically based pharmacokinetic models adequately describe the available clinical data, including the investigated drug–gene interaction, drug–drug interaction, and drug–drug–gene interaction studies, as well as the metformin exposure during renal impairment. All modeled drug–drug interaction area under the curve and maximum concentration ratios are within 1.5-fold of the observed ratios. The clinical data of renally impaired patients shows the expected increase in metformin exposure with declining kidney function, but also indicates counter-regulatory mechanisms in severe renal disease; these mechanisms were implemented into the model based on findings in preclinical species.

**Conclusions** Whole-body physiologically based pharmacokinetic models of metformin and cimetidine were built and qualified for the prediction of metformin pharmacokinetics during drug–gene interaction, drug–drug interaction, and different stages of renal disease. The model files will be freely available in the Open Systems Pharmacology model repository. Current guidelines for metformin treatment of renally impaired patients should be reviewed to avoid overdosing in CKD3 and to allow metformin therapy of CKD4 patients.

**Electronic supplementary material** The online version of this article (<https://doi.org/10.1007/s40262-020-00896-w>) contains supplementary material, which is available to authorized users.

✉ Thorsten Lehr  
 thorsten.lehr@mx.uni-saarland.de

Extended author information available on the last page of the article

## 1 Introduction

Metformin is an oral antidiabetic that reduces blood glucose levels. It is the first-line therapy for type 2 diabetes mellitus (T2DM) and the fourth most commonly prescribed outpatient medication in the USA, with almost 80 million prescriptions in 2017 [1].

Metformin is a BCS Class III drug of high solubility and very low permeability, positively charged at physiological pH and depends on active transport to cross biological

### Key Points

A whole-body physiologically based pharmacokinetic model of metformin, the fourth most commonly prescribed drug in the USA, has been carefully developed and evaluated to describe the metformin concentrations in blood, kidney, and urine. In addition, a whole-body physiologically based pharmacokinetic model of cimetidine, a potent multidrug and toxin extrusion protein 1 inhibitor used in drug–drug interaction studies, has been established.

These models have been applied to describe and predict the metformin-*SLC22A2* 808G>T drug–gene interaction, the cimetidine-metformin drug–drug interaction, and a combined drug–drug–gene interaction study, in which different *SLC22A2* genotypes were additionally challenged with cimetidine co-administration.

Furthermore, the pathophysiological changes during renal impairment have been assessed and implemented to describe the increased metformin exposure of patients with different stages of chronic kidney disease. For severe chronic kidney disease, this analysis indicates an induction of organic cation transporter 2 and multidrug and toxin extrusion protein 1, possibly as an adaptation to progressing uremia/hyperuricemia. The final pathophysiological based pharmacokinetic model was applied to generate metformin dosing recommendations for CKD3A–4 patients.

membranes. The metformin rate of absorption is slower than its rate of elimination [2] and the absorption is restricted to the upper intestine [3], leading to incomplete absorption of metformin, an oral bioavailability of 50–60%, and the excretion of approximately 30% of an oral dose, unabsorbed, with the feces [2, 4]. Furthermore, the absorption of metformin is saturable, with higher doses showing decreased dose-normalized plasma concentrations and a decreased fraction excreted to urine [4, 5]. Following its absorption, metformin is not bound to plasma proteins [2, 4, 6], not metabolized [2, 6], and not secreted to bile [2, 4, 7], but excreted unchanged with the urine by passive glomerular filtration and active renal secretion through the sequential action of organic cation transporter 2 (OCT2) and multidrug and toxin extrusion protein 1 (MATE1). Although there are early reports of MATE2-K expression in the human kidney [8, 9], a recent quantitative study found only negligible amounts of MATE2-K compared to MATE1 [10]. Renal clearance is approximately 500 mL/min [11] with a strong correlation between the renal clearances of metformin and

creatinine [4]. Patients with renal impairment show a marked increase in metformin exposure, with three- to ten-fold higher plasma trough concentrations in chronic kidney disease (CKD) stages 3A–5 [12]. As a consequence, metformin is contraindicated in patients with a glomerular filtration rate (GFR) < 30 mL/min (i.e., CKD stages 4 and 5) [13, 14], depriving these patients of metformin as a treatment option.

The impact of genetic polymorphisms on the absorption and disposition of metformin (drug–gene interactions or “DGIs”) has been investigated in a multitude of clinical trials, yielding to some extent contradictory results. The transporters of primary interest in these studies were the plasma membrane monoamine transporter (PMAT), OCT1, OCT2, and MATE1, where variations in OCT2 seem to have the largest impact on the plasma concentrations of metformin [15–19]. The most common polymorphism in the gene encoding for OCT2 is the *SLC22A2* 808G>T single-nucleotide polymorphism [20], which results in an amino acid exchange from alanine to serine (A270S) and presumably increased function, leading to decreased exposure with ~ 13–20% decreased maximum concentration ( $C_{max}$ ) [17, 18, 21].

A third factor that impacts metformin exposure is drug–drug interactions (DDIs). Metformin displays a list of 333 DDIs, with 13 major and 293 moderate interactions [22]. Even though some of these occur on the pharmacodynamic level, pharmacokinetic DDIs are clinically relevant and may call for an adjustment of the co-administration regimen. As metformin is exclusively eliminated by glomerular filtration and secretion through the renal organic cation transport system, co-treatment with a potent inhibitor of this transport pathway, such as cimetidine, decreases the renal clearance of metformin and increases metformin exposure (+50% area under the curve [AUC]) [21, 23]. Metformin is recommended by the US Food and Drug Administration as an OCT2/MATE victim drug for clinical DDI studies [24].

The aim of this study was to build and evaluate a whole-body physiologically based pharmacokinetic (PBPK) model of metformin, applicable (1) to describe the impact of the metformin-*SLC22A2* 808G>T DGI on metformin exposure, (2) to dynamically model the cimetidine-metformin DDI, and (3) to analyze the impact of renal impairment on metformin exposure and generate dose recommendations for different stages of CKD. The newly developed and thoroughly evaluated metformin and cimetidine models will be freely available in the Open Systems Pharmacology PBPK model repository (<https://www.open-systems-pharmacology.org>), and the Electronic Supplementary Material (ESM) to this article is compiled to serve as a comprehensive and transparent documentation and reference.

## 2 Methods

### 2.1 Software

Physiologically based pharmacokinetic models were developed using PK-Sim<sup>®</sup> and MoBi<sup>®</sup> modeling software (Open Systems Pharmacology Suite 8.0, <https://www.open-systems-pharmacology.org>). Published clinical study data were digitized with GetData Graph Digitizer 2.26.0.20 (© S. Fedorov). Model input parameter optimization (Levenberg–Marquardt algorithm, multiple starting values) and sensitivity analysis were performed in PK-Sim<sup>®</sup>. All pharmacokinetic parameters and model performance measures derived from simulated and/or observed data were calculated in R 3.6.1 (The R Foundation for Statistical Computing, Vienna, Austria). Plots were generated in R and RStudio 1.1.423 (RStudio, Inc., Boston, MA, USA).

### 2.2 Physiologically Based Pharmacokinetic Model Building

Physiologically based pharmacokinetic model building was started with an extensive literature search to collect physicochemical parameters, mechanistic information on absorption, distribution, metabolism, and excretion processes, as well as published clinical studies. The general procedure of PBPK model building, including parameter optimization and generation of virtual individuals and virtual populations, is described in the ESM.

### 2.3 Physiologically Based Pharmacokinetic Model Evaluation

Model performance was evaluated with multiple methods. First, predicted population plasma concentration–time profiles were compared with the data observed in the respective clinical studies. As the clinical data from literature is mostly reported as arithmetic means  $\pm$  standard deviation, population prediction arithmetic means and 68% prediction intervals were plotted, which corresponds to the range of  $\pm 1$  standard deviation around the mean, if normal distribution is assumed. In addition, the predicted plasma concentration values of all studies were plotted against their corresponding observed values in goodness-of-fit plots.

Furthermore, model performance was evaluated by comparison of predicted to observed AUC and  $C_{\max}$  values. All AUC values were calculated from the time of drug administration to the time of the last concentration measurement ( $AUC_{\text{last}}$ ).

As quantitative measures of model performance, mean relative deviation (MRD) of all predicted plasma concentrations (Eq. 1) and geometric mean fold error (GMFE) of all

predicted  $AUC_{\text{last}}$  and  $C_{\max}$  values (Eq. 2) were calculated. MRD and GMFE values  $\leq 2$  characterize an adequate model performance.

$$\text{MRD} = 10^x; x = \sqrt{\frac{\sum_{i=1}^k (\log_{10} c_{\text{predicted},i} - \log_{10} c_{\text{observed},i})^2}{k}}, \quad (1)$$

where  $c_{\text{predicted},i}$  is the predicted plasma concentration,  $c_{\text{observed},i}$  is the corresponding observed plasma concentration, and  $k$  is the number of observed values.

$$\text{GMFE} = 10^x; x = \frac{\sum_{i=1}^m \left| \log_{10} \left( \frac{\text{predicted PK parameter}_i}{\text{observed PK parameter}_i} \right) \right|}{m}, \quad (2)$$

where predicted PK parameter<sub>*i*</sub> is the predicted  $AUC_{\text{last}}$  or  $C_{\max}$  value, observed PK parameter<sub>*i*</sub> is the corresponding observed  $AUC_{\text{last}}$  or  $C_{\max}$  value, and  $m$  is the number of studies.

Finally, the physiological plausibility of the parameter estimates and the results of sensitivity analyses were assessed. A detailed description of the sensitivity calculation is given in the ESM.

### 2.4 Modeling the Impact of Polymorphism

The impact of genetic polymorphism on the pharmacokinetics of metformin was implemented by splitting the polymorphic transporter in question into two transporters with half of the initial reference concentration each, corresponding to the two homologous chromosomal alleles in diploid humans. Each “wild-type” allele present in the simulated population (one in heterozygous individuals and two in homozygous individuals) was modeled with the transport rate constant identified during the initial model development. Each “variant” allele was modeled with an adapted transport rate constant that was identified based on clinical studies of metformin in homozygous “variant” individuals.

### 2.5 Drug–Drug Interaction Modeling

For mechanistic DDI modeling, the type of interaction (competitive inhibition, mechanism-based inhibition, induction) and the interaction parameters were extracted from in-vitro literature. These parameters were incorporated into the perpetrator PBPK model, to dynamically describe the impact of the perpetrator on the victim drug. The mathematical implementation is shown in the ESM.

The DDI modeling performance was assessed by comparison of predicted vs observed victim drug plasma concentration–time profiles when administered alone and during co-administration. In addition, predicted DDI  $AUC_{\text{last}}$  ratios (Eq. 3) and DDI  $C_{\max}$  ratios (Eq. 4) were evaluated.

$$\text{DDI AUC}_{\text{last}} \text{ ratio} = \frac{\text{AUC}_{\text{last}} \text{ victim drug during co-administration}}{\text{AUC}_{\text{last}} \text{ victim drug control}} \quad (3)$$

$$\text{DDI } C_{\text{max}} \text{ ratio} = \frac{C_{\text{max}} \text{ victim drug during co-administration}}{C_{\text{max}} \text{ victim drug control}} \quad (4)$$

As a quantitative measure of the prediction accuracy, GMFE values of the predicted DDI  $\text{AUC}_{\text{last}}$  ratios and DDI  $C_{\text{max}}$  ratios were calculated according to Eq. (2).

## 2.6 Modeling of Renal Impairment

To model the impact of renal impairment on the pharmacokinetics of metformin, a literature search was conducted to identify the pathophysiological changes that occur in conjunction with renal impairment, including their extent at the different stages of CKD. In a next step, these differences in anatomy and physiology were implemented to create renally impaired individuals and to describe the published clinical studies of metformin in patients with CKD.

## 3 Results

### 3.1 Metformin Physiologically Based Pharmacokinetic Model Building and Evaluation

A whole-body PBPK model of metformin has been successfully developed. Thirty-nine clinical studies of intravenous or oral administration covering a broad dosing range (0.001–2550 mg), 22 studies thereof with corresponding metformin fraction excreted to urine data, were utilized for PBPK model building and evaluation. In addition, human  $^{11}\text{C}$ -metformin tissue concentration positron emission tomography (PET) measurements in the kidneys, liver, skeletal muscle, and intestines were included. Clinical studies are listed in the ESM.

To describe the pharmacokinetics of metformin, active transport processes by PMAT, OCT1, OCT2, and MATE1 were implemented. These transporters were distributed and localized according to the current state of the literature, with their main sites of action illustrated in Fig. 1. PMAT was chosen to model the saturable absorption of metformin based on its good apparent affinity, high expression in the human small intestine, and localization at the luminal surface of enterocytes [25, 26], though the thiamine transporter 2 is also a likely candidate to contribute to the intestinal absorption of metformin [27, 28]. Renal excretion is modeled as passive glomerular filtration and active secretion through the sequential action of OCT2 and MATE1. Transporter distribution, localization, and transport directions are summarized

in the system-dependent parameter table in the ESM; transport parameters are summarized in the metformin drug-dependent parameter table in the ESM.

The good model performance is demonstrated in Fig. 2, using representative studies. Population predictions of all 39 clinical studies compared to observed data, shown in semi-logarithmic as well as linear plots, goodness-of-fit plots, and MRD values, are presented in the ESM. Predictions of metformin fraction excreted to urine are shown for all studies that provided observed data. For further evaluation of the model performance, predicted compared to observed  $\text{AUC}_{\text{last}}$  and  $C_{\text{max}}$  values,  $\text{AUC}_{\text{last}}$  and  $C_{\text{max}}$  GMFEs (1.20 and 1.24, respectively), and the results of the sensitivity analysis are documented in the ESM.

An important and novel feature of the presented model is the use of human  $^{11}\text{C}$ -metformin tissue concentration PET measurements for model development. As metformin is not metabolized, these PET images are unbiased by labeled metabolites. The unique transporter-controlled distribution of an intravenous  $^{11}\text{C}$ -metformin microdose over time [7] is shown in the upper part of Fig. 3. Noteworthy are the very high concentrations in the kidney, bladder, and liver, and the low permeation into other tissues. Population predictions of the quantified tissue concentrations are presented in the lower part of Fig. 3 and in the ESM. Metformin plasma, whole blood, kidney, and muscle concentrations are accurately described by the model, governed by the implemented transport processes and the low passive permeability of metformin.

### 3.2 Impact of Organic Cation Transporter 2 Polymorphism

The impact of the *SLC22A2* 808G>T single-nucleotide polymorphism on metformin exposure (DGI) was implemented using the same Michaelis–Menten constant for both isoforms [17, 20, 29], but an increased transport rate constant for each minor OCT2 allele (808T) present in the simulated population. The 2.67-fold higher transport rate constant to describe the activity of the variant OCT2 (see metformin drug-dependent parameter table in the ESM) was optimized, based on the metformin plasma profiles of the homozygous 808TT populations studied by Christensen et al. and Wang et al. [18, 21]. The metformin plasma concentrations of all other 808TT and 808GT study populations were predicted and are presented in Fig. 4. Except for one study reporting a higher metformin exposure with the variant OCT2 [29], the DGI  $\text{AUC}_{\text{last}}$  ratios for the hetero- and homozygous groups are well predicted, with 6/7 within two-fold of the observed ratios (see the ESM).

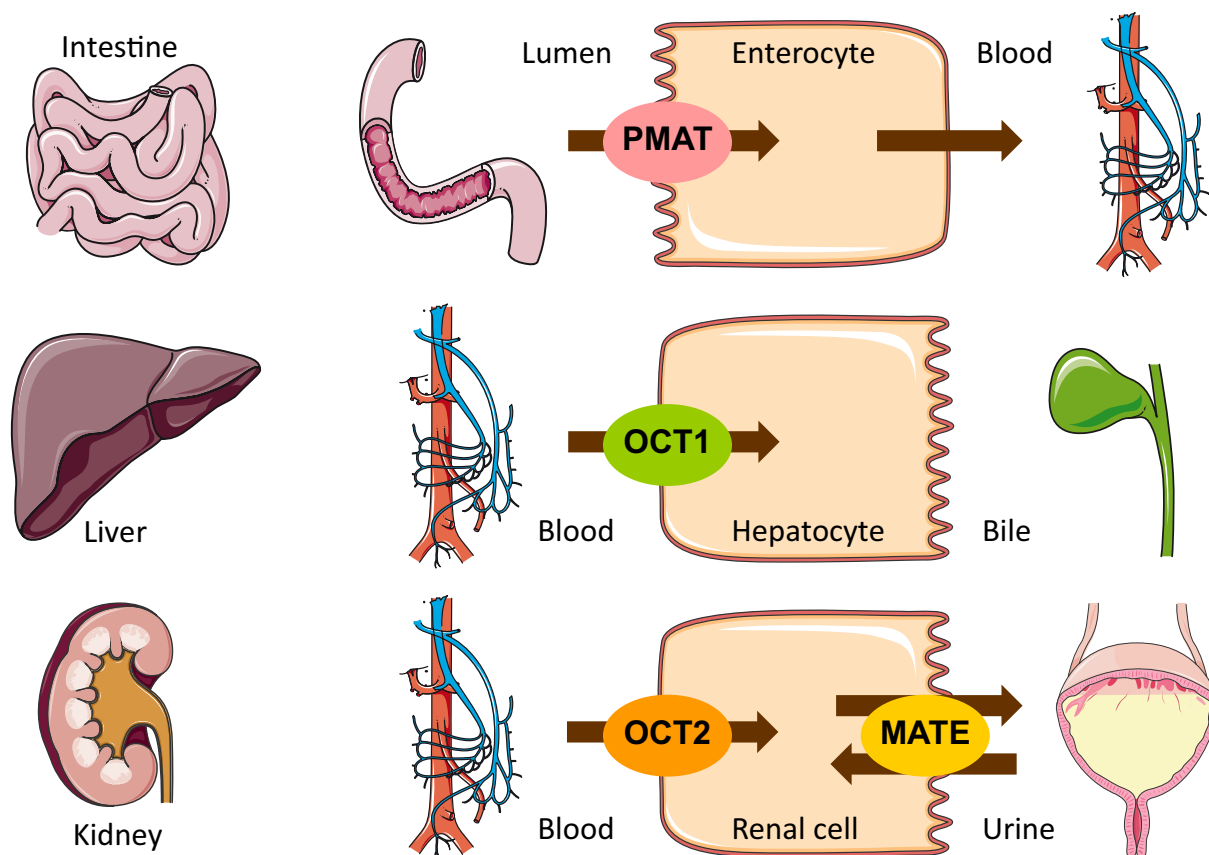


**Fig. 1** Metformin transporters. Main sites of action of the transporters that were implemented to model the absorption, distribution, and excretion of metformin. Several different studies report that they found no secretion of metformin to bile [2, 4, 7]. Drawings by Servier

Medical Art, licensed under CC BY 3.0. *MATE* multidrug and toxin extrusion protein, *OCT* organic cation transporter, *PMAT* plasma membrane monoamine transporter

### 3.3 Drug–Drug Interaction Modeling with Cimetine

In addition to the metformin model, a whole-body PBPK model of the potent *MATE1* inhibitor cimetine was developed. A detailed description of the cimetine model development and evaluation is given in the ESM. The good model performance is demonstrated by population simulations compared to observed data, a goodness-of-fit plot, and MRD values. Furthermore, predicted  $AUC_{last}$  and  $C_{max}$  values are documented, which are in good agreement with the observed data with GMFEs of 1.14 and 1.17, respectively.

The cimetine-metformin DDI was modeled as competitive inhibition of *OCT1*, *OCT2*, and *MATE1* by cimetine, using inhibition parameters from the literature [30]. However, cimetine also is a BCS Class III drug (high solubility and low permeability) that is primarily excreted unchanged in the urine (renal clearance of approximately 400 mL/min [31]), indicating an important role of active transport in its

distribution and excretion. As the only published information on cimetine kidney concentrations is a postmortem tissue-to-serum partition coefficient of 14.9 [32], which is not applicable for parameter optimization, the cimetine interaction parameters were fixed to literature values and one of the cimetine-metformin DDI studies [33] was utilized to inform the intracellular kidney concentration in the cimetine model parameter optimization. Population predictions of all clinical cimetine-metformin DDI studies are presented in Fig. 5a–d. Predicted DDI  $AUC_{last}$  and  $C_{max}$  ratios are close to the observed values, with low GMFEs of 1.22 and 1.20, respectively (see the ESM).

In the *OCT2* polymorphism study by Wang et al. [21], the different *SLC22A2* genotypes were additionally challenged with cimetine co-administration, to show the combined effects of *SLC22A2* 808G>T DGI (decreased metformin plasma concentrations) and cimetine DDI (increased metformin plasma concentrations). The predictions of this drug–drug–gene interaction (DDGI) are presented in Fig. 5e,

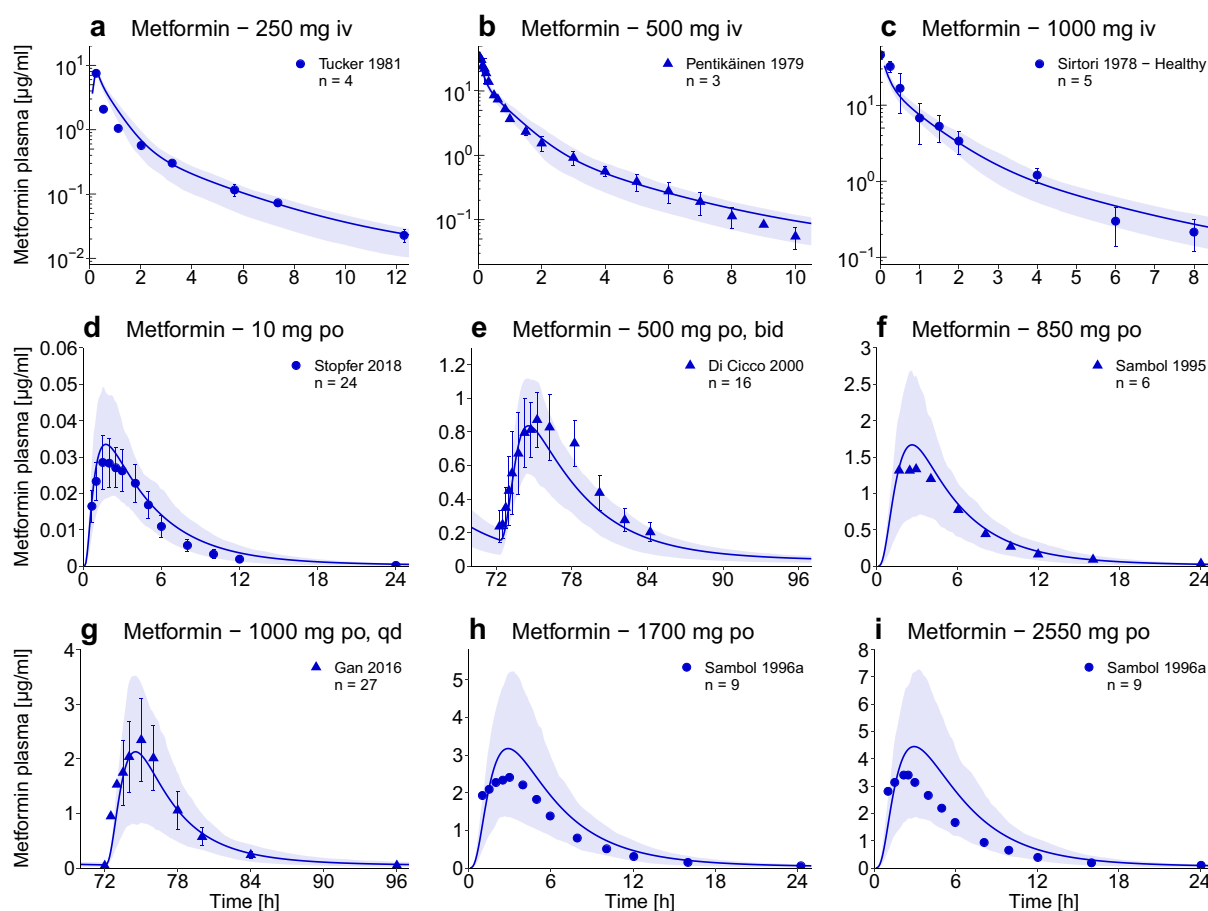


**Fig. 2** Metformin plasma concentrations. Population predictions of metformin plasma concentration–time profiles of representative intravenous (iv) and oral (po) studies, compared to observed data [2, 4–6, 39, 52–54]. Population prediction arithmetic means are shown as lines; the shaded areas illustrate the 68% population prediction inter-

vals. Observed data are shown as dots (training dataset) or triangles (test dataset)  $\pm$  standard deviation. Details on the study protocols, further studies, and quantitative model performance measures are provided in the ESM. *bid* twice daily, *qd* once daily

f. Comparison of the metformin exposure of the three different genotypes during cimetidine treatment (Fig. 5d–f, red triangles) shows that the impact of the polymorphism becomes more pronounced with inhibition of MATE1. Quantitative evaluation of all DDI and DDGI predictions with plots of predicted vs observed  $AUC_{last}$  and  $C_{max}$  ratios are presented in the ESM.

### 3.4 Modeling of Renal Impairment

The impact of renal impairment on metformin pharmacokinetics was modeled by implementation of pathophysiological changes for individuals with a  $GFR < 60$  mL/min (CKD3A–CKD5). First, the actual individual GFR was used as reported. Second, renal secretion through OCT2 and MATE1 was decreased in proportion to the decrease in GFR,

according to the “intact nephron hypothesis” [34–36]. Third, as metformin does not bind to plasma proteins, the levels of albumin and alpha-1-acid glycoprotein were not changed, but the hematocrit was gradually decreased with progressing stages of CKD [37]. As observed in previous PBPK analyses of drug pharmacokinetics during renal impairment [36, 38], these changes were not sufficient to describe the high metformin plasma concentrations in patients with CKD, suggesting the inhibition of further elimination pathways by uremic solutes that accumulate during renal impairment.

To incorporate this hypothesis by inhibition of basolateral OCT1 (liver uptake) and PMAT (skeletal muscle uptake), observed data of intravenously administered metformin in CKD3A–5 patients [6] were used to adjust the transport activities of OCT1 and PMAT for the different stages of CKD, yielding a linear correlation between transporter

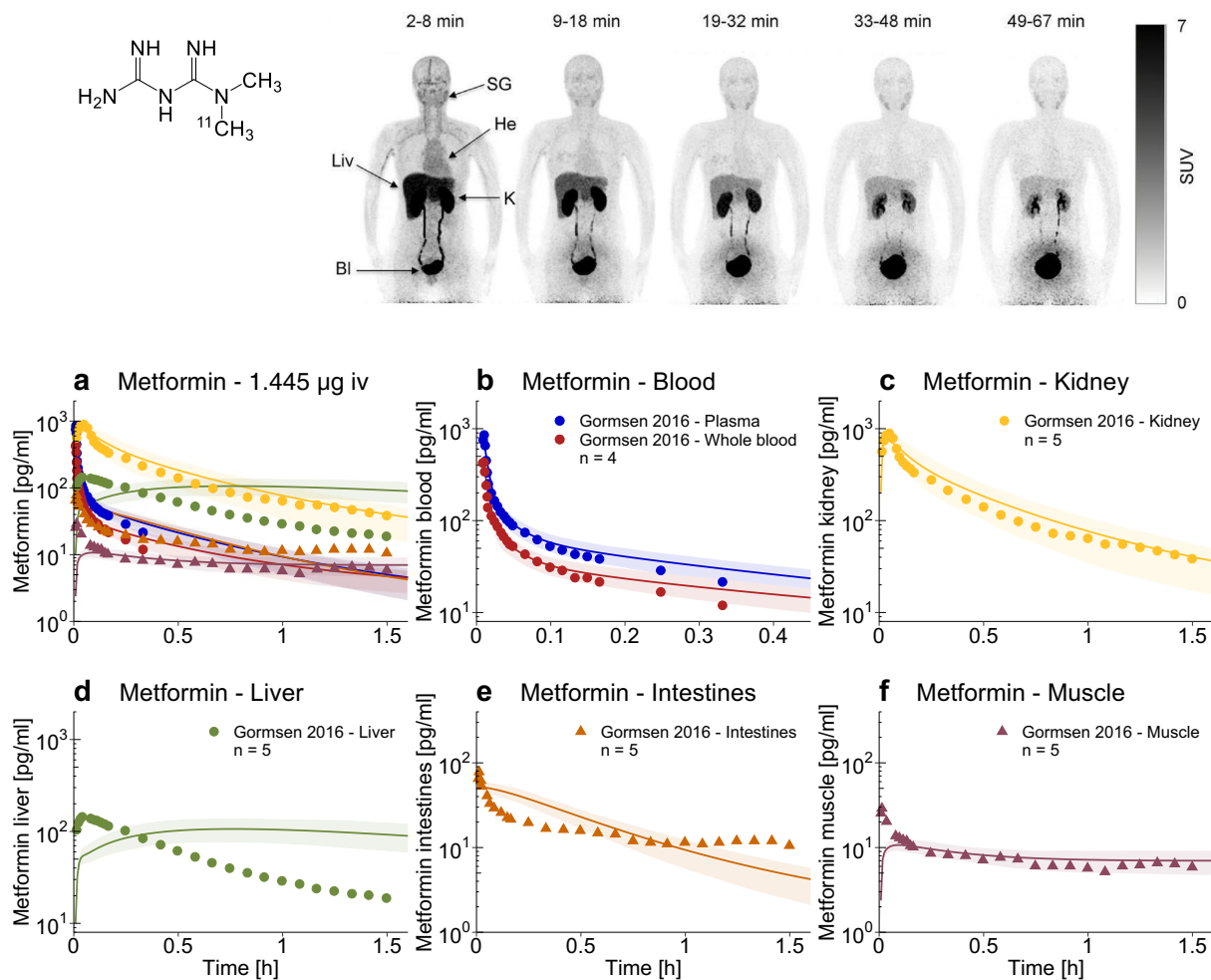


**Fig. 3** Metformin tissue concentrations. Upper panel: pseudodynamic whole-body positron emission tomography imaging of a representative patient following an intravenous microdose of  $^{11}\text{C}$ -metformin [7] © SNMMI. **a-f** Population predictions of metformin blood and tissue concentration–time profiles measured in the  $^{11}\text{C}$ -metformin positron emission tomography study, compared to observed data [7]. Population prediction arithmetic means are shown as lines; the shaded areas

illustrate the 68% population prediction intervals. Observed data are shown as dots (training dataset) or triangles (test dataset). Linear plots are presented in the ESM. *Bl* bladder, *He* heart, *iv* intravenous, *K* kidney, *Liv* liver, *SG* submandibular gland, *SUV* standardized uptake value = concentration [kBq/mL]·body weight [g]/injected dose [kBq]

inhibition and GFR. This correlation was implemented and used to predict orally administered metformin in CKD. Furthermore, to capture the broader shape of the metformin plasma concentration–time profiles in patients with CKD, the permeability at the basolateral side of the small intestinal mucosa cells was decreased. This permeability was already adjusted in the model for healthy individuals, to release the metformin from the enterocytes into the blood. Considering the negligible passive permeability of metformin, there are probably transporters involved at this membrane barrier as well, but because of the current lack of information on the identity of such transporters, the local passive permeability

was adjusted in the model. Decreasing the basolateral small intestinal permeability in CKD might well be a surrogate for the inhibition of these unknown transporters by accumulating uremic solutes, consistent with their inhibition of basolateral transporters of the liver.

Finally, although one would expect a progressive or even exponential increase of metformin plasma concentrations with decreasing kidney function, no apparent difference in the exposure of CKD3B and CKD4 patients could be observed in the available clinical data [12, 39], indicating adaptive processes in severe renal disease. Therefore, induction of OCT2 and MATE1, as observed in hyperuricemic

**Fig. 4** Impact of organic cation transporter 2 (OCT2) polymorphism. Population predictions of metformin plasma concentration–time profiles in different *SLC22A2* genotypes, compared to observed data [17, 18, 21, 29]. Population prediction arithmetic means are shown as dark blue (*SLC22A2* 808GG, reference genotype) or lighter blue (*SLC22A2* 808GT and 808TT, variant genotypes) lines. The shaded areas illustrate the respective 68% population prediction intervals. Observed data are shown as dots  $\pm$  standard deviation. Details on the study protocols, semilogarithmic plots, and quantitative model performance measures are provided in the ESM. *GG* *SLC22A2* 808GG genotype, *GT* *SLC22A2* 808GT genotype, *po* oral, *TT* *SLC22A2* 808TT genotype

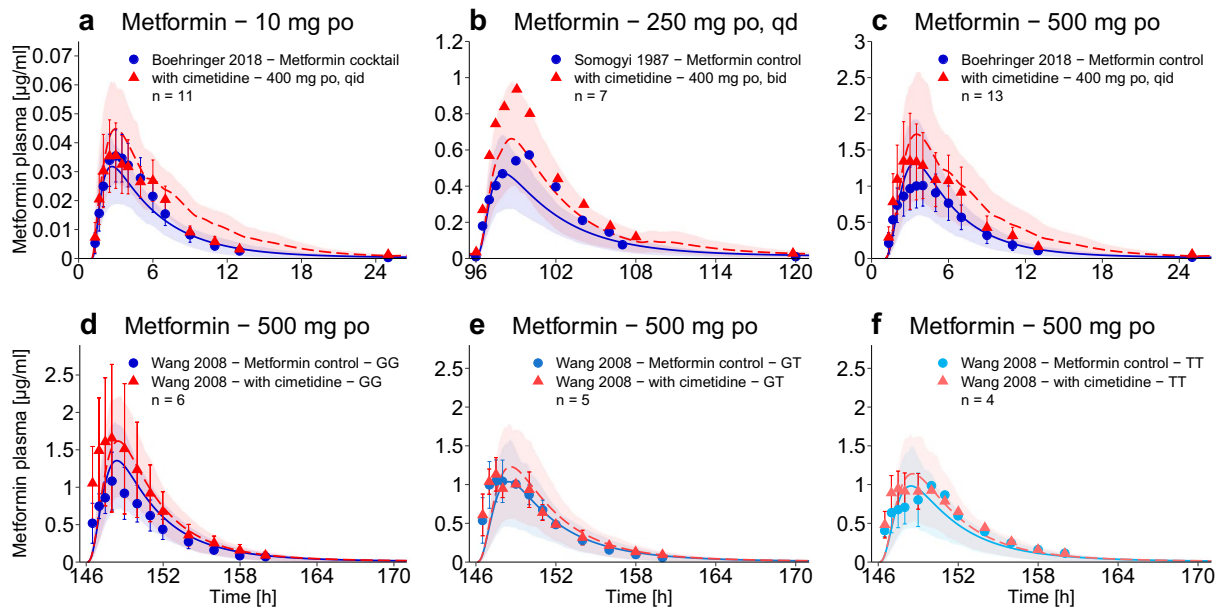
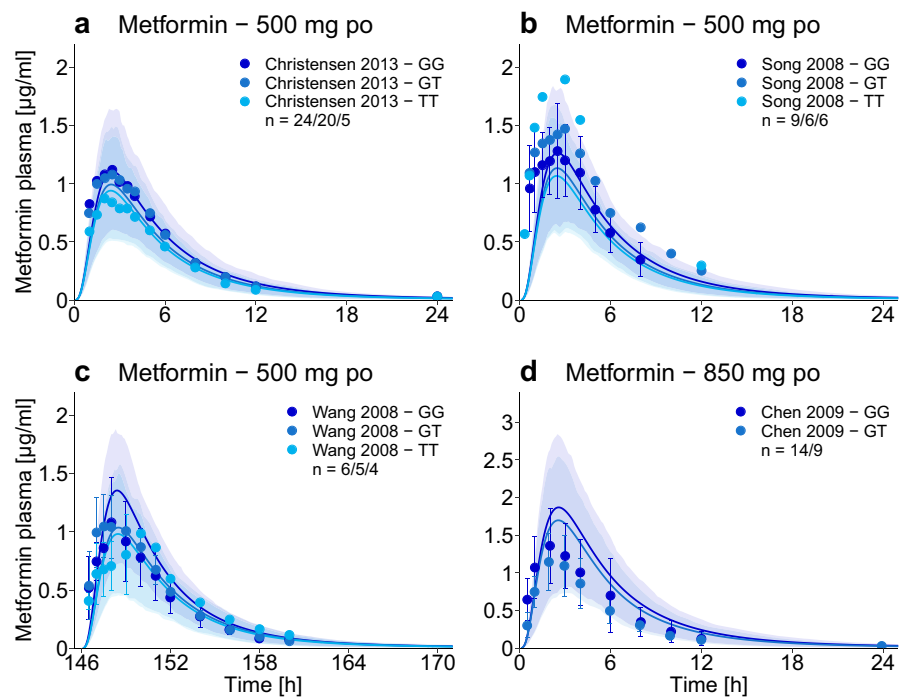


**Fig. 5** Impact of drug–drug interaction (DDI) and drug–drug–gene interaction (DDGI). Population predictions of metformin plasma concentration–time profiles before and during cimetidine co-treatment of different *SLC22A2* genotypes, compared to observed data [21, 23, 33]. Population prediction arithmetic means are shown as solid blue (metformin only) or dashed red (DDI or DDGI) lines; the shaded areas illustrate the respective 68% population prediction inter-

vals. Observed data are shown as dots (metformin only) or triangles (DDI or DDGI)  $\pm$  standard deviation. Details on the study protocols, semilogarithmic plots, and quantitative DDI and DDGI prediction performance measures are provided in the ESM. *bid* twice daily, *GG* *SLC22A2* 808GG genotype, *GT* *SLC22A2* 808GT genotype, *po* oral, *qd* once daily, *qid* four times daily, *TT* *SLC22A2* 808TT genotype



rats [40], was assumed and incorporated for CKD4-5 patients, greatly improving the predictions in severe renal disease (Fig. 6a, b). These changes in system-dependent parameters to model CKD3A-5 are summarized in Fig. 6 (left table). The model performance for all available clinical studies of metformin in renal disease is documented in the ESM.

The developed model of metformin in renal impairment was applied to generate dose recommendations for patients with CKD, that match the steady-state AUC of renally healthy individuals. Simulations of metformin plasma concentrations in CKD3A-5 patients compared to healthy volunteers, all treated with 1000 mg of metformin three times daily, are shown in Fig. 6c. Simulations of metformin in patients with CKD administered with the model-based dose recommendations are shown in Fig. 6d. In the table below, these recommendations are compared to the guidance in the US and German labels. While the US label provides no quantitative advice [13], the German label recommends a reduction to 67% of the dose for CKD3A and to 33% for CKD3B patients [14]. Based on the scarce clinical data of metformin exposure in renally impaired patients, the presented model suggests much lower doses of about 30% for CKD3A and of 20% for CKD3B and 4.

## 4 Discussion

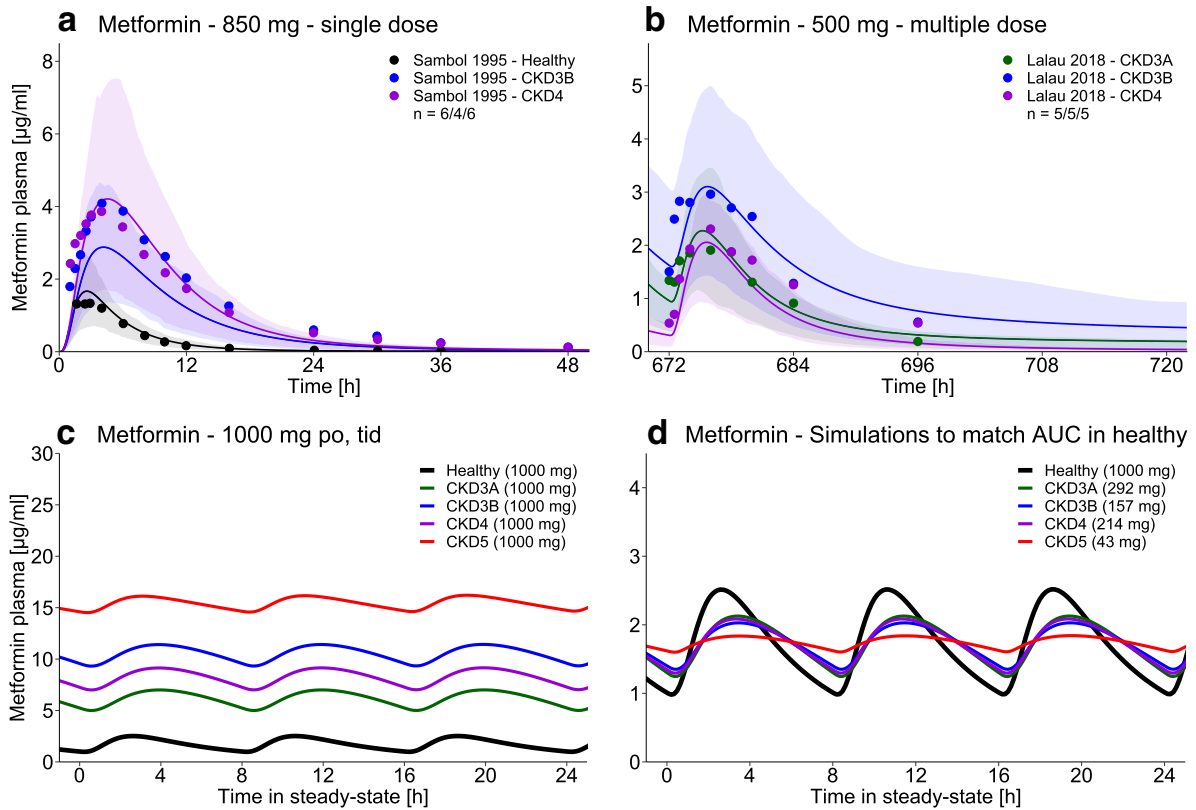
A comprehensive whole-body PBPK model of metformin has been thoroughly built and evaluated, integrating the current knowledge on the mechanisms controlling the pharmacokinetics of this widely prescribed drug. The established model has been evaluated for prediction of the effects of the *SLC22A2* 808G>T polymorphism, the cimetidine-metformin DDI, and the impact of renal impairment, a frequent co-morbidity in patients with T2DM.

Several other PBPK models of metformin have been published previously [41–44], but our newly developed model is the first to integrate PET-measured human in-vivo metformin kidney concentrations, clinical data of microdose studies, and a mechanistic description of the saturable transporter-dependent absorption of metformin. The limitations of the presented model result from our lack of knowledge regarding the metformin pharmacokinetic processes in the liver and the expression levels of the different transporters throughout the body. As shown in Fig. 3d, the liver concentration–time profile following the intravenous <sup>11</sup>C-metformin microdose is not adequately described. The uptake of metformin into the liver is modeled via OCT1, but, in accordance with the literature, no process for metformin metabolism or secretion to bile has been implemented. An unspecific hepatic metabolic clearance was tested, but did not improve the model (causing underestimation of the plasma concentrations in studies with

therapeutic doses), supporting the idea that metformin is not metabolized. The plasma concentrations following the oral <sup>11</sup>C-metformin microdose, and consequently also the measured tissue concentrations, are underpredicted for the 2 h of the oral PET study (see the ESM). However, the administered microdoses (1.445 µg intravenously and 0.856 µg orally) were more than 300,000 and 500,000 times below the lowest therapeutic dose of 500 mg. Given that the metformin pharmacokinetics are completely governed by saturable transport processes and that the plasma, whole blood, kidney, and muscle concentrations following the intravenous microdose are well described, this underprediction might be caused by a missing process for metformin absorption.

The effect of the *SLC22A2* 808G>T polymorphism is difficult to assess from the literature. In-vitro studies report a decreased metformin transport rate [29], equal activity [20], as well as increased transport velocity [17] for the variant OCT2 protein. In-vivo, two studies report decreased clearance by renal secretion in Korean and Chinese 808TT individuals [21, 29], whereof the Chinese study nevertheless shows a non-significantly lower metformin plasma  $C_{max}$  for the 808TT group. However, two different studies report increased clearance by renal secretion in American and European individuals [17, 18], with corresponding decreases in metformin exposure in association with the minor allele. Given that OCT2 and MATE1 are working sequentially to transport metformin through the kidney, it is difficult to distinguish their impacts on renal secretion. Therefore, statements regarding the effect of polymorphisms or co-medications on OCT2 function should not be based on plasma concentrations or renal secretion alone, without concomitant assessment of MATE1 genotype/activity or kidney concentrations. This also holds true for the DDGI results by Wang et al. [21] (Fig. 5f), where the observed lack of cimetidine-metformin DDI in *SLC22A2* 808TT individuals is difficult to explain, because (1) this DDI is mainly caused by inhibition of MATE1, (2) the MATE1 genotypes were not analyzed in this study, and (3) so far there are no in-vitro results available on the impact of cimetidine on MATE1 variants. Another explanation for the weak effect of cimetidine in the *SLC22A2* 808TT group might be reduced transport of cimetidine by this OCT2 variant into the kidney and therefore less inhibition of MATE1, as previously proposed [30].

To model the renal impairment, renal secretion was decreased in proportion to the impaired GFR, based on the “intact nephron hypothesis”, which postulates that structurally damaged nephrons stop contributing to both passive renal filtration and active secretion, and that the remaining intact nephrons continue to function in glomerulo-tubular balance with appropriate adaptation to the patient’s needs [35]. This hypothesis has been successfully applied in previous PBPK analyses of renal impairment [36, 42, 45, 46]. The inhibition of liver drug uptake by uremic toxins in renal



CKD stage	GFR [ml/min]	Individual GFR [ml/min]	Factor <sup>a</sup> OCT2 and MATE1 <sup>34-36</sup>	Factor <sup>b</sup> HKT <sup>37</sup> muscle and OCT1	Factor <sup>c</sup> PMAT basolateral intest. perm.	Induction OCT2 <sup>40</sup> [fold]	Induction MATE1 <sup>40</sup> [fold]	Model-based dose [Dose %] <sup>d</sup>	German Label [Dose %]	US Label [Dose %]
Healthy	≥ 90	116.6	1.00	1.00	1.000	1.00	-	100.0	100.0	100.0
3A	45-59	52.5	0.45	0.90	0.019	0.50	-	29.2	66.7	?
3B	30-44	37.5	0.32	0.90	0.026	0.50	-	15.7	33.3	?
4	15-29	22.5	0.19	0.82	0.045	0.50	1.33	2.99	contraind.	contraind.
5	< 15	7.5	0.06	0.63	0.144	0.50	1.33	2.99	contraind.	contraind.

<sup>a</sup> Factor = actual GFR / age-based healthy GFR, <sup>b</sup> Factor = 1 / (1.027 \* GFR - 0.758), <sup>c</sup> Hypothesis <sup>d</sup> of a 3-times daily 1000 mg regimen

**Fig. 6** Impact of renal impairment and model-based chronic kidney disease (CKD) dose recommendations. **a, b** Population predictions of metformin plasma concentration–time profiles in different stages of CKD, compared to observed data [12, 39]. Population prediction arithmetic means are shown as black (healthy) or colored (CKD3A-4) lines. The shaded areas illustrate the respective 68% population prediction intervals. Observed data are shown as dots in corresponding colors. **c** Simulations of metformin exposure in CKD3A-5 patients compared to healthy individuals using an oral (po) dose of 1000 mg,

three times daily (tid). **d** Simulations of metformin exposure in CKD3A-5 patients to match the steady-state area under the curve (AUC) of 1000 mg po, tid in healthy individuals. The tables show the implementation of renal impairment (on the left) and the model-based dose recommendations compared to the guidance in the US and German labels (on the right). *contraind.* contraindicated, *GFR* glomerular filtration rate, *HKT* hematocrit, *intest. perm.* intestinal permeability, *MATE* multidrug and toxin extrusion protein, *OCT* organic cation transporter, *PMAT* plasma membrane monoamine transporter

impairment has been postulated by Zhao et al. [38], based on the fact that the clearance of many nonrenally eliminated drugs is decreased in CKD, and based on their PBPK analysis of repaglinide in CKD4.

We used an empirical approach to model the inhibition of liver and muscle uptake as a function of the degree of

renal impairment. The inhibition of the basolateral intestinal permeability/transport in CKD is purely hypothetical, but was essential to describe the shape and elimination phase of the clinically observed data. The induction of OCT2 and MATE1 was demonstrated in hyperuricemic rats [40]. To confirm and refine these hypotheses, in-vitro studies of

OCT1 and PMAT inhibition by uremic solutes are needed, to identify the toxins involved and to assess their inhibitory potential; the expression and role of transporters at the basolateral membrane of the intestinal mucosa has to be investigated; and the clinical relevance of OCT2 and MATE1 induction by uric acid in humans needs to be established.

Future applications include the modeling of further DGIs and DDIs, and ultimately, the individualized dose recommendation for real patients with multiple polymorphisms, co-medications, and co-morbidities. Although the effects of some of these interactions do not reach statistical significance in the blood, their impact on kidney or liver concentrations might well be substantial and of therapeutic relevance. The model application with the most immediate medical benefit is the generation of dose recommendations for renally impaired patients with T2DM. Chronic kidney disease is a frequent co-morbidity, but physicians are reluctant to prescribe metformin to patients with reduced renal function because of the contraindication given in most guidelines and fear of lactic acidosis caused by metformin accumulation [47]. These contraindications are based solely on the estimated GFR of the patient, even though for patients with stable renal disease, a dose adjustment based on renal function, with monitoring of the metformin plasma concentrations, would be perfectly feasible. A reduced dose of 500 mg metformin daily was reported to be safe for creatinine clearances as low as 20 mL/min [48] and in a group of CKD4 patients [12], which is in line with the presented model-based recommendation of 200 mg three times daily for CKD4 patients with T2DM.

## 5 Conclusions

Mechanistic whole-body PBPK models of metformin and cimetidine have been carefully developed and evaluated to integrate the current pharmacokinetic knowledge on these drugs and to describe the impact of the *SLC22A2* 808G>T polymorphism, the cimetidine-metformin DDI, and the pathophysiological changes during renal impairment on the exposure of metformin. Both models will be released open-source (<https://www.open-systems-pharmacology.org>) [49], to support metformin therapy, OCT2/MATE DDI studies during drug development, and to be used as input for pharmacodynamic glucose-homeostasis models [50, 51] and other PBPK/pharmacodynamic analyses. The presented analysis has generated insights into the pharmacokinetics during renal impairment, indicating that the kidneys of patients with severe renal disease might be able to adapt to uremia/hyperuricemia by induction of OCT2 and MATE1, as has been shown for hyperuricemic rats [40].

**Acknowledgements** Open Access funding provided by Projekt DEAL.

## Compliance with Ethical Standards

**Funding** This project has received funding from Boehringer Ingelheim Pharma GmbH & Co. KG and from the German Federal Ministry of Education and Research “NanoCare4.0 – Anwendungssichere Materialinnovationen” Program (BMBF Grant 03XP0196).

**Conflict of Interest** Naoki Ishiguro, Thomas Ebner, Sabrina Wiebe, Fabian Müller, Peter Stopfer, and Valerie Nock are employees of Boehringer Ingelheim Pharma GmbH & Co. KG. Thorsten Lehr has received research grants from Boehringer Ingelheim Pharma GmbH & Co. KG and from the German Federal Ministry of Education and Research. Nina Hanke, Denise Türk, and Dominik Selzer have no conflicts of interest that are directly relevant to the content of this article.

**Ethics Approval** All procedures performed in studies involving human participants were in accordance with the ethical standards of the institutional and/or national research committee and with the 1964 Helsinki Declaration and its later amendments or comparable ethical standards.

**Consent to Participate** Informed consent was obtained from all individual participants included in the studies.

**Open Access** This article is licensed under a Creative Commons Attribution-NonCommercial 4.0 International License, which permits any non-commercial use, sharing, adaptation, distribution and reproduction in any medium or format, as long as you give appropriate credit to the original author(s) and the source, provide a link to the Creative Commons licence, and indicate if changes were made. The images or other third party material in this article are included in the article's Creative Commons licence, unless indicated otherwise in a credit line to the material. If material is not included in the article's Creative Commons licence and your intended use is not permitted by statutory regulation or exceeds the permitted use, you will need to obtain permission directly from the copyright holder. To view a copy of this licence, visit <http://creativecommons.org/licenses/by-nc/4.0/>.


## References

1. ClinCalc LLC. ClinCalc DrugStats database. 2019. Available from: <https://clincalc.com/DrugStats/>. Accessed 20 Nov 2019.
2. Pentikäinen PJ, Neuvonen PJ, Penttilä A. Pharmacokinetics of metformin after intravenous and oral administration to man. *Eur J Clin Pharmacol*. 1979;16:195–202. <https://doi.org/10.1007/bf00562061>.
3. Vidon N, Chaussade S, Noel M, Franchisseur C, Huchet B, Bernier JJ. Metformin in the digestive tract. *Diabetes Res Clin Pract*. 1988;4:223–9. [https://doi.org/10.1016/s0168-8227\(88\)80022-6](https://doi.org/10.1016/s0168-8227(88)80022-6).
4. Tucker GT, Casey C, Phillips PJ, Connor H, Ward JD, Woods HF. Metformin kinetics in healthy subjects and in patients with diabetes mellitus. *Br J Clin Pharmacol*. 1981;12:235–46. <https://doi.org/10.1111/j.1365-2125.1981.tb01206.x>.
5. Sambol NC, Chiang J, O’Conner M, Liu CY, Lin ET, Goodman AM, et al. Pharmacokinetics and pharmacodynamics of metformin in healthy subjects and patients with noninsulin-dependent diabetes mellitus. *J Clin Pharmacol*. 1996;36:1012–21. <https://doi.org/10.1177/009127009603601105>.
6. Sirtori CR, Franceschini G, Galli-Kienle M, Cighetti G, Galli G, Bondioli A, et al. Disposition of metformin (*N,N*-dimethylbiguanide) in man. *Clin Pharmacol Ther*. 1978;24:683–93. <https://doi.org/10.1002/cpt.1978246683>.

7. Gormsen LC, Sundelin EI, Jensen JB, Vendelbo MH, Jakobsen S, Munk OL, et al. In vivo imaging of human 11C-metformin in peripheral organs: dosimetry, biodistribution, and kinetic analyses. *J Nucl Med*. 2016;57:1920–6. <https://doi.org/10.2967/jnume.d.116.177774>.
8. Otsuka M, Matsumoto T, Morimoto R, Arioka S, Omote H, Moriyama Y. A human transporter protein that mediates the final excretion step for toxic organic cations. *Proc Natl Acad Sci USA*. 2005;102:17923–8. <https://doi.org/10.1073/pnas.0506483102>.
9. Masuda S, Terada T, Yonezawa A, Tanihara Y, Kishimoto K, Katsura T, et al. Identification and functional characterization of a new human kidney-specific H<sup>+</sup>/organic cation antiporter, kidney-specific multidrug and toxin extrusion 2. *J Am Soc Nephrol*. 2006;17:2127–35. <https://doi.org/10.1681/ASN.2006030205>.
10. Prasad B, Johnson K, Billington S, Lee C, Chung GW, Brown CDA, et al. Abundance of drug transporters in the human kidney cortex as quantified by quantitative targeted proteomics. *Drug Metab Dispos*. 2016;44:1920–4. <https://doi.org/10.1124/dmd.116.072066>.
11. Graham GG, Punt J, Arora M, Day RO, Doogue MP, Duong JK, et al. Clinical pharmacokinetics of metformin. *Clin Pharmacokinet*. 2011;50:81–988. <https://doi.org/10.2165/11534750-000000000-00000>.
12. Lalau J-D, Kajbaf F, Bennis Y, Hurtel-Lemaire A-S, Belpaire F, De Broe ME. Metformin treatment in patients with type 2 diabetes and chronic kidney disease stages 3A, 3B, or 4. *Diabetes Care*. 2018;41:547–53. <https://doi.org/10.2337/dc17-2231>.
13. Bristol-Myers Squibb Company. Prescribing information: Glucophage<sup>®</sup> (metformin hydrochloride) tablets. 2017. [https://www.accessdata.fda.gov/drugsatfda\\_docs/label/2017/020357s037s039,021202s021s0231bl.pdf](https://www.accessdata.fda.gov/drugsatfda_docs/label/2017/020357s037s039,021202s021s0231bl.pdf). Accessed 20 Nov 2019.
14. Heumann Pharma GmbH & Co. Generica KG. Prescribing information: metformin Heumann. 2017. Available from: [https://www.heumann.de/fileadmin/user\\_upload/produkte/infos/Fachinformation-Metformin-Heumann.pdf](https://www.heumann.de/fileadmin/user_upload/produkte/infos/Fachinformation-Metformin-Heumann.pdf). Accessed 20 Nov 2019.
15. Christensen MMH, Brasch-Andersen C, Green H, Nielsen F, Damkier P, Beck-Nielsen H, et al. The pharmacogenetics of metformin and its impact on plasma metformin steady-state levels and glycosylated hemoglobin A1c. *Pharmacogenet Genomics*. 2011;21:837–50. <https://doi.org/10.1097/FPC.0b013e32834c0010>.
16. Duong JK, Kumar SS, Kirkpatrick CM, Greenup LC, Arora M, Lee TC, et al. Population pharmacokinetics of metformin in healthy subjects and patients with type 2 diabetes mellitus: simulation of doses according to renal function. *Clin Pharmacokinet*. 2013;52:373–84. <https://doi.org/10.1007/s40262-013-0046-9>.
17. Chen Y, Li S, Brown C, Cheatham S, Castro RA, Leabman MK, et al. Effect of genetic variation in the organic cation transporter 2 on the renal elimination of metformin. *Pharmacogenet Genomics*. 2009;19:497–504. <https://doi.org/10.1097/FPC.0b013e32832cc7e9>.
18. Christensen MMH, Pedersen RS, Stage TB, Brasch-Andersen C, Nielsen F, Damkier P, et al. A gene-gene interaction between polymorphisms in the OCT2 and MATE1 genes influences the renal clearance of metformin. *Pharmacogenet Genomics*. 2013;23:526–34. <https://doi.org/10.1097/FPC.0b013e328364a57d>.
19. Stocker SL, Morrissey KM, Yee SW, Castro RA, Xu L, Dahlin A, et al. The effect of novel promoter variants in MATE1 and MATE2 on the pharmacokinetics and pharmacodynamics of metformin. *Clin Pharmacol Ther*. 2013;93:186–94. <https://doi.org/10.1038/clpt.2012.210>.
20. Zolk O, Solbach TF, König J, Fromm MF. Functional characterization of the human organic cation transporter 2 variant p270Ala%3eSer. *Drug Metab Dispos*. 2009;37:1312–8. <https://doi.org/10.1124/dmd.108.023762>.
21. Wang Z-J, Yin OQP, Tomlinson B, Chow MSS. OCT2 polymorphisms and in-vivo renal functional consequence: studies with metformin and cimetidine. *Pharmacogenet Genomics*. 2008;18:637–45. <https://doi.org/10.1097/FPC.0b013e328302cd41>.
22. Drugs.com. Drug interactions checker. 2019. Available from: <https://www.drugs.com/drug-interactions/metformin.html>. Accessed 20 Nov 2019.
23. Somogyi A, Stockley C, Keal J, Rolan P, Bochner F. Reduction of metformin renal tubular secretion by cimetidine in man. *Br J Clin Pharmacol*. 1987;23:545–51. <https://doi.org/10.1111/j.1365-2125.1987.tb03090.x>.
24. US Food and Drug Administration. Drug development and drug interactions: table of substrates, inhibitors and inducers. 2019. Available from: <https://www.fda.gov/drugs/drug-interactions-labeling/drug-development-and-drug-interactions-table-substrates-inhibitors-and-inducers>. Accessed 15 Nov 2019.
25. Zhou M, Xia L, Wang J. Metformin transport by a newly cloned proton-stimulated organic cation transporter (plasma membrane monoamine transporter) expressed in human intestine. *Drug Metab Dispos*. 2007;35:1956–62. <https://doi.org/10.1124/dmd.107.015495>.
26. Han TK, Proctor WR, Costales CL, Cai H, Everett RS, Thacker DR. Four cation-selective transporters contribute to apical uptake and accumulation of metformin in Caco-2 cell monolayers. *J Pharmacol Exp Ther*. 2015;352:519–28. <https://doi.org/10.1124/jpet.114.220350>.
27. Liang X, Chien H-C, Yee SW, Giacomini MM, Chen EC, Piao M, et al. Metformin is a substrate and inhibitor of the human thiamine transporter, THTR-2 (SLC19A3). *Mol Pharm*. 2015;12:4301–10. <https://doi.org/10.1021/acs.molpharmaceut.5b00501>.
28. Liang X, Giacomini KM. Transporters involved in metformin pharmacokinetics and treatment response. *J Pharm Sci*. 2017;106:2245–50. <https://doi.org/10.1016/j.xphs.2017.04.078>.
29. Song IS, Shin HJ, Shim EJ, Jung IS, Kim WY, Shon JH, et al. Genetic variants of the organic cation transporter 2 influence the disposition of metformin. *Clin Pharmacol Ther*. 2008;84:559–62. <https://doi.org/10.1038/clpt.2008.61>.
30. Ito S, Kusahara H, Yokochi M, Toyoshima J, Inoue K, Yuasa H, et al. Competitive inhibition of the luminal efflux by multidrug and toxin extrusions, but not basolateral uptake by organic cation transporter 2, is the likely mechanism underlying the pharmacokinetic drug-drug interactions caused by cimetidine in the kidney. *J Pharmacol Exp Ther*. 2012;340:393–403. <https://doi.org/10.1124/jpet.111.184986>.
31. Somogyi A, Gugler R. Clinical pharmacokinetics of cimetidine. *Clin Pharmacokinet*. 1983;8:463–95. <https://doi.org/10.2165/00003088-198308060-00001>.
32. Schentag JJ, Cerra FB, Calleri GM, Leising ME, French MA, Bernhard H. Age, disease, and cimetidine disposition in healthy subjects and chronically ill patients. *Clin Pharmacol Ther*. 1981;29:737–43. <https://doi.org/10.1038/clpt.1981.104>.
33. Boehringer Ingelheim Pharma GmbH & Co. KG. The effect of potent inhibitors of drug transporters (verapamil, rifampin, cimetidine, probenecid) on pharmacokinetics of a transporter probe drug cocktail consisting of digoxin, furosemide, metformin and rosuvastatin. EudraCT 2017-001549-29. 2018. Available from: <https://clinicaltrials.gov/ct2/show/record/NCT03307252>. Accessed 20 Nov 2019.
34. Bricker NS, Morrin PAF, Kime SW. The pathologic physiology of chronic Bright's disease: an exposition of the "intact nephron hypothesis". *Am J Med*. 1960;28:77–97. [https://doi.org/10.1016/0002-9343\(60\)90225-4](https://doi.org/10.1016/0002-9343(60)90225-4).
35. Bricker NS. On the meaning of the intact nephron hypothesis. *Am J Med*. 1969;46:1–11. [https://doi.org/10.1016/0002-9343\(69\)90053-9](https://doi.org/10.1016/0002-9343(69)90053-9).

36. Hsueh C-H, Hsu V, Zhao P, Zhang L, Giacomini KM, Huang S-M. PBPK Modeling of the effect of reduced kidney function on the pharmacokinetics of drugs excreted renally by organic anion transporters. *Clin Pharmacol Ther.* 2018;103:485–92. <https://doi.org/10.1002/cpt.750>.
37. Schmulenson E, Schlender J-F, Frechen S, Jaehde U. A physiologically-based pharmacokinetic modeling approach to assess the impact of chronic kidney disease. Annual Meeting of Population Approach Group Europe (PAGE); 2018; Montreux, Switzerland: abstract 8630. Available from: <https://www.page-meeting.org/?abstract=8630>. Accessed 30 Apr 2020.
38. Zhao P, Vieira MLT, Grillo JA, Song P, Wu T-C, Zheng JH, et al. Evaluation of exposure change of nonrenally eliminated drugs in patients with chronic kidney disease using physiologically based pharmacokinetic modeling and simulation. *J Clin Pharmacol.* 2012;52:91–108. <https://doi.org/10.1177/0091270011415528>.
39. Sambol NC, Chiang J, Lin ET, Goodman AM, Liu CY, Benet LZ, et al. Kidney function and age are both predictors of pharmacokinetics of metformin. *J Clin Pharmacol.* 1995;35:1094–102. <https://doi.org/10.1002/j.1552-4604.1995.tb04033.x>.
40. Zhang G, Ma Y, Xi D, Rao Z, Sun X, Wu X. Effect of high uric acid on the disposition of metformin: in vivo and in vitro studies. *Biopharm Drug Dispos.* 2019;40:3–11. <https://doi.org/10.1002/bdd.2164>.
41. Xia B, Heimbach T, Gollen R, Nanavati C, He H. A simplified PBPK modeling approach for prediction of pharmacokinetics of four primarily renally excreted and CYP3A metabolized compounds during pregnancy. *AAPS J.* 2013;15:1012–24. <https://doi.org/10.1208/s12248-013-9505-3>.
42. Li J, Guo H-F, Liu C, Zhong Z, Liu L, Liu X-D. Prediction of drug disposition in diabetic patients by means of a physiologically based pharmacokinetic model. *Clin Pharmacokinet.* 2015;54:179–93. <https://doi.org/10.1007/s40262-014-0192-8>.
43. Burt HJ, Neuhoff S, Almond L, Gaohua L, Harwood MD, Jamei M, et al. Metformin and cimetidine: physiologically based pharmacokinetic modelling to investigate transporter mediated drug-drug interactions. *Eur J Pharm Sci.* 2016;88:70–82. <https://doi.org/10.1016/j.ejps.2016.03.020>.
44. Nishiyama K, Toshimoto K, Lee W, Ishiguro N, Bister B, Sugiyama Y. Physiologically-based pharmacokinetic modeling analysis for quantitative prediction of renal transporter-mediated interactions between metformin and cimetidine. *CPT Pharmacometr Syst Pharmacol.* 2019;8:396–406. <https://doi.org/10.1002/psp4.12398>.
45. Li G, Wang K, Chen R, Zhao H, Yang J, Zheng Q. Simulation of the pharmacokinetics of bisoprolol in healthy adults and patients with impaired renal function using whole-body physiologically based pharmacokinetic modeling. *Acta Pharmacol Sin.* 2012;33:1359–71. <https://doi.org/10.1038/aps.2012.103>.
46. Posada MM, Bacon JA, Schneck KB, Tirona RG, Kim RB, Higgins JW, et al. Prediction of renal transporter mediated drug-drug interactions for pemetrexed using physiologically based pharmacokinetic modeling. *Drug Metab Dispos.* 2015;43:325–34. <https://doi.org/10.1124/dmd.114.059618>.
47. Kajbaf F, Arnouts P, de Broe M, Lalau J-D. Metformin therapy and kidney disease: a review of guidelines and proposals for metformin withdrawal around the world. *Pharmacoepidemiol Drug Saf.* 2013;22:1027–35. <https://doi.org/10.1002/pds.3501>.
48. Duong JK, Roberts DM, Furlong TJ, Kumar SS, Greenfield JR, Kirkpatrick CM, et al. Metformin therapy in patients with chronic kidney disease. *Diabetes Obes Metab.* 2012;14:963–5. <https://doi.org/10.1111/j.1463-1326.2012.01617.x>.
49. Lippert J, Burghaus R, Edginton A, Frechen S, Karlsson M, Kovar A, et al. Open systems pharmacology community: an open access, open source, open science approach to modeling and simulation in pharmaceutical sciences. *CPT Pharmacometrics Syst Pharmacol.* 2019;8:878–82. <https://doi.org/10.1002/psp4.12473>.
50. Schaller S, Willmann S, Lippert J, Schaupp L, Pieber TR, Schuppert A, et al. A generic integrated physiologically based whole-body model of the glucose-insulin-glucagon regulatory system. *CPT Pharmacometrics Syst Pharmacol.* 2013;2:e65. <https://doi.org/10.1038/psp.2013.40>.
51. Balazki P, Schaller S, Eissing T, Lehr T. A quantitative systems pharmacology kidney model of diabetes associated renal hyperfiltration and the effects of SGLT inhibitors. *CPT Pharmacometrics Syst Pharmacol.* 2018;7:788–97. <https://doi.org/10.1002/psp4.12359>.
52. Stopfer P, Giessmann T, Hohl K, Hutzl S, Schmidt S, Gansser D, et al. Optimization of a drug transporter probe cocktail: potential screening tool for transporter-mediated drug-drug interactions. *Br J Clin Pharmacol.* 2018;84:1941–9. <https://doi.org/10.1111/bcp.13609>.
53. Di Cicco RA, Allen A, Carr A, Fowles S, Jorkasky DK, Freed MI. Rosiglitazone does not alter the pharmacokinetics of metformin. *J Clin Pharmacol.* 2000;40:1280–5.
54. Gan L, Jiang X, Mendonza A, Swan T, Reynolds C, Nguyen J, et al. Pharmacokinetic drug-drug interaction assessment of LCZ696 (an angiotensin receptor neprilysin inhibitor) with omeprazole, metformin or levonorgestrel-ethinyl estradiol in healthy subjects. *Clin Pharmacol Drug Dev.* 2016;5:27–39. <https://doi.org/10.1002/cpdd.181>.

## Affiliations

Nina Hanke<sup>1</sup> · Denise Türk<sup>1</sup> · Dominik Selzer<sup>1</sup> · Naoki Ishiguro<sup>2</sup> · Thomas Ebner<sup>3</sup> · Sabrina Wiebe<sup>3,4</sup> · Fabian Müller<sup>3,5</sup> · Peter Stopfer<sup>3</sup> · Valerie Nock<sup>3</sup> · Thorsten Lehr<sup>1</sup> 

<sup>1</sup> Clinical Pharmacy, Saarland University, Campus C2 2, 66123 Saarbrücken, Germany

<sup>2</sup> Kobe Pharma Research Institute, Nippon Boehringer Ingelheim Co. Ltd., Kobe, Japan

<sup>3</sup> Boehringer Ingelheim Pharma GmbH & Co. KG, Biberach, Germany

<sup>4</sup> Department of Clinical Pharmacology and Pharmacoepidemiology, Heidelberg University Hospital, Heidelberg, Germany

<sup>5</sup> Institute of Experimental and Clinical Pharmacology and Toxicology, Friedrich-Alexander-Universität Erlangen-Nürnberg, Erlangen, Germany



#### 4.2 PROJECT II - A PHYSIOLOGICALLY-BASED PHARMACOKINETIC MODEL OF TRIMETHOPRIM FOR MATE1, OCT1, OCT2, AND CYP2C8 DRUG-DRUG-GENE INTERACTION PREDICTIONS

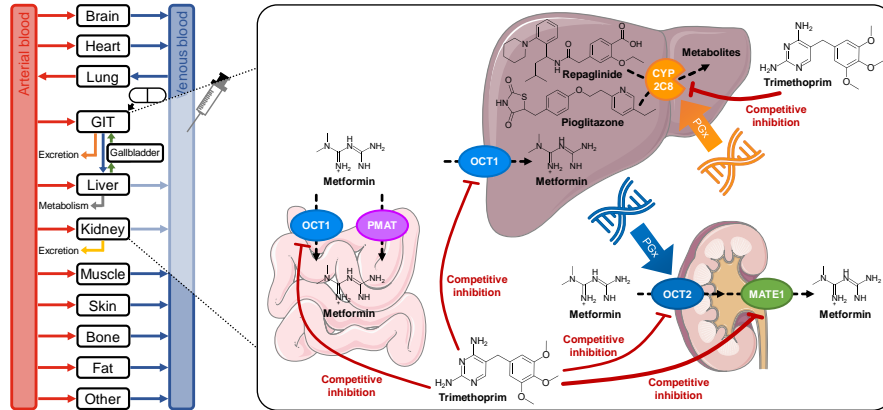


**Figure 4.2.** Whole-body physiologically based pharmacokinetic (PBPK) modeling of trimethoprim for drug-drug-gene interaction predictions. Illustrations of organs were taken from Servier [5], licensed under CC BY 3.0 (<https://creativecommons.org/licenses/by/3.0/>). CYP, cytochrome P450; GIT, gastrointestinal tract; MATE, multidrug and toxin extrusion protein; OCT, organic cation transporter; PG<sub>x</sub>, pharmacogenetics; PMAT, plasma membrane monoamine transporter.

#### Publication

Türk D, Hanke N, and Lehr T. A physiologically-based pharmacokinetic model of trimethoprim for MATE<sub>1</sub>, OCT<sub>1</sub>, OCT<sub>2</sub>, and CYP<sub>2C8</sub> drug-drug-gene interaction predictions. *Pharmaceutics*. 2020;12(11):1074. DOI: [10.3390/pharmaceutics12111074](https://doi.org/10.3390/pharmaceutics12111074)

Publication II

#### Supplementary material

The supplementary material to this publication can be found on the accompanying compact disk or can be accessed online via: [https://mdpi-res.com/d\\_attachment/pharmaceutics/pharmaceutics-12-01074/article\\_deploy/pharmaceutics-12-01074-s001.pdf?version=1605014473](https://mdpi-res.com/d_attachment/pharmaceutics/pharmaceutics-12-01074/article_deploy/pharmaceutics-12-01074-s001.pdf?version=1605014473).

### Copyright

This article is an open access article distributed under the terms and conditions of CC BY 4.0 (<https://creativecommons.org/licenses/by/4.0/>), which permits unrestricted use, distribution, and reproduction in any medium, provided the original work is properly cited.

© 2020 by the authors. Licensee MDPI, Basel, Switzerland.

### Author contributions

Declaration of author contributions to the publication related to project II according to CRediT [4]:

Denise Feick (née Türk):	Conceptualization, Investigation, Visualization, Writing - Original Draft, Writing - Review & Editing
Nina Hanke:	Conceptualization, Investigation, Writing - Original Draft, Writing - Review & Editing
Thorsten Lehr:	Conceptualization, Funding Acquisition, Investigation, Writing - Original Draft, Writing - Review & Editing





Article

# A Physiologically-Based Pharmacokinetic Model of Trimethoprim for MATE1, OCT1, OCT2, and CYP2C8 Drug–Drug–Gene Interaction Predictions

Denise Türk, Nina Hanke  and Thorsten Lehr \* 

Clinical Pharmacy, Saarland University, 66123 Saarbrücken, Germany; denise.tuerk@uni-saarland.de (D.T.); n.hanke@mx.uni-saarland.de (N.H.)

\* Correspondence: thorsten.lehr@mx.uni-saarland.de; Tel.: +49-681-302-70255

Received: 25 September 2020; Accepted: 4 November 2020; Published: 10 November 2020



**Abstract:** Trimethoprim is a frequently-prescribed antibiotic and therefore likely to be co-administered with other medications, but it is also a potent inhibitor of multidrug and toxin extrusion protein (MATE) and a weak inhibitor of cytochrome P450 (CYP) 2C8. The aim of this work was to develop a physiologically-based pharmacokinetic (PBPK) model of trimethoprim to investigate and predict its drug–drug interactions (DDIs). The model was developed in PK-Sim<sup>®</sup>, using a large number of clinical studies (66 plasma concentration–time profiles with 36 corresponding fractions excreted in urine) to describe the trimethoprim pharmacokinetics over the entire published dosing range (40 to 960 mg). The key features of the model include intestinal efflux via P-glycoprotein (P-gp), metabolism by CYP3A4, an unspecific hepatic clearance process, and a renal clearance consisting of glomerular filtration and tubular secretion. The DDI performance of this new model was demonstrated by prediction of DDIs and drug–drug–gene interactions (DDGIs) of trimethoprim with metformin, repaglinide, pioglitazone, and rifampicin, with all predicted DDI and DDGI  $AUC_{last}$  and  $C_{max}$  ratios within 1.5-fold of the clinically-observed values. The model will be freely available in the Open Systems Pharmacology model repository, to support DDI studies during drug development.

**Keywords:** physiologically-based pharmacokinetic (PBPK) modeling; trimethoprim; drug–drug interaction (DDI); multidrug and toxin extrusion protein (MATE); organic cation transporter (OCT); cytochrome P450 2C8 (CYP2C8)

## 1. Introduction

Trimethoprim is an inhibitor of bacterial folic acid metabolism used to treat bacterial infections. It is either applied as monotherapy or in combination with sulfonamides, e.g., sulfamethoxazole (“cotrimoxazole”). Trimethoprim is one of the most frequently-used antibiotics worldwide, ranking fifth after penicillins, cephalosporins, macrolides, and fluoroquinolones, with a global consumption of  $5 \times 10^9$  standard units in 2010 [1].

Due to the frequent prescription of trimethoprim, investigation of its drug–drug interaction (DDI) potential is clinically relevant. The antibiotic is a potent inhibitor of multidrug and toxin-extrusion protein (MATE) 1 and MATE2-K [2], and therefore recommended by the FDA as a clinical MATE inhibitor. Furthermore, trimethoprim less potently inhibits organic cation transporter (OCT) 1 and OCT2 [3,4]. This combined inhibition potential can be observed during clinical studies of trimethoprim with metformin, where co-administration of trimethoprim increases the area under the concentration–time curve ( $AUC$ ) of metformin by 30% [4]. Metformin is listed by the FDA as the only recommended MATE1, MATE2-K, and OCT2 substrate for clinical DDI studies [2].

In addition to its inhibition of transporters, trimethoprim is a weak inhibitor of cytochrome P450 (CYP) 2C8 [2]. Co-administration of trimethoprim increases the *AUC* of repaglinide and pioglitazone by 61% and 42%, respectively [5,6]. Both victim drugs are mainly metabolized by CYP2C8 and listed as sensitive CYP2C8 index substrate (repaglinide) or moderately-sensitive CYP2C8 substrate (pioglitazone) for the use in clinical DDI studies [2].

Similar to DDIs, polymorphisms in transporters or metabolizing enzymes can affect the pharmacokinetics of a drug (drug–gene interactions, DGIs), leading to loss of efficacy or adverse drug reactions. Naturally, DDIs and DGIs may occur simultaneously (drug–drug–gene interactions, DDGIs), counteracting or adding their respective effects on drug exposure, which urgently needs to be considered in clinical practice as it can lead to very strong interaction effects. Two DDGIs with trimethoprim as the perpetrator, co-administered with metformin in *SLC22A2 808G>T* polymorphic subjects or with pioglitazone in *CYP2C8\*3* polymorphic volunteers, are reported in the literature [6,7]. The *SLC22A2 808G>T* allele frequency is between 10 and 14% in most populations [8]. This missense variant is associated with decreased metformin maximum plasma concentrations ( $C_{max}$ ) in vivo [7,9–11] and might be associated with cisplatin-induced ototoxicity [12]. The *CYP2C8\*3* allele frequency varies between populations and is reported at 13% in Caucasians and 2% in African Americans [13]. In vitro data suggest that the *CYP2C8\*3* allele is associated with decreased metabolism of e.g., paclitaxel [13]. However, clinical data showed controversial results with increased metabolism of repaglinide and pioglitazone [6,14].

In addition to its DDI liability as a perpetrator drug, trimethoprim can also be the victim drug in polypharmaceutical drug regimens. Co-administration of trimethoprim with rifampicin, an inducer of CYP enzymes and P-glycoprotein (P-gp) [2,15], has been shown to increase the urinary excretion of trimethoprim due to increased expression of P-gp [16].

The aims of this study were (1) to develop a whole-body physiologically-based pharmacokinetic (PBPK) model of trimethoprim that accurately describes the observed concentrations in plasma and urine over time, (2) to predict the DDIs of trimethoprim with the victim drugs metformin, repaglinide and pioglitazone, (3) to predict the clinically-significant DDGIs of trimethoprim with metformin in *SLC22A2 808G>T* carriers and with pioglitazone in *CYP2C8\*3* carriers, and (4) to describe the rifampicin–trimethoprim DDI with trimethoprim in the role of the victim drug. The newly-developed trimethoprim model will be freely available in the Open Systems Pharmacology model repository ([www.open-systems-pharmacology.org](http://www.open-systems-pharmacology.org)) and the Supplementary Materials to this manuscript were compiled as one comprehensive reference manual with transparent documentation of the model performance to support DDI investigations during drug development, labeling, and submission for regulatory approval of new drugs.

## 2. Materials and Methods

### 2.1. Software

The PBPK model of trimethoprim was developed using PK-Sim<sup>®</sup> modeling software (Open Systems Pharmacology Suite 8.0, [www.open-systems-pharmacology.org](http://www.open-systems-pharmacology.org), 2019). Clinical study data from literature were digitized with Engauge Digitizer 10.12 (© M. Mitchell [17], 2019) according to best practices [18]. Model parameter optimization (Levenberg–Marquardt algorithm) and sensitivity analysis were performed within PK-Sim<sup>®</sup>. Calculation of pharmacokinetic parameters, quantitative model performance analysis, and generation of plots were accomplished using R 3.6.2 (The R Foundation for Statistical Computing, Vienna, Austria, 2019) and RStudio 1.2.5033 (RStudio, Inc., Boston, MA, USA, 2019).

### 2.2. Trimethoprim Clinical Data

Plasma or whole blood concentration–time profiles and fraction excreted unchanged ( $f_e$ ) in urine data of single- and multiple-dose trimethoprim studies were collected from literature and digitized.

The obtained profiles were divided into a training dataset and a test dataset, which were used for model building and model evaluation, respectively.

### 2.3. Trimethoprim PBPK Model Building

Model building was started with an extensive literature search to gain information about physicochemical parameters as well as absorption, distribution, metabolism, and excretion (ADME) processes of trimethoprim.

To simulate trimethoprim in the different organs of the body, virtual individuals were created according to the demographics of the respective clinical studies (ethnicity, sex, age, body weight, and height). If no information was provided, a European, male, 30-year-old individual was assumed, with body weight and height characteristics taken from the PK-Sim<sup>®</sup> population database.

Transporters and enzymes involved in trimethoprim ADME were implemented according to current literature, using the PK-Sim<sup>®</sup> expression database [19]. Details on their expression and localization in the different organs of the body are provided in the system-dependent parameter table in the Supplementary Materials (Table S19).

Model parameters that could not be informed from literature were optimized by fitting the model simultaneously to all plasma or whole blood concentration–time profiles and *fe* in urine data of the training dataset.

### 2.4. Trimethoprim PBPK Model Evaluation

Trimethoprim model performance was evaluated by comparison of (1) the predicted plasma or whole blood concentration–time and *fe* in urine profiles to the clinically-observed data of the respective clinical studies, (2) predicted plasma or whole blood concentration values of all studies to their corresponding observed values in goodness-of-fit plots, and (3) predicted to observed *fe* in urine, *AUC*, and *C*<sub>max</sub> values, where *AUC* was calculated from the time of drug administration to the time of the last concentration measurement (*AUC*<sub>last</sub>) for both predicted and observed plasma or whole blood concentration–time profiles.

As quantitative measures of the model performance, the mean relative deviation (MRD) of all predicted plasma and whole blood concentrations and the geometric mean fold error (GMFE) of all predicted *fe* in urine, *AUC*<sub>last</sub>, and *C*<sub>max</sub> values were calculated according to Equations (1) and (2), respectively. MRD and GMFE values ≤ 2 characterize an adequate model performance.

$$\text{MRD} = 10^x; x = \sqrt{\frac{\sum_{i=1}^k (\log_{10} c_{\text{predicted},i} - \log_{10} c_{\text{observed},i})^2}{k}} \quad (1)$$

where *c*<sub>predicted,*i*</sub> = predicted plasma (or whole blood) concentration, *c*<sub>observed,*i*</sub> = corresponding observed plasma (or whole blood) concentration, and *k* = number of observed values.

$$\text{GMFE} = 10^x; x = \frac{\sum_{i=1}^m \left| \log_{10} \left( \frac{\text{predicted PK parameter}_i}{\text{observed PK parameter}_i} \right) \right|}{m} \quad (2)$$

where predicted PK parameter<sub>*i*</sub> = predicted *fe* in urine, *AUC*<sub>last</sub>, or *C*<sub>max</sub> value; observed PK parameter<sub>*i*</sub> = corresponding observed *fe* in urine, *AUC*<sub>last</sub>, or *C*<sub>max</sub> value; *m* = number of studies.

### 2.5. DDI and DDGI Modeling

In addition to the previously-described methods for PBPK model evaluation, the ability of the trimethoprim model to adequately predict DDIs was tested. Trimethoprim DD(G)I modeling was performed with three different victim drugs (metformin, repaglinide, and pioglitazone) and one perpetrator drug (rifampicin). The parameters of the previously-developed PBPK models of metformin [20], repaglinide, pioglitazone [21], and rifampicin [22] that were applied for DDI modeling

are reproduced in Tables S8, S11, S14 and S17 and DDI model processes are illustrated in Figures S14, S18, S21 and S25 of the Supplementary Materials.

To predict the trimethoprim–metformin DDI, competitive inhibition of MATE1, OCT1, and OCT2 by trimethoprim was implemented, using  $K_i$  values of 4.45  $\mu\text{mol/L}$ , 32.20  $\mu\text{mol/L}$ , and 47.82  $\mu\text{mol/L}$ , respectively [3,4,23–27]. The trimethoprim–repaglinide and trimethoprim–pioglitazone DDIs were predicted as competitive inhibition of CYP2C8 by trimethoprim with a  $K_i$  value of 4.85  $\mu\text{mol/L}$  [28]. All trimethoprim  $K_i$  values and in vitro references are listed in the trimethoprim drug-dependent parameter table in Section 3.1.

To predict the published trimethoprim DDGI studies with metformin (*SLC22A2 808G>T*, increased metformin transport) and pioglitazone (*CYP2C8\*3*, increased pioglitazone metabolism), the trimethoprim model was applied with previously-built and evaluated DGI models of metformin and pioglitazone [20,21]. For the competitive inhibition of the variant OCT2 or CYP2C8 isoforms by trimethoprim, the same  $K_i$  values as for the wildtype transporter or enzyme were applied.

The rifampicin–trimethoprim DDI was modeled as induction of P-gp trimethoprim transport and CYP3A4 trimethoprim metabolism by rifampicin, with simultaneous competitive inhibition of P-gp and CYP3A4. The parameter values to model these interactions were taken from literature (values and references are listed in the rifampicin drug-dependent parameter Table S17 in the Supplementary Materials) and have been evaluated in previous DDI analyses [21,22]. Due to the lack of in vitro information regarding the metabolism of trimethoprim, the clinical data of the rifampicin–trimethoprim DDI were included into the training dataset, and the inducible fraction of trimethoprim metabolism was attributed to metabolism by CYP3A4.

The mathematical implementation of competitive inhibition and rifampicin-dependent induction is shown in Section 1.5 of the Supplementary Materials.

## 2.6. DDI and DDGI Model Performance Evaluation

The DDI and DDGI modeling performance was evaluated by comparison of predicted to observed plasma concentration–time profiles of the respective victim drugs metformin, repaglinide, pioglitazone, or trimethoprim, administered alone and during perpetrator drug co-treatment (trimethoprim or rifampicin). Furthermore, predicted DDI or DDGI  $AUC_{\text{last}}$  ratios (Equation (3)) and DDI or DDGI  $C_{\text{max}}$  ratios (Equation (4)) were calculated, and compared to the observed ratios.

$$\text{DDI or DDGI } AUC_{\text{last}} \text{ ratio} = \frac{AUC_{\text{last}} \text{ victim drug during co - administration}}{AUC_{\text{last}} \text{ victim drug control}} \quad (3)$$

$$\text{DDI or DDGI } C_{\text{max}} \text{ ratio} = \frac{C_{\text{max}} \text{ victim drug during co - administration}}{C_{\text{max}} \text{ victim drug control}} \quad (4)$$

As a quantitative measure of the DDI and DDGI model performance, GMFE values of the predicted  $AUC_{\text{last}}$  ratios and  $C_{\text{max}}$  ratios were calculated according to Equation (2).

## 2.7. Sensitivity Analysis

Local sensitivity analysis was performed on the trimethoprim model to investigate the impact of single-model parameters on the predicted  $AUC$ ,  $C_{\text{max}}$ , and  $t_{\text{max}}$  at steady state. Parameters were included in the analysis if they have been optimized, if they were associated with optimized parameters or if they might had a strong impact on the model predictions due to their use in the calculation of permeabilities or partition coefficients. A list of the analyzed parameters is provided in Table S6 of the Supplementary Materials.

Sensitivity was calculated as the ratio of the relative change of the simulated  $AUC$ ,  $C_{\max}$ , or  $t_{\max}$  to the relative variation of the tested parameter around the parameter value used in the model, according to Equation (5):

$$S = \frac{\Delta PK}{PK} \cdot \frac{p}{\Delta p} \quad (5)$$

where  $S$  = sensitivity of the  $AUC$ ,  $C_{\max}$ , or  $t_{\max}$  to the tested model parameter;  $\Delta PK$  = change of the  $AUC$ ,  $C_{\max}$ , or  $t_{\max}$ ;  $PK$  =  $AUC$ ,  $C_{\max}$ , or  $t_{\max}$  predicted with the original model parameter value;  $p$  = original model parameter value;  $\Delta p$  = change of the tested model parameter value.

Sensitivity analysis was performed using the highest recommended dose and a relative parameter perturbation of 1000%. The threshold value for sensitivity was set to 0.5; this value signifies that a 100% change of the investigated parameter value causes a 50% change of the predicted  $AUC$ ,  $C_{\max}$  or  $t_{\max}$ .

### 3. Results

#### 3.1. Trimethoprim PBPK Model Building and Evaluation

The trimethoprim whole-body PBPK model was built and evaluated using a total number of 66 trimethoprim plasma or whole blood concentration–time profiles and 36  $fe$  in urine profiles (intravenous and oral, single-, and multiple-dose administration), covering a broad dosing range from of 40 to 960 mg. In 47 of the 66 clinical studies, trimethoprim was administered as “cotrimoxazole”, i.e., in combination with sulfamethoxazole. According to literature [29,30] and our own analyses, trimethoprim pharmacokinetic profiles are not altered by simultaneous administration of sulfamethoxazole (see Figure S2 in the Supplementary Materials). Consequently, studies with co-administration of trimethoprim and sulfamethoxazole were included for model development. A table listing all utilized clinical studies is provided in the Supplementary Materials (Table S1).

The final trimethoprim PBPK model applies active efflux via P-gp (most strongly expressed in the intestine and kidney), metabolism by CYP3A4 (mainly in the liver with lower expression in the intestine), an unspecific hepatic clearance, and passive glomerular filtration. Trimethoprim is primarily excreted unchanged in the urine (46–67% of an oral dose [30–32]). The implemented ADME processes are visualized in Figure 1 and in Figure S3 of the Supplementary Materials. The drug-dependent parameters of the final model are given in Table 1 and in Table S2 of the Supplementary Materials. The model-specific, system-dependent parameters, with the expression profiles of the incorporated transporter and metabolizing enzymes, are summarized in the system-dependent parameter table in the Supplementary Materials (Table S19).

The good descriptive (training dataset, 13 studies) and predictive (test dataset, 53 studies) performance of the trimethoprim model is demonstrated in Figure 2, showing representative population predictions of plasma concentration–time profiles and  $fe$  in urine, compared to observed data. The population predictions of all 66 analyzed clinical studies, compared to their respective observed data, are shown in Figures S4–S9 of the Supplementary Materials (semilogarithmic as well as linear plots). Furthermore, goodness-of-fit plots with predicted versus observed (a) plasma or whole blood concentrations and (b)  $fe$  in urine values, are presented in Figure 3 and in Figures S10 and S11 of the Supplementary Materials, where 93% of all predicted plasma or whole blood concentrations and 100% of all predicted  $fe$  in urine values are within 2-fold of the observed data. MRD values for all predicted plasma or whole blood concentration–time profiles (58/66 with  $MRD \leq 2$ ) and GMFE values for predicted  $fe$  in urine (overall GMFE of 1.19) are documented in the Supplementary Materials (Tables S3 and S4).

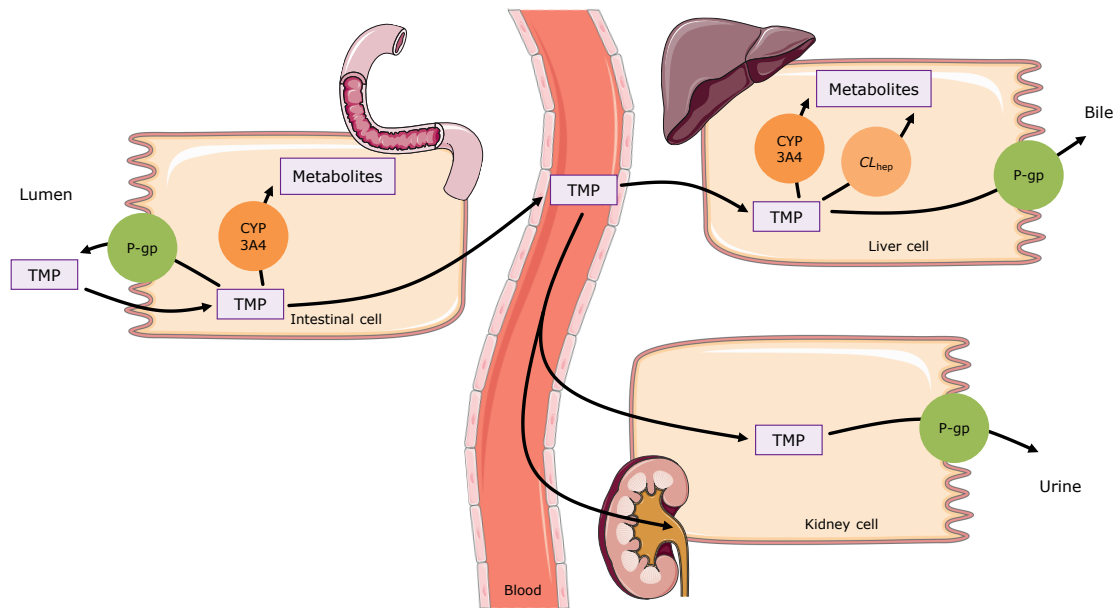


**Figure 1.** Schematic illustration of the trimethoprim absorption, distribution, metabolism, and excretion (ADME) processes in the model. Trimethoprim is absorbed in the intestine with counteractive efflux via P-gp. About 20% of a trimethoprim dose is metabolized [33] (modeled via CYP3A4 and an additional  $CL_{hep}$ ). The main route of trimethoprim elimination is urinary excretion (46–67% of an oral dose [30–32]) via glomerular filtration and active tubular secretion via P-gp. Drawings by Servier, licensed under CC BY 3.0 [34].  $CL_{hep}$ : hepatic metabolic clearance, CYP: cytochrome P450, P-gp: P-glycoprotein, TMP: trimethoprim.

**Table 1.** Trimethoprim drug-dependent parameters.

Parameter	Value	Unit	Source	Literature	Reference	Description
MW	290.32	g/mol	Literature	290.32	[35]	Molecular weight
pK <sub>a</sub> (base)	7.12	-	Literature	6.60, 7.12, 7.30	[35–37]	Acid dissociation constant
Solubility (pH 7.0)	0.40	g/L	Literature	0.40	[35]	Solubility
logP	1.01	-	Optimized	0.60, 0.73, 0.91, 1.43	[35,38–40]	Lipophilicity
f <sub>u</sub>	56	%	Literature	42–65	[41–47]	Fraction unbound plasma
P-gp K <sub>M</sub>	195.75	μmol/L	Optimized	-	-	Michaelis–Menten constant
P-gp k <sub>cat</sub>	1.44	1/min	Optimized	-	-	Transport rate constant
CYP3A4 K <sub>M</sub>	375.57	μmol/L	Optimized	-	-	Michaelis–Menten constant
CYP3A4 k <sub>cat</sub>	0.56	1/min	Optimized	-	-	Catalytic rate constant
CL <sub>hep</sub>	1.61 × 10 <sup>-2</sup>	1/min	Optimized	-	-	Hepatic metabolic clearance
GFR fraction	1	-	Assumed	-	-	Fraction of filtered drug in the urine
EHC continuous fraction	1	-	Assumed	-	-	Fraction of bile continually released
MATE1 K <sub>i</sub>	4.45	μmol/L	Literature	0.51, 2.64, 3.29, 3.94, 4.06, 4.58, 6.30, 6.73, 7.99 *	[3,4,23–25]	Conc. for 50% inhibition (competitive)
OCT1 K <sub>i</sub>	32.20	μmol/L	Literature	27.70, 36.70 *	[3,4]	Conc. for 50% inhibition (competitive)
OCT2 K <sub>i</sub>	47.82	μmol/L	Literature	13.20, 19.80, 27.20, 32.30, 57.40, 137.00 *	[3,4,23,26,27]	Conc. for 50% inhibition (competitive)
CYP2C8 K <sub>i</sub>	4.85	μmol/L	Literature	2.25, 3.80, 8.50 *	[28]	Conc. for 50% inhibition (competitive)
Partition coefficients	Diverse	-	Calculated	Berezhkovskiy	[48]	Cell to plasma partition coefficients
Cellular permeability	4.96 × 10 <sup>-4</sup>	cm/min	Calculated	CDS	[49]	Permeability into the cellular space
Intestinal permeability	1.24 × 10 <sup>-2</sup>	cm/min	Optimized	1.36 × 10 <sup>-6</sup>	Calculated	Transcellular intestinal permeability
Formulation	Weibull °	-	Optimized	-	-	Formulation used in predictions

\* if half maximal inhibitory concentrations ( $IC_{50}$ ) were reported,  $K_i$  values were calculated using the Cheng–Prusoff equation [50], and then the mean  $K_i$  was used in the model; ° Weibull function with a dissolution time of 53.47, 94.86, 71.83, or 52.59 min (50% dissolved) and a dissolution shape of 0.91, 0.91, 0.89, or 1.00 (all optimized) for oral suspension fasted [51,52], oral suspension fed [53], for capsule fasted [51], and tablet fasted [33,54–57], respectively. Berezhkovskiy, Berezhkovskiy calculation method; CDS, charge-dependent Schmitt calculation method;  $CL_{hep}$ , hepatic metabolic clearance; conc., concentration; CYP, cytochrome P450; EHC, enterohepatic circulation; GFR, glomerular filtration rate; MATE, multidrug and toxin extrusion protein; OCT, organic cation transporter; P-gp, P-glycoprotein.

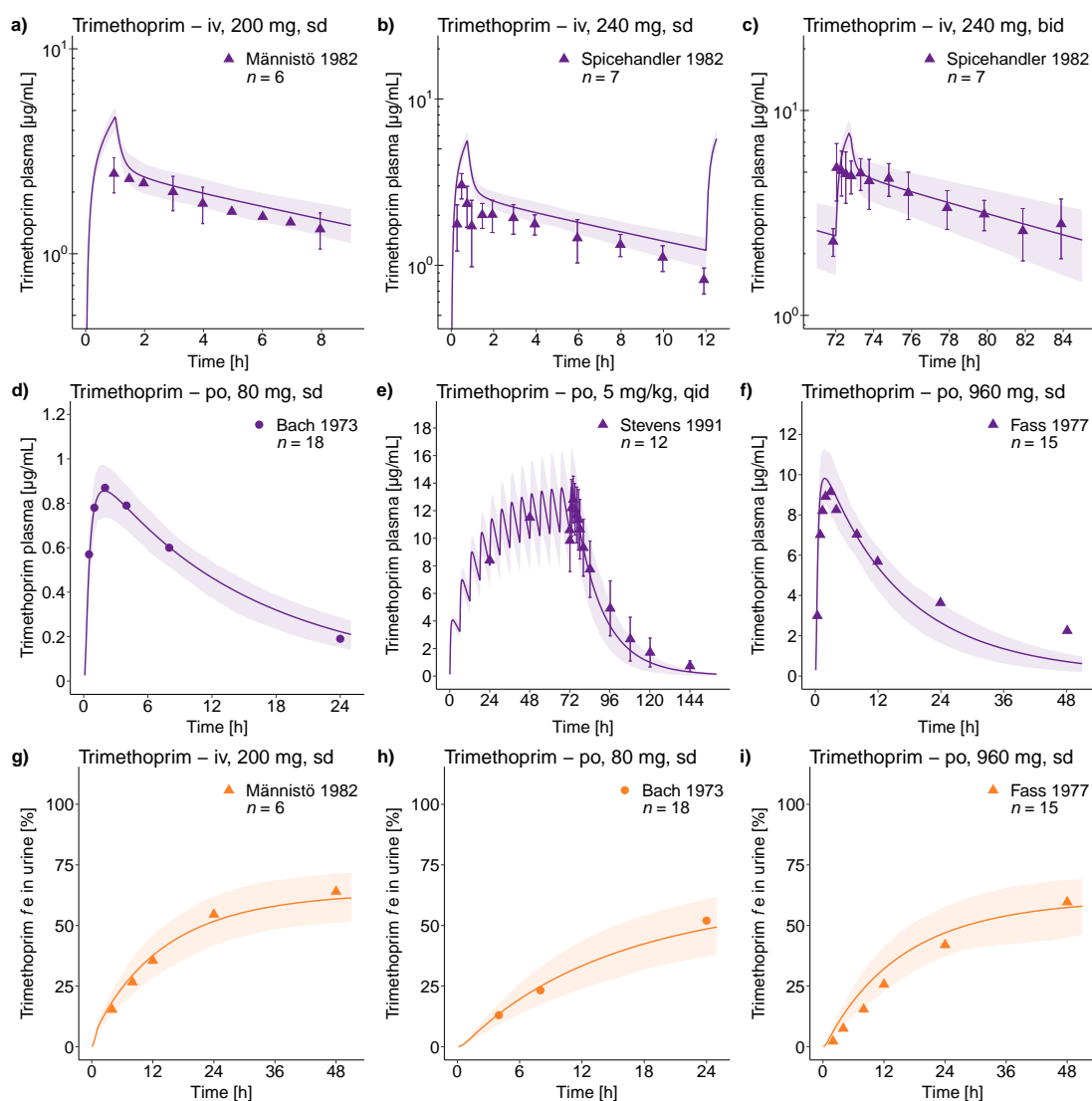


**Figure 2.** Trimethoprim in plasma and urine. Population predictions of trimethoprim (a–f) plasma concentration–time profiles and (g–i) fraction excreted unchanged in urine profiles compared to observed data [43,54,55,57,58] of representative intravenous and oral studies. Population prediction arithmetic means are shown as lines; the shaded areas illustrate the 68% population prediction intervals. Observed data are shown as triangles (training dataset) or dots (test dataset)  $\pm$  standard deviation. Details on the study protocols and model simulations of all 66 clinical studies used for model building and evaluation are provided in the Supplementary Materials. bid, twice daily; *fe* in urine, fraction excreted unchanged in urine; iv, intravenous; po, oral; qid, four times daily; sd, single dose.

Correlations of predicted with observed  $AUC_{last}$  (97% within 2-fold) and  $C_{max}$  values (98% within 2-fold) are presented in Figure 4 and in Figure S12 of the Supplementary Materials. The plotted values for all studies are provided in the Supplementary Materials (Table S5), including calculated GMFE values, with overall GMFEs of 1.29 and 1.20 for  $AUC_{last}$  and  $C_{max}$ , respectively.



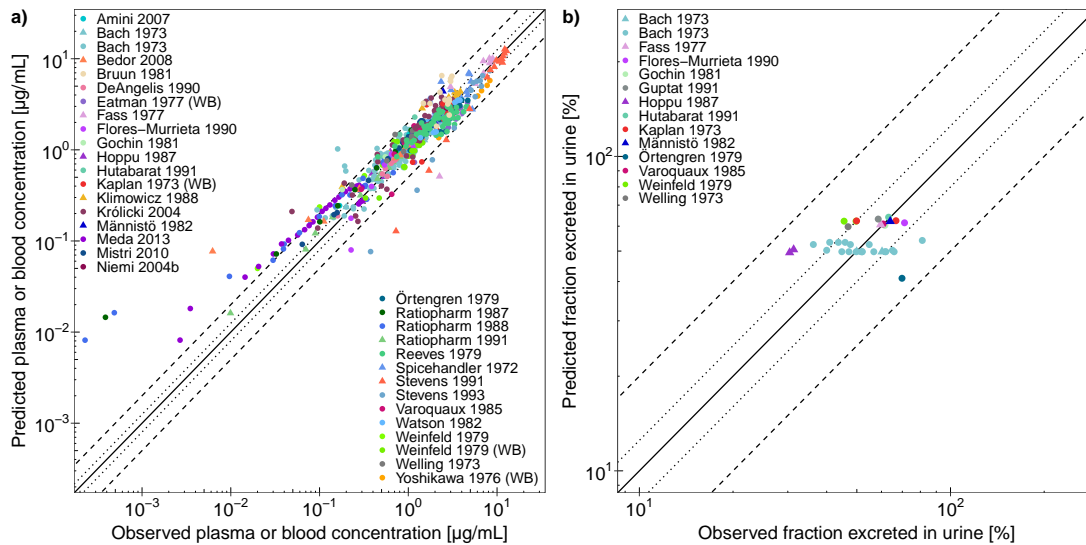


**Figure 3.** Trimethoprim physiologically-based pharmacokinetic (PBPK) model performance. The goodness-of-fit plots show predicted compared to observed (a) plasma or whole blood concentrations and (b) fractions excreted unchanged in urine of all studies used for model building and evaluation. The solid line marks the line of identity and dotted lines indicate 1.25-fold and dashed lines indicate 2-fold deviation. Data are shown as triangles (training dataset) or dots (test dataset) [30,31,33,37,41,43,46,51–73]. Details on the predicted clinical studies and the individual fraction excreted unchanged in urine values are provided in the Supplementary Materials. WB, whole blood.

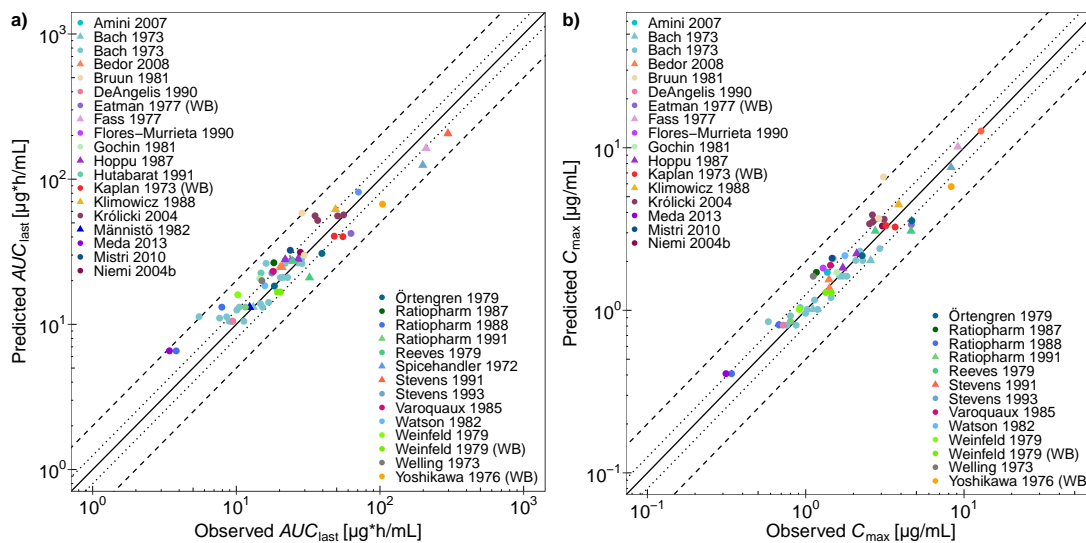


**Figure 4.** Trimethoprim PBPK model performance. The goodness-of-fit plots show predicted compared to observed (a)  $AUC_{last}$  values and (b)  $C_{max}$  values of all studies used for model building and evaluation. The solid line marks the line of identity and dotted lines indicate 1.25-fold and dashed lines indicate 2-fold deviation. Data are shown as triangles (training dataset) or dots (test dataset) [30,31,33,37,41,43,46,51–73]. Details on the predicted clinical studies and the individual  $AUC_{last}$  and  $C_{max}$  values are provided in the Supplementary Materials. WB, whole blood.

Sensitivity analysis of a simulation of 160 mg trimethoprim twice daily, using a parameter perturbation of 1000% and a sensitivity threshold of 0.5, showed that the only parameter value the model predictions are sensitive to is the trimethoprim fraction unbound in plasma, for which a literature

value is used in the model (56% [44]). The full quantitative results of the sensitivity analysis are shown in Section 2.5 (Figure S13) of the Supplementary Materials.

### 3.2. Trimethoprim DDI and DDGI Modeling

Trimethoprim DD(G)I modeling was performed with three different victim drugs (metformin, repaglinide, and pioglitazone) and one perpetrator drug (rifampicin). Tables listing all utilized clinical DDI studies are provided in the Supplementary Materials (Tables S7, S10, S13 and S16). The resulting trimethoprim DDI network with the affected transporters and enzymes is illustrated in Figure 5 and in Figure S1 of the Supplementary Materials.

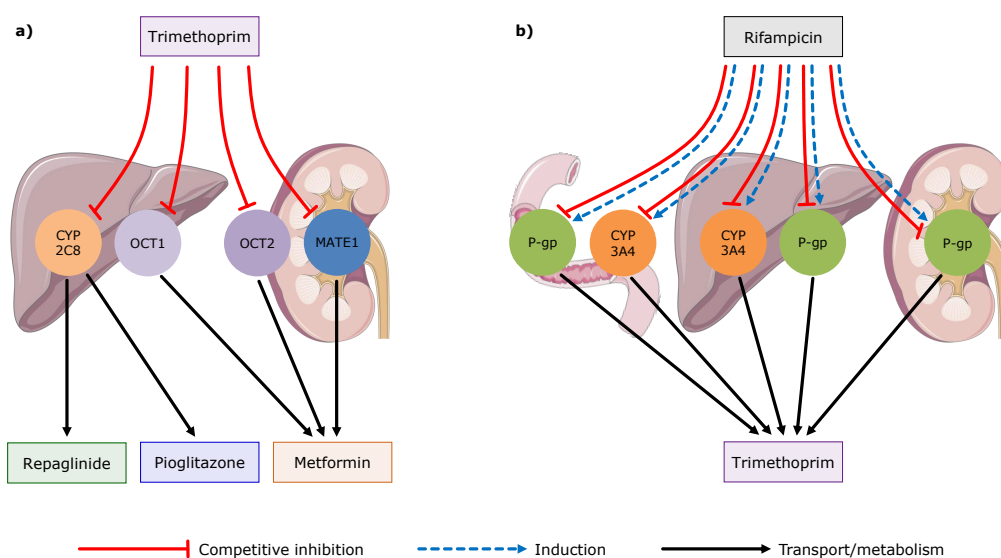


**Figure 5.** Trimethoprim drug–drug interaction (DDI) network. (a) Trimethoprim is a MATE1, OCT1, OCT2 and CYP2C8 inhibitor that impacts the pharmacokinetics of metformin, repaglinide, and pioglitazone. (b) On the other hand, trimethoprim is a victim drug in the DDI with rifampicin. Rifampicin inhibits and in the long term induces P-gp and CYP3A4, and thereby impacts the pharmacokinetics of trimethoprim. Drawings by Servier, licensed under CC BY 3.0 [34]. CYP: cytochrome P450, MATE: multidrug and toxin extrusion protein, OCT: organic cation transporter, P-gp: P-glycoprotein.

The good DDI model performance is demonstrated in Figure 6, showing representative population predictions of victim drug plasma concentration–time profiles before and during the four different DDIs, compared to observed data. For the rifampicin–trimethoprim DDI study, no plasma concentrations of trimethoprim without rifampicin co-administration were reported. Instead, day 1 and day 8 of the rifampicin–trimethoprim co-administration were shown, and therefore modeled and evaluated. Semilogarithmic as well as linear plots of population predicted compared to observed victim drug plasma concentration–time profiles of all DDI and DDGI studies are shown in Figures S15, S16, S19, S22, S23, S26, and S27 of the Supplementary Materials.

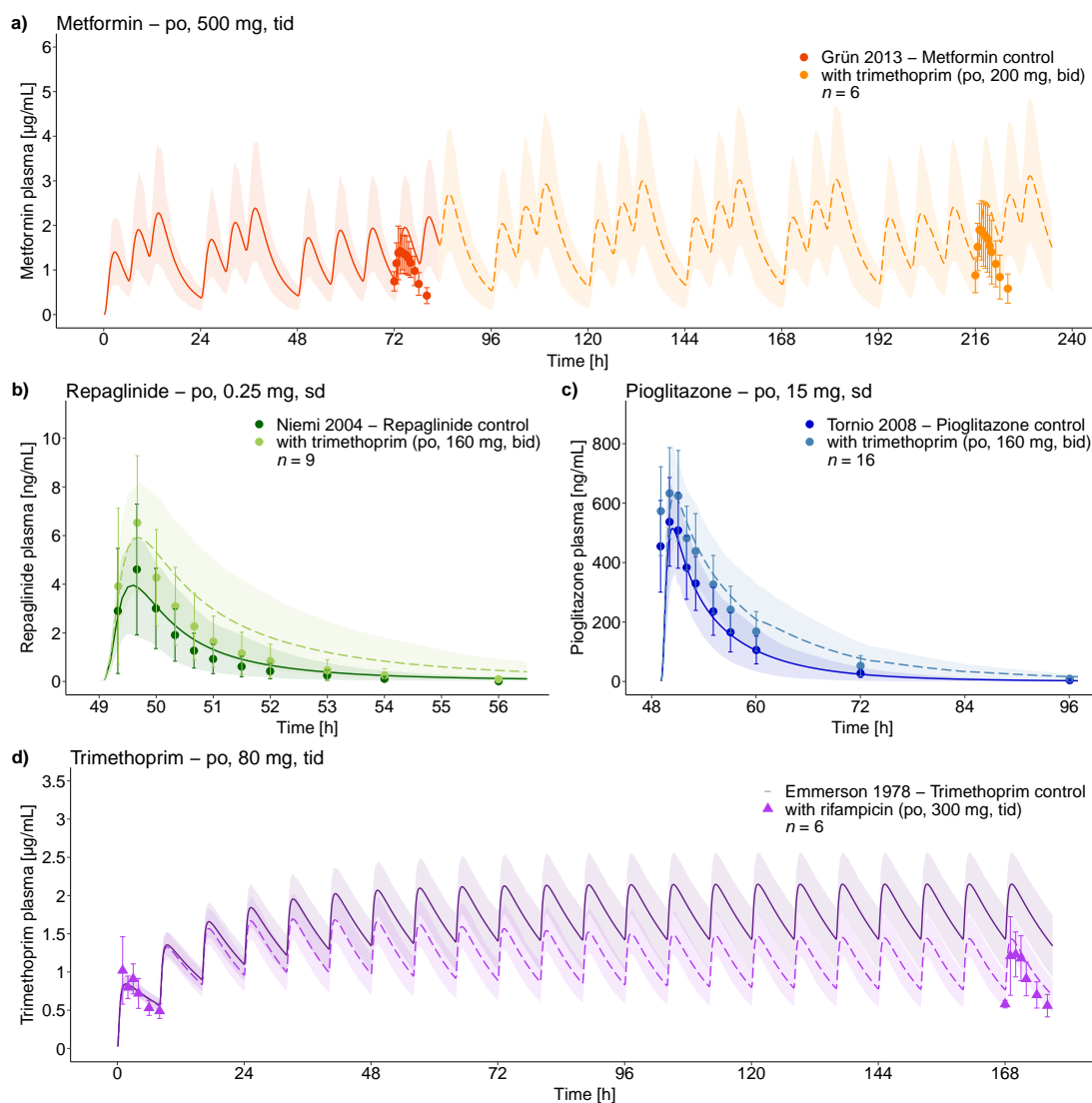


**Figure 6.** Trimethoprim DDI victim drug plasma profiles. Population predictions of victim drug plasma concentration–time profiles of the (a) trimethoprim–metformin, (b) trimethoprim–repaglinide, (c) trimethoprim–pioglitazone, and (d) rifampicin–trimethoprim DDIs, compared to observed data [5–7,16]. Population prediction arithmetic means are shown as lines (solid, victim drug alone and dashed, victim drug during perpetrator co-administration); the shaded areas illustrate the respective 68% population prediction intervals. Observed data are shown as triangles (training dataset) or dots (test dataset)  $\pm$  standard deviation. Perpetrator application starts at (a) 83 h or (b–d) 0 h. Details on the study protocols and model simulations of all clinical DDI and DDGI studies used to evaluate the DDI performance of the trimethoprim model are provided in the Supplementary Materials. bid, twice daily; po, oral; sd, single dose; tid, three times daily.

For a quantitative evaluation of the DDI performance, predicted and observed DDI and DDGI  $AUC_{last}$  and  $C_{max}$  ratios are compared in Figure 7 and listed in the Supplementary Materials, showing overall GMFEs of 1.08, 1.27, 1.32, and 1.08 ( $AUC_{last}$  ratios) and of 1.14, 1.11, 1.04, and 1.30 ( $C_{max}$  ratios) for the four modeled DDIs (trimethoprim–metformin, trimethoprim–repaglinide, trimethoprim–pioglitazone, and rifampicin–trimethoprim), respectively. All predicted DDI and DDGI  $AUC_{last}$  and  $C_{max}$  ratios are within 1.5-fold of the observed values. The full quantitative evaluation showing all ratios and GMFE values with ranges is presented in the Supplementary Materials (Tables S9, S12, S15 and S18 and Figures S17, S20, S24 and S28).

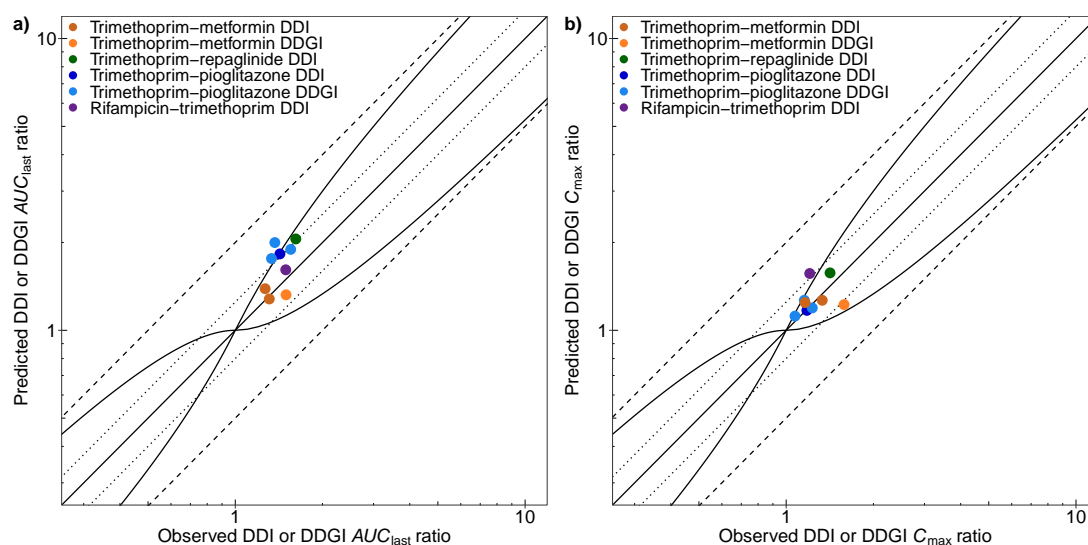


**Figure 7.** Trimethoprim DDI model performance. Predicted compared to observed DDI and DDGI (a)  $AUC_{last}$  ratios and (b)  $C_{max}$  ratios of all clinical studies used to evaluate the DDI performance of the trimethoprim model. The straight solid line marks the line of identity and the curved solid lines show the DDI prediction acceptance limits proposed by Guest et al. [74]. Dotted lines indicate 1.25-fold and dashed lines indicate 2-fold deviation. Data are shown as dots [4–7,16]. Details on the predicted clinical studies and the individual DDI and DDGI  $AUC_{last}$  and  $C_{max}$  ratios are provided in the Supplementary Materials.

#### 4. Discussion

A whole-body PBPK model of trimethoprim for the investigation and prediction of DDIs has been successfully built and evaluated. The model reliably captures the trimethoprim plasma and urine concentration–time profiles over a broad dosing range, for intravenous and oral administration as well as for single- and multiple-dose regimens. Good model performance has been demonstrated by (1) comparison of population predicted plasma or whole blood concentration and  $f_e$  in urine profiles to observed data, (2) a goodness-of-fit plot and MRD values of the predicted plasma concentrations, (3) goodness-of-fit plots and GMFE values of the predicted  $f_e$  in urine,  $AUC_{last}$ , and  $C_{max}$  values, and (4) the good DDI and DDGI performance.

The processes involved in the absorption, distribution, metabolism, and excretion of trimethoprim are not completely characterized or understood. It is known that trimethoprim is mainly excreted unchanged in urine (46–67% of an oral dose [30–32]), via glomerular filtration and tubular secretion. In vitro, trimethoprim is a substrate of P-gp [75], MATE1, and MATE2-K [76], but MATE2-K expression in the human kidney is extremely low [77]. The active tubular secretion of trimethoprim via MATE1 also seems unlikely, because the renal clearance of trimethoprim increased after eight days of rifampicin co-administration [16], and induction of MATE1 by rifampicin has not been demonstrated, yet. Furthermore, about 20% of a trimethoprim dose is reported to be metabolized [33], but there is no information available, as to which enzymes are involved in vivo. Implementation of P-gp and CYP3A4 into the trimethoprim model resulted in a good description of the trimethoprim concentration–time profiles observed in plasma and urine. In addition, the trimethoprim plasma concentrations measured during the first and eighth day of rifampicin co-administration and the observed increase in trimethoprim renal clearance on the eighth day of this DDI [16] are well captured by the model after implementation of P-gp and CYP3A4. Another candidate enzyme for trimethoprim metabolism in vivo is CYP2C9 [78], but co-administration of high doses of the CYP2C9 inhibitor, sulfamethoxazole ( $K_i = 271 \mu\text{M}$  [79]) showed no effect on trimethoprim plasma concentrations (see [29,30] and Figure S2 in the Supplementary Materials). In addition, the induction of CYP2C9 by

rifampicin is not as strong as that of CYP3A4 and using CYP2C9 as the main enzyme for trimethoprim metabolism in the model resulted in an underprediction of the rifampicin DDI effect.

One shortcoming of the presented model might be that according to literature, about 20% of a trimethoprim dose is metabolized [33], but fitting the model to this low value (CYP3A4 metabolism assumed) led to an overprediction of the urinary excretion and to an underprediction of the rifampicin-trimethoprim DDI. By implementation of CYP3A4 metabolism and addition of an unspecific hepatic clearance process, both urinary excretion and rifampicin-trimethoprim DDI could be well described, accepting a higher total fraction metabolized of 30–40%. Summed up, these 30–40% match well with the observed 46–67% of trimethoprim excreted unchanged in urine [30–32] and the reported fraction excreted in feces of 4% [80]. Unfortunately, the *in vivo* trimethoprim metabolism is not completely understood, which led us to include an unspecific clearance into the model. It might be speculated that trimethoprim undergoes tubular reabsorption, which was not implemented in our model but could reduce the slight overprediction of trimethoprim urinary excretion that we see without the unspecific hepatic clearance. However, no transporters involved in tubular reabsorption of trimethoprim are described in the literature, so far. Therefore, the extent of trimethoprim metabolism and the involved enzymes, as well as possible tubular reabsorption mechanisms need to be further investigated experimentally, to confirm or reject our model assumptions.

The presented trimethoprim model is able to adequately predict the MATE1, OCT1, and OCT2 DDI (metformin) as well as the CYP2C8 DDIs (repaglinide and pioglitazone), shown by comparison of predicted to observed plasma concentration–time profiles and predicted compared to observed DDI *AUC* and  $C_{\max}$  ratios, with all predicted ratios within 1.5-fold of the observed ratios. Metformin, the only recommended MATE1, MATE2-K, and OCT2 substrate for clinical DDI studies [2], is frequently prescribed (almost 80 million prescriptions in the USA in 2017 [81]) to treat type 2 diabetes mellitus. Also, as trimethoprim is regularly prescribed, co-administration with metformin, leading to increased metformin exposure, can frequently occur. The resulting increased risk of adverse drug events, e.g., in patients treated with high metformin doses or patients with impaired renal function, could be mitigated by applying the model to calculate metformin dose adaptations for the duration of this co-administration.

In addition, the model was successfully applied to predict plasma concentration–time profiles of metformin and pioglitazone in carriers of the *SLC22A2 808G>T* and *CYP2C8\*3* alleles, respectively, during co-administration with trimethoprim. The *SLC22A2 808G>T* allele investigated in this study occurs with a global frequency of 10–14% [8]. Therefore, investigation of its related DDGIs is clinically relevant. Plasma concentration time–profiles are well predicted using an OCT2  $K_i$  value from *in vitro* literature (same value assumed for wildtype and polymorphic transporter), resulting in predicted DDGI *AUC* and  $C_{\max}$  ratios within 1.5-fold of the observed values. The second variant allele investigated is the *CYP2C8\*3* allele, occurring with a frequency of 13% in Caucasians [13]. The model was applied to predict the trimethoprim–pioglitazone DDGI using a CYP2C8  $K_i$  value taken from *in vitro* literature. For the DDGI, no plasma concentration–time profiles were reported and therefore, only predicted and observed DDGI *AUC* and  $C_{\max}$  ratios were compared, resulting in predicted DDGI *AUC* and  $C_{\max}$  ratios within 1.5-fold and 1.25-fold of observed values, respectively.

Regarding previously-published PBPK models of trimethoprim, there are four earlier models of trimethoprim described in the literature [82–85]. These models have been built to predict the CYP2C8 DDI and DDGI with rosiglitazone (whole-body PBPK model) [82], to investigate the basolateral and apical kidney transporter DDI with creatinine (two semi-PBPK models) [83,84], or for pediatric scaling (whole-body PBPK model) [85]. The trimethoprim–rosiglitazone DDGI model [82] well describes the rosiglitazone plasma concentration–time profiles in CYP2C8 wildtype and carriers of the *CYP2C8\*3* allele. Also, the two minimal PBPK models built to describe the creatinine plasma concentration–time profiles during trimethoprim co-administration show a good DDI performance [83,84], without taking *SLC22A2* polymorphism into account. Our model was built and evaluated to assess DDIs mediated via CYP2C8, MATE1, OCT1, and OCT2, as well as DDGIs caused by *CYP2C8\*3* and *SLC22A2808G>T*

polymorphisms, applying one and the same whole-body PBPK model. Our model differs further from the previously-published models, as (1) none of these models was developed using such a large number of clinical studies (66 blood and 36 urine profiles) and (2) this is the first model which attempts to mechanistically describe the tubular secretion of trimethoprim. The good ability of the presented model to describe these different DDIs and DDGIs increases the confidence regarding the modeled trimethoprim concentrations at different sites of action (liver and kidney) and its general applicability for future investigations.

## 5. Conclusions

In this study, a carefully-developed mechanistic whole-body PBPK model of trimethoprim is presented. The model adequately predicts the trimethoprim pharmacokinetics following intravenous and oral administration over a broad range of dosing regimens. In addition, the model was qualified by prediction of DDI studies with the victim drugs metformin, repaglinide, and pioglitazone and by prediction of DDGI studies with metformin and pioglitazone. The model evaluation is transparently documented in the Supplementary Materials, showing the model performance for all 66 analyzed trimethoprim studies as well as for all DDI and DDGI studies utilized for model evaluation. The model will be shared with the research and drug development community via the Open Systems Pharmacology repository ([www.open-systems-pharmacology.org](http://www.open-systems-pharmacology.org)) [86], for the investigation of new DDI scenarios with MATE1, OCT1, OCT2, and CYP2C8 victim drugs.

**Supplementary Materials:** The following are available online at <http://www.mdpi.com/1999-4923/12/11/1074/s1>, Supplementary Materials: Comprehensive reference manual, providing documentation of the complete model performance assessment. Table S1: Clinical studies of trimethoprim; Table S2: Drug-dependent parameters of the final trimethoprim PBPK model; Table S3: MRD values of trimethoprim plasma (or whole blood) concentration predictions; Table S4: Predicted and observed trimethoprim fractions excreted unchanged in urine; Table S5: Predicted and observed trimethoprim  $AUC_{last}$  and  $C_{max}$  values; Table S6: Parameters evaluated during trimethoprim sensitivity analysis; Table S7: Clinical studies investigating the trimethoprim-metformin DDI and DDGI; Table S8: Drug-dependent parameters of the metformin PBPK model; Table S9: Predicted and observed trimethoprim-metformin DDI and DDGI  $AUC_{last}$  and  $C_{max}$  ratios; Table S10: Clinical studies investigating the trimethoprim-repaglinide DDI; Table S11: Drug-dependent parameters of the repaglinide PBPK model; Table S12: Predicted and observed trimethoprim-repaglinide DDI  $AUC_{last}$  and  $C_{max}$  ratios; Table S13: Clinical studies investigating the trimethoprim-pioglitazone DDI and DDGI; Table S14: Drug-dependent parameters of the pioglitazone PBPK model; Table S15: Predicted and observed trimethoprim-pioglitazone DDI and DDGI  $AUC_{last}$  and  $C_{max}$  ratios; Table S16: Clinical studies investigating the rifampicin-trimethoprim DDI; Table S17: Drug-dependent parameters of the rifampicin PBPK model; Table S18: Predicted and observed rifampicin-trimethoprim DDI  $AUC_{last}$  and  $C_{max}$  ratios; Table S19: System-dependent parameters; Figure S1: Trimethoprim DDI network; Figure S2: Comparison of trimethoprim administered alone or together with sulfamethoxazole as “cotrimoxazole”; Figure S3: Schematic illustration of the trimethoprim ADME processes in the model; Figure S4: Trimethoprim plasma concentration-time profiles (semilogarithmic); Figure S5: Trimethoprim plasma concentration-time profiles after “cotrimoxazole” administration (semilogarithmic); Figure S6: Trimethoprim plasma concentration-time profiles (linear); Figure S7: Trimethoprim plasma concentration-time profiles after “cotrimoxazole” administration (linear); Figure S8: Trimethoprim fraction excreted unchanged in urine profiles; Figure S9: Trimethoprim fraction excreted unchanged in urine profiles after “cotrimoxazole” administration; Figure S10: Trimethoprim predicted compared to observed plasma concentration values; Figure S11: Trimethoprim predicted compared to observed fractions excreted unchanged in urine; Figure S12: Trimethoprim predicted compared to observed  $AUC_{last}$  and  $C_{max}$  values; Figure S13: Trimethoprim sensitivity analysis; Figure S14: Trimethoprim-metformin DDI model processes; Figure S15: Metformin plasma concentration-time profiles before and during trimethoprim DDI and DDGI (semilogarithmic); Figure S16: Metformin plasma concentration-time profiles before and during trimethoprim DDI and DDGI (linear); Figure S17: Metformin predicted compared to observed DDI and DDGI  $AUC_{last}$  and  $C_{max}$  ratios; Figure S18: Trimethoprim-repaglinide DDI model processes; Figure S19: Repaglinide plasma concentration-time profiles before and during trimethoprim DDI; Figure S20: Repaglinide predicted compared to observed DDI  $AUC_{last}$  and  $C_{max}$  ratios; Figure S21: Trimethoprim-pioglitazone DDI model processes; Figure S22: Pioglitazone plasma concentration-time profiles before and during trimethoprim DDI and DDGI (semilogarithmic); Figure S23: Pioglitazone plasma concentration-time profiles before and during trimethoprim DDI and DDGI (linear); Figure S24: Pioglitazone predicted compared to observed DDI and DDGI  $AUC_{last}$  and  $C_{max}$  ratios; Figure S25: Rifampicin-trimethoprim DDI model processes; Figure S26: Trimethoprim and rifampicin plasma concentration-time profiles of the rifampicin DDI (semilogarithmic); Figure S27: Trimethoprim and rifampicin plasma concentration-time profiles of the rifampicin DDI (linear); Figure S28: Trimethoprim predicted compared to observed DDI  $AUC_{last}$  and  $C_{max}$  ratios.

**Author Contributions:** Conceptualization, D.T., N.H., and T.L.; funding acquisition, T.L.; investigation, D.T., N.H., and T.L.; visualization, D.T.; writing—original draft, D.T., N.H., and T.L.; writing—review and editing, D.T., N.H., and T.L. All authors have read and agreed to the published version of the manuscript.

**Funding:** This project was partly funded by the German Federal Ministry of Education and Research (BMBF), grant number 031L0161C (“OSMOSES”). The APC was funded by the German Research Foundation (DFG) and Saarland University within the funding program “Open Access Publishing”.

**Conflicts of Interest:** Thorsten Lehr has received funding from the German Federal Ministry of Education and Research (grant 031L0161C). Denise Türk and Nina Hanke declare no conflict of interest. The funders had no role in the design of the study; in the collection, analyses, or interpretation of data; in the writing of the manuscript, or in the decision to publish the results.

## References

1. Van Boeckel, T.P.; Gandra, S.; Ashok, A.; Caudron, Q.; Grenfell, B.T.; Levin, S.A.; Laxminarayan, R. Global antibiotic consumption 2000 to 2010: An analysis of national pharmaceutical sales data. *Lancet. Infect. Dis.* **2014**, *14*, 742–750. [CrossRef]
2. U.S. Food and Drug Administration. Drug Development and Drug Interactions: Table of Substrates, Inhibitors and Inducers. Available online: <https://www.fda.gov/drugs/drug-interactions-labeling/drug-development-and-drug-interactions-table-substrates-inhibitors-and-inducers> (accessed on 24 August 2020).
3. Elsbj, R.; Chidlaw, S.; Outteridge, S.; Pickering, S.; Radcliffe, A.; Sullivan, R.; Jones, H.; Butler, P. Mechanistic in vitro studies confirm that inhibition of the renal apical efflux transporter multidrug and toxin extrusion (MATE) 1, and not altered absorption, underlies the increased metformin exposure observed in clinical interactions with cimetidine, trimethoprim or pyrimethamine. *Pharmacol. Res. Perspect.* **2017**, *5*, 1–13.
4. Müller, F.; Pontones, C.A.; Renner, B.; Mieth, M.; Hoier, E.; Auge, D.; Maas, R.; Zolk, O.; Fromm, M.F. N(1)-methylnicotinamide as an endogenous probe for drug interactions by renal cation transporters: Studies on the metformin-trimethoprim interaction. *Eur. J. Clin. Pharmacol.* **2015**, *71*, 85–94. [CrossRef] [PubMed]
5. Niemi, M.; Kajosaari, L.L.; Neuvonen, M.; Backman, J.T.; Neuvonen, P.J. The CYP2C8 inhibitor trimethoprim increases the plasma concentrations of repaglinide in healthy subjects. *Br. J. Clin. Pharmacol.* **2004**, *57*, 441–447. [CrossRef] [PubMed]
6. Tornio, A.; Niemi, M.; Neuvonen, P.J.; Backman, J.T. Trimethoprim and the CYP2C8\*3 allele have opposite effects on the pharmacokinetics of pioglitazone. *Drug Metab. Dispos.* **2008**, *36*, 73–80. [CrossRef] [PubMed]
7. Grün, B.; Kiessling, M.K.; Burhenne, J.; Riedel, K.-D.; Weiss, J.; Rauch, G.; Haefeli, W.E.; Czock, D. Trimethoprim-metformin interaction and its genetic modulation by OCT2 and MATE1 transporters. *Br. J. Clin. Pharmacol.* **2013**, *76*, 787–796. [CrossRef] [PubMed]
8. National Center for Biotechnology Information (NCBI) dbSNP-rs316019. Available online: <https://www.ncbi.nlm.nih.gov/snp/rs316019> (accessed on 16 October 2020).
9. Wang, Z.-J.; Yin, O.Q.P.; Tomlinson, B.; Chow, M.S.S. OCT2 polymorphisms and in-vivo renal functional consequence: Studies with metformin and cimetidine. *Pharmacogenet. Genom.* **2008**, *18*, 637–645. [CrossRef] [PubMed]
10. Chen, Y.; Li, S.; Brown, C.; Cheatham, S.; Castro, R.A.; Leabman, M.K.; Urban, T.J.; Chen, L.; Yee, S.W.; Choi, J.H.; et al. Effect of genetic variation in the organic cation transporter 2 on the renal elimination of metformin. *Pharmacogenet. Genom.* **2009**, *19*, 497–504. [CrossRef] [PubMed]
11. Christensen, M.M.H.; Pedersen, R.S.; Stage, T.B.; Brasch-Andersen, C.; Nielsen, F.; Damkier, P.; Beck-Nielsen, H.; Brøsen, K. A gene-gene interaction between polymorphisms in the OCT2 and MATE1 genes influences the renal clearance of metformin. *Pharmacogenet. Genom.* **2013**, *23*, 526–534. [CrossRef] [PubMed]
12. Clemens, E.; Broer, L.; Langer, T.; Uitterlinden, A.G.; de Vries, A.C.H.; van Grotel, M.; Pluijijm, S.F.M.; Binder, H.; Byrne, J.; van Dulmen-den Broeder, E.; et al. Genetic variation of cisplatin-induced ototoxicity in non-cranial-irradiated pediatric patients using a candidate gene approach: The International PanCareLIFE Study. *Pharm. J.* **2020**, *20*, 294–305. [CrossRef]
13. Dai, D.; Zeldin, D.C.; Blaisdell, J.A.; Chanas, B.; Coulter, S.J.; Ghanayem, B.I.; Goldstein, J.A. Polymorphisms in human CYP2C8 decrease metabolism of the anticancer drug paclitaxel and arachidonic acid. *Pharmacogenetics* **2001**, *11*, 597–607. [CrossRef] [PubMed]

14. Niemi, M.; Leathart, J.B.; Neuvonen, M.; Backman, J.T.; Daly, A.K.; Neuvonen, P.J. Polymorphism in CYP2C8 is associated with reduced plasma concentrations of repaglinide. *Clin. Pharmacol. Ther.* **2003**, *74*, 380–387. [[CrossRef](#)]
15. Greiner, B.; Eichelbaum, M.; Fritz, P.; Kreichgauer, H.P.; von Richter, O.; Zundler, J.; Kroemer, H.K. The role of intestinal P-glycoprotein in the interaction of digoxin and rifampin. *J. Clin. Invest.* **1999**, *104*, 147–153. [[CrossRef](#)] [[PubMed](#)]
16. Emmerson, A.M.; Grüneberg, R.N.; Johnson, E.S. The pharmacokinetics in man of a combination of rifampicin and trimethoprim. *J. Antimicrob. Chemother.* **1978**, *4*, 523–531. [[CrossRef](#)]
17. Mitchell, M.; Muftakhidinov, B.; Winchen, T.; Jedrzejewski-Szmek, Z.; Trande, A.; Weingrill, J.; Langer, S.; Lane, D.; Sower, K. Engauge Digitizer Software. Available online: <https://markumitchell.github.io/engauge-digitizer> (accessed on 24 August 2020).
18. Wojtyniak, J.-G.; Britz, H.; Selzer, D.; Schwab, M.; Lehr, T. Data digitizing: Accurate and precise data extraction for quantitative systems pharmacology and physiologically-based pharmacokinetic modeling. *CPT Pharmacomet. Syst. Pharmacol.* **2020**, *9*, 322–331. [[CrossRef](#)]
19. Open Systems Pharmacology Suite Community. PK-Sim<sup>®</sup> Ontogeny Database Documentation, Version 7.3. Available online: <https://github.com/Open-Systems-Pharmacology/OSPSuite.Documentation/blob/master/PK-SimOntogenyDatabaseVersion7.3.pdf> (accessed on 24 August 2020).
20. Hanke, N.; Türk, D.; Selzer, D.; Ishiguro, N.; Ebner, T.; Wiebe, S.; Müller, F.; Stopfer, P.; Nock, V.; Lehr, T. A comprehensive whole-body physiologically based pharmacokinetic drug-drug-gene interaction model of metformin and cimetidine in healthy adults and renally impaired individuals. *Clin. Pharmacokinet.* **2020**. [[CrossRef](#)]
21. Türk, D.; Hanke, N.; Wolf, S.; Frechen, S.; Eissing, T.; Wendl, T.; Schwab, M.; Lehr, T. Physiologically based pharmacokinetic models for prediction of complex CYP2C8 and OATP1B1 (SLCO1B1) drug-drug-gene interactions: A modeling network of gemfibrozil, repaglinide, pioglitazone, rifampicin, clarithromycin and itraconazole. *Clin. Pharmacokinet.* **2019**, *58*, 1595–1607. [[CrossRef](#)]
22. Hanke, N.; Frechen, S.; Moj, D.; Britz, H.; Eissing, T.; Wendl, T.; Lehr, T. PBPK models for CYP3A4 and P-gp DDI prediction: A modeling network of rifampicin, itraconazole, clarithromycin, midazolam, alfentanil, and digoxin. *CPT Pharmacomet. Syst. Pharmacol.* **2018**, *7*, 647–659. [[CrossRef](#)]
23. Lepistö, E.-I.; Zhang, X.; Hao, J.; Huang, J.; Kosaka, A.; Birkus, G.; Murray, B.P.; Bannister, R.; Cihlar, T.; Huang, Y.; et al. Contribution of the organic anion transporter OAT2 to the renal active tubular secretion of creatinine and mechanism for serum creatinine elevations caused by cobicistat. *Kidney Int.* **2014**, *86*, 350–357. [[CrossRef](#)]
24. Müller, F.; König, J.; Glaeser, H.; Schmidt, I.; Zolk, O.; Fromm, M.F.; Maas, R. Molecular mechanism of renal tubular secretion of the antimalarial drug chloroquine. *Antimicrob. Agents Chemother.* **2011**, *55*, 3091–3098. [[CrossRef](#)]
25. Lechner, C.; Ishiguro, N.; Fukuhara, A.; Shimizu, H.; Ohtsu, N.; Takatani, M.; Nishiyama, K.; Washio, I.; Yamamura, N.; Kusuhara, H. Impact of experimental conditions on the evaluation of interactions between multidrug and toxin extrusion proteins and candidate drugs. *Drug Metab. Dispos.* **2016**, *44*, 1381–1389. [[CrossRef](#)] [[PubMed](#)]
26. Müller, F.; König, J.; Hoier, E.; Mandery, K.; Fromm, M.F. Role of organic cation transporter OCT2 and multidrug and toxin extrusion proteins MATE1 and MATE2-K for transport and drug interactions of the antiviral lamivudine. *Biochem. Pharmacol.* **2013**, *86*, 808–815. [[CrossRef](#)] [[PubMed](#)]
27. Chu, X.; Bleasby, K.; Chan, G.H.; Nunes, I.; Evers, R. The complexities of interpreting elevated serum creatinine levels in drug development: Does a correlation with inhibition of renal transporters exist? *Drug Metab. Dispos.* **2016**, *44*, 1498–1509. [[CrossRef](#)] [[PubMed](#)]
28. Dinger, J.; Meyer, M.R.; Maurer, H.H. Development of an in vitro cytochrome P450 cocktail inhibition assay for assessing the inhibition risk of drugs of abuse. *Toxicol. Lett.* **2014**, *230*, 28–35. [[CrossRef](#)] [[PubMed](#)]
29. Nolte, H.; Büttner, H. Pharmacokinetics of trimethoprim and its combination with sulfamethoxazole in man after single and chronic oral administration. *Chemotherapy* **1973**, *18*, 274–284. [[CrossRef](#)] [[PubMed](#)]
30. Kaplan, S.A.; Weinfeld, R.E.; Abruzzo, C.W.; McFaden, K.; Lewis Jack, M.; Weissman, L. Pharmacokinetic profile of trimethoprim-sulfamethoxazole in man. *J. Infect. Dis.* **1973**, *128*, S547–S555. [[CrossRef](#)]
31. Weinfeld, R.E.; Macasieb, T.C. Determination of trimethoprim in biological fluids by high-performance liquid chromatography. *J. Chromatogr. B* **1979**, *164*, 73–84. [[CrossRef](#)]



32. Guptat, R.L.; Kumar, R.; Singla, A.K. Enhanced dissolution and absorption of trimethoprim from coprecipitates with polyethylene glycols and polyvinylpyrrolidone. *Drug Dev. Ind. Pharm.* **1991**, *17*, 463–468. [CrossRef]
33. Ratiopharm GmbH. *Fachinformation Cotrim-ratiopharm® 480 mg Tabletten, Cotrim forte-ratiopharm® 960 mg Tabletten (Bioavailability Study 1987 and 1991)*; Ratiopharm GmbH.: Ulm, Germany, 2017.
34. Les Laboratoires Servier. Servier Medical Art. Available online: <https://smart.servier.com/> (accessed on 24 August 2020).
35. Wishart, D.S.; Knox, C.; Guo, A.C.; Shrivastava, S.; Hassanali, M.; Stothard, P.; Chang, Z.; Woolsey, J. DrugBank: A comprehensive resource for in silico drug discovery and exploration. *Nucleic Acids Res.* **2006**, *34*, D668–D672. [CrossRef]
36. O'Neil, M.J.; Heckelman, P.E.; Koch, C.B.; Roman, K.J.; Kenny, C.M.; D'Arecca, M.R. *The Merck Index: An Encyclopedia of Chemicals, Drugs, and Biologicals*, 14th ed.; O'Neil, M.J., Heckelman, P.E., Koch, C.B., Roman, K.J., Eds.; Merck and Co. Inc.: Whitehouse Station, NJ, USA, 2006.
37. Reeves, D.S.; Wilkinson, P.J. The pharmacokinetics of trimethoprim and trimethoprim/sulphonamide combinations, including penetration into body tissues. *Infection* **1979**, *7* (Suppl. 4), S330–S341. [CrossRef]
38. Kim, S.; Chen, J.; Cheng, T.; Gindulyte, A.; He, J.; He, S.; Li, Q.; Shoemaker, B.A.; Thiessen, P.A.; Yu, B.; et al. PubChem 2019 update: Improved access to chemical data. *Nucleic Acids Res.* **2019**, *47*, D1102–D1109. [CrossRef] [PubMed]
39. Fresta, M.; Furneri, P.M.; Mezzasalma, E.; Nicolosi, V.M.; Puglisi, G. Correlation of trimethoprim and brodimoprim physicochemical and lipid membrane interaction properties with their accumulation in human neutrophils. *Antimicrob. Agents Chemother.* **1996**, *40*, 2865–2873. [CrossRef] [PubMed]
40. Kasim, N.A.; Whitehouse, M.; Ramachandran, C.; Bermejo, M.; Lennernäs, H.; Hussain, A.S.; Junginger, H.E.; Stavchansky, S.A.; Midha, K.K.; Shah, V.P.; et al. Molecular properties of WHO essential drugs and provisional biopharmaceutical classification. *Mol. Pharm.* **2004**, *1*, 85–96. [CrossRef] [PubMed]
41. Varoquaux, O.; Lajoie, D.; Gobert, C.; Cordonnier, P.; Ducreuzet, C.; Pays, M.; Advenier, C. Pharmacokinetics of the trimethoprim-sulphamethoxazole combination in the elderly. *Br. J. Clin. Pharmacol.* **1985**, *20*, 575–581. [CrossRef] [PubMed]
42. Wijkström, A.; Westerlund, D. Plasma protein binding of sulphadiazine, sulphamethoxazole and trimethoprim determined by ultrafiltration. *J. Pharm. Biomed. Anal.* **1983**, *1*, 293–299. [CrossRef]
43. Männistö, P.T.; Mäntylä, R.; Mattila, J.; Nykänen, S.; Lamminsivu, U. Comparison of pharmacokinetics of sulphadiazine and sulphamethoxazole after intravenous infusion. *J. Antimicrob. Chemother.* **1982**, *9*, 461–470. [CrossRef]
44. Hoffmann-La Roche Inc. *BACTRIM™ Sulfamethoxazole and Trimethoprim DS (Double Strength) Tablets and Tablets USP*; Hoffmann-La Roche Inc.: Basel, Switzerland, 2013.
45. Singlas, E.; Colin, J.N.; Rottembourg, J.; Meessen, J.P.; de Martin, A.; Legrain, M.; Simon, P. Pharmacokinetics of sulfamethoxazole - trimethoprim combination during chronic peritoneal dialysis: Effect of peritonitis. *Eur. J. Clin. Pharmacol.* **1982**, *21*, 409–415. [CrossRef]
46. Hutabarat, R.M.; Unadkat, J.D.; Sahajwalla, C.; McNamara, S.; Ramsey, B.; Smith, A.L. Disposition of drugs in cystic fibrosis. I. Sulfamethoxazole and trimethoprim. *Clin. Pharmacol. Ther.* **1991**, *49*, 402–409. [CrossRef]
47. Gonzalez, D.; Schmidt, S.; Derendorf, H. Importance of relating efficacy measures to unbound drug concentrations for anti-infective agents. *Clin. Microbiol. Rev.* **2013**, *26*, 274–288. [CrossRef]
48. Berezhkovskiy, L.M. Volume of distribution at steady state for a linear pharmacokinetic system with peripheral elimination. *J. Pharm. Sci.* **2004**, *93*, 1628–1640. [CrossRef]
49. Open Systems Pharmacology Suite Community. *Open Systems Pharmacology Suite Manual, Version 7.4*. Available online: <https://github.com/Open-Systems-Pharmacology/OSPSuite.Documentation/blob/master/OpenSystemsPharmacologySuite.pdf> (accessed on 24 August 2020).
50. Cheng, Y.C.; Prusoff, W.H. Relationship between the inhibition constant (KI) and the concentration of inhibitor which causes 50 per cent inhibition (I50) of an enzymatic reaction. *Biochem. Pharmacol.* **1973**, *22*, 3099–3108. [PubMed]
51. Bedor, D.C.G.; Gonçalves, T.M.; Ferreira, M.L.L.; de Sousa, C.E.M.; Menezes, A.L.; Oliveira, E.J.; de Santana, D.P. Simultaneous determination of sulfamethoxazole and trimethoprim in biological fluids for high-throughput analysis: Comparison of HPLC with ultraviolet and tandem mass spectrometric detection. *J. Chromatogr. B* **2008**, *863*, 46–54. [CrossRef] [PubMed]

52. Ratiopharm GmbH. *Fachinformation Cotrim K-ratiopharm<sup>®</sup> 240 mg/5 mL Saft, Cotrim E-ratiopharm<sup>®</sup> 480 mg/5 mL Saft (Bioavailability Study 1988)*; Ratiopharm GmbH.: Ulm, Germany, 2013.
53. Hoppu, K.; Tuomisto, J.; Koskimies, O.; Simell, O. Food and guar decrease absorption of trimethoprim. *Eur. J. Clin. Pharmacol.* **1987**, *32*, 427–429. [[CrossRef](#)]
54. Bach, M.C.; Gold, O.; Finland, M. Absorption and urinary excretion of trimethoprim, sulfamethoxazole, and trimethoprim-sulfamethoxazole: Results with single doses in normal young adults and preliminary observations during therapy with trimethoprim-sulfamethoxazole. *J. Infect. Dis.* **1973**, *128* (Suppl. 5), C84–C99. [[CrossRef](#)] [[PubMed](#)]
55. Fass, R.J.; Prior, R.B.; Perkins, R.L. Pharmacokinetics and tolerance of a single twelve-tablet dose of trimethoprim (960 mg)-sulfamethoxazole (4800 mg). *Antimicrob. Agents Chemother.* **1977**, *12*, 102–106. [[CrossRef](#)]
56. Klimowicz, A.; Nowak, A.; Kadyków, M. Plasma and skin blister fluid concentrations of trimethoprim following its oral administration. *Eur. J. Clin. Pharmacol.* **1988**, *34*, 377–380. [[CrossRef](#)] [[PubMed](#)]
57. Stevens, R.C.; Laizure, S.C.; Williams, C.L.; Stein, D.S. Pharmacokinetics and adverse effects of 20-mg/kg/day trimethoprim and 100-mg/kg/day sulfamethoxazole in healthy adult subjects. *Antimicrob. Agents Chemother.* **1991**, *35*, 1884–1890. [[CrossRef](#)]
58. Spicehandler, J.; Pollock, A.A.; Simberkoff, M.S.; Rahal, J.J. Intravenous pharmacokinetics and in vitro bactericidal activity of trimethoprim-sulfamethoxazole. *Rev. Infect. Dis.* **1982**, *4*, 562–565. [[CrossRef](#)]
59. Amini, H.; Ahmadiani, A. Rapid and simultaneous determination of sulfamethoxazole and trimethoprim in human plasma by high-performance liquid chromatography. *J. Pharm. Biomed. Anal.* **2007**, *43*, 1146–1150. [[CrossRef](#)]
60. Bruun, J.N.; Ostby, N.; Bredesen, J.E.; Kierulf, P.; Lunde, P.K. Sulfonamide and trimethoprim concentrations in human serum and skin blister fluid. *Antimicrob. Agents Chemother.* **1981**, *19*, 82–85. [[CrossRef](#)]
61. DeAngelis, D.V.; Woolley, J.L.; Sigel, C.W. High-performance liquid chromatographic assay for the simultaneous measurement of trimethoprim and sulfamethoxazole in plasma or urine. *Ther. Drug Monit.* **1990**, *12*, 382–392. [[CrossRef](#)] [[PubMed](#)]
62. Eatman, F.B.; Maggio, A.C.; Pocolinko, R.; Boxenbaum, H.G.; Geitner, K.A.; Glover, W.; Macasieb, T.; Holazo, A.; Weinfeld, R.E.; Kaplan, S.A. Blood and salivary concentrations of sulfamethoxazole and trimethoprim in man. *J. Pharmacokinet. Biopharm.* **1977**, *5*, 615–624. [[CrossRef](#)] [[PubMed](#)]
63. Flores-Murrieta, F.J.; Castañeda-Hernández, G.; Menéndez, J.C.; Chávez, F.; Herrera, J.E.; Hong, E. Pharmacokinetics of sulfamethoxazole and trimethoprim in Mexicans: Bioequivalence of two oral formulations (URO-TS D<sup>®</sup> and Bactrim F<sup>®</sup>). *Biopharm. Drug Dispos.* **1990**, *11*, 765–772. [[CrossRef](#)]
64. Gochin, R.; Kanfer, I.; Haigh, J.M. Simultaneous determination of trimethoprim, sulphamethoxazole and N4-acetylsulphamethoxazole in serum and urine by high-performance liquid chromatography. *J. Chromatogr.* **1981**, *223*, 139–145. [[CrossRef](#)]
65. Królicki, A.; Klimowicz, A.; Bielecka-Grzela, S.; Nowak, A.; Maleszka, R. Penetration of cotrimoxazole components into skin after a single oral dose. Theoretical versus experimental approach. *Pol. J. Pharmacol.* **2004**, *56*, 257–263.
66. MEDA Pharma GmbH & Co KG. *Fachinformation Cotrim-Diolan<sup>®</sup> Suspension Zum Einnehmen*; MEDA Pharma GmbH & Co. KG: Bad Homburg, Germany, 2013.
67. Mistri, H.N.; Jangid, A.G.; Pudage, A.; Shah, A.; Shrivastav, P.S. Simultaneous determination of sulfamethoxazole and trimethoprim in microgram quantities from low plasma volume by liquid chromatography–tandem mass spectrometry. *Microchem. J.* **2010**, *94*, 130–138. [[CrossRef](#)]
68. Niemi, M.; Backman, J.T.; Neuvonen, P.J. Effects of trimethoprim and rifampin on the pharmacokinetics of the cytochrome P450 2C8 substrate rosiglitazone. *Clin. Pharmacol. Ther.* **2004**, *76*, 239–249. [[CrossRef](#)]
69. Örtengren, B.; Magni, L.; Bergan, T. Development of sulphonamide-trimethoprim combinations for urinary tract infections. Part 3: Pharmacokinetic characterization of sulphadiazine and sulphamethoxazole given with trimethoprim. *Infection* **1979**, *7*, S371–S381. [[CrossRef](#)]
70. Stevens, R.C.; Laizure, S.C.; Sanders, P.L.; Stein, D.S. Multiple-dose pharmacokinetics of 12 milligrams of trimethoprim and 60 milligrams of sulfamethoxazole per kilogram of body weight per day in healthy volunteers. *Antimicrob. Agents Chemother.* **1993**, *37*, 448–452. [[CrossRef](#)]

71. Watson, I.D.; Cohen, H.N.; Stewart, M.J.; McIntosh, S.J.; Shenkin, A.; Thomson, J.A. Comparative pharmacokinetics of co-trimazole and co-trimoxazole to “steady state” in normal subjects. *Br. J. Clin. Pharmacol.* **1982**, *14*, 437–443. [CrossRef]
72. Welling, P.G.; Craig, W.A.; Amidon, G.L.; Kunin, C.M. Pharmacokinetics of trimethoprim and sulfamethoxazole in normal subjects and in patients with renal failure. *J. Infect. Dis.* **1973**, *128*, 556–566. [CrossRef] [PubMed]
73. Yoshikawa, T.T.; Guze, L.B. Concentrations of trimethoprim-sulfamethoxazole in blood after a single, large oral dose. *Antimicrob. Agents Chemother.* **1976**, *10*, 462–463. [CrossRef] [PubMed]
74. Guest, E.J.; Aarons, L.; Houston, J.B.; Rostami-Hodjegan, A.; Galetin, A. Critique of the two-fold measure of prediction success for ratios: Application for the assessment of drug-drug interactions. *Drug Metab. Dispos.* **2011**, *39*, 170–173. [CrossRef] [PubMed]
75. Susanto, M.; Benet, L.Z. Can the enhanced renal clearance of antibiotics in cystic fibrosis patients be explained by P-glycoprotein transport? *Pharm. Res.* **2002**, *19*, 457–462. [CrossRef] [PubMed]
76. Kito, T.; Ito, S.; Mizuno, T.; Maeda, K.; Kusuhara, H. Investigation of non-linear MATE1-mediated efflux of trimethoprim in the mouse kidney as the mechanism underlying drug-drug interactions between trimethoprim and organic cations in the kidney. *Drug Metab. Pharmacokinet.* **2019**, *34*, 87–94. [CrossRef] [PubMed]
77. Prasad, B.; Johnson, K.; Billington, S.; Lee, C.; Chung, G.W.; Brown, C.D.A.; Kelly, E.J.; Himmelfarb, J.; Unadkat, J.D. Abundance of drug transporters in the human kidney cortex as quantified by quantitative targeted proteomics. *Drug Metab. Dispos.* **2016**, *44*, 1920–1924. [CrossRef] [PubMed]
78. Ribera, E.; Pou, L.; Fernandez-Sola, A.; Campos, F.; Lopez, R.M.; Ocaña, I.; Ruiz, I.; Pahissa, A. Rifampin reduces concentrations of trimethoprim and sulfamethoxazole in serum in human immunodeficiency virus-infected patients. *Antimicrob. Agents Chemother.* **2001**, *45*, 3238–3241. [CrossRef]
79. Wen, X.; Wang, J.; Backman, J.T.; Laitila, J.; Neuvonen, P.J. Trimethoprim and sulfamethoxazole are selective inhibitors of CYP2C8 and CYP2C9, respectively. *Drug Metab. Dispos.* **2002**, *30*, 631–635. [CrossRef]
80. Rylance, G.W.; George, R.H.; Healing, D.E.; Roberts, D.G. Single dose pharmacokinetics of trimethoprim. *Arch. Dis. Child.* **1985**, *60*, 29–33. [CrossRef]
81. ClinCalc LLC. ClinCalc DrugStats Database. Available online: <https://clincalc.com/DrugStats/> (accessed on 30 October 2020).
82. Rowland Yeo, K.; Kenny, J.R.; Rostami-Hodjegan, A. Application of in vitro-in vivo extrapolation (IVIVE) and physiologically based pharmacokinetic (PBPK) modelling to investigate the impact of the CYP2C8 polymorphism on rosiglitazone exposure. *Eur. J. Clin. Pharmacol.* **2013**, *69*, 1311–1320.
83. Scotcher, D.; Arya, V.; Yang, X.; Zhao, P.; Zhang, L.; Huang, S.-M.; Rostami-Hodjegan, A.; Galetin, A. A novel physiologically based model of creatinine renal disposition to integrate current knowledge of systems parameters and clinical observations. *CPT Pharmacomet. Syst. Pharmacol.* **2020**, *9*, 310–321. [CrossRef] [PubMed]
84. Nakada, T.; Kudo, T.; Kume, T.; Kusuhara, H.; Ito, K. Quantitative analysis of elevation of serum creatinine via renal transporter inhibition by trimethoprim in healthy subjects using physiologically-based pharmacokinetic model. *Drug Metab. Pharmacokinet.* **2018**, *33*, 103–110. [CrossRef] [PubMed]
85. Thompson, E.J.; Wu, H.; Maharaj, A.; Edginton, A.N.; Balevic, S.J.; Cobbaert, M.; Cunningham, A.P.; Hornik, C.P.; Cohen-Wolkowicz, M. Physiologically based pharmacokinetic modeling for trimethoprim and sulfamethoxazole in children. *Clin. Pharmacokinet.* **2019**, *58*, 887–898. [CrossRef] [PubMed]
86. Lippert, J.; Burghaus, R.; Edginton, A.; Frechen, S.; Karlsson, M.; Kovar, A.; Lehr, T.; Milligan, P.; Nock, V.; Ramusovic, S.; et al. Open Systems Pharmacology Community - An open access, open source, open science approach to modeling and simulation in pharmaceutical sciences. *CPT Pharmacomet. Syst. Pharmacol.* **2019**, *8*, 878–882. [CrossRef] [PubMed]

**Publisher’s Note:** MDPI stays neutral with regard to jurisdictional claims in published maps and institutional affiliations.



© 2020 by the authors. Licensee MDPI, Basel, Switzerland. This article is an open access article distributed under the terms and conditions of the Creative Commons Attribution (CC BY) license (<http://creativecommons.org/licenses/by/4.0/>).



#### 4.3 PROJECT III - RENAL TRANSPORTER-MEDIATED DRUG-BIOMARKER INTERACTIONS OF THE ENDOGENOUS SUBSTRATES CREATININE AND N<sup>1</sup>-METHYLNICOTINAMIDE: A PBPK MODELING APPROACH

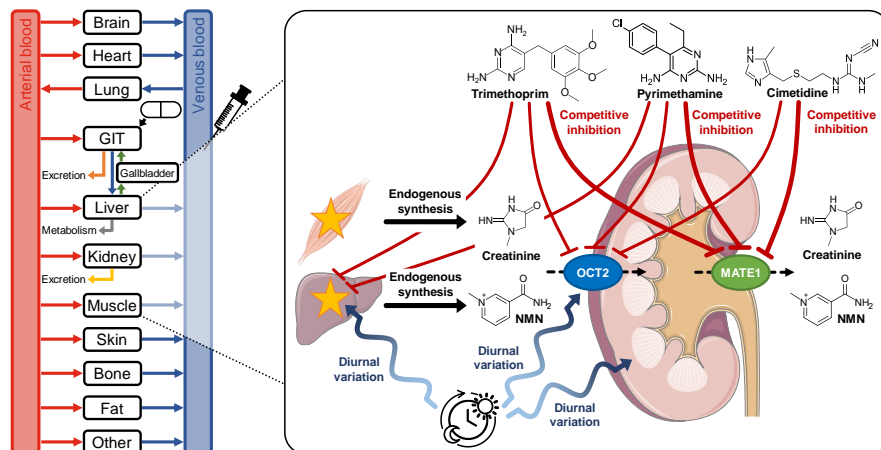


**Figure 4.3.** Whole-body physiologically based pharmacokinetic (PBPK) modeling of the endogenous organic cation transporter (OCT) 2 and multidrug and toxin extrusion protein (MATE) 1 substrates creatinine and N<sup>1</sup>-methylnicotinamide (NMN) for drug-biomarker interaction predictions, incorporating the effect of diurnal variation. Illustrations of organs were taken from Servier [5], licensed under CC BY 3.0 (<https://creativecommons.org/licenses/by/3.0/>). GIT, gastrointestinal tract.

#### Publication

Türk D, Müller F, Fromm MF, Selzer D, Dallmann R, and Lehr T. Renal transporter-mediated drug-biomarker interactions of the endogenous substrates creatinine and N<sup>1</sup>-methylnicotinamide: a PBPK modeling approach. *Clinical Pharmacology & Therapeutics*. 2022. Online ahead of print. DOI: [10.1002/cpt.2636](https://doi.org/10.1002/cpt.2636)

Publication III

#### Supplementary material

The supplementary material to this publication can be found on the accompanying compact disk or can be accessed online via: <https://ascpt.onlinelibrary.wiley.com/action/downloadSupplement?doi=10.1002%2Fcpt.2636&file=cpt2636-sup-0001-SupinfoS1.pdf>.

### Copyright

This is an open access article under the terms of CC BY-NC 4.0 (<https://creativecommons.org/licenses/by-nc/4.0/>), which permits use, distribution and reproduction in any medium, provided the original work is properly cited and is not used for commercial purposes.

© 2022 The Authors. Clinical Pharmacology & Therapeutics published by Wiley Periodicals LLC on behalf of American Society for Clinical Pharmacology and Therapeutics.

### Author contributions

Declaration of author contributions to the publication related to project III according to CRediT [4]:

Denise Feick (née Türk):	Conceptualization, Formal Analysis, Investigation, Visualization, Writing - Original Draft, Writing - Review & Editing
Fabian Müller:	Formal Analysis, Writing - Review & Editing
Martin F. Fromm:	Formal Analysis, Writing - Review & Editing
Dominik Selzer:	Formal Analysis, Writing - Review & Editing
Robert Dallmann:	Formal Analysis, Writing - Review & Editing
Thorsten Lehr:	Conceptualization, Formal Analysis, Funding Acquisition, Investigation, Writing - Review & Editing



# Renal Transporter-Mediated Drug-Biomarker Interactions of the Endogenous Substrates Creatinine and N<sup>1</sup>-Methylnicotinamide: A PBPK Modeling Approach

Denise Türk<sup>1</sup> , Fabian Müller<sup>2</sup>, Martin F. Fromm<sup>2</sup> , Dominik Selzer<sup>1</sup>, Robert Dallmann<sup>3</sup> and Thorsten Lehr<sup>1,\*</sup>

Endogenous biomarkers for transporter-mediated drug-drug interaction (DDI) predictions represent a promising approach to facilitate and improve conventional DDI investigations in clinical studies. This approach requires high sensitivity and specificity of biomarkers for the targets of interest (e.g., transport proteins), as well as rigorous characterization of their kinetics, which can be accomplished utilizing physiologically-based pharmacokinetic (PBPK) modeling. Therefore, the objective of this study was to develop PBPK models of the endogenous organic cation transporter (OCT)2 and multidrug and toxin extrusion protein (MATE)1 substrates creatinine and N<sup>1</sup>-methylnicotinamide (NMN). Additionally, this study aimed to predict kinetic changes of the biomarkers during administration of the OCT2 and MATE1 perpetrator drugs trimethoprim, pyrimethamine, and cimetidine. Whole-body PBPK models of creatinine and NMN were developed utilizing studies investigating creatinine or NMN exogenous administration and endogenous synthesis. The newly developed models accurately describe and predict observed plasma concentration-time profiles and urinary excretion of both biomarkers. Subsequently, models were coupled to the previously built and evaluated perpetrator models of trimethoprim, pyrimethamine, and cimetidine for interaction predictions. Increased creatinine plasma concentrations and decreased urinary excretion during the drug-biomarker interactions with trimethoprim, pyrimethamine, and cimetidine were well-described. An additional inhibition of NMN synthesis by trimethoprim and pyrimethamine was hypothesized, improving NMN plasma and urine interaction predictions. To summarize, whole-body PBPK models of creatinine and NMN were built and evaluated to better assess creatinine and NMN kinetics while uncovering knowledge gaps for future research. The models can support investigations of renal transporter-mediated DDIs during drug development.

## Study Highlights

### WHAT IS THE CURRENT KNOWLEDGE ON THE TOPIC?

Investigations on renal transporter-mediated drug-drug interactions (DDIs) are impeded due to challenging *in vitro* to *in vivo* translation.

### WHAT QUESTION DID THIS STUDY ADDRESS?

How can the application of a biomarker-informed approach support conventional investigation on DDIs and how can mechanistic mathematical modeling contribute to assess biomarker kinetics?

### WHAT DOES THIS STUDY ADD TO OUR KNOWLEDGE?

The endogenous biomarkers creatinine and N<sup>1</sup>-methylnicotinamide have been proposed as biomarkers to

support investigations on renal transporter-mediated DDIs. Whole-body physiologically-based pharmacokinetic models have been developed and successfully applied for interaction predictions with three established renal transporter inhibitors.

### HOW MIGHT THIS CHANGE CLINICAL PHARMACOLOGY OR TRANSLATIONAL SCIENCE?

Mechanistic pharmacokinetic modeling has been shown to support characterization of endogenous compounds and a biomarker-informed strategy for investigations on interactions might be a promising approach during drug development.

<sup>1</sup>Clinical Pharmacy, Saarland University, Saarbrücken, Germany; <sup>2</sup>Institute of Experimental and Clinical Pharmacology and Toxicology, Friedrich-Alexander-Universität Erlangen-Nürnberg, Erlangen, Germany; <sup>3</sup>Division of Biomedical Sciences, Warwick Medical School, University of Warwick, Coventry, UK. \*Correspondence: Thorsten Lehr ([thorsten.lehr@mx.uni-saarland.de](mailto:thorsten.lehr@mx.uni-saarland.de))

Received March 11, 2022; accepted April 28, 2022. doi:10.1002/cpt.2636

## ARTICLE

Endogenous compounds measured in blood or urine can serve as biomarkers, providing information about physiological and pharmacological processes. Pathophysiological conditions or interaction of a perpetrator drug with the synthesis, distribution, metabolism, or excretion of a biomarker can result in changes of plasma, tissue, or urine levels. Measuring biomarkers can complement investigations on drug-drug interactions (DDIs) by broadening and augmenting the understanding of underlying interaction mechanisms, thus, estimating DDI risks in early-stage *in vivo* studies and supporting study planning and prioritization.<sup>1</sup> Mathialagan *et al.*<sup>2</sup> pointed out challenges of *in vitro-in vivo* translation for renal transporter-mediated DDIs and emphasized the need for a biomarker-informed strategy to improve DDI risk predictions from *in vitro* data. For the renal organic cation secretion axis, represented by consecutive action of organic cation transporter (OCT)2 and multidrug and toxin extrusion proteins (MATEs),<sup>3</sup> two endogenous compounds have been identified as potential biomarkers to investigate interactions: creatinine and N<sup>1</sup>-methylnicotinamide (NMN).<sup>4</sup> Creatinine, a breakdown product of muscle creatine, is mainly excreted passively via glomerular filtration, but 10–40% are actively secreted,<sup>5</sup> mainly by OCT2 and MATEs,<sup>6</sup> whereas no metabolism of creatinine has been described previously. NMN, a molecule formed during tryptophan and vitamin B3 metabolism, is metabolized via aldehyde oxidase (AOX)<sup>7</sup> and passively renally cleared as well as actively transported into urine by OCT2 and MATEs.<sup>8,9</sup> NMN renal clearance is concentration-dependent comparing intravenous administration to endogenously synthesized NMN, attributed to saturable reabsorption from urine.<sup>10</sup>

When identifying and selecting a biomarker for interaction studies, various factors need to be considered, such as sensitivity, specificity, predictivity, robustness, and ease of accessibility.<sup>11,12</sup> Furthermore, biomarkers need to be well-characterized regarding their kinetics, including their endogenous synthesis, active transport, and metabolic transformation. However, detailed information on these processes is often lacking (e.g., due to the complex interplay of transport and metabolism as well as requirements for dedicated studies and analytical procedures<sup>12,13</sup>). Here, physiologically-based pharmacokinetic (PBPK) modeling can help to support investigations on endogenous compounds and to gain a mechanistic understanding of the underlying kinetics.<sup>12</sup> Over the past years, PBPK modeling has become an increasingly important tool during drug development,<sup>14</sup> and has shown its strengths and advantages (e.g., in accurately describing and predicting (pharmacokinetic) of victims during perpetrator co-administration<sup>15</sup> or in assessing the influence of genetic polymorphisms<sup>16</sup>). Furthermore, PBPK models have proven their capability for hypothesis testing (e.g., regarding causes for altered renal transport of drugs in patients with chronic kidney disease<sup>17</sup>). For endogenous biomarkers, there are examples of successfully utilizing PBPK models, to assess and understand transporter-mediated interactions using coproporphyrin I or creatinine.<sup>18-23</sup> However, there is still an apparent lack of PBPK models for endogenous compounds to overcome,<sup>12</sup> in particular for renal OCT2/MATE substrates.

Biomarker PBPK models can support investigations on transporter-mediated DDIs. A PBPK model for an investigational

drug (and potential OCT2 and/or MATE inhibitor) can be linked with biomarker PBPK models in early clinical phases during drug development, to assess the interaction potential. For instance, inhibitory constant ( $K_i$ ) values from *in vitro* tests can be implemented and model predictions can be compared with biomarker plasma and clearance measurements from phase I studies, to complement the workflow for utilization of endogenous biomarkers in drug development, as proposed by Mathialagan *et al.*<sup>2</sup> This includes assessing the influence of a new drug on biomarker renal clearance before performing a metformin DDI study, if *in vitro* inhibition studies hint toward OCT2 and/or MATE inhibition potential.

The objectives of this study were (1) to develop whole-body PBPK models of the endogenous biomarkers creatinine and NMN that mechanistically describe their absorption, synthesis, metabolic transformation, and active transport also considering causes of observed diurnal variation, and (2) to test the ability of the newly developed models to adequately describe drug-biomarker interactions (DBIs) with the potent OCT2 and MATE inhibitors trimethoprim, pyrimethamine, and cimetidine,<sup>24</sup> by coupling the biomarker models to already evaluated and published perpetrator models within a PBPK DDI/DBI modeling network.<sup>17,25,26</sup>

## METHODS

## Software

PBPK models of creatinine and NMN were developed using the PK-Sim and MoBi modeling software suite (Open Systems Pharmacology Suite 9.1, [www.open-systems-pharmacology.org](http://www.open-systems-pharmacology.org)). Plasma and urine measurements from literature were digitized with Engauge Digitizer 10.12 (M. Mitchell<sup>27</sup>) according to best practices.<sup>28</sup> Model parameter optimization and sensitivity analysis were performed within MoBi. Calculation of (pharmacokinetic) parameters, quantitative model performance analysis, and generation of plots were accomplished using the statistical programming language R 4.1.1 (The R Foundation for Statistical Computing, Vienna, Austria) and RStudio 1.4.1717 (RStudio, Boston, MA).

## PBPK model building

An extensive literature search was performed to gather physicochemical information about creatinine and NMN as well as information about important kinetic processes, such as absorption, synthesis, distribution, metabolism, and excretion (compound-dependent parameters). Additionally, studies reporting human blood and urine measurements after intravenous and oral administration in single- and multiple-dose regimens were collected alongside concentration measurements of endogenous creatinine and NMN. For creatinine, studies investigating its kinetics after ingestion of cooked meat were also included by calculating creatinine intake from the amount of ingested meat considering the animal source and method of preparation (e.g., 1.5 mg creatinine per gram of boiled beef<sup>29</sup>). Profiles extracted from clinical studies were digitized and subsequently divided into a training dataset for model building and a test dataset for model evaluation. Data for model building were selected to include plasma and urine measurements after exogenous administration of different doses and regimens of creatinine or NMN (corrected for endogenous levels) as well as endogenous concentrations. Virtual twins of (mean) study subjects were created with demographic information taken from the respective study reports. Detailed information about virtual individuals and system-dependent parameters is provided in **Supplementary Section S1.1**. Endogenous synthesis of creatinine and NMN was implemented in the respective organs in agreement with literature reports. Diurnal variation of kidney-related processes has been recently observed to affect the pharmacokinetics of the renal transporter



substrate metformin (D. Türk *et al.*, unpublished data) and was therefore implemented for both creatinine and NMN (**Supplementary Section S1.1**). Creatinine and NMN model parameters which could not be based on published values, were optimized by fitting training simulations to their respective observed data. Details on parameter optimizations are provided in **Supplementary Section S1.1**.

### PBPK model evaluation

Creatinine and NMN model performances were evaluated by comparison of predicted to observed plasma concentration-time and urine profiles as well as by goodness-of-fit plots. Quantitative model performance was evaluated by calculating mean relative deviations of predicted plasma concentrations and urinary excretion rates ( $Ae_{urine}$  rates) as well as geometric mean fold errors (GMFEs) of predicted area under the concentration-time curve calculated from the time of compound administration (or first data sampling point) to the time of the last concentration measurement ( $AUC_{last}$ ) and maximum plasma concentration ( $C_{max}$ ) values, amounts excreted unchanged in urine ( $Ae_{urine}$ ) and renal clearances, as described elsewhere.<sup>17,25</sup> Local sensitivity analyses were performed for the creatinine and NMN models to investigate the impact of single parameter changes on predicted  $AUC_{last}$  values.

### Drug-biomarker interaction modeling

Models of trimethoprim,<sup>25</sup> pyrimethamine,<sup>26</sup> and cimetidine<sup>17</sup> have been recently or, in the case of pyrimethamine, during this analysis (**Supplementary Section S5**), successfully applied to predict DDIs with the OCT1, OCT2, and MATE substrate metformin using interaction parameters from the literature. Hence, these models were considered eligible for interaction predictions with the newly developed creatinine and NMN models. Model parameters are reproduced in **Tables S18, S21, S28, and S32**.

DBI model performances were evaluated by comparison of predicted to observed plasma concentration-time or urine profiles before and during, or without and with perpetrator drug administration, depending on the

respective observed dataset. Furthermore, comparison of predicted to observed DBI  $AUC_{last}$ ,  $C_{max}$ , and urinary excretion ratios, calculated as ratio of the respective DBI kinetic parameter to the respective control kinetic parameter, was displayed in goodness-of-fit plots and GMFEs were calculated as quantitative measures.

## RESULTS

### Creatinine PBPK model building and evaluation

A total of 26 studies were included to develop a whole-body creatinine PBPK model, covering creatinine kinetics of endogenous creatinine as well as kinetics after intravenous and oral administration and after dietary meat consumption. All clinical studies used for model building and evaluation are listed in **Table S2**.

The final creatinine PBPK model covers its synthesis in muscle cells (individually optimized for each study, range synthesis rate ( $R_{syn}$ ) 6.50–11.88  $\mu\text{mol}/\text{min}$ ; **Table S5**) based on endogenously synthesized creatinine. Creatinine is mainly excreted passively via glomerular filtration, but to a lower extent actively secreted by sequential action of OCT2 and MATE1. Tubular secretion accounts for about 17% of renal clearance in the model. This is in accordance with the literature, which reports a contribution of tubular secretion by 10–40% to renal creatinine clearance ( $CL_{cr}$ ).<sup>5</sup> An increase in serum creatinine by meat ingestion has been shown by several studies, being most pronounced for cooked beef.<sup>30</sup> For instance, ingestion of 225 g cooked beef corresponds to about 340 mg creatinine<sup>29</sup> and leads to a transient increase in plasma creatinine by 40%,<sup>31</sup> which was reproduced by the model. Observed intraday variation of creatinine plasma concentrations was described by diurnal renal excretion comprising diurnal glomerular filtration rate (GFR), renal blood flow, and OCT2

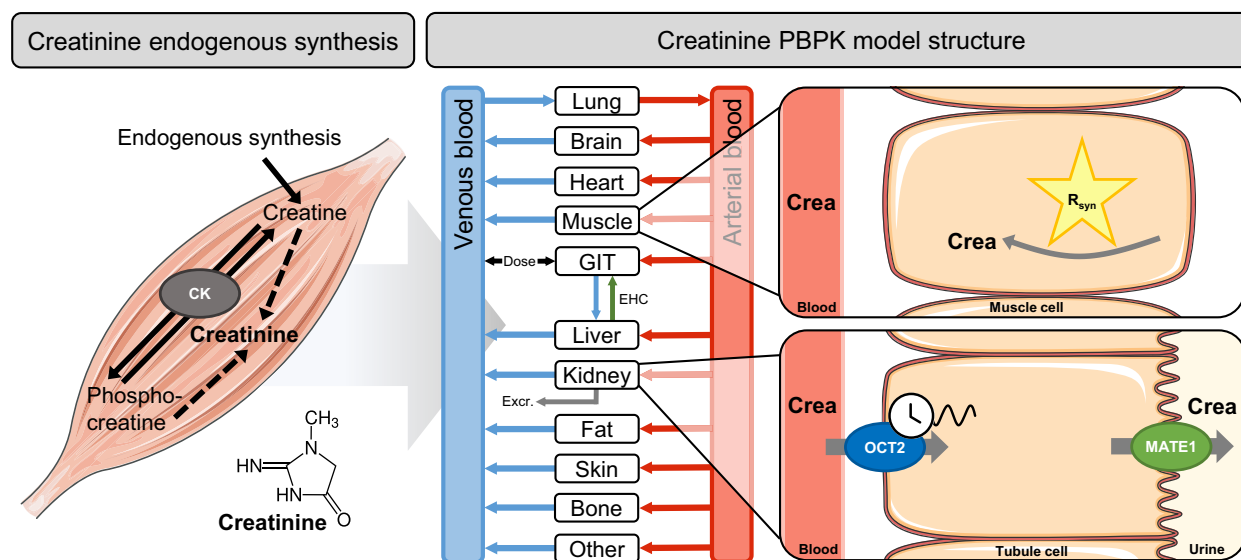


**Figure 1** Synthesis of endogenous creatinine and whole-body physiologically-based pharmacokinetic (PBPK) model processes. Creatinine is formed as breakdown product during reaction of creatine to phosphocreatine and vice versa via creatine kinase (CK). The creatinine PBPK model includes creatinine synthesis in muscle cells (implemented as  $R_{syn}$ , synthesis rate) and renal excretion, passively via glomerular filtration (not shown) and actively via consecutive action of organic cation transporter (OCT)2 and multidrug and toxin extrusion protein (MATE)1 in tubule epithelial cells. Diurnal rhythm is implemented for glomerular filtration rate (GFR), renal blood flow (both not shown) and OCT2 activity (clock symbol). Drawings by Servier, licensed under CC BY 3.0.<sup>44</sup> Crea, creatinine; EHC, enterohepatic circulation; excr., excretion; GIT, gastrointestinal tract.

## ARTICLE

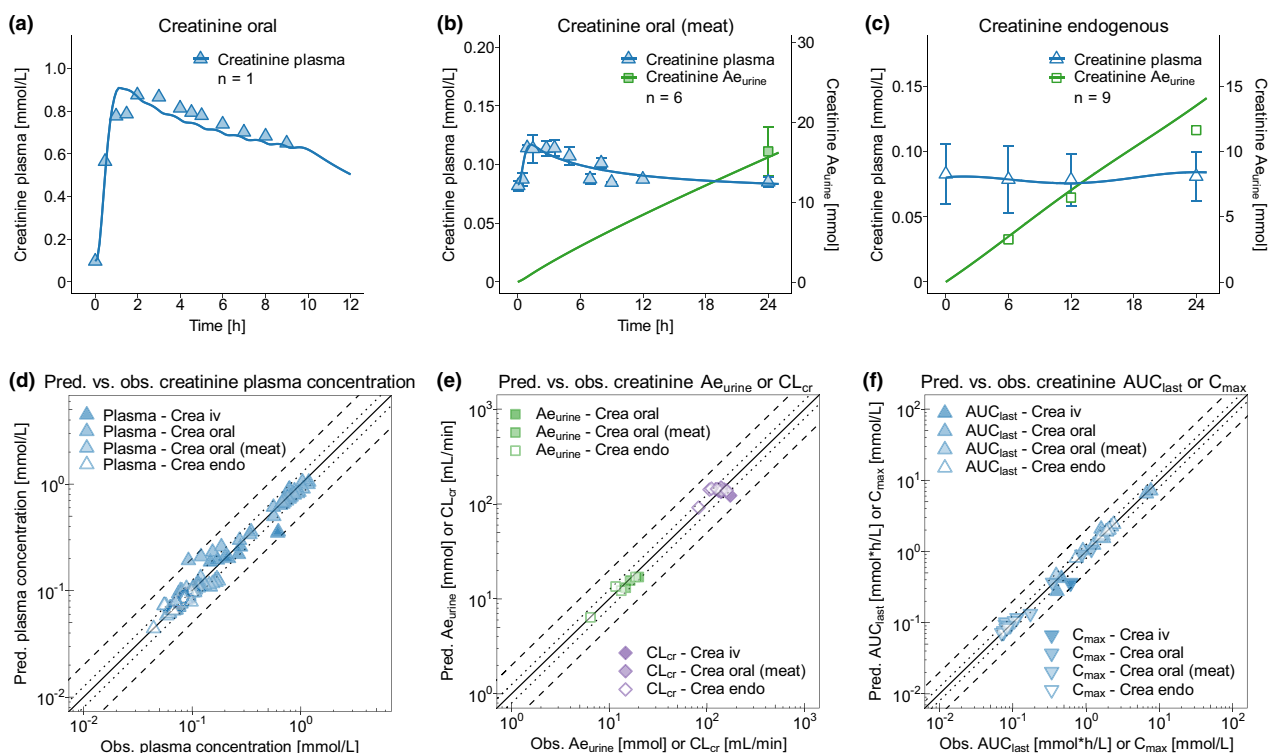


**Figure 2** Creatinine physiologically-based pharmacokinetic (PBPK) model performance. Predictions of creatinine (a–c) plasma concentration-time (blue) and cumulative amount excreted unchanged in urine ( $Ae_{urine}$ , green) profiles compared with observed data of representative studies<sup>31,45,46</sup> of exogenous creatinine application **a** initial oral dose of 8 g creatinine followed by 0.5 g every hour; **b** ingestion of 225 g cooked beef, or **c** endogenous measurements. Time refers to the time after dose (exogenous) or time after first concentration measurement (endogenous). Goodness-of-fit plots showing predicted compared with observed creatinine (d) plasma concentration, (e)  $Ae_{urine}$  and renal creatinine clearance ( $CL_{cr}$ ) and (f) area under the concentration-time curve ( $AUC_{last}$ ) and maximum plasma concentration ( $C_{max}$ ) values of all studies used for model building and evaluation. The solid line marks the line of identity and dotted lines indicate 1.25-fold and dashed lines indicate 2-fold deviation. Data are shown as blue triangles (plasma), green squares ( $Ae_{urine}$ ), and purple diamonds ( $CL_{cr}$ ); filled symbols indicate creatinine administration, empty symbols indicate endogenous creatinine. Details on the clinical studies and individual values alongside mean relative deviations (MRDs) and geometric mean fold errors (GMFEs) are provided in **Supplementary Section S2**. Crea, creatinine; endo, endogenous; iv, intravenous; n, number of individuals studied; obs., observed; pred., predicted.

activity. An overview of the creatinine synthesis, model structure, and implemented kinetic processes is illustrated in **Figure 1**. Creatinine compound-dependent model parameters are summarized in **Table S3**.

Representative creatinine plasma concentration-time and  $Ae_{urine}$  profiles are shown in **Figure 2a–c**, demonstrating the good performance of the creatinine model. Profiles of all studies are provided in **Supplementary Section S2.2**. Comparison of predicted to observed creatinine plasma concentration,  $Ae_{urine}$ ,  $CL_{cr}$ ,  $AUC_{last}$ , and  $C_{max}$  values in goodness-of-fit plots further underlines the good performance of the creatinine model with all predictions within twofold of observed values (**Figure 2d–f**). A local sensitivity analysis revealed that simulations of creatinine are sensitive to the fraction unbound in plasma (literature value), GFR (calculated), and creatinine  $R_{syn}$  (optimized).

### NMN PBPK model building and evaluation

A total of 11 studies was used to develop a whole-body NMN PBPK model, covering NMN kinetics after intravenous administration and endogenous NMN. All clinical studies used for model building and evaluation are listed in **Table S10**.

The final NMN PBPK model covers synthesis in liver cells (individually optimized for each study; **Table S13**), metabolism via AOX1 as well as glomerular filtration and active transport into urine by OCT2 and MATE1. Furthermore, a saturable tubular re-absorption process has been implemented as efflux transport at the basolateral site of tubule cells, whereas Michaelis-Menten and transport rate constants were inferred from high (intravenous administration) and low (baseline) NMN plasma levels and the corresponding urinary excretion rates. For an intravenous administration of 224 mg NMN, the model predicts a metabolized fraction of about 40% compared with 33% reported in literature.<sup>32</sup> Regarding endogenously synthesized NMN, renal clearance accounts for 18–36% of total clearance (depending on the daytime), which is in accordance with the observed data, where 35% of NMN and its carboxamide metabolites in urine are unchanged NMN.<sup>7</sup> Observed intraday variation of NMN plasma concentrations was described by a combination of diurnal NMN synthesis and renal excretion comprising diurnal GFR, renal blood flow, and OCT2 activity, using a modified equation<sup>33</sup> for NMN  $R_{syn}$  (**Supplementary Section S1.1**). An overview of the NMN synthesis, model structure, and implemented kinetic processes is

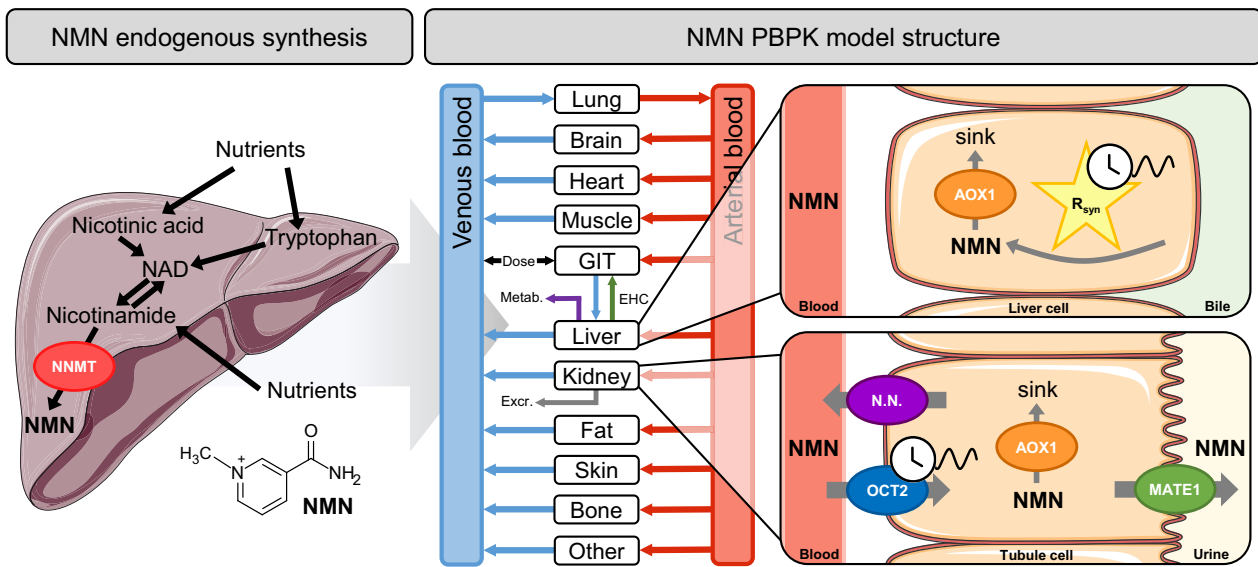


**Figure 3** Synthesis of endogenous N<sup>1</sup>-methylnicotinamide (NMN) and whole-body physiologically-based pharmacokinetic (PBPK) model processes. NMN is synthesized from nutrients via various intermediates. The direct precursor nicotinamide is converted to NMN via nicotinamide N-methyltransferase (NNMT), which is mainly expressed in liver cells.<sup>47</sup> The NMN PBPK model covers NMN synthesis in the liver (implemented as  $R_{syn}$ , synthesis rate) and metabolism by aldehyde oxidase (AOX)1, where resulting carboxamide metabolites are not included in the model (“sink” process). NMN is passively excreted in urine via glomerular filtration (not shown), actively secreted via organic cation transporter (OCT)2 and multidrug and toxin extrusion protein (MATE)1 and re-absorbed from urine via a saturable process (“N.N.”), implemented at the basolateral site of tubule cells. Diurnal rhythm is implemented for glomerular filtration rate (GFR), renal blood flow (both not shown), OCT2 activity, and NMN  $R_{syn}$  (clock symbols). Drawings by Servier, licensed under CC BY 3.0.<sup>44</sup> EHC, enterohepatic circulation; excr., excretion; GIT, gastrointestinal tract; metab., metabolism, NAD, nicotinamide adenine dinucleotide.

illustrated in **Figure 3**. NMN compound-dependent model parameters are summarized in **Table S11**.

Representative NMN plasma concentration-time,  $Ae_{urine}$  rate and  $Ae_{urine}$  profiles are shown in **Figure 4a–c**, demonstrating the good performance of the NMN model. Profiles of all studies are provided in **Supplementary Section S3.2**. Comparison of predicted to observed NMN plasma concentration,  $Ae_{urine}$  rate and  $Ae_{urine}$  and  $AUC_{last}$  and  $C_{max}$  values in goodness-of-fit plots further underlines the good performance of the NMN model with about 90% of predictions within twofold of observed values (**Figure 4d–f**). A local sensitivity analysis revealed that both simulations of intravenously administered and endogenous NMN are sensitive to the fraction unbound in plasma (literature value) and simulations of endogenous NMN are sensitive to OCT2 activity (optimized), AOX1 clearance (optimized), and organ permeability (calculated).

#### Drug-biomarker interaction modeling

A renal transporter DBI network was established (**Figure 5**) by linking the biomarker models with models of trimethoprim, pyrimethamine, and cimetidine. Specifically, OCT2 competitive inhibition was modeled with literature  $K_i$  values of 47.8  $\mu\text{mol/L}$ , 0.61  $\mu\text{mol/L}$ , and 124  $\mu\text{mol/L}$ , and MATE1 competitive inhibition was modeled with literature  $K_i$  values of 4.45  $\mu\text{mol/L}$ , 0.02  $\mu\text{mol/L}$ , and 3.80  $\mu\text{mol/L}$  for trimethoprim, pyrimethamine, and cimetidine, respectively (**Tables S18, S21, S32**). For all perpetrators, the same inhibition constants were used as for previous interaction predictions with metformin.

To evaluate the drug-creatinine interactions, eight, three and two studies with trimethoprim, pyrimethamine, and cimetidine, respectively, have been utilized and are listed in **Tables S34, S37, and S40**. During administration of trimethoprim, pyrimethamine, and cimetidine, an increase in serum creatinine and a decrease of creatinine  $Ae_{urine}$  and  $CL_{cr}$  has been observed. This kinetic interaction can be attributed to inhibition of tubular secretion of creatinine. Observed plasma concentration-time and urine profiles are well-described, indicating a good drug-creatinine interaction model performance. Representative predicted creatinine profiles before and during trimethoprim or cimetidine and without and with pyrimethamine compared with observed data are shown in **Figure 6**. Plots of all profiles are provided in **Supplementary Section S7**.

Predicted DBI  $AUC_{last}$ ,  $C_{max}$ ,  $Ae_{urine}$ , and  $CL_{cr}$  ratios are all within twofold of observed ratios and within prediction limits proposed by Guest *et al.*<sup>34</sup> (**Figure 6**). Corresponding values for all clinical studies are provided in **Tables S35, S36, S38, S39, and S41**, including calculated overall GMFEs.

To model the drug-NMN interactions, one trimethoprim and two pyrimethamine studies were incorporated and are listed in **Tables S42 and S46**. During administration of trimethoprim and pyrimethamine, a decrease of NMN  $Ae_{urine}$  has been observed, resulting from inhibition of NMN transport by OCT2 and MATE1, which the model was able to (partially) reproduce. Conversely, NMN plasma concentration time profiles during trimethoprim and pyrimethamine interaction result in lower mean NMN concentrations compared with control profiles<sup>8,9,35</sup> and

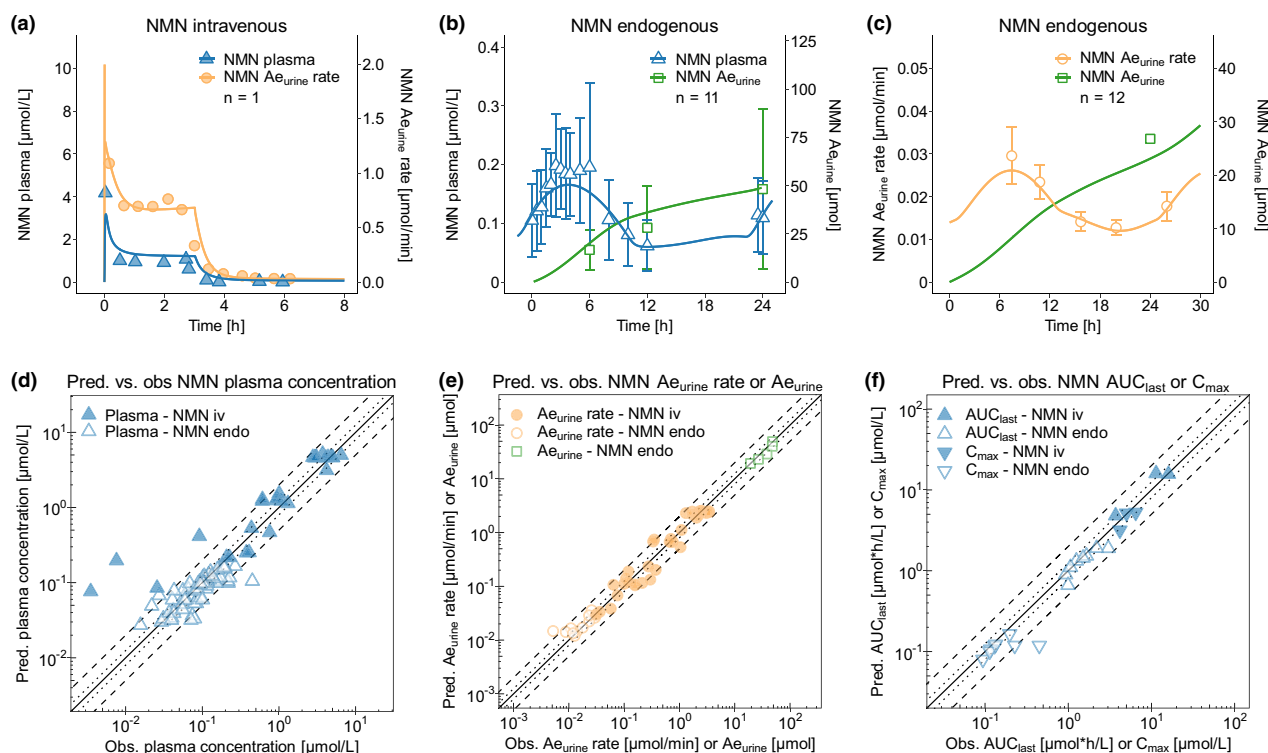


**Figure 4**  $N^1$ -methylnicotinamide (NMN) physiologically-based pharmacokinetic (PBPK) model performance. Predictions of NMN (a–c) plasma concentration-time (blue), urinary excretion rate ( $Ae_{urine}$  rate, orange), and cumulative amount excreted unchanged in urine ( $Ae_{urine}$ , green) profiles compared with observed data of representative studies<sup>7,9,10</sup> of a intravenous NMN administration of 8.3 mg loading dose followed by a 30.9 mg 3-hour infusion or b and c endogenous measurements. Time refers to the time after dose (exogenous) or time after first concentration measurement (endogenous). Goodness-of-fit plots showing predicted compared with observed NMN (d) plasma concentration, (e)  $Ae_{urine}$  and  $Ae_{urine}$  rate, and (f) area under the concentration-time curve ( $AUC_{last}$ ) and maximum plasma concentration ( $C_{max}$ ) values of all studies used for model building and evaluation. The solid line marks the line of identity and dotted lines indicate 1.25-fold and dashed lines indicate 2-fold deviation. Data are shown as blue triangles (plasma), orange dots ( $Ae_{urine}$  rate), and green squares ( $Ae_{urine}$ ); filled symbols indicate NMN administration, and empty symbols indicate endogenous NMN. Details on the clinical studies and individual values alongside mean relative deviations (MRDs) and geometric mean fold errors (GMFEs) are provided in **Supplementary Section S3**. Endo, endogenous; iv, intravenous;  $n$ , number of individuals studied; obs., observed; pred. predicted.

also an apparently decreased diurnal variation. The mechanisms underlying these observations have not been described. Thus, it was hypothesized that trimethoprim and pyrimethamine inhibit nicotinamide N-methyltransferase (NNMT), and, hence, NMN synthesis. Consequently, an additional inhibition process of NMN  $R_{syn}$  was implemented (equation provided in **Supplementary Section S1.3**). After applying this hypothetical NNMT inhibition using optimized values for the inhibitory constant of NMN synthesis ( $K_{i, syn}$ ), with  $K_{i, syn} = 32.61 \mu\text{mol/L}$  and  $K_{i, syn} = 1.39 \mu\text{mol/L}$  for trimethoprim and pyrimethamine, respectively, in addition to inhibition of OCT2 and MATE1, urine and plasma-concentration-time profiles were well described, indicating a good drug-NMN interaction model performance. Representative predicted NMN profiles without and with inhibitor compared with observed data are shown in **Figure 7**. Plots of profiles are provided in **Supplementary Section S8**.

Predicted DBI  $AUC_{last}$ ,  $C_{max}$ , and  $Ae_{urine}$  ratios are all within twofold of observed ratios and within prediction limits proposed by Guest *et al.*<sup>34</sup> (**Figure 7**). Corresponding values for all clinical studies are provided in **Tables S43, S44, S45, S47, S48, and S49**, including calculated overall GMFEs.

## DISCUSSION

Whole-body PBPK models of the endogenous OCT2 and MATE1 substrates creatinine and NMN were built and thoroughly evaluated, accurately simulating and predicting plasma as well as urine profiles of both compounds. Two important scenarios were evaluated: (1) simulation and prediction of endogenous baseline creatinine and NMN as well as (2) creatinine and NMN kinetics after exogenous intake and administration. For this, PBPK models implemented relevant metabolism and transport processes and covered the influence of diurnal rhythm on significant physiological processes. These models have been successfully applied to simulate and predict the fate of creatinine and NMN during administration of trimethoprim, pyrimethamine, and cimetidine, focusing on renal transporter inhibition.

Since creatinine concentrations are not only affected by (co-)administered drugs, but also by important covariates, such as sex, age, body and muscle mass, diet, and disease state,<sup>36</sup> a holistic pharmacokinetic modeling approach is required to incorporate these factors. In lieu of previously published creatinine PBPK models that only focused on a specific topic (e.g., prediction of creatinine transporter

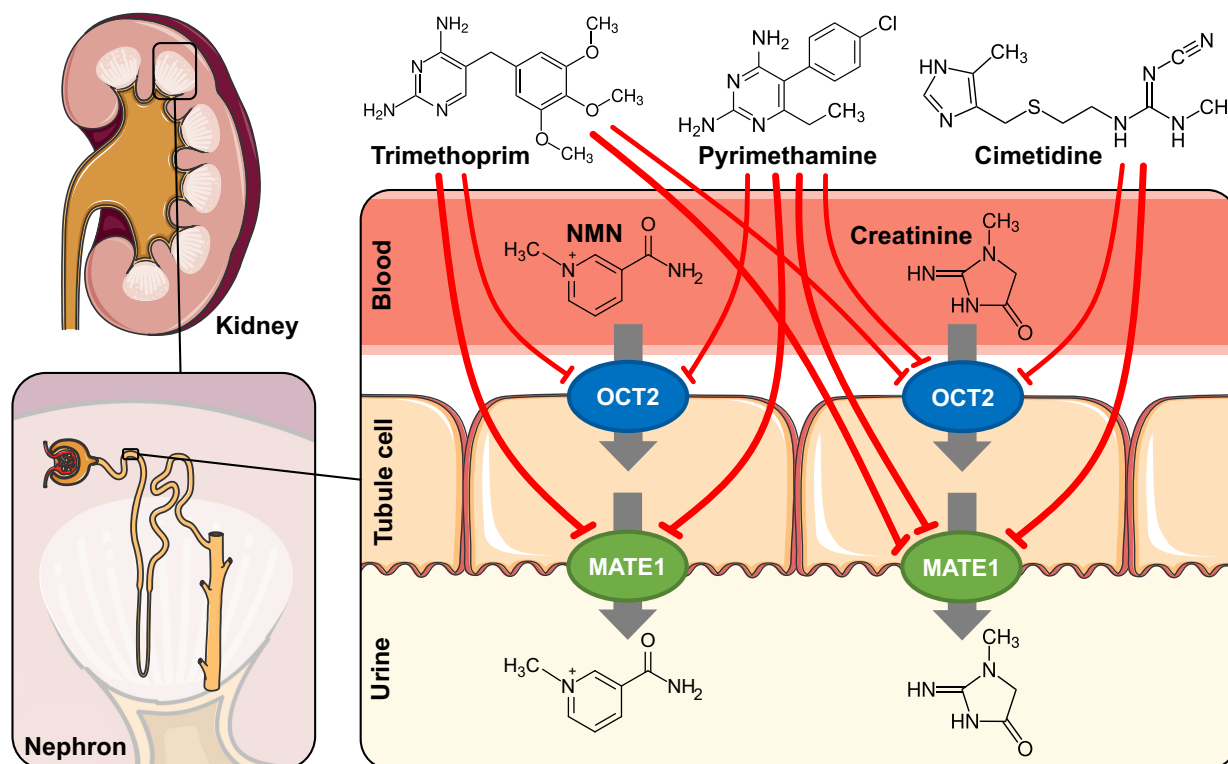


**Figure 5** Renal transporter drug-biomarker interaction network. Creatinine and N<sup>1</sup>-methylnicotinamide (NMN) are actively secreted into urine by sequential action of organic cation transporter (OCT)2, an influx transporter located at the basolateral membrane of proximal tubule epithelial cells, and multidrug and toxin extrusion protein (MATE)1, an efflux transporter located at the apical site of the same cells. Trimethoprim, pyrimethamine, and cimetidine are competitive inhibitors of OCT2 and MATE1, resulting in decreased renal excretion of creatinine and NMN. Gray arrows represent active transport, and red lines indicate transporter inhibition. Drawings by Servier, licensed under CC BY 3.0.<sup>44</sup>

interactions<sup>20-23</sup> or creatinine in chronic kidney disease<sup>37</sup>), the presented whole-body PBPK model is the first to mechanistically describe creatinine synthesis in muscle cells with respect to varying muscle mass while incorporating diurnal renal elimination as well as renal transporter-mediated DBIs. Optimized values for creatinine synthesis in muscle cells exhibit a large intra- and interstudy variability, which is plausible due to the influence of the aforementioned covariates. Moreover, the effect of a creatinine-rich diet on plasma levels and urinary excretion is covered by the model, allowing simulation of creatinine kinetics after ingestion of differently prepared meat meals. Creatinine intake was implemented as an oral solution by calculating the ingested amount from the meal-specific creatinine content informed by the literature.<sup>29</sup> For this, creatinine must be absorbed from the gastrointestinal tract. Due to its hydrophilic properties, creatinine has been discussed as organic cation and anion transporter substrate,<sup>6</sup> which might also be relevant for the intestinal barrier. A significant increase in intestinal permeability has been observed after fitting simulations regarding oral creatinine intake in comparison to quantitative structure-activity relationship estimated permeability and might hint toward additional unspecified transport processes in the gut. At the renal barrier, organic anion transporter (OAT)2, OCT2, MATE1, and MATE2-K have been shown to transport creatinine *in vitro*<sup>6</sup> with OAT2 also discussed to be involved in creatinine re-absorption.<sup>38</sup> However, only

tubular secretion via OCT2 and MATE1 has been implemented in the model, as they show the most pronounced creatinine uptake *in vitro*.<sup>6</sup> Furthermore, a distinction between two transporters at the same membrane (i.e., OAT2 and OCT2), is challenging without knowledge of the amount transported and MATE2-K expression is controversial, as in a recent study, MATE2-K was below the lower limit of quantification in human kidneys.<sup>39</sup>

For the transporter substrate metformin, which is exclusively renally excreted, about 75% of clearance can be attributed to active secretion,<sup>2</sup> and diurnal variation of GFR, renal blood flow, and OCT2 activity have been observed to affect metformin pharmacokinetics (D. Türk *et al.*, unpublished data). As the same renal excretion axis is also relevant for creatinine, insights from metformin were transferred to the biomarker model. For creatinine, diurnal variation observed in plasma can be fully explained by varying GFR and renal blood flow, whereas only a neglectable amount can be attributed to varying OCT2 activity. This is in accordance with literature, as a much smaller extent of creatinine is actively secreted compared with metformin.<sup>2</sup> Fluctuation in creatinine synthesis attributed to varying activity of creatine kinase (e.g., due to physical activity<sup>40</sup>) might contribute to observed intraday variation in plasma concentrations and modeled diurnal synthesis showed expected plasma level pattern. However, varying GFR and renal blood flow already lead to an adequate description of observed data with parametrization derived

## ARTICLE

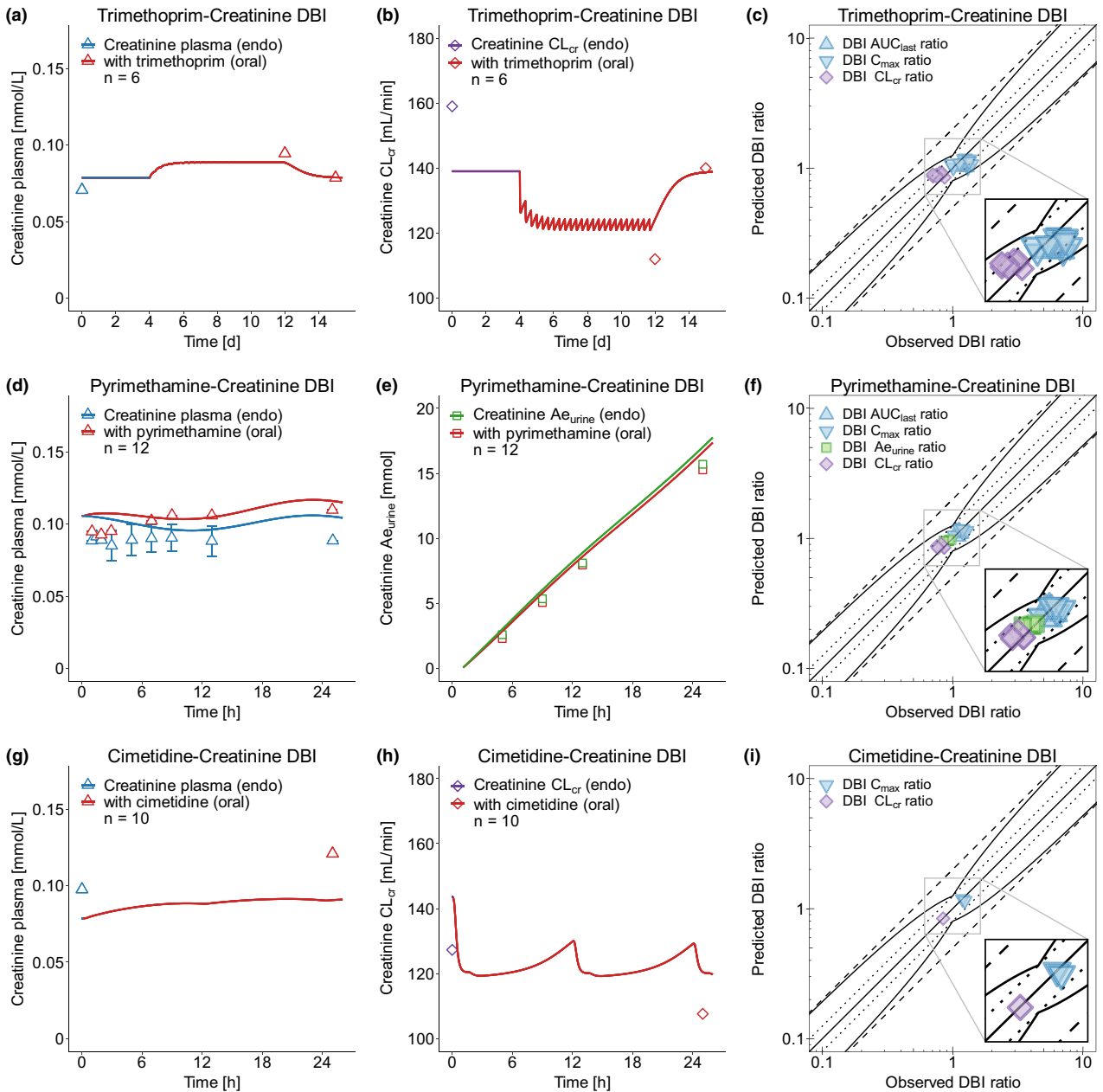


**Figure 6** Drug-creatinine interaction model performance. Predictions of creatinine plasma concentration-time (blue), renal creatinine clearance ( $CL_{cr}$ , purple), and cumulative amount excreted unchanged in urine ( $Ae_{urine}$ , green) profiles of the (a, b) trimethoprim-creatinine, (d, e) pyrimethamine-creatinine, and (g, h) cimetidine-creatinine interactions, compared with observed data.<sup>35,48,49</sup> Predictions are shown as lines. Predicted compared with observed DBI area under the concentration-time curve ( $AUC_{last}$ ), maximum plasma concentration ( $C_{max}$ ),  $Ae_{urine}$ , and  $CL_{cr}$  ratios of all clinical studies used are shown to evaluate the performance of the (c) trimethoprim-creatinine, (f) pyrimethamine-creatinine, and (i) cimetidine-creatinine interaction models. The straight solid line marks the line of identity and the curved solid lines show the DBI prediction acceptance limits proposed by Guest *et al.*<sup>34</sup> Dotted lines indicate 1.25-fold and dashed lines indicate 2-fold deviation. Data are shown as blue triangles (DBI  $AUC_{last}$  and  $C_{max}$  ratios), green squares (DBI  $Ae_{urine}$  ratios) or purple diamonds (DBI  $CL_{cr}$  ratios). Details on the study protocols, model simulations and individual DBI  $AUC_{last}$ ,  $C_{max}$ ,  $Ae_{urine}$ , and  $CL_{cr}$  ratios of all clinical studies used to evaluate the DBI performance of the creatinine model are provided in **Supplementary Section S7**. DBI, drug-biomarker interaction; endo, endogenous;  $n$ , number of individuals studied.

from previously reported values. Therefore, diurnal synthesis has not been implemented in the final model.

The implementation of only two renal transporters for tubular secretion might limit the creatinine model regarding physiological

precision, which could be overcome by further research in this area, especially regarding transporters involved in re-absorption. Moreover, the number of well-controlled creatinine studies, especially with nonaggregated data, is limited and many older studies,

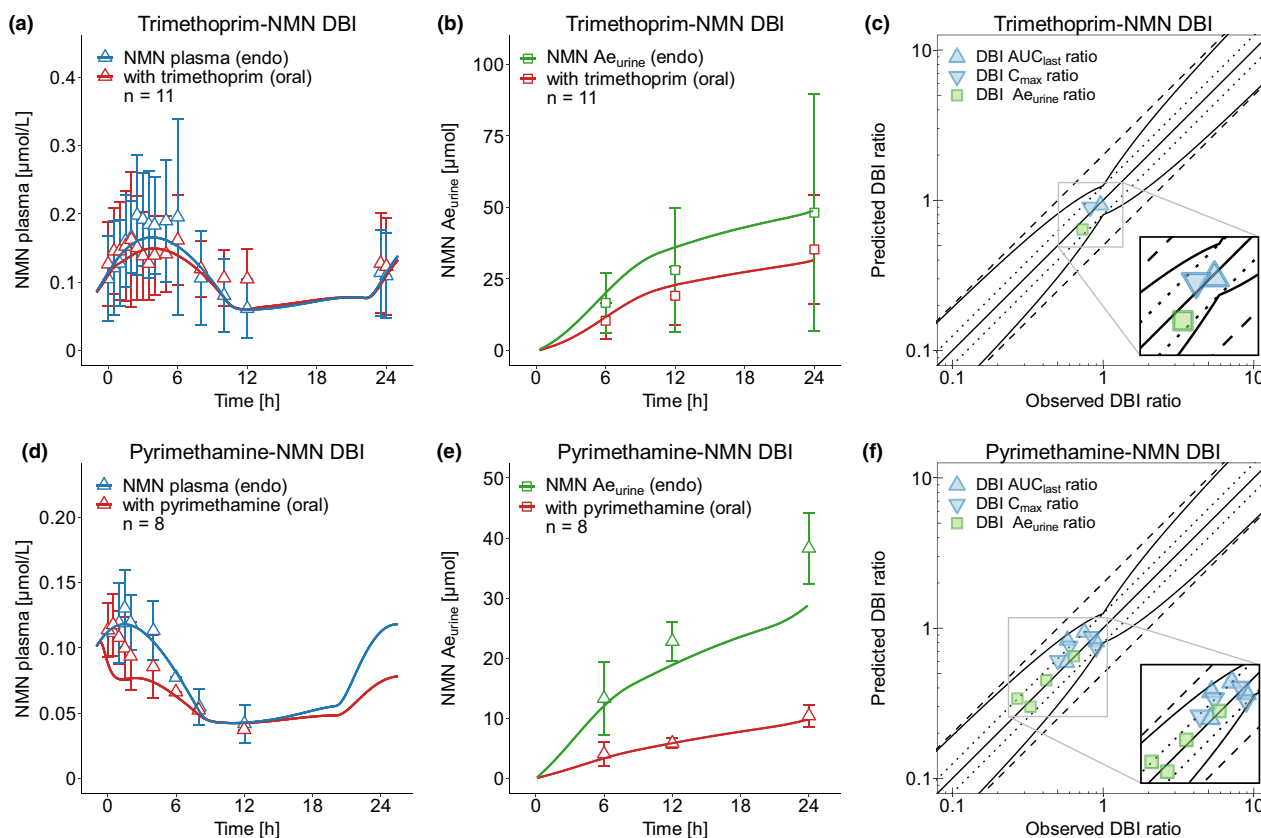


**Figure 7** Drug- $N^1$ -methylnicotinamide (NMN) interaction model performance. Predictions of NMN plasma concentration-time (blue) and cumulative amount excreted unchanged in urine ( $Ae_{urine}$ , green) profiles of the (a, b) trimethoprim-NMN and (d, e) pyrimethamine-NMN interactions, compared with observed data.<sup>8,9</sup> Predictions are shown as lines. Predicted compared with observed DBI area under the concentration-time curve ( $AUC_{last}$ ), maximum plasma concentration ( $C_{max}$ ), and  $Ae_{urine}$  ratios of all clinical studies used are shown to evaluate the performance of the (c) trimethoprim-NMN and (f) pyrimethamine-NMN interaction models. The straight solid line marks the line of identity and the curved solid lines show the DBI prediction acceptance limits proposed by Guest *et al.*<sup>34</sup> Dotted lines indicate 1.25-fold and dashed lines indicate 2-fold deviation. Data are shown as blue triangles (DBI  $AUC_{last}$  and  $C_{max}$  ratios) or green squares (DBI  $Ae_{urine}$  ratios). Details on the study protocols, model simulations and individual DBI  $AUC_{last}$ ,  $C_{max}$ , and  $Ae_{urine}$  ratios of all clinical studies used to evaluate the DBI performance of the NMN model are provided in **Supplementary Section S8**. DBI, drug-biomarker interaction; endo, endogenous;  $n$ , number of individuals studied.

used in model development and evaluation, measured creatinine by varying analytical methods which might contribute to inter-study variability of creatinine levels that are already prone to large inter- and intraindividual differences, including diurnal variation. Nevertheless, the final model met the required model performance evaluation criteria, typically applied to drug models<sup>17,25</sup> and all predicted plasma and urine concentrations deviated less than twofold from the observed data.

The NMN PBPK model presented in this work is the first kinetic model of this biomarker, mechanistically describing its synthesis, biotransformation, tubular secretion, and re-absorption. Because no NMN  $R_{syn}$  has been reported yet, an approximate value for NMN  $R_{syn}$  has been calculated from measurements of NMN and its carboxamide metabolites in urine,<sup>7</sup> assuming no further metabolization. This revealed an NMN  $R_{syn}$  of about 77  $\mu\text{mol}$  per day, which is much lower than the creatinine synthesis of about 18 mmol per day.<sup>41</sup>

NMN is metabolized by AOX1 and urinary excretion rates of NMN and its metabolites in urine were also utilized to assess the fraction of endogenous NMN metabolized, revealing that about

65% of NMN undergo further biotransformation.<sup>7</sup> Regarding renal excretion, a saturable tubular re-absorption process has been described in addition to tubular secretion via OCT2 and MATEs, as the ratio of renal NMN clearance and creatinine clearance is concentration dependent.<sup>10</sup> A transport process has been implemented at the basolateral site of tubule epithelial cells, informing Michaelis-Menten and transport rate constant values by simultaneously fitting observed plasma and urine data to simulations of endogenous NMN and after intravenous administration, leading to an accurate description of NMN levels. However, involved transporters, their location in the kidneys, the mechanism of transportation, and real NMN concentrations in kidney cells remain unknown. Moreover, sequential actions of two transporters are also plausible, which requires further investigations.

In contrast to modeling metformin (D. Türk *et al.*, unpublished data) and creatinine, the pronounced diurnal variation in observed NMN plasma concentrations could not be sufficiently described by solely implementing a diurnal rhythm of GFR, renal blood flow, and OCT2, as each of these accounted for only 0%, 1%, and 9% of

## ARTICLE

the observed amplitude, respectively. This variation could be explained, however, by the large influence of varying synthesis due to nicotinamide adenine dinucleotide utilization and, hence, affected nicotinamide levels.<sup>7</sup> Therefore, a mixed effect of diurnal synthesis and elimination was assumed to model NMN in plasma and urine. For this, the model implements an additional intermittent synthesis process with study-specific optimized values for amplitude and acrophase to address the observed large interstudy variability (Table S13). These differences might be attributed to expected intersubject variability in activity levels before the first NMN measurement that are correlated to NAD utilization. Additionally, a diurnal pattern of AOX4 activity has been observed in Harderian glands of mice,<sup>42</sup> but was not considered in the model, as data in humans are lacking and effect separation (e.g., from diurnal elimination) is not possible analyzing the available clinical data on urine measurements of NMN carboxamide metabolites.

Due to lack of information and data, some assumptions have been made during the development of the NMN model. This included uninformed priors regarding the extent of synthesis and involved transporters at the renal barrier as well as the diurnal processes to cover highly variable intraday NMN plasma levels. Moreover, the large observed interindividual differences in NMN plasma levels have been modeled by implementing a varying extent of NMN synthesis. However, only a limited number of studies could be included during model development, because many studies reported only very sparse NMN plasma data without specification of clock time. Furthermore, only studies on healthy subjects could be included, as increased expression of NNMT has been described (e.g., in patients with cancer, metabolic, and cardiovascular diseases<sup>43</sup>), where NMN levels should be interpreted with great caution. Despite these challenges, the PBPK model met the performance evaluation criteria with about 90% of predicted plasma and urine concentrations within twofold of observed data.

Sensitivity analyses of both biomarkers reveal highest sensitivity to the fraction unbound in plasma, where a literature value of 100% was used in both models. Furthermore, the analyses highlight the most important model processes, showing that transporter-mediated tubular secretion plays a minor role for creatinine pharmacokinetics compared with NMN.

This work was complemented by the development and evaluation of a DDI/DBI network involving three perpetrators of OCT2 and MATE1, trimethoprim, pyrimethamine, and cimetidine, all previously evaluated for DDI predictions with metformin, and extended by models of the endogenous substrates, creatinine and NMN. According to the magnitude of  $K_i$  values and simulated (unbound) plasma and kidney concentrations, the main contributor to DDIs/DBIs is MATE inhibition. Whereas interactions lead to an expected decrease in renal clearance and increase in plasma levels of creatinine, similar interaction scenarios lead to a decrease in NMN renal clearance with simultaneously paradox decrease in plasma levels. Previously, this effect has been attributed to a possible inhibition of NMN synthesis by trimethoprim and pyrimethamine with unclear underlying mechanisms.<sup>1</sup> Hence, recent recommendations suggest focusing on NMN renal clearance instead of plasma concentrations during renal transporter perpetrator drug administration.<sup>1,8,11</sup> To apply PBPK models for

transporter-mediated interaction predictions, a close interdisciplinary collaboration between pharmacometricians and laboratory scientists should be enforced, to obtain reliable  $K_i$  values.

Because PBPK modeling is helpful for hypothesis generation and testing, inhibition of NMN synthesis by trimethoprim and pyrimethamine was implemented, leading to a satisfactory description of observed data by including  $K_i$  values at the same scale as OCT2 inhibition. Underlying effects, such as direct inhibition of NNMT, indirect NNMT inhibition due to reduction of the methyl donor S-adenosylmethionine by interference with human folate metabolism (trimethoprim and pyrimethamine are both inhibitors of bacterial folate metabolism), or direct interaction with the methionine cycle might be plausible. To verify or reject these hypotheses, additional *in vitro* inhibition assays and, especially, *in vivo* metabolomic investigations are necessary.

The previously mentioned covariates, such as muscle mass and disease state, might compromise the suitability of creatinine as a biomarker to assess transporter-mediated DDIs. However, the new creatinine PBPK model can compensate for these shortcomings. Standardized measurements of this low-cost and easily detectable marker supported by model-based analyses in early drug development will allow to gain insights into possible transporter-mediated interactions. NMN has been previously proposed to be a more suitable biomarker, due to the higher proportion of active secretion compared with creatinine (70% vs. 10–40%<sup>2,5</sup>) and good correlation of NMN and metformin renal clearances,<sup>35</sup> also applying to the trimethoprim-induced reduction of renal clearances.<sup>9</sup> The newly developed NMN PBPK model can support NMN measurements in context of a biomarker-informed strategy during drug development, as changes in NMN urine as well as plasma during interactions can be assessed and further strengthens the validity of the whole interaction network of three perpetrators and three victims.

In summary, whole-body PBPK models of the currently proposed biomarkers for OCT2 and MATE1 activity, creatinine, and NMN, have been developed that support the vision of a biomarker-informed strategy to improve DDI investigations during drug development. Here, all perpetrator and victim models were thoroughly studied and validated in a comprehensive interaction network. During development and evaluation stages, knowledge gaps could be identified as starting point for future research. The comprehensive models can be further extended (e.g., to include predictions in renally impaired individuals) and will be shared with the research and drug development community ([www.open-systems-pharmacology.org](http://www.open-systems-pharmacology.org)), to assist in future OCT2 and MATE interaction studies. Next to depicting a complement to a proposed biomarker-informed workflow,<sup>2</sup> a further biomarker model application might be the estimation of *in vivo*  $K_i$  values from phase I biomarker measurements without prior knowledge of interaction potential from *in vitro* tests.

## SUPPORTING INFORMATION

Supplementary information accompanies this paper on the *Clinical Pharmacology & Therapeutics* website ([www.cpt-journal.com](http://www.cpt-journal.com)).

## FUNDING

This project was partly funded by the German Federal Ministry of Education and Research (BMBF), grant number 031L0161C (“OSMOSES”). Open Access funding enabled and organized by Projekt DEAL.



**CONFLICT OF INTEREST**

F.M. is an employee of Boehringer Ingelheim Pharma GmbH & Co. KG. All other authors declared no competing interests for this work.

**AUTHOR CONTRIBUTIONS**

D.T., F.M., M.F.F., D.S., R.D., and T.L. wrote the manuscript. D.T. and T.L. designed the research. D.T. performed the research. D.T., F.M., M.F.F., D.S., R.D., and T.L. analyzed the data.

© 2022 The Authors. *Clinical Pharmacology & Therapeutics* published by Wiley Periodicals LLC on behalf of American Society for Clinical Pharmacology and Therapeutics.

This is an open access article under the terms of the [Creative Commons Attribution-NonCommercial](https://creativecommons.org/licenses/by-nc/4.0/) License, which permits use, distribution and reproduction in any medium, provided the original work is properly cited and is not used for commercial purposes.

- Shen, H. A pharmaceutical industry perspective on transporter and CYP-mediated drug-drug interactions: kidney transporter biomarkers. *Bioanalysis* **10**, 625–631 (2018).
- Mathialagan, S., Feng, B., Rodrigues, A.D. & Varma, M.V.S. Drug-drug interactions involving renal OCT2/MATE transporters: clinical risk assessment may require endogenous biomarker-informed approach. *Clin. Pharmacol. Ther.* **110**, 855–859 (2021).
- Oswald, S. *et al.* Protein abundance of clinically relevant drug transporters in the human kidneys. *Int. J. Mol. Sci.* **20**, 1–12 (2019).
- Fromm, M.F. Prediction of transporter-mediated drug-drug interactions using endogenous compounds. *Clin. Pharmacol. Ther.* **92**, 546–548 (2012).
- Levey, A.S., Perrone, R.D. & Madias, N.E. Serum creatinine and renal function. *Ann. Rev. Med.* **39**, 465–490 (1988).
- Mathialagan, S., Rodrigues, A.D. & Feng, B. Evaluation of renal transporter inhibition using creatinine as a substrate in vitro to assess the clinical risk of elevated serum creatinine. *J. Pharm. Sci.* **106**, 2535–2541 (2017).
- Okamoto, H. *et al.* Diurnal variations in human urinary excretion of nicotinamide catabolites: effects of stress on the metabolism of nicotinamide. *Am. J. Clin. Nutr.* **77**, 406–410 (2003).
- Ito, S. *et al.* N-methylnicotinamide is an endogenous probe for evaluation of drug-drug interactions involving multidrug and toxin extrusions (MATE1 and MATE2-K). *Clin. Pharmacol. Ther.* **92**, 635–641 (2012).
- Müller, F. *et al.* N(1)-methylnicotinamide as an endogenous probe for drug interactions by renal cation transporters: studies on the metformin-trimethoprim interaction. *Eur. J. Clin. Pharmacol.* **71**, 85–94 (2015).
- Weber, W., Toussaint, S., Looby, M., Nitz, M. & Kewitz, H. System analysis in multiple dose kinetics: evidence for saturable tubular reabsorption of the organic cation N1-methylnicotinamide in humans. *J. Pharmacokin. Biopharm.* **19**, 553–574 (1991).
- Müller, F., Sharma, A., König, J. & Fromm, M.F. Biomarkers for in vivo assessment of transporter function. *Pharmacol. Rev.* **70**, 246–277 (2018).
- Rodrigues, A.D., Taskar, K.S., Kusuvara, H. & Sugiyama, Y. Endogenous probes for drug transporters: balancing vision with reality. *Clin. Pharmacol. Ther.* **103**, 434–448 (2018).
- Chu, X. *et al.* Clinical probes and endogenous biomarkers as substrates for transporter drug-drug interaction evaluation: perspectives from the International Transporter Consortium. *Clin. Pharmacol. Ther.* **104**, 836–864 (2018).
- Grimstein, M. *et al.* Physiologically based pharmacokinetic modeling in regulatory science: an update from the U.S. Food and Drug Administration's Office of Clinical Pharmacology. *J. Pharm. Sci.* **108**, 21–25 (2019).
- Türk, D. *et al.* Physiologically based pharmacokinetic models for prediction of complex CYP2C8 and OATP1B1 (SLC01B1) drug-drug-gene interactions: a modeling network of gemfibrozil, repaglinide, pioglitazone, rifampicin, clarithromycin and itraconazole. *Clin. Pharmacokin. Ther.* **58**, 1595–1607 (2019).
- Türk, D. *et al.* Novel models for the prediction of drug-gene interactions. *Expert Opin. Drug Metab. Toxicol.* **17**, 1293–1310 (2021).
- Hanke, N. *et al.* A comprehensive whole-body physiologically based pharmacokinetic drug–drug–gene interaction model of metformin and cimetidine in healthy adults and renally impaired individuals. *Clin. Pharmacokin. Ther.* **59**, 1419–1431 (2020).
- Yoshikado, T. *et al.* PBPK modeling of coproporphyrin I as an endogenous biomarker for drug interactions involving inhibition of hepatic OATP1B1 and OATP1B3. *CPT Pharmacometrics Syst. Pharmacol.* **7**, 739–747 (2018).
- Takita, H. *et al.* PBPK model of coproporphyrin I: evaluation of the impact of SLC01B1 genotype, ethnicity, and sex on its inter-individual variability. *CPT Pharmacometrics Syst. Pharmacol.* **10**, 137–147 (2021).
- Nakada, T., Kudo, T., Kume, T., Kusuvara, H. & Ito, K. Quantitative analysis of elevation of serum creatinine via renal transporter inhibition by trimethoprim in healthy subjects using physiologically-based pharmacokinetic model. *Drug Metab. Pharmacokin. Ther.* **33**, 103–110 (2018).
- Nakada, T., Kudo, T., Kume, T., Kusuvara, H. & Ito, K. Estimation of changes in serum creatinine and creatinine clearance caused by renal transporter inhibition in healthy subjects. *Drug Metab. Pharmacokin. Ther.* **34**, 233–238 (2019).
- Imamura, Y. *et al.* Prediction of fluoroquinolone-induced elevation in serum creatinine levels: a case of drug-endogenous substance interaction involving the inhibition of renal secretion. *Clin. Pharmacol. Ther.* **89**, 81–88 (2011).
- Scotcher, D. *et al.* Mechanistic models as framework for understanding biomarker disposition: prediction of creatinine-drug interactions. *CPT Pharmacometrics Syst. Pharmacol.* **9**, 282–293 (2020).
- U.S. Food and Drug Administration. *Drug development and drug interactions: table of substrates, inhibitors and inducers.* <<https://www.fda.gov/drugs/drug-interactions-labeling/drug-development-and-drug-interactions-table-substrates-inhibitors-and-inducers>> (2017). Accessed March 1, 2022.
- Türk, D., Hanke, N. & Lehr, T. A physiologically-based pharmacokinetic model of trimethoprim for MATE1, OCT1, OCT2, and CYP2C8 drug-drug-gene interaction predictions. *Pharmaceutics* **12**, 1074 (2020).
- Sjögren, E., Tarning, J., Barnes, K.I. & Jonsson, E.N. A physiologically-based pharmacokinetic framework for prediction of drug exposure in malnourished children. *Pharmaceutics* **13**, 204 (2021).
- Mitchell, M., Muftakhidinov, B. & Winchen, T. *Engauge Digitizer Software.* <<https://markumitchell.github.io/engauge-digitizer>>. Accessed March 1, 2022.
- Wojtyniak, J.-G., Britz, H., Selzer, D., Schwab, M. & Lehr, T. Data digitizing: accurate and precise data extraction for quantitative systems pharmacology and physiologically-based pharmacokinetic modeling. *CPT Pharmacometrics Syst. Pharmacol.* **9**, 322–331 (2020).
- Camara, A.A., Arn, K.D., Reimer, A. & Newburgh, L.H. The twenty-four hourly endogenous creatinine clearance as a clinical measure of the functional state of the kidneys. *J. Lab. Clin. Med.* **37**, 743–763 (1951).
- Jacobsen, F.K., Christensen, C.K., Mogensen, C.E., Andreassen, F. & Heilskov, N.S. Postprandial serum creatinine increase in normal subjects after eating cooked meat. *Proc. Eur. Dial. Transpl. Assoc.* **16**, 506–512 (1979).
- Mayersohn, M., Conrad, K.A. & Achari, R. The influence of a cooked meat meal on creatinine plasma concentration and creatinine clearance. *Br. J. Clin. Pharmacol.* **15**, 227–230 (1983).
- Perlzweig, W.A. & Huff, J.W. The fate of N1-methylnicotinamide in man. *J. Biol. Chem.* **161**, 417 (1945).
- Lehr, T. *et al.* A quantitative enterohepatic circulation model. *Clin. Pharmacokin. Ther.* **48**, 529–542 (2009).
- Guest, E.J., Aarons, L., Houston, J.B., Rostami-Hodjegan, A. & Galetin, A. Critique of the two-fold measure of prediction success for ratios: application for the assessment of drug-drug interactions. *Drug Metab. Dispos.* **39**, 170–173 (2011).
- Miyake, T. *et al.* Identification of appropriate endogenous biomarker for risk assessment of multidrug and toxin extrusion

## ARTICLE

- protein-mediated drug-drug interactions in healthy volunteers. *Clin. Pharmacol. Ther.* **109**, 507–516 (2021).
36. Chu, X., Chan, G.H. & Evers, R. Identification of endogenous biomarkers to predict the propensity of drug candidates to cause hepatic or renal transporter-mediated drug-drug interactions. *J. Pharm. Sci.* **106**, 2357–2367 (2017).
  37. Takita, H., Scotcher, D., Chinnadurai, R., Kalra, P.A. & Galetin, A. Physiologically-based pharmacokinetic modelling of creatinine-drug interactions in the chronic kidney disease population. *CPT Pharmacometrics Syst. Pharmacol.* **9**, 695–706 (2020).
  38. Chu, X., Bleasby, K., Chan, G.H., Nunes, I. & Evers, R. The complexities of interpreting reversible elevated serum creatinine levels in drug development: Does a correlation with inhibition of renal transporters exist? *Drug Metab. Dispos.* **44**, 1498–1509 (2016).
  39. Prasad, B. et al. Abundance of drug transporters in the human kidney cortex as quantified by quantitative targeted proteomics. *Drug Metab. Dispos.* **44**, 1920–1924 (2016).
  40. Gutenbrunner, C. Circadian variations of the serum creatine kinase level—a masking effect? *Chronobiol. Int.* **17**, 583–590 (2000).
  41. Feher, J. (ed.) 7.4–Tubular reabsorption and secretion. In *Quantitative Human Physiology* 719–729 (Academic Press, Boston, 2017).
  42. Terao, M. et al. Mouse aldehyde-oxidase-4 controls diurnal rhythms, fat deposition and locomotor activity. *Sci. Rep.* **6**, 30343 (2016).
  43. Gao, Y. et al. Bisubstrate inhibitors of nicotinamide N-methyltransferase (NNMT) with enhanced activity. *J. Med. Chem.* **62**, 6597–6614 (2019).
  44. Les Laboratoires Servier. *Servier Medical Art.* <<https://smart.servier.com/>>. Accessed November 30, 2021.
  45. Berglund, F., Killander, J. & Pompeius, R. Effect of trimethoprim-sulfamethoxazole on the renal excretion of creatinine in man. *J. Urol.* **114**, 802–808 (1975).
  46. Pasternack, A. & Kuhlback, B. Diurnal variations of serum and urine creatine and creatinine. *Scand. J. Clin. Lab. Invest.* **27**, 1–7 (1971).
  47. Pissios, P. Nicotinamide N-methyltransferase: more than a vitamin B3 clearance enzyme. *Trends Endocrinol. Metab.* **28**, 340–353 (2017).
  48. Shouval, D., Ligumsky, M. & Ben-Ishay, D. Effect of co-trimoxazole on normal creatinine clearance. *Lancet* **1**, 244–245 (1978).
  49. Serdar, M.A. et al. A practical approach to glomerular filtration rate measurements: creatinine clearance estimation using cimetidine. *Ann. Clin. Lab. Sci.* **31**, 265–273 (2001).

## DISCUSSION AND PERSPECTIVE

---

Different research questions have been addressed in this thesis by applying mechanistic pharmacokinetic modeling techniques to (i) predict transporter-mediated DDGIs, (ii) suggest dose adaptations in renally impaired individuals and (iii) assess the impact of diurnal variation on ADME processes. PBPK models of the renal transporter inhibitors trimethoprim, pyrimethamine and cimetidine and of the substrates metformin (exogenous), creatinine and NMN (endogenous) have been successfully developed. These models mechanistically describe absorption, synthesis, biotransformation and transporter-mediated renal clearance, taking the current state of knowledge about pharmacokinetic processes and localization of involved transporters into account. Modeling revealed knowledge gaps that can be starting points for future research activities, to test generated hypotheses.

### 5.1 MEMBRANE TRANSPORTERS

Membrane transporters mediate compound transport to cross biological membranes and thus, contribute to pharmacokinetics by affecting absorption, distribution and excretion. The renal barrier is one of the most important transporter sites, controlling compound excretion as well as reabsorption. However, knowledge gaps exist, including controversial reports of membrane transporter expression (Section 1.2) as well as unknown transporter abundance and function. High variability in transporter abundances reported by different laboratories has been described, presumably due to a lack of harmonized guidelines for sample analyses [196]. Furthermore, several transporters are involved at the same barrier and hence, distinguishing their activity and determining specific substrates is challenging. Accordingly, index perpetrators and substrates, as available for CYP enzymes, have not yet been defined for transporters [28, 54]. Knowledge of actual intracellular concentrations of transporter substrates and perpetrators, e.g., accessible by PET measurements as reported for metformin [195], as well as tissue-specific inhibition information are also rarely available.

PBPK modeling requires various input data and informative *in vitro* and *in vivo* measurements are crucial to increase model reliability and versatility. With PBPK modeling, it is possible to test different assumptions and optimize parameters if knowledge gaps exist, e.g., with respect to protein abundances or the extent of ADME processes. For instance, unknown transporter abundance could be estimated using

*Availability of  
experimental data*

*Opportunities of transporter physiologically based pharmacokinetic modeling*

pharmacokinetic information from multiple substrates and/or perpetrators of the transporter of interest. Tissue distribution of substrates and inhibitors could be informed by assessing intracellular concentrations of perpetrators and substrates using plasma concentration-time profiles from various interaction studies. These assumptions were made for the cimetidine model in project I, to accurately model cimetidine concentrations at sites of inhibitory action in the liver (CYP and transporter inhibition) and kidneys (renal transporter inhibition), taking one interaction study each with midazolam and metformin into account while incorporating  $K_i$  values from experimental reports.

## 5.2 RENAL TRANSPORTER-MEDIATED DRUG-DRUG AND DRUG-BIOMARKER INTERACTIONS

*Renal transporter drug-drug and drug-biomarker interaction network*

DDI models account for 67% of PBPK model submissions to the FDA. However, only 10% of these DDI submissions could be attributed to transporter-based DDIs [165]. This apparent underrepresentation emphasizes the need for further modeling activities in this research area. The presented perpetrator models of trimethoprim, pyrimethamine and cimetidine and victim models of metformin, creatinine and NMN have been successfully applied to establish an OCT and MATE DDI/DBI network (Figure 5.1). First, the perpetrator models have been evaluated for DDI predictions with metformin (projects I–III) and were therefore considered qualified for further OCT- and MATE-mediated interaction predictions. Second, the interaction network was extended by including models of the biomarkers creatinine and NMN (project III), to advance the vision of biomarker-informed DDI investigations during drug development and to serve as additional validation of the whole DDI/DBI network.

*Metformin, cimetidine and trimethoprim drug-drug interactions*

Transporter-mediated DDIs were successfully predicted using the presented models, representing a cornerstone for further DDI predictions involving OCTs and MATEs. Next to its inhibitory activity on membrane transporters, cimetidine is listed as inhibitor of CYP3A4-mediated metabolism by the FDA [54]. Therefore, the model was applied for DDI predictions with the sensitive CYP3A4 substrate midazolam. Likewise, the trimethoprim model was applied for DDI and DDGI predictions with the CYP2C8 substrates repaglinide and pioglitazone. The additionally modeled CYP3A4- and CYP2C8-mediated DDI predictions involving cimetidine and trimethoprim emphasize the good overall interaction model performance by also extending the previously developed DD(G)I networks with further compounds [26, 188]. The various tested applications of the models, i.e., successful DDI and DDGI predictions with diverse target proteins, organs and victim drugs, increased the confidence of modeled drug concentrations at different sites of action (liver and kidney) as well as the general applicability of the models.

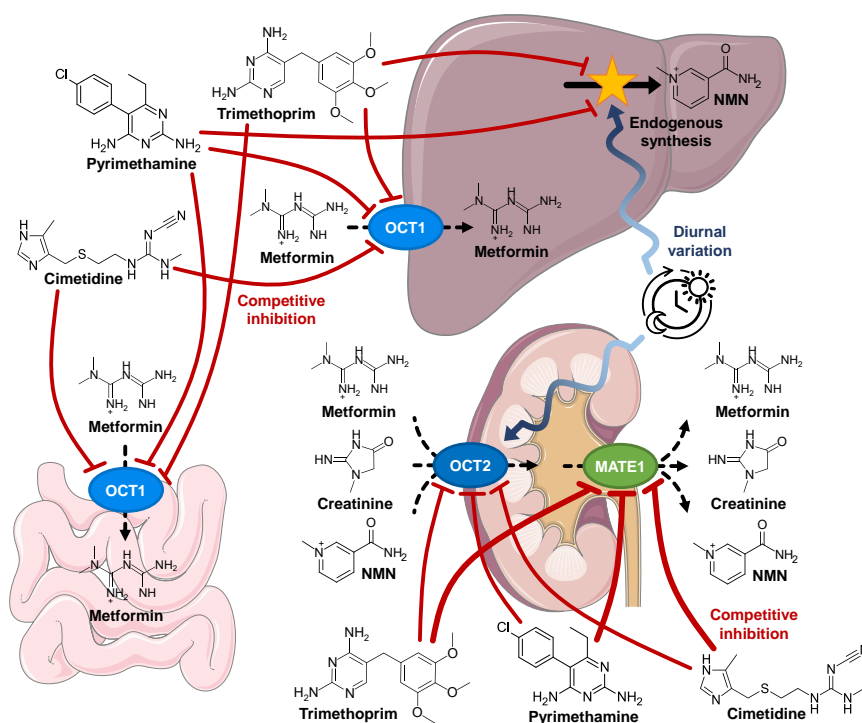


**Figure 5.1.** Organic cation transporter (OCT) and multidrug and toxin extrusion protein (MATE) drug-drug and drug-biomarker interaction network involving trimethoprim, pyrimethamine and cimetidine (perpetrators) and metformin, creatinine and N<sup>1</sup>-methylnicotinamide (NMN) (victims). Illustrations of organs were taken from Servier [5], licensed under CC BY 3.0 (<https://creativecommons.org/licenses/by/3.0/>).

Creatinine plasma and urine profiles from literature were successfully described by the model. Additionally, the creatinine model could predict the effect of DBIs with trimethoprim, pyrimethamine and cimetidine. Creatinine kinetics are susceptible to the influence of various factors, e.g., sex, age, muscle mass, diet, and renal function [197], while the newly developed PBPK model incorporated most of these covariates. For instance, the impact of differently prepared meat meals on creatinine concentrations in blood and urine can be assessed with the creatinine PBPK model. Furthermore, the model holds the potential to be extended in the future e.g., for predictions in renally impaired individuals requiring the necessary information from clinical studies.

To our knowledge, the NMN model developed in project III is the first comprehensive model of this biomarker, allowing the prediction of plasma and urine profiles covering endogenous synthesis, metabolism, tubular secretion and reabsorption. Due to unexpected lower NMN plasma concentrations during renal transporter perpetrator drug administration, recent publications recommend to particularly focus on NMN renal clearance in lieu of plasma concentrations [74, 75, 77]. With our newly developed NMN model, inhibition of NMN

*Drug-N<sup>1</sup>-  
methylnicotinamide  
interactions*

synthesis by trimethoprim and pyrimethamine was hypothesized, resulting in accurate predictions of NMN in urine as well as in plasma. As underlying mechanisms are still unclear [74], *in vitro* inhibition assays and *in vivo* metabolomic studies are necessary to test these hypotheses. NMN has been previously proposed as superior biomarker for OCT2 and MATE interactions compared to creatinine, as (i) NMN displays a higher proportion of active secretion than creatinine (70% compared to 10–40% [19, 83]) and (ii) NMN and metformin renal clearances are in good correlation, also applying to the extent of clearance reduction during interactions [58, 68].

*Biomarker-informed  
strategy for  
drug-drug  
interaction risk  
assessment during  
drug development  
including  
pharmacokinetic  
modeling*

The newly developed biomarker PBPK models can compensate for potential shortcomings in suitability of both creatinine and NMN, including apparently low contribution of transporter-mediated excretion to total clearance (creatinine) and incomplete information about absorption, synthesis, biotransformation and excretion (NMN). Both models can successfully describe and predict changes in urine as well as plasma during DBIs. The creatinine and NMN models could provide important insights into transporter-mediated interactions by model-based analyses of biomarker concentrations in early clinical phases of drug development, to support a biomarker-informed strategy. Here,  $K_i$  and  $IC_{50}$  values of NMEs from *in vitro* tests could be incorporated and model predictions could be compared to biomarker measurements in plasma and urine from phase I studies. Here, the presented models can serve as helpful tools to implement the analysis of endogenous biomarkers in drug development for OCT2 and MATE-related DDIs as proposed by Mathialagan et al. (Figure 1.4) [19].

*Future directions of  
biomarker models*

Thorough characterization of biomarker kinetics is a necessary cornerstone for routinely implementing biomarker analysis in the process of drug development. Here, PBPK modeling can contribute to the characterization of biomarkers, particularly in hypothesis generation and testing. Several examples are available, showcasing the implementation of coproporphyrin I (CPI) as OATP biomarker and how CPI could support drug development [198]. For OATP-related DDIs, a biomarker-informed, model-driven workflow has been proposed, where *in vivo*  $K_i$  values are determined and subsequently incorporated into PBPK model predictions with drug transporter substrates [199]. This approach presented by Yoshida et al. also further emphasizes the potential of model-based biomarker analyses to assess interaction potential of NMEs in early drug development [199]. The presented PBPK models for creatinine and NMN have shown their predictive capabilities in DBI scenarios within a thoroughly evaluated OCT2 and MATE DDI/DBI network. Additional biomarkers, such as N<sup>1</sup>-methyladenosine, as well as other perpetrator and victim drugs could expand the established network, to support future MID<sub>3</sub>.

## 5.3 DRUG-(DRUG-)GENE INTERACTIONS

In project I, the metformin model has been successfully applied to model the metformin-*SLC22A2* 808G>T DGI and was additionally challenged with predictions in *SLC22A2* wild-type and 808G>T polymorphic subjects during co-administration of cimetidine. Although controversial reports from *in vitro* experiments and *in vivo* studies impede the accurate assessment of the effect of the *SLC22A2* 808G>T polymorphism on the pharmacokinetics of metformin (Section 1.4.2), the presented metformin DGI model is capable of accurately predicting observed metformin concentrations assuming higher transport activity of OCT2 in *SLC22A2* variant allele carriers. However, due to sequential action of OCT2 and MATE1 contributing to metformin renal clearance, DGI modeling results should be interpreted with caution, as neither MATE genotypes or phenotypes nor kidney tissue concentrations were investigated in the studies utilized for model development. Moreover, the importance of considering variants in both *SLC22A2* and *SLC41A1* genes has been pointed out in Section 1.4.2. The presented metformin model is readily extensible to include further DGI scenarios in the future, if required input data become available [27]. The cimetidine-metformin DDGI was modeled assuming similar interaction constants for predictions in *SLC22A2* wild-type and variant allele carriers, leading to adequate prediction of observed data. However, a difference in interaction magnitude has been described for cimetidine in the respective variants *in vitro* [117], but was not incorporated due to sparse information from literature.

In project II, the new trimethoprim model was challenged with metformin interaction predictions in *SLC22A2* wild-type and 808G>T polymorphic subjects and, by linking our previously developed pioglitazone-CYP2C8 DGI model [26], to predict the trimethoprim-pioglitazone DDGI. Therefore, identical  $K_i$  values for OCT2 (as indicated by an *in vitro* study [117]) and CYP2C8 inhibition were used for wild-type and variant proteins. This resulted in good DDGI predictions, however, no *in vitro* studies investigating the effect of trimethoprim on variant CYP2C8 were available. Assuming the same inhibitory activity for wild-type and variant protein is often a compromise and additional *in vitro* experiments determining the required parameters for variant enzymes and transporters could improve DDGI modeling.

Clinical DDGI studies are rarely performed for risk assessment during drug development, due to ethical concerns of putting study participants at an increased risk of experiencing ADRs. Additionally, as some variant alleles may occur with low frequencies, an extensive number of eligible study participants would have to be screened for these alleles to acquire sufficiently large study sample sizes [27, 200]. Although often assumptions need to be made, PBPK models are flexible and helpful tools to predict various DDGI scenarios [27]. These

*Modeling of  
metformin  
transporter-mediated  
drug-(drug-)gene  
interactions*

*Modeling of  
trimethoprim  
drug-(drug-)gene  
interactions*

*Physiologically  
based  
pharmacokinetic  
modeling to assess  
drug-drug-gene  
interactions*

models cannot only be helpful during drug development, but also in performing individual dose optimizations. This aspect has been demonstrated in an article by Wojtyniak et al., where a model-based precision dosing approach focusing on a comprehensive network involving simvastatin was chosen [167]. Nevertheless, successful DDGI predictions with cimetidine, trimethoprim, metformin and pioglitazone and different polymorphisms emphasize the validity of the presented models and interaction networks, which could be easily extended to additional DDGI scenarios in the future. A recent literature analysis showed that in the last two decades, the interest in DGI modeling has been steadily increasing [27]. According to this analysis, published DGI models focused more frequently on polymorphisms affecting metabolism than on transporter DGIs (*SLCO1B1* and *ABCB1* DGIs most frequently analyzed with respect to transporter DGI models), emphasizing the importance of further research on the topic.

#### 5.4 DRUG-DISEASE INTERACTIONS

*Modeling of  
metformin in  
patients with  
different chronic  
kidney disease stages*

The metformin base model developed with data from healthy subjects has been successfully extended to describe and predict the impact of CKD, which depicts a common comorbidity in patients with type 2 diabetes [16]. The model considers proportional decrease of renal secretion to impaired GFR according to the “intact nephron hypothesis” [201] and the effect of CKD on non-renal elimination due to inhibited liver drug uptake by uremic toxins. These hypotheses were tested in previous PBPK modeling analyses [202–206]. The newly developed model followed an empirical approach to also incorporate the inhibition of hepatic and muscular uptake by OCT1 and PMAT proportional to the decreased GFR. Furthermore, an inhibition of basolateral intestinal permeability/transport in CKD was hypothesized and implemented in the model to describe the respective observed data. Additionally, induction of OCT2 and MATE1, which was reported in hyperuricemic rats [139], was included in the model for subjects with CKD stages 4 and 5. These hypotheses require further verification in human *in vivo* studies. A previously published PBPK modeling analysis of creatinine in CKD patients supports our modeling results, as the authors suggested a smaller decline of OCT2 and MATE activity compared to GFR [207]. Recently, a white paper was published by the ITC, focusing on transporter modulation in different populations such as CKD patients, elaborating the possible clinical implications and future directions [208]. The authors highlight the potential of thoroughly developed PBPK models as valuable tools to translate pharmacokinetics from healthy subjects to patient populations. Additionally, the authors noted the need for reliable information on pathophysiological changes from *in vivo* experiments, such as tissue transporter abundances in patients compared to healthy individuals [208].



Model-based dose calculations for metformin were performed in patients with different stages of CKD. These included a subsequent comparison with current guideline recommendations. According to these guidelines, metformin should be administered in a reduced dose, or an alternative drug should be selected in patients with GFR below 60 mL/min [24, 25]. Furthermore, a GFR below 30 mL/min was denoted as contraindication for metformin therapy, due to an increased risk of lactic acidosis [24, 25]. Model-based dose adaptations, developed on basis of AUC in healthy subjects, suggest much lower doses in patients with CKD stage 3A and 3B than recommended by the guidelines, but an adapted dose of 200 mg three times daily for CKD4 patients was inferred from model simulations. This is in line with clinical studies testing 500 mg metformin daily in patients with stable creatinine clearances as low as 20 mL/min [209] or in a group of CKD4 patients [210]. Additionally, the authors recommended to monitor blood metformin regarding drug accumulation [209], to educate patients with respect to symptoms of lactic acidosis [209] and to measure lactate levels in these fragile patients [210]. The drug-disease interaction model developed in this work supports the approach of integrating mechanistic modeling into investigations of drug pharmacology in patients. As a first step towards MIPD, the metformin model in CKD patients was utilized to calculate dose adaptations and could also be expanded to include concomitant drug administration and genetic predisposition.

*Model-based dose adaptations*

## 5.5 DIURNAL VARIATION

Both modeled biomarkers, creatinine and NMN, exhibit pronounced diurnal variation in their kinetics, which was assessed using the presented PBPK models. The observed diurnal plasma level pattern of creatinine could be completely explained by varying GFR and renal blood flow, with only an insignificant effect of diurnal tubular secretion. This was in line with the literature, as only a small amount of creatinine is actively secreted [19]. Additionally, intraday variability of creatinine synthesis attributed to varying activity of creatine kinase might contribute to the observed variation in plasma concentrations. However, this effect was not incorporated in the model, as implementation of a diurnal effect on renal clearance led to an accurate description of observed data with parametrization derived from literature reports.

*Modeling of diurnal creatinine renal excretion*

In contrast, the considerable diurnal variation in observed NMN plasma concentrations was insufficiently covered by solely incorporating diurnal rhythm of renal excretion, as this effect accounted only for a small fraction of the observed amplitude. Complex NMN synthesis, consisting of multiple steps with NAD as one important intermediate (Figure 1.3), was implemented as one surrogate parameter (“ $R_{syn}$ ”)

*Modeling of diurnal  
N<sup>1</sup>-  
methylnicotinamide  
synthesis*

in the NMN model. Sizeable diurnal variation in NMN plasma levels could be attributed to NAD utilization over day and correlated degradation to nicotinamide, the direct precursor of NMN [99]. Implementation of an additional intermittent NMN synthesis process greatly improved model performance. Here, the necessary parameters such as amplitude and acrophase were optimized for each respective study, presumably attributed to intersubject variability in activity levels before the first NMN measurement, which are correlated to NAD utilization. With respect to NMN biotransformation by AOX, a diurnal pattern of enzyme activity was not considered, as experimental data in humans or human cells are missing and this effect could not adequately be differentiated from others such as diurnal synthesis or elimination taking the available clinical data into account. Hence, further *in vivo* measurements could contribute to an adequate analysis of NMN and its carboxamide metabolites in urine.

*Perspectives of  
chronotherapy and  
modeling of diurnal  
variation*

For different medical conditions, such as cancer or metabolic diseases, chronotherapy has been proposed as an advantageous treatment option [149, 211]. Furthermore, a disrupted diurnal rhythm has been associated with various diseases, such as cancer, cardiovascular diseases and psychiatric disorders [212, 213]. Although personalized chronomodulated treatment has been suggested to contribute to more effective and safe therapies, only few dedicated clinical trials investigating chronopharmacology are available for a limited number of drugs. Here, project III demonstrated that the creatinine and NMN PBPK models are excellent tools for generating and testing hypotheses, such as the causes of diurnal variation. Insights gained with the biomarker models regarding diurnal ADME processes could be transferred to other biomarkers and drugs in the future, contributing greatly to investigations of the impact of diurnal rhythm and possible implications for chronotherapy.

## 5.6 MECHANISTIC PHARMACOKINETIC MODELING - CHALLENGES AND OPPORTUNITIES

### 5.6.1 Model development

*Data acquisition and  
availability*

PBPK modeling depicts a mechanistic but simultaneously “data hungry” approach, providing the opportunity to cover complex scenarios, while requiring many necessary input values [27]. Reliable experimental data for the compound of interest including system-dependent data such as organ volumes and tissue composition, physicochemical properties and ADME-related processes are crucial components [166]. Extensive data on human and animal anatomy and physiology are usually provided through large databases within modern PBPK software solutions. Physicochemical properties are frequently reported for parent drugs, but often sparsely for metabolites or biomarkers.

Additionally, ADME-related parameters, often referred to as drug-biological properties due to interplay of a drug with the biological system, are needed. These include cellular and intestinal permeabilities, fraction unbound in plasma, and information about enzyme and transporter affinity and activity [166]. Here, pharmacometricians are typically confronted with missing or incomplete *in vitro* data, especially when models are predominantly based on reported values from literature. However, these parameters can also be estimated using quantitative structure activity relationship approaches or can be complemented by optimizing parameters utilizing *in vivo* profiles [27].

Different modeling approaches come with their special advantages and disadvantages and a combination of different approaches can be beneficial to answer the respective research questions. This was demonstrated in project I, where cimetidine data were analyzed with a PopPK approach prior to a PBPK analysis, to gain knowledge about the absorption behavior of cimetidine. This example highlights the interplay of different model types and how PopPK analyses can support PBPK model development and improve reliability of input data. PBPK modeling presents a highly flexible method, with the possibility to extend developed models to answer additional research questions.

*Combination of modeling approaches*

### 5.6.2 Model-informed drug development and discovery

PBPK models are established tools to support drug development as well as regulatory submissions. Therefore, careful model building and thorough evaluation is crucial. Here, the FDA and EMA provide guidelines on how to report modeling results [171, 214]. The PBPK models published during this work are accompanied by comprehensive supporting information, including modeling strategy, utilized data and performance evaluation. Furthermore, models have to be sustainable and need continuous maintenance. To support knowledge exchange between scientists, easy access to model files and data is beneficial, which could be accomplished by an open-source approach. All presented models are freely available to the research community, to serve as a basis for future investigations involving these models. Qualification of models and available platforms is crucial to assess model quality and predictive capability. Recently, a white paper was published working out how model qualification activities could be performed and harmonized [215].

*Model publication and sustainability*

The interaction PBPK models presented in this work were evaluated within DDI networks. Comprehensive interaction networks, e.g., focusing on CYP1A2, CYP2C19 and CYP3A4 were published [188, 216] and maintained by the Open Systems Pharmacology consortium ([www.open-systems-pharmacology.org](http://www.open-systems-pharmacology.org)), where also a generic and sustainable framework for model (re-)qualification [217] and a compound library are provided. In a recent example, the nonsteroidal, selec-

*Interaction network models*

tive mineralocorticoid receptor antagonist finerenone was integrated into the existing CYP3A4 network, to predict untested interactions with strong CYP3A4 inhibitors [218]. Results of these PBPK modeling analyses are included in the prescribing information of Kerendia<sup>®</sup> (finerenone) [219]. This example highlights the importance of PBPK modeling during drug development also from an ethical perspective, as the knowledge obtained from model simulations can help in reducing the number and costs of potentially harmful DDI studies.

### 5.6.3 *Model-informed precision dosing*

PBPK models can contribute to investigate the effect of pathophysiology, genetic predisposition, and co-medication, which might be inaccessible from clinical studies. Furthermore, models can help to explain the causes of interindividual variability [27], but for reliable investigation and implementation, accessibility of individual measurements and related information such as demographics and genetic polymorphisms, should be promoted. PBPK models hold a great potential to provide personalized dosing adaptations for special populations like patients. However, these models are not routinely applied in clinical practice, yet. This can typically be attributed to difficult assessment of model quality, reliability and predictive performance as well as non-trivial handling of such models, especially for potential users without pharmacometric experience [27].

To implement models in clinical practice, interdisciplinary collaboration is essential [27, 220]. These multidisciplinary consortia should include clinical pharmacists, pharmacometricians, healthcare professionals, experts on pharmacogenetics and specialists for diseases of interest. The development of easy-to-use software and web applications to provide decision support, tailored to the needs of clinicians, physicians and patients, should be advanced. Furthermore, accountability and legal conflicts pose one major hurdle in implementing models in clinical practice [220], and a legal basis regarding accountability for model development, implementation and application needs to be created [27, 220].

*Physiologically  
based  
pharmacokinetic  
models for  
personalized dosing  
adaptations*

*Opportunities to  
integrate models in  
clinical practice*

## CONCLUSION

---

The role of transporters in drug pharmacology represents an important research area, as disregard can adversely affect drug development and safety of pharmacotherapy. New approaches to assess transporter-mediated DDIs, DGIs and drug-disease interactions include *in silico* approaches and, for DDI investigations, incorporation of a biomarker-informed strategy. Mechanistic pharmacokinetic models, especially whole-body PBPK models in the scope of this thesis, have demonstrated their usefulness over time and application areas are versatile. Models have been successfully applied to describe and predict the effect of DDIs, DBIs, DGIs, drug-disease interactions and diurnal variation on pharmacokinetics of exogenous and endogenous renal transporter substrates even in complex interaction scenarios and for hypothesis testing. The validity of all perpetrator and victim models involved in a comprehensive interaction network has been emphasized. The newly developed models are freely available in the Open Systems Pharmacology model repository ([www.open-systems-pharmacology.org](http://www.open-systems-pharmacology.org)), (i) to support investigations during MID<sub>3</sub> and submissions for regulatory approval of new drugs or (ii) to estimate dose adaptations, contributing to an effective and safe pharmacotherapy for patients. Furthermore, investigations of other OCT2 and MATE substrates and inhibitors could benefit from findings in this work.



## BIBLIOGRAPHY

---

1. Hanke N, Türk D, Selzer D, Ishiguro N, Ebner T, Wiebe S, Müller F, Stopfer P, Nock V, and Lehr T. A comprehensive whole-body physiologically based pharmacokinetic drug–drug–gene interaction model of metformin and cimetidine in healthy adults and renally impaired individuals. *Clinical Pharmacokinetics*. 2020;59(11):1419–31. DOI: [10 . 1007 / s40262 - 020 - 00896 - w](https://doi.org/10.1007/s40262-020-00896-w)
2. Türk D, Hanke N, and Lehr T. A physiologically-based pharmacokinetic model of trimethoprim for MATE<sub>1</sub>, OCT<sub>1</sub>, OCT<sub>2</sub>, and CYP2C8 drug-drug-gene interaction predictions. *Pharmaceutics*. 2020;12(11):1074. DOI: [10.3390/pharmaceutics12111074](https://doi.org/10.3390/pharmaceutics12111074)
3. Türk D, Müller F, Fromm MF, Selzer D, Dallmann R, and Lehr T. Renal transporter-mediated drug-biomarker interactions of the endogenous substrates creatinine and N<sup>1</sup>-methylnicotinamide: a PBPK modeling approach. *Clinical Pharmacology & Therapeutics*. 2022. Online ahead of print. DOI: [10.1002/cpt.2636](https://doi.org/10.1002/cpt.2636)
4. Brand A, Allen L, Altman M, Hlava M, and Scott J. Beyond authorship: attribution, contribution, collaboration, and credit. *Learned Publishing*. 2015;28(2):151–5. DOI: [10.1087/20150211](https://doi.org/10.1087/20150211)
5. Les Laboratoires Servier. Servier Medical Art. Available from: <https://smart.servier.com/> [Internet] [cited 14 Dec 2021]
6. Lazarou J, Pomeranz BH, and Corey PN. Incidence of adverse drug reactions in hospitalized patients: a meta-analysis of prospective studies. *Journal of the American Medical Association*. 1998;279(15):1200–5. DOI: [10.1001/jama.279.15.1200](https://doi.org/10.1001/jama.279.15.1200)
7. Shehab N, Lovegrove MC, Geller AI, Rose KO, Weidle NJ, and Budnitz DS. US emergency department visits for outpatient adverse drug events, 2013-2014. *Journal of the American Medical Association*. 2016;316(20):2115–25. DOI: [10 . 1001 / jama . 2016 . 16201](https://doi.org/10.1001/jama.2016.16201)
8. Hakkarainen KM, Hedna K, Petzold M, and Hägg S. Percentage of patients with preventable adverse drug reactions and preventability of adverse drug reactions - a meta-analysis. *PloS One*. 2012;7(3):e33236. DOI: [10.1371/journal.pone.0033236](https://doi.org/10.1371/journal.pone.0033236)
9. Masnoon N, Shakib S, Kalisch-Ellett L, and Caughey GE. What is polypharmacy? A systematic review of definitions. *BMC Geriatrics*. 2017;17(1):230. DOI: [10.1186/s12877-017-0621-2](https://doi.org/10.1186/s12877-017-0621-2)

10. Franceschi M, Scarcelli C, Niro V, Seripa D, Pazienza AM, Pepe G, Colusso AM, Pacilli L, and Pilotto A. Prevalence, clinical features and avoidability of adverse drug reactions as cause of admission to a geriatric unit: a prospective study of 1756 patients. *Drug Safety*. 2008;31(6):545–56. DOI: [10.2165/00002018-200831060-00009](https://doi.org/10.2165/00002018-200831060-00009)
11. Qato DM, Wilder J, Schumm LP, Gillet V, and Alexander GC. Changes in prescription and over-the-counter medication and dietary supplement use among older adults in the United States, 2005 vs 2011. *JAMA Internal Medicine*. 2016;176(4):473–82. DOI: [10.1001/jamainternmed.2015.8581](https://doi.org/10.1001/jamainternmed.2015.8581)
12. Cacabelos R, Cacabelos N, and Carril JC. The role of pharmacogenomics in adverse drug reactions. *Expert Review of Clinical Pharmacology*. 2019;12(5):407–42. DOI: [10.1080/17512433.2019.1597706](https://doi.org/10.1080/17512433.2019.1597706)
13. Morrissey KM, Stocker SL, Wittwer MB, Xu L, and Giacomini KM. Renal transporters in drug development. *Annual Review of Pharmacology and Toxicology*. 2013;53:503–29. DOI: [10.1146/annurev-pharmtox-011112-140317](https://doi.org/10.1146/annurev-pharmtox-011112-140317)
14. Sommer J, Seeling A, and Rupprecht H. Adverse drug events in patients with chronic kidney disease associated with multiple drug interactions and polypharmacy. *Drugs & Aging*. 2020;37(5):359–72. DOI: [10.1007/s40266-020-00747-0](https://doi.org/10.1007/s40266-020-00747-0)
15. Laville SM, Gras-Champel V, Moragny J, et al. Adverse drug reactions in patients with CKD. *Clinical Journal of the American Society of Nephrology*. 2020;15(8):1090–102. DOI: [10.2215/CJN.01030120](https://doi.org/10.2215/CJN.01030120)
16. Thomas MC, Cooper ME, and Zimmet P. Changing epidemiology of type 2 diabetes mellitus and associated chronic kidney disease. *Nature Reviews Nephrology*. 2016;12(2):73–81. DOI: [10.1038/nrneph.2015.173](https://doi.org/10.1038/nrneph.2015.173)
17. Khan MAB, Hashim MJ, King JK, Govender RD, Mustafa H, and Al Kaabi J. Epidemiology of type 2 diabetes - global burden of disease and forecasted trends. *Journal of Epidemiology and Global Health*. 2020;10(1):107–11. DOI: [10.2991/jegh.k.191028.001](https://doi.org/10.2991/jegh.k.191028.001)
18. Zhou Y, Zhang GQ, Wei YH, Zhang JP, Zhang GR, Ren JX, Duan HG, Rao Z, and Wu XA. The impact of drug transporters on adverse drug reaction. *European Journal of Drug Metabolism and Pharmacokinetics*. 2013;38(2):77–85. DOI: [10.1007/s13318-013-0117-1](https://doi.org/10.1007/s13318-013-0117-1)



19. Mathialagan S, Feng B, Rodrigues AD, and Varma MVS. Drug-drug interactions involving renal OCT2/MATE transporters: clinical risk assessment may require endogenous biomarker-informed approach. *Clinical Pharmacology & Therapeutics*. 2021;110(4):855–9. DOI: [10.1002/cpt.2089](https://doi.org/10.1002/cpt.2089)
20. American Diabetes Association. 9. Pharmacologic approaches to glycemic treatment: standards of medical care in diabetes—2020. *Diabetes Care*. 2020;43(Suppl 1):S98–S110. DOI: [10.2337/dc20-S009](https://doi.org/10.2337/dc20-S009)
21. ClinCalc LLC. ClinCalc DrugStats database. 2022. Available from: <https://clincalc.com/DrugStats/> [Internet] [cited 10 Jan 2022]
22. Zolk O. Disposition of metformin: variability due to polymorphisms of organic cation transporters. *Annals of Medicine*. 2012;44(2):119–29. DOI: [10.3109/07853890.2010.549144](https://doi.org/10.3109/07853890.2010.549144)
23. Graham GG, Punt J, Arora M, et al. Clinical pharmacokinetics of metformin. *Clinical Pharmacokinetics*. 2011;50(2):81–98. DOI: [10.2165/11534750-000000000-00000](https://doi.org/10.2165/11534750-000000000-00000)
24. Bristol-Myers Squibb Company. GLUCOPHAGE® (metformin hydrochloride) Tablets, GLUCOPHAGE® XR (metformin hydrochloride) Extended-Release Tablets. Prescribing information. 2017. Available from: [https://www.accessdata.fda.gov/drugsatfda\\_docs/label/2017/020357s037s039\\_021202s021s0231bl.pdf](https://www.accessdata.fda.gov/drugsatfda_docs/label/2017/020357s037s039_021202s021s0231bl.pdf) [Internet] [cited 30 May 2022]
25. Merck. Glucophage® 500 mg/- 850 mg/- 1000 mg Filmtabletten. Fachinformation. 2022. Available from: <https://www.fachinfo.de/pdf/000959> [Internet] [cited 30 May 2022]
26. Türk D, Hanke N, Wolf S, Frechen S, Eissing T, Wendl T, Schwab M, and Lehr T. Physiologically based pharmacokinetic models for prediction of complex CYP2C8 and OATP1B1 (*SLCO1B1*) drug-drug-gene interactions: a modeling network of gemfibrozil, repaglinide, pioglitazone, rifampicin, clarithromycin and itraconazole. *Clinical Pharmacokinetics*. 2019;58(12):1595–607. DOI: [10.1007/s40262-019-00777-x](https://doi.org/10.1007/s40262-019-00777-x)
27. Türk D, Fuhr LM, Marok FZ, Rüdeshheim S, Kühn A, Selzer D, Schwab M, and Lehr T. Novel models for the prediction of drug-gene interactions. *Expert Opinion on Drug Metabolism & Toxicology*. 2021;17(11):1293–310. DOI: [10.1080/17425255.2021.1998455](https://doi.org/10.1080/17425255.2021.1998455)
28. Zhang L, Huang SM, Reynolds K, Madabushi R, and Zineh I. Transporters in drug development: scientific and regulatory considerations. *Clinical Pharmacology & Therapeutics*. 2018;104(5):793–6. DOI: [10.1002/cpt.1214](https://doi.org/10.1002/cpt.1214)

29. Galetin A, Zhao P, and Huang SM. Physiologically based pharmacokinetic modeling of drug transporters to facilitate individualized dose prediction. *Journal of Pharmaceutical Sciences*. 2017;106(9):2204–8. DOI: [10.1016/j.xphs.2017.03.036](https://doi.org/10.1016/j.xphs.2017.03.036)
30. Jala A, Ponneganti S, Vishnubhatla DS, Bhuvanam G, Mekala PR, Varghese B, Radhakrishnanand P, Adela R, Murty US, and Borkar RM. Transporter-mediated drug-drug interactions: advancement in models, analytical tools, and regulatory perspective. *Drug Metabolism Reviews*. 2021;53(3):285–320. DOI: [10.1080/03602532.2021.1928687](https://doi.org/10.1080/03602532.2021.1928687)
31. Giacomini KM and Sugiyama Y. Membrane transporters and drug response. *Goodman and Gilman's The pharmacological basis of therapeutics*. Ed. by Brunton L, Lazo J, and Parker R. McGraw-Hill, New York, 2006:41–70
32. Drozdik M, Drozdik M, and Oswald S. Membrane carriers and transporters in kidney physiology and disease. *Biomedicines*. 2021;9(4):426. DOI: [10.3390/biomedicines9040426](https://doi.org/10.3390/biomedicines9040426)
33. Fu S, Yu F, Sun T, and Hu Z. Transporter-mediated drug–drug interactions – Study design, data analysis, and implications for in vitro evaluations. *Medicine in Drug Discovery*. 2021;11:100096. DOI: [10.1016/j.medidd.2021.100096](https://doi.org/10.1016/j.medidd.2021.100096)
34. Ivanyuk A, Livio F, Biollaz J, and Buclin T. Renal drug transporters and drug interactions. *Clinical Pharmacokinetics*. 2017;56(8):825–92. DOI: [10.1007/s40262-017-0506-8](https://doi.org/10.1007/s40262-017-0506-8)
35. Huang SM, Zhang L, and Giacomini KM. The International Transporter Consortium: a collaborative group of scientists from academia, industry, and the FDA. *Clinical Pharmacology & Therapeutics*. 2010;87(1):32–6. DOI: [10.1038/clpt.2009.236](https://doi.org/10.1038/clpt.2009.236)
36. International Transporter Consortium, Giacomini KM, Huang SM, et al. Membrane transporters in drug development. *Nature Reviews Drug Discovery*. 2010;9(3):215–36. DOI: [10.1038/nrd3028](https://doi.org/10.1038/nrd3028)
37. U.S. Food and Drug Administration. In vitro drug interaction studies - Cytochrome P450 enzyme- and transporter-mediated drug interactions. Guidance for industry. 2020. Available from: <https://www.fda.gov/media/134582/download> [Internet] [cited 20 Jan 2022]
38. University of California, San Francisco. UCSF-FDA TransPortal. 2022. Available from: <https://transportal.compbio.ucsf.edu/> [Internet] [cited 17 Jan 2022]

39. Morrissey KM, Wen CC, Johns SJ, Zhang L, Huang SM, and Giacomini KM. The UCSF-FDA TransPortal: a public drug transporter database. *Clinical Pharmacology & Therapeutics*. 2012;92(5):545–6. DOI: [10.1038/clpt.2012.44](https://doi.org/10.1038/clpt.2012.44)
40. Oswald S, Müller J, Neugebauer U, Schröter R, Herrmann E, Pavenstädt H, and Ciarimboli G. Protein abundance of clinically relevant drug transporters in the human kidneys. *International Journal of Molecular Sciences*. 2019;20(21):1–12. DOI: [10.3390/ijms20215303](https://doi.org/10.3390/ijms20215303)
41. Zamek-Gliszczynski MJ, Taub ME, Chothe PP, et al. Transporters in drug development: 2018 ITC recommendations for transporters of emerging clinical importance. *Clinical Pharmacology & Therapeutics*. 2018;104(5):890–9. DOI: [10.1002/cpt.1112](https://doi.org/10.1002/cpt.1112)
42. Prasad B, Johnson K, Billington S, Lee C, Chung GW, Brown CDA, Kelly EJ, Himmelfarb J, and Unadkat JD. Abundance of drug transporters in the human kidney cortex as quantified by quantitative targeted proteomics. 2016;44(12):1920–4
43. U.S. Food and Drug Administration. Clinical drug interaction studies - Cytochrome P450 enzyme- and transporter-mediated drug interactions. Guidance for industry. 2020. Available from: <https://www.fda.gov/media/134581/download> [Internet] [cited 20 Jan 2022]
44. Neuhoff S, Ungell AL, Zamora I, and Artursson P. pH-dependent bidirectional transport of weakly basic drugs across Caco-2 monolayers: implications for drug-drug interactions. *Pharmaceutical Research*. 2003;20(8):1141–8. DOI: [10.1023/a:1025032511040](https://doi.org/10.1023/a:1025032511040)
45. Varma MVS, Feng B, Obach RS, Troutman DC, Chupka J, Miller HR, and El-Kattan A. Physicochemical determinants of human renal clearance. *Journal of Medicinal Chemistry*. 2009;52(15):4844–52. DOI: [10.1021/jm900403j](https://doi.org/10.1021/jm900403j)
46. Koepsell H. Update on drug-drug interaction at organic cation transporters: mechanisms, clinical impact, and proposal for advanced *in vitro* testing. *Expert Opinion on Drug Metabolism & Toxicology*. 2021;17(6):635–53. DOI: [10.1080/17425255.2021.1915284](https://doi.org/10.1080/17425255.2021.1915284)
47. Otsuka M, Matsumoto T, Morimoto R, Arioka S, Omote H, and Moriyama Y. A human transporter protein that mediates the final excretion step for toxic organic cations. *Proceedings of the National Academy of Sciences of the United States of America*. 2005;102(50):17923–8. DOI: [10.1073/pnas.0506483102](https://doi.org/10.1073/pnas.0506483102)

48. Masuda S, Terada T, Yonezawa A, Tanihara Y, Kishimoto K, Katsura T, Ogawa O, and Inui KI. Identification and functional characterization of a new human kidney-specific H<sup>+</sup>/organic cation antiporter, kidney-specific multidrug and toxin extrusion 2. *Journal of the American Society of Nephrology*. 2006;17(8):2127–35. DOI: [10.1681/ASN.2006030205](https://doi.org/10.1681/ASN.2006030205)
49. EMA Committee for Human Medicinal Products (CHMP). Guideline on the investigation of drug interactions. 2013. Available from: [https://www.ema.europa.eu/en/documents/scientific-guideline/guideline-investigation-drug-interactions-revision-1\\_en.pdf](https://www.ema.europa.eu/en/documents/scientific-guideline/guideline-investigation-drug-interactions-revision-1_en.pdf) [Internet] [cited 20 Jan 2022]
50. Freedman MD. Drug interactions: classification and systematic approach. *American Journal of Therapeutics*. 1995;2(6):433–43
51. Cleland WW. The kinetics of enzyme-catalyzed reactions with two or more substrates or products. II. Inhibition: nomenclature and theory. *Biochimica et Biophysica Acta*. 1963;67(C):173–87. DOI: [10.1016/0006-3002\(63\)91815-8](https://doi.org/10.1016/0006-3002(63)91815-8)
52. Tipton KF. Enzyme kinetics in relation to enzyme inhibitors. *Biochemical Pharmacology*. 1973;22(23):2933–41. DOI: [10.1016/0006-2952\(73\)90179-2](https://doi.org/10.1016/0006-2952(73)90179-2)
53. Silverman RB. Mechanism-based enzyme inactivators. *Methods in Enzymology*. 1995;249:240–83. DOI: [10.1016/0076-6879\(95\)49038-8](https://doi.org/10.1016/0076-6879(95)49038-8)
54. U.S. Food and Drug Administration. Drug development and drug interactions: table of substrates, inhibitors and inducers. 2017. Available from: <https://www.fda.gov/drugs/drug-interactions-labeling/drug-development-and-drug-interactions-table-substrates-inhibitors-and-inducers> [Internet] [cited 01 Mar 2022]
55. Gessner A, König J, and Fromm MF. Clinical aspects of transporter-mediated drug-drug interactions. *Clinical Pharmacology & Therapeutics*. 2019;105(6):1386–94. DOI: [10.1002/cpt.1360](https://doi.org/10.1002/cpt.1360)
56. Peng Y, Cheng Z, and Xie F. Evaluation of pharmacokinetic drug-drug interactions: a review of the mechanisms, in vitro and in silico approaches. 2021;11(2):1–16. DOI: [10.3390/metabo11020075](https://doi.org/10.3390/metabo11020075)
57. Pan Y, Hsu V, Grimstein M, Zhang L, Arya V, Sinha V, Grillo JA, and Zhao P. The application of physiologically based pharmacokinetic modeling to predict the role of drug transporters: scientific and regulatory perspectives. *Journal of Clinical Pharmacology*. 2016;56 (Suppl 7):S122–31. DOI: [10.1002/jcph.740](https://doi.org/10.1002/jcph.740)

58. Miyake T, Kimoto E, Luo L, et al. Identification of appropriate endogenous biomarker for risk assessment of multidrug and toxin extrusion protein-mediated drug-drug interactions in healthy volunteers. *Clinical Pharmacology & Therapeutics*. 2021;109(2):507–16. DOI: [10.1002/cpt.2022](https://doi.org/10.1002/cpt.2022)
59. Mariappan TT, Shen H, and Marathe P. Endogenous biomarkers to assess drug-drug interactions by drug transporters and enzymes. *Current Drug Metabolism*. 2017;18(8):757–68. DOI: [10.2174/1389200218666170724110818](https://doi.org/10.2174/1389200218666170724110818)
60. Hacker K, Maas R, Kornhuber J, Fromm MF, and Zolk O. Substrate-dependent inhibition of the human organic cation transporter OCT2: a comparison of metformin with experimental substrates. *PloS One*. 2015;10(9):e0136451. DOI: [10.1371/journal.pone.0136451](https://doi.org/10.1371/journal.pone.0136451)
61. U.S. Food and Drug Administration. Drug development and drug interactions. Possible models for decision-making. Evaluation of investigational drugs as substrates for P-gp, BCRP, OATP1B1, OATP1B3, OAT1, OAT3, and OCT2 transporters and an interacting drug. 2015. Available from: <https://web.archive.org/web/20130702231323/http://www.fda.gov/downloads/Drugs/DevelopmentApprovalProcess/DevelopmentResources/DrugInteractionsLabeling/UCM269211.pdf> [Internet] [cited 18 Jan 2022]
62. U.S. Food and Drug Administration. Drug development and drug interactions. Possible models for decision-making. Decision tree to determine whether an investigational drug is a substrate for P-gp and when an in vivo clinical study is needed. 2015. Available from: <https://web.archive.org/web/20130702192726/http://www.fda.gov/downloads/Drugs/DevelopmentApprovalProcess/DevelopmentResources/DrugInteractionsLabeling/UCM269213.pdf> [Internet] [cited 18 Jan 2022]
63. U.S. Food and Drug Administration. Drug development and drug interactions. Possible models for decision-making. Decision tree to determine whether an investigational drug is a substrate for OATP1B1 or OATP1B3 and when an in vivo clinical study is needed. 2015. Available from: <https://web.archive.org/web/20130702225617/http://www.fda.gov/downloads/Drugs/DevelopmentApprovalProcess/DevelopmentResources/DrugInteractionsLabeling/UCM269216.pdf> [Internet] [cited 18 Jan 2022]
64. U.S. Food and Drug Administration. Drug development and drug interactions. Possible models for decision-making. Decision tree to determine whether an investigational drug is a substrate for OCT2, OAT1, or OAT3 and when an in vivo clinical

- study is needed. 2015. Available from: <https://web.archive.org/web/20130702185028/http://www.fda.gov/downloads/Drugs/DevelopmentApprovalProcess/DevelopmentResources/DrugInteractionsLabeling/UCM269220.pdf> [Internet] [cited 18 Jan 2022]
65. U.S. Food and Drug Administration. Drug development and drug interactions. Possible models for decision-making. Decision tree to determine whether an investigational drug is an inhibitor of P-gp and when an in vivo clinical study is needed. 2015. Available from: <https://web.archive.org/web/20130702181140/http://www.fda.gov/downloads/Drugs/DevelopmentApprovalProcess/DevelopmentResources/DrugInteractionsLabeling/UCM269215.pdf> [Internet] [cited 18 Jan 2022]
66. U.S. Food and Drug Administration. Drug development and drug interactions. Possible models for decision-making. Decision tree to determine whether an investigational drug is an inhibitor of OATP1B1 or OATP1B3 and when an in vivo clinical study is needed. 2015. Available from: <https://web.archive.org/web/20130703014006/http://www.fda.gov/downloads/Drugs/DevelopmentApprovalProcess/DevelopmentResources/DrugInteractionsLabeling/UCM269218.pdf> [Internet] [cited 18 Jan 2022]
67. U.S. Food and Drug Administration. Drug development and drug interactions. Possible models for decision-making. Decision tree to determine whether an investigational drug is an inhibitor of OCT2, OAT1, or OAT3 and when an in vivo clinical study is needed. 2015. Available from: <https://web.archive.org/web/20130702202736/http://www.fda.gov/downloads/Drugs/DevelopmentApprovalProcess/DevelopmentResources/DrugInteractionsLabeling/UCM269222.pdf> [Internet] [cited 18 Jan 2022]
68. Müller F, Pontones CA, Renner B, Mieth M, Hoier E, Auge D, Maas R, Zolk O, and Fromm MF. N<sup>1</sup>-methylnicotinamide as an endogenous probe for drug interactions by renal cation transporters: studies on the metformin-trimethoprim interaction. *European Journal of Clinical Pharmacology*. 2015;71(1):85–94. DOI: [10.1007/s00228-014-1770-2](https://doi.org/10.1007/s00228-014-1770-2)
69. Kusuhara H, Ito S, Kumagai Y, Jiang M, Shiroshita T, Moriyama Y, Inoue K, Yuasa H, and Sugiyama Y. Effects of a MATE protein inhibitor, pyrimethamine, on the renal elimination of metformin at oral microdose and at therapeutic dose in healthy subjects. *Clinical Pharmacology & Therapeutics*. 2011;89(6):837–44. DOI: [10.1038/clpt.2011.36](https://doi.org/10.1038/clpt.2011.36)

70. Oh J, Chung H, Park SI, et al. Inhibition of the multidrug and toxin extrusion (MATE) transporter by pyrimethamine increases the plasma concentration of metformin but does not increase antihyperglycaemic activity in humans. *Diabetes, Obesity and Metabolism*. 2016;18(1):104–8. DOI: [10.1111/dom.12577](https://doi.org/10.1111/dom.12577)
71. Wang ZJ, Yin OQP, Tomlinson B, and Chow MSS. OCT2 polymorphisms and in-vivo renal functional consequence: studies with metformin and cimetidine. *Pharmacogenetics and Genomics*. 2008;18(7):637–45. DOI: [10.1097/FPC.0b013e328302cd41](https://doi.org/10.1097/FPC.0b013e328302cd41)
72. Somogyi A, Stockley C, Keal J, Rolan P, and Bochner F. Reduction of metformin renal tubular secretion by cimetidine in man. *British Journal of Clinical Pharmacology*. 1987;23(5):545–51. DOI: [10.1111/j.1365-2125.1987.tb03090.x](https://doi.org/10.1111/j.1365-2125.1987.tb03090.x)
73. Rodrigues D and Rowland A. From endogenous compounds as biomarkers to plasma-derived nanovesicles as liquid biopsy; has the golden age of translational pharmacokinetics-absorption, distribution, metabolism, excretion-drug-drug interaction science finally arrived? *Clinical Pharmacology & Therapeutics*. 2019;105(6):1407–20. DOI: [10.1002/cpt.1328](https://doi.org/10.1002/cpt.1328)
74. Shen H. A pharmaceutical industry perspective on transporter and CYP-mediated drug-drug interactions: kidney transporter biomarkers. *Bioanalysis*. 2018;10(9):625–31. DOI: [10.4155/bio-2017-0265](https://doi.org/10.4155/bio-2017-0265)
75. Müller F, Sharma A, König J, and Fromm MF. Biomarkers for in vivo assessment of transporter function. *Pharmacological Reviews*. 2018;70(2):246–77. DOI: [10.1124/pr.116.013326](https://doi.org/10.1124/pr.116.013326)
76. Rodrigues AD, Taskar KS, Kusuhara H, and Sugiyama Y. Endogenous probes for drug transporters: balancing vision with reality. *Clinical Pharmacology & Therapeutics*. 2018;103(3):434–48. DOI: [10.1002/cpt.749](https://doi.org/10.1002/cpt.749)
77. Ito S, Kusuhara H, Kumagai Y, et al. N-methylnicotinamide is an endogenous probe for evaluation of drug-drug interactions involving multidrug and toxin extrusions (MATE<sub>1</sub> and MATE<sub>2-K</sub>). *Clinical Pharmacology & Therapeutics*. 2012;92(5):635–41. DOI: [10.1038/clpt.2012.138](https://doi.org/10.1038/clpt.2012.138)
78. Chu X, Bleasby K, Chan GH, Nunes I, and Evers R. The complexities of interpreting reversible elevated serum creatinine levels in drug development: does a correlation with inhibition of renal transporters exist? *Drug Metabolism & Disposition*. 2016;44(9):1498–509. DOI: [10.1124/dmd.115.067694](https://doi.org/10.1124/dmd.115.067694)

79. Chu X, Liao M, Shen H, et al. Clinical probes and endogenous biomarkers as substrates for transporter drug-drug interaction evaluation: perspectives from the International Transporter Consortium. *Clinical Pharmacology & Therapeutics*. 2018;104(5):836–64. DOI: [10.1002/cpt.1216](https://doi.org/10.1002/cpt.1216)
80. Fromm MF. Prediction of transporter-mediated drug-drug interactions using endogenous compounds. *Clinical Pharmacology & Therapeutics*. 2012;92(5):546–8. DOI: [10.1038/clpt.2012.145](https://doi.org/10.1038/clpt.2012.145)
81. Miyake T, Mizuno T, Takehara I, et al. Elucidation of N<sup>1</sup>-methyladenosine as a potential surrogate biomarker for drug interaction studies involving renal organic cation transporters. *Drug Metabolism & Disposition*. 2019;47(11):1270–80. DOI: [10.1124/dmd.119.087262](https://doi.org/10.1124/dmd.119.087262)
82. Brosnan JT, Silva RP da, and Brosnan ME. The metabolic burden of creatine synthesis. *Amino Acids*. 2011;40(5):1325–31. DOI: [10.1007/s00726-011-0853-y](https://doi.org/10.1007/s00726-011-0853-y)
83. Levey AS, Perrone RD, and Madias NE. Serum creatinine and renal function. *Annual Review of Medicine*. 1988;39(1):465–90. DOI: [10.1146/annurev.me.39.020188.002341](https://doi.org/10.1146/annurev.me.39.020188.002341)
84. Lepist EI, Zhang X, Hao J, et al. Contribution of the organic anion transporter OAT2 to the renal active tubular secretion of creatinine and mechanism for serum creatinine elevations caused by cobicistat. *Kidney International*. 2014;86(2):350–7. DOI: [10.1038/ki.2014.66](https://doi.org/10.1038/ki.2014.66)
85. Mathialagan S, Rodrigues AD, and Feng B. Evaluation of renal transporter inhibition using creatinine as a substrate *in vitro* to assess the clinical risk of elevated serum creatinine. *Journal of Pharmaceutical Sciences*. 2017;106(9):2535–41. DOI: [10.1016/j.xphs.2017.04.009](https://doi.org/10.1016/j.xphs.2017.04.009)
86. Koopman MG, Koomen GCM, Krediet RT, Moor EA de, Hoek FJ, and Arisz L. Circadian rhythm of glomerular filtration rate in normal individuals. *Clinical Science*. 1989;77(1):105–11. DOI: [10.1042/cs0770105](https://doi.org/10.1042/cs0770105)
87. Myre SA, McCann J, First MR, and Cluxton RJ. Effect of trimethoprim on serum creatinine in healthy and chronic renal failure volunteers. *Therapeutic Drug Monitoring*. 1987;9(2):161–5. DOI: [10.1097/00007691-198706000-00006](https://doi.org/10.1097/00007691-198706000-00006)
88. Roy MT, First MR, Myre SA, and Cacini W. Effect of cotrimoxazole and sulfamethoxazole on serum creatinine in normal subjects. *Therapeutic Drug Monitoring*. 1982;4(1):77–9. DOI: [10.1097/00007691-198204000-00011](https://doi.org/10.1097/00007691-198204000-00011)



89. Bräutigam M, Froese P, Baethke R, and Kessel M. [Effect of co-trimoxazole on renal creatinine excretion in man (author's transl)]. *Klinische Wochenschrift*. 1979;57(2):95–6. DOI: [10.1007/BF01491342](https://doi.org/10.1007/BF01491342)
90. Berglund F, Killander J, and Pompeius R. Effect of trimethoprim-sulfamethoxazole on the renal excretion of creatinine in man. *Journal of Urology*. 1975;114(6):802–8. DOI: [10.1016/S0022-5347\(17\)67149-0](https://doi.org/10.1016/S0022-5347(17)67149-0)
91. Grün B, Kiessling MK, Burhenne J, Riedel KD, Weiss J, Rauch G, Haefeli WE, and Czock D. Trimethoprim-metformin interaction and its genetic modulation by OCT2 and MATE1 transporters. *British Journal of Clinical Pharmacology*. 2013;76(5):787–96. DOI: [10.1111/bcp.12079](https://doi.org/10.1111/bcp.12079)
92. Naderer O, Nafziger AN, and Bertino JS. Effects of moderate-dose versus high-dose trimethoprim on serum creatinine and creatinine clearance and adverse reactions. *Antimicrobial Agents and Chemotherapy*. 1997;41(11):2466–70. DOI: [10.1128/AAC.41.11.2466](https://doi.org/10.1128/AAC.41.11.2466)
93. Shouval D, Ligumsky M, and Ben-Ishay D. Effect of co-trimoxazole on normal creatinine clearance. *Lancet*. 1978;1(8058):244–5. DOI: [10.1016/s0140-6736\(78\)90486-5](https://doi.org/10.1016/s0140-6736(78)90486-5)
94. Opravil M, Keusch G, and Luthy R. Pyrimethamine inhibits renal secretion of creatinine. *Antimicrobial Agents and Chemotherapy*. 1993;37(5):1056–60. DOI: [10.1128/AAC.37.5.1056](https://doi.org/10.1128/AAC.37.5.1056)
95. Hilbrands LB, Artz MA, Wetzels JFM, and Koene RAP. Cimetidine improves the reliability of creatinine as a marker of glomerular filtration. *Kidney International*. 1991;40(6):1171–6. DOI: [10.1038/ki.1991.331](https://doi.org/10.1038/ki.1991.331)
96. Serdar MA, Kurt I, Ozcelik F, Urhan M, Ilgan S, Yenicesu M, Kenar L, and Kutluay T. A practical approach to glomerular filtration rate measurements: creatinine clearance estimation using cimetidine. *Annals of Clinical and Laboratory Science*. 2001;31(3):265–73
97. van Acker BAC, Koomen GCM, Koopman MG, Krediet RT, and Arisz L. Discrepancy between circadian rhythms of inulin and creatinine clearance. *The Journal of Laboratory and Clinical Medicine*. 1992;120(3):400–10. DOI: [10.5555/uri:pii:002221439290040R](https://doi.org/10.5555/uri:pii:002221439290040R)
98. Weber W, Toussaint S, Looby M, Nitz M, and Kewitz H. System analysis in multiple dose kinetics: evidence for saturable tubular reabsorption of the organic cation N<sup>1</sup>-methylnicotinamide in humans. *Journal of Pharmacokinetics and Biopharmaceutics*. 1991;19(5):553–74. DOI: [10.1007/BF01062963](https://doi.org/10.1007/BF01062963)

99. Okamoto H, Ishikawa A, Yoshitake Y, Kodama N, Nishimuta M, Fukuwatari T, and Shibata K. Diurnal variations in human urinary excretion of nicotinamide catabolites: effects of stress on the metabolism of nicotinamide. *The American Journal of Clinical Nutrition*. 2003;77(2):406–10. DOI: [10.1093/ajcn/77.2.406](https://doi.org/10.1093/ajcn/77.2.406)
100. Badawy AAB. Kynurenine pathway of tryptophan metabolism: regulatory and functional aspects. *International Journal of Tryptophan Research*. 2017;10:1–20. DOI: [10.1177/1178646917691938](https://doi.org/10.1177/1178646917691938)
101. Bieganowski P and Brenner C. Discoveries of nicotinamide riboside as a nutrient and conserved NRK genes establish a Preiss-Handler independent route to NAD<sup>+</sup> in fungi and humans. *Cell*. 2004;117(4):495–502. DOI: [10.1016/s0092-8674\(04\)00416-7](https://doi.org/10.1016/s0092-8674(04)00416-7)
102. Pissios P. Nicotinamide N-methyltransferase: more than a vitamin B<sub>3</sub> clearance enzyme. *Trends in Endocrinology & Metabolism*. 2017;28(5):340–53. DOI: [10.1016/j.tem.2017.02.004](https://doi.org/10.1016/j.tem.2017.02.004)
103. Zanger U, Klein K, Kugler N, Petrikat T, and Ryu C. Chapter two - epigenetics and microRNAs in pharmacogenetics. *Pharmacogenetics*. Ed. by Brøsen K and Damkier P. Vol. 83. *Advances in Pharmacology*. Academic Press, 2018:33–64. DOI: <https://doi.org/10.1016/bs.apha.2018.02.003>
104. Zanger UM and Schwab M. Cytochrome P450 enzymes in drug metabolism: regulation of gene expression, enzyme activities, and impact of genetic variation. 2013;138(1):103–41. DOI: [10.1016/j.pharmthera.2012.12.007](https://doi.org/10.1016/j.pharmthera.2012.12.007)
105. Yee SW, Brackman DJ, Ennis EA, Sugiyama Y, Kamdem LK, Blanchard R, Galetin A, Zhang L, and Giacomini KM. Influence of transporter polymorphisms on drug disposition and response: a perspective from the International Transporter Consortium. *Clinical Pharmacology & Therapeutics*. 2018;104(5):803–17. DOI: [10.1002/cpt.1098](https://doi.org/10.1002/cpt.1098)
106. Shastry BS. SNP alleles in human disease and evolution. *Journal of Human Genetics*. 2002;47(11):561–6. DOI: [10.1007/s100380200086](https://doi.org/10.1007/s100380200086)
107. Schwarz UI, Gulilat M, and Kim RB. The role of next-generation sequencing in pharmacogenetics and pharmacogenomics. *Cold Spring Harbor Perspectives in Medicine*. 2019;9(2):a033027. DOI: [10.1101/cshperspect.a033027](https://doi.org/10.1101/cshperspect.a033027)

108. Caudle KE, Dunnenberger HM, Freimuth RR, et al. Standardizing terms for clinical pharmacogenetic test results: consensus terms from the Clinical Pharmacogenetics Implementation Consortium (CPIC). *Genetics in Medicine*. 2017;19(2):215–23. DOI: [10.1038/gim.2016.87](https://doi.org/10.1038/gim.2016.87)
109. Kuehl P, Zhang J, Lin Y, et al. Sequence diversity in *CYP3A* promoters and characterization of the genetic basis of polymorphic *CYP3A5* expression. *Nature Genetics*. 2001;27(4):383–91. DOI: [10.1038/86882](https://doi.org/10.1038/86882)
110. Balram C, Zhou Q, Cheung YB, and Lee EJD. *CYP3A5*\*3 and \*6 single nucleotide polymorphisms in three distinct Asian populations. *European Journal of Clinical Pharmacology*. 2003;59(2):123–6. DOI: [10.1007/s00228-003-0594-2](https://doi.org/10.1007/s00228-003-0594-2)
111. Pharmacogenomics Knowledgebase. FDA drug label annotations. Available from: <https://www.pharmgkb.org/fdaLabelAnnotations> [Internet] [cited 19 Jan 2022]
112. Whirl-Carrillo M, McDonagh EM, Hebert JM, Gong L, Sangkuhl K, Thorn CF, Altman RB, and Klein TE. Pharmacogenomics knowledge for personalized medicine. *Clinical Pharmacology & Therapeutics*. 2012;92(4):414–7. DOI: [10.1038/clpt.2012.96](https://doi.org/10.1038/clpt.2012.96)
113. Whirl-Carrillo M, Huddart R, Gong L, Sangkuhl K, Thorn CF, Whaley R, and Klein TE. An evidence-based framework for evaluating pharmacogenomics knowledge for personalized medicine. *Clinical Pharmacology & Therapeutics*. 2021;110(3):563–72. DOI: [10.1002/cpt.2350](https://doi.org/10.1002/cpt.2350)
114. Pharmacogenomics Knowledgebase. VIPs: Very Important Pharmacogenes. Available from: <https://www.pharmgkb.org/vips> [Internet] [cited 19 Jan 2022]
115. National Center for Biotechnology Information (NCBI). dbSNP - rs316019. Available from: <https://www.ncbi.nlm.nih.gov/snp/rs316019> [Internet] [cited 16 Oct 2020]
116. Song IS, Shin HJ, Shim EJ, Jung IS, Kim WY, Shon JH, and Shin JG. Genetic variants of the organic cation transporter 2 influence the disposition of metformin. *Clinical Pharmacology & Therapeutics*. 2008;84(5):559–62. DOI: [10.1038/clpt.2008.61](https://doi.org/10.1038/clpt.2008.61)
117. Zolk O, Solbach TF, König J, and Fromm MF. Functional characterization of the human organic cation transporter 2 variant p.270Ala>Ser. *Drug Metabolism & Disposition*. 2009;37(6):1312–8. DOI: [10.1124/dmd.108.023762](https://doi.org/10.1124/dmd.108.023762)
118. Chen Y, Li S, Brown C, et al. Effect of genetic variation in the organic cation transporter 2 on the renal elimination of metformin. *Pharmacogenetics and Genomics*. 2009;19(7):497–504. DOI: [10.1097/FPC.0b013e32832cc7e9](https://doi.org/10.1097/FPC.0b013e32832cc7e9)

119. Christensen MMH, Pedersen RS, Stage TB, Brasch-Andersen C, Nielsen F, Damkier P, Beck-Nielsen H, and Brøsen K. A gene–gene interaction between polymorphisms in the OCT2 and MATE1 genes influences the renal clearance of metformin. *Pharmacogenetics and Genomics*. 2013;23(10):526–34. DOI: [10.1097/FPC.0b013e328364a57d](https://doi.org/10.1097/FPC.0b013e328364a57d)
120. Filipski KK, Mathijssen RH, Mikkelsen TS, Schinkel AH, and Sparreboom A. Contribution of organic cation transporter 2 (OCT2) to cisplatin-induced nephrotoxicity. *Clinical Pharmacology & Therapeutics*. 2009;86(4):396–402. DOI: [10.1038/clpt.2009.139](https://doi.org/10.1038/clpt.2009.139)
121. Frenzel D, Köppen C, Bauer OB, Karst U, Schröter R, Tzvetkov MV, and Ciarimboli G. Effects of single nucleotide polymorphism Ala270Ser (rs316019) on the function and regulation of hOCT2. *Biomolecules*. 2019;9(10):578. DOI: [10.3390/biom9100578](https://doi.org/10.3390/biom9100578)
122. Iwata K, Aizawa K, Kamitsu S, Jingami S, Fukunaga E, Yoshida M, Yoshimura M, Hamada A, and Saito H. Effects of genetic variants in SLC22A2 organic cation transporter 2 and SLC47A1 multidrug and toxin extrusion 1 transporter on cisplatin-induced adverse events. *Clinical and Experimental Nephrology*. 2012;16(6):843–51. DOI: [10.1007/s10157-012-0638-y](https://doi.org/10.1007/s10157-012-0638-y)
123. Hinai Y, Motoyama S, Niioka T, and Miura M. Absence of effect of *SLC22A2* genotype on cisplatin-induced nephrotoxicity in oesophageal cancer patients receiving cisplatin and 5-fluorouracil: report of results discordant with those of earlier studies. *Journal of Clinical Pharmacy and Therapeutics*. 2013;38(6):498–503. DOI: [10.1111/jcpt.12097](https://doi.org/10.1111/jcpt.12097)
124. National Center for Biotechnology Information (NCBI). dbSNP - rs2252281. Available from: <https://www.ncbi.nlm.nih.gov/snp/rs2252281> [Internet] [cited 20 Jan 2022]
125. Ha Choi J, Wah Yee S, Kim MJ, et al. Identification and characterization of novel polymorphisms in the basal promoter of the human transporter, MATE1. *Pharmacogenetics and Genomics*. 2009;19(10):770–80. DOI: [10.1097/FPC.0b013e328330eeca](https://doi.org/10.1097/FPC.0b013e328330eeca)
126. National Center for Biotechnology Information (NCBI). dbSNP - rs2289669. Available from: <https://www.ncbi.nlm.nih.gov/snp/rs2289669> [Internet] [cited 20 Jan 2022]
127. He R, Zhang D, Lu W, Zheng T, Wan L, Liu F, and Jia W. SLC47A1 gene rs2289669 G>A variants enhance the glucose-lowering effect of metformin via delaying its excretion in Chinese type 2 diabetes patients. *Diabetes Research and Clinical*

- Practice. 2015;109(1):57–63. DOI: [10.1016/j.diabres.2015.05.003](https://doi.org/10.1016/j.diabres.2015.05.003)
128. Evers R, Piquette-Miller M, Polli JW, et al. Disease-associated changes in drug transporters may impact the pharmacokinetics and/or toxicity of drugs: a white paper from the International Transporter Consortium. *Clinical Pharmacology & Therapeutics*. 2018;104(5):900–15. DOI: [10.1002/cpt.1115](https://doi.org/10.1002/cpt.1115)
  129. Lv JC and Zhang LX. Prevalence and disease burden of chronic kidney disease. *Renal fibrosis: mechanisms and therapies*. Ed. by Liu BC, Lan HY, and Lv LL. Singapore: Springer Singapore, 2019:3–15. DOI: [10.1007/978-981-13-8871-2\\_1](https://doi.org/10.1007/978-981-13-8871-2_1)
  130. Levey AS, Eckardt KU, Tsukamoto Y, Levin A, Coresh J, Rossert J, De Zeeuw D, Hostetter TH, Lameire N, and Eknoyan G. Definition and classification of chronic kidney disease: a position statement from Kidney Disease: Improving Global Outcomes (KDIGO). *Kidney International*. 2005;67(6):2089–100. DOI: [10.1111/j.1523-1755.2005.00365.x](https://doi.org/10.1111/j.1523-1755.2005.00365.x)
  131. KDIGO. KDIGO 2012 Clinical practice guideline for the evaluation and management of chronic kidney disease. Official Journal of the international Society of nephrology KDIGO. 2013. Available from: [https://kdigo.org/wp-content/uploads/2017/02/KDIGO\\_2012\\_CKD\\_GL.pdf](https://kdigo.org/wp-content/uploads/2017/02/KDIGO_2012_CKD_GL.pdf) [Internet] [cited 14 Jun 2022]
  132. Ladda MA and Goralski KB. The effects of CKD on cytochrome P450-mediated drug metabolism. *Advances in Chronic Kidney Disease*. 2016;23(2):67–75. DOI: [10.1053/j.ackd.2015.10.002](https://doi.org/10.1053/j.ackd.2015.10.002)
  133. Lalande L, Charpiat B, Leboucher G, and Tod M. Consequences of renal failure on non-renal clearance of drugs. *Clinical Pharmacokinetics*. 2014;53(6):521–32. DOI: [10.1007/s40262-014-0146-1](https://doi.org/10.1007/s40262-014-0146-1)
  134. Miners JO, Yang X, Knights KM, and Zhang L. The role of the kidney in drug elimination: transport, metabolism, and the impact of kidney disease on drug clearance. *Clinical Pharmacology & Therapeutics*. 2017;102(3):436–49. DOI: [10.1002/cpt.757](https://doi.org/10.1002/cpt.757)
  135. Haller C. Hypoalbuminemia in renal failure: pathogenesis and therapeutic considerations. *Kidney and Blood Pressure Research*. 2005;28(5-6):307–10. DOI: [10.1159/000090185](https://doi.org/10.1159/000090185)
  136. Cheung KWK, Hsueh CH, Zhao P, Meyer TW, Zhang L, Huang SM, and Giacomini KM. The effect of uremic solutes on the organic cation transporter 2. *Journal of Pharmaceutical Sciences*. 2017;106(9):2551–7. DOI: [10.1016/j.xphs.2017.04.076](https://doi.org/10.1016/j.xphs.2017.04.076)

137. Hsueh CH, Yoshida K, Zhao P, Meyer TW, Zhang L, Huang SM, and Giacomini KM. Identification and quantitative assessment of uremic solutes as inhibitors of renal organic anion transporters, OAT<sub>1</sub> and OAT<sub>3</sub>. *Molecular Pharmaceutics*. 2016;13(9):3130–40. DOI: [10.1021/acs.molpharmaceut.6b00332](https://doi.org/10.1021/acs.molpharmaceut.6b00332)
138. Nishihara K, Masuda S, Ji L, Katsura T, and Inui KI. Pharmacokinetic significance of luminal multidrug and toxin extrusion 1 in chronic renal failure rats. *Journal of Biopharmaceutics and Clinical Pharmacokinetics*. 2007;73(9):1482–90. DOI: [10.1016/j.bcp.2006.12.034](https://doi.org/10.1016/j.bcp.2006.12.034)
139. Zhang G, Ma Y, Xi D, Rao Z, Sun X, and Wu X. Effect of high uric acid on the disposition of metformin: *in vivo* and *in vitro* studies. *Biopharmaceutics & Drug Disposition*. 2019;40(1):3–11. DOI: [10.1002/bdd.2164](https://doi.org/10.1002/bdd.2164)
140. U.S. Food and Drug Administration. Pharmacokinetics in patients with impaired renal function - study design, data analysis and impact on dosing and labeling. Guidance for industry. 2020. Available from: <https://www.fda.gov/regulatory-information/search-fda-guidance-documents/pharmacokinetics-patients-impaired-renal-function-study-design-data-analysis-and-impact-dosing-and-labeling> [Internet] [cited 20 Jan 2022]
141. European Medicines Agency. Guideline on the evaluation of the pharmacokinetics of medicinal products in patients with decreased renal function. 2015. Available from: [https://www.ema.europa.eu/en/documents/scientific-guideline/guideline-evaluation-pharmacokinetics-medicinal-products-patients-decreased-renal-function\\_en.pdf](https://www.ema.europa.eu/en/documents/scientific-guideline/guideline-evaluation-pharmacokinetics-medicinal-products-patients-decreased-renal-function_en.pdf) [Internet] [cited 20 Jan 2022]
142. Xiao JJ, Chen JS, Lum BL, and Graham RA. A survey of renal impairment pharmacokinetic studies for new oncology drug approvals in the USA from 2010 to early 2015: a focus on development strategies and future directions. *Anti-Cancer Drugs*. 2017;28(7):677–701. DOI: [10.1097/CAD.0000000000000513](https://doi.org/10.1097/CAD.0000000000000513)
143. Rowland Yeo K and Gil Berglund E. An integrated approach for assessing the impact of renal impairment on pharmacokinetics of drugs in development: pivotal role of PBPK modelling. *Journal of Clinical Pharmacology and Therapeutics*. 2021;110(5):1168–71. DOI: [10.1002/cpt.2243](https://doi.org/10.1002/cpt.2243)
144. Dallmann R, Brown SA, and Gachon F. Chronopharmacology: new insights and therapeutic implications. *Annual Review of Pharmacology and Toxicology*. 2014;54(1):339–61. DOI: [10.1146/annurev-pharmtox-011613-135923](https://doi.org/10.1146/annurev-pharmtox-011613-135923)

145. Mohawk JA, Green CB, and Takahashi JS. Central and peripheral circadian clocks in mammals. *Annual Review of Neuroscience*. 2012;35(1):445–62. DOI: [10.1146/annurev-neuro-060909-153128](https://doi.org/10.1146/annurev-neuro-060909-153128)
146. Dakup PP, Porter KI, Little AA, Gajula RP, Zhang H, Skorniyakov E, Kemp MG, Van Dongen HPA, and Gaddameedhi S. The circadian clock regulates cisplatin-induced toxicity and tumor regression in melanoma mouse and human models. *Oncotarget*. 2018;9(18):14524–38. DOI: [10.18632/oncotarget.24539](https://doi.org/10.18632/oncotarget.24539)
147. Levi F, Hrushesky WJM, Borch RF, Pleasants ME, Kennedy BJ, and Halberg F. Cisplatin urinary pharmacokinetics and nephrotoxicity: a common circadian mechanism. *Cancer Treatment Reports*. 1982;66(11):1933–8
148. Hrushesky WJM, Borch R, and Levi F. Circadian time dependence of cisplatin urinary kinetics. *Clinical Pharmacology & Therapeutics*. 1982;32(3):330–9. DOI: [10.1038/clpt.1982.168](https://doi.org/10.1038/clpt.1982.168)
149. Zhou J, Wang J, Zhang X, and Tang Q. New insights into cancer chronotherapies. *Frontiers in Pharmacology*. 2021;12:741295. DOI: [10.3389/fphar.2021.741295](https://doi.org/10.3389/fphar.2021.741295)
150. Moore JG and Englert E. Circadian rhythm of gastric acid secretion in man. *Nature*. 1970;226(5252):1261–2. DOI: [10.1038/2261261a0](https://doi.org/10.1038/2261261a0)
151. Goo RH, Moore JG, Greenberg E, and Alazraki NP. Circadian variation in gastric emptying of meals in humans. *Gastroenterology*. 1987;93(3):515–8. DOI: [10.1016/0016-5085\(87\)90913-9](https://doi.org/10.1016/0016-5085(87)90913-9)
152. Vaughn B, Rotolo S, and Roth H. Circadian rhythm and sleep influences on digestive physiology and disorders. *ChronoPhysiology and Therapy*. 2014;4:67–77. DOI: [10.2147/CPT.S44806](https://doi.org/10.2147/CPT.S44806)
153. Lemmer B and Nold G. Circadian changes in estimated hepatic blood flow in healthy subjects. *British Journal of Clinical Pharmacology*. 1991;32(5):627–9. DOI: [10.1111/j.1365-2125.1991.tb03964.x](https://doi.org/10.1111/j.1365-2125.1991.tb03964.x)
154. Wesson LG. Electrolyte excretion in relation to diurnal cycles of renal function. *Medicine*. 1964;43(5):547–92. DOI: [10.1097/00005792-196409000-00002](https://doi.org/10.1097/00005792-196409000-00002)
155. Cameron MA, Maalouf NM, Poindexter J, Adams-Huet B, Sakhaee K, and Moe OW. The diurnal variation in urine acidification differs between normal individuals and uric acid stone formers. *Kidney International*. 2012;81(1):1123–30. DOI: [10.1038/ki.2011.480](https://doi.org/10.1038/ki.2011.480)

156. Ansermet C, Centeno G, Nikolaeva S, Maillard M, Pradervand S, and Firsov D. The intrinsic circadian clock in podocytes controls glomerular filtration rate. *Scientific Reports*. 2019;9(1):1–9. DOI: [10.1038/s41598-019-52682-9](https://doi.org/10.1038/s41598-019-52682-9)
157. Wuerzner G, Firsov D, and Bonny O. Circadian glomerular function: from physiology to molecular and therapeutical aspects. *Nephrology Dialysis Transplantation*. 2014;29(8):1475–80. DOI: [10.1093/ndt/gft525](https://doi.org/10.1093/ndt/gft525)
158. Oda M, Koyanagi S, Tsurudome Y, Kanemitsu T, Matsunaga N, and Ohdo S. Renal circadian clock regulates the dosing-time dependency of cisplatin-induced nephrotoxicity in mice. *Molecular Pharmacology*. 2014;85(5):715–22. DOI: [10.1124/mol.113.089805](https://doi.org/10.1124/mol.113.089805)
159. Barrett JS, Fossler MJ, Cadieu KD, and Gastonguay MR. Pharmacometrics: a multidisciplinary field to facilitate critical thinking in drug development and translational research settings. *Journal of Clinical Pharmacology*. 2008;48(5):632–49. DOI: [10.1177/0091270008315318](https://doi.org/10.1177/0091270008315318)
160. Williams PJ and Ette EI. Pharmacometrics: impacting drug development and pharmacotherapy. *Pharmacometrics*. Hoboken, NJ, USA: John Wiley Sons, Inc., 2007:1–21. DOI: [10.1002/9780470087978.ch1](https://doi.org/10.1002/9780470087978.ch1)
161. Ette EI and Williams PJ. Pharmacometrics: the science of quantitative pharmacology. Ed. by Ette EI and Williams PJ. Hoboken, NJ, USA: John Wiley Sons, Inc., 2006. DOI: [10.1002/0470087978](https://doi.org/10.1002/0470087978)
162. Peters SA. Physiologically-based pharmacokinetic (PBPK) modeling and simulations. Hoboken, NJ, USA: John Wiley Sons, Inc., 2012. DOI: [10.1002/9781118140291](https://doi.org/10.1002/9781118140291)
163. Taddio MF, Mu L, Keller C, Schibli R, and Krämer SD. Physiologically based pharmacokinetic modelling with dynamic PET data to study the *in vivo* effects of transporter inhibition on hepatobiliary clearance in mice. *Contrast Media & Molecular Imaging*. 2018;2018:5849047. DOI: [10.1155/2018/5849047](https://doi.org/10.1155/2018/5849047)
164. El-Khateeb E, Burkhill S, Murby S, Amirat H, Rostami-Hodjegan A, and Ahmad A. Physiological-based pharmacokinetic modeling trends in pharmaceutical drug development over the last 20-years; in-depth analysis of applications, organizations, and platforms. *Biopharmaceutics & Drug Disposition*. 2021;42(4):107–17. DOI: [10.1002/bdd.2257](https://doi.org/10.1002/bdd.2257)
165. Grimstein M, Yang Y, Zhang X, Grillo J, Huang S, Zineh I, and Wang Y. Physiologically based pharmacokinetic modeling in regulatory science: an update from the U.S. Food and Drug Administration’s Office of Clinical Pharmacology. *Journal of*



- Pharmaceutical Sciences. 2019;108(1):21–5. DOI: [10.1016/j.xphs.2018.10.033](https://doi.org/10.1016/j.xphs.2018.10.033)
166. Kuepfer L, Niederal C, Wendl T, Schlender JF, Willmann S, Lippert J, Block M, Eissing T, and Teutonico D. Applied concepts in PBPK modeling: how to build a PBPK/PD model. *CPT: Pharmacometrics & Systems Pharmacology*. 2016;5(10):516–31. DOI: [10.1002/psp4.12134](https://doi.org/10.1002/psp4.12134)
  167. Wojtyniak JG, Selzer D, Schwab M, and Lehr T. Physiologically based precision dosing approach for drug-drug-gene interactions: a simvastatin network analysis. *Clinical Pharmacology & Therapeutics*. 2021;109(1):201–11. DOI: [10.1002/cpt.2111](https://doi.org/10.1002/cpt.2111)
  168. Wang Y, Zhu H, Madabushi R, Liu Q, Huang SM, and Zineh I. Model-informed drug development: current US regulatory practice and future considerations. *Clinical Pharmacology & Therapeutics*. 2019;105(4):899–911. DOI: [10.1002/cpt.1363](https://doi.org/10.1002/cpt.1363)
  169. Kim TH, Shin S, and Shin BS. Model-based drug development: application of modeling and simulation in drug development. *Journal of Pharmaceutical Investigation*. 2018;48(4):431–41. DOI: [10.1007/s40005-017-0371-3](https://doi.org/10.1007/s40005-017-0371-3)
  170. U.S. Food and Drug Administration. Exposure-response relationships - study design, data analysis, and regulatory applications. Guidance for industry. 2003. Available from: <https://www.fda.gov/regulatory-information/search-fda-guidance-documents/exposure-response-relationships-study-design-data-analysis-and-regulatory-applications> [Internet] [cited 14 Jun 2022]
  171. U.S. Food and Drug Administration. Physiologically based pharmacokinetic analyses - format and content. Guidance for industry. 2018. Available from: <https://www.fda.gov/regulatory-information/search-fda-guidance-documents/physiologically-based-pharmacokinetic-analyses-format-and-content-guidance-industry> [Internet] [cited 14 Jun 2022]
  172. U.S. Food and Drug Administration. Population pharmacokinetics. Guidance for industry. 2022. Available from: <https://www.fda.gov/regulatory-information/search-fda-guidance-documents/population-pharmacokinetics> [Internet] [cited 14 Jun 2022]
  173. European Medicines Agency. Guideline on reporting the results of population pharmacokinetic analyses. 2007. Available from: [https://www.ema.europa.eu/en/documents/scientific-guideline/guideline-reporting-results-population-pharmacokinetic-analyses\\_en.pdf](https://www.ema.europa.eu/en/documents/scientific-guideline/guideline-reporting-results-population-pharmacokinetic-analyses_en.pdf) [Internet] [cited 14 Jun 2022]

174. EMA Committee for Human Medicinal Products (CHMP). Guideline on the reporting of physiologically based pharmacokinetic (PBPK) modelling and simulation. 2018. Available from: [https://www.ema.europa.eu/en/documents/scientific-guideline/guideline-reporting-physiologically-based-pharmacokinetic-pbpb-modelling-simulation\\_en.pdf](https://www.ema.europa.eu/en/documents/scientific-guideline/guideline-reporting-physiologically-based-pharmacokinetic-pbpb-modelling-simulation_en.pdf) [Internet] [cited 14 Jun 2022]
175. Meyer M, Schneckener S, Ludewig B, Kuepfer L, and Lipfert J. Using expression data for quantification of active processes in physiologically based pharmacokinetic modeling. *Drug Metabolism & Disposition*. 2012;40(5):892–901. DOI: [10.1124/dmd.111.043174](https://doi.org/10.1124/dmd.111.043174)
176. Nishimura M and Naito S. Tissue-specific mRNA expression profiles of human phase I metabolizing enzymes except for cytochrome P450 and phase II metabolizing enzymes. *Drug Metabolism & Pharmacokinetics*. 2006;21(5):357–74. DOI: [10.2133/dmpk.21.357](https://doi.org/10.2133/dmpk.21.357)
177. Rodrigues AD. Integrated cytochrome P450 reaction phenotyping: attempting to bridge the gap between cDNA-expressed cytochromes P450 and native human liver microsomes. *Biochemical Pharmacology*. 1999;57(5):465–80. DOI: [10.1016/S0006-2952\(98\)00268-8](https://doi.org/10.1016/S0006-2952(98)00268-8)
178. Nishimura M, Yaguti H, Yoshitsugu H, Naito S, and Satoh T. Tissue distribution of mRNA expression of human cytochrome P450 isoforms assessed by high-sensitivity real-time reverse transcription PCR. *Yakugaku Zasshi: Journal of the Pharmaceutical Society of Japan*. 2003;123(5):369–75. DOI: [10.1248/yakushi.123.369](https://doi.org/10.1248/yakushi.123.369)
179. Rowland Yeo K, Walsky RL, Jamei M, Rostami-Hodjegan A, and Tucker GT. Prediction of time-dependent CYP3A4 drug-drug interactions by physiologically based pharmacokinetic modelling: impact of inactivation parameters and enzyme turnover. *European Journal of Pharmaceutical Sciences*. 2011;43(3):160–73. DOI: [10.1016/j.ejps.2011.04.008](https://doi.org/10.1016/j.ejps.2011.04.008)
180. Greenblatt DJ, Moltke LL von, Harmatz JS, Chen G, Weemhoff JL, Jen C, Kelley CJ, LeDuc BW, and Zinny MA. Time course of recovery of cytochrome p450 3A function after single doses of grapefruit juice. *Clinical Pharmacology & Therapeutics*. 2003;74(2):121–9. DOI: [10.1016/S0009-9236\(03\)00118-8](https://doi.org/10.1016/S0009-9236(03)00118-8)
181. Scotcher D, Billington S, Brown J, Jones CR, Brown CDA, Rostami-Hodjegan A, and Galetin A. Microsomal and cytosolic scaling factors in dog and human kidney cortex and application for in vitro-in vivo extrapolation of renal metabolic clearance. *Drug Metabolism & Disposition*. 2017;45(5):556–68. DOI: [10.1124/dmd.117.075242](https://doi.org/10.1124/dmd.117.075242)

182. Otsuka M, Matsumoto T, Morimoto R, Arioka S, Omote H, and Moriyama Y. A human transporter protein that mediates the final excretion step for toxic organic cations. *Proceedings of the National Academy of Sciences of the United States of America*. 2005;102(50):17923–8. DOI: [10.1073/pnas.0506483102](https://doi.org/10.1073/pnas.0506483102)
183. Nishimura M and Naito S. Tissue-specific mRNA expression profiles of human ATP-binding cassette and solute carrier transporter superfamilies. *Drug Metabolism and Pharmacokinetics*. 2005;20(6):452–77. DOI: [10.2133/dmpk.20.452](https://doi.org/10.2133/dmpk.20.452)
184. Prasad B, Evers R, Gupta A, Hop CECA, Salphati L, Shukla S, Ambudkar SV, and Unadkat JD. Interindividual variability in hepatic organic anion-transporting polypeptides and P-glycoprotein (ABCB1) protein expression: quantification by liquid chromatography tandem mass spectroscopy and influence of genotype, age, and sex. *Drug Metabolism & Disposition*. 2014;42(1):78–88. DOI: [10.1124/dmd.113.053819](https://doi.org/10.1124/dmd.113.053819)
185. Wang L, Prasad B, Salphati L, Chu X, Gupta A, Hop CECA, Evers R, and Unadkat JD. Interspecies variability in expression of hepatobiliary transporters across human, dog, monkey, and rat as determined by quantitative proteomics. *Drug Metabolism & Disposition*. 2015;43(3):367–74. DOI: [10.1124/dmd.114.061580](https://doi.org/10.1124/dmd.114.061580)
186. Kolesnikov N, Hastings E, Keays M, et al. ArrayExpress update - simplifying data submissions. *Nucleic Acids Research*. 2015;43(D1):D1113–6. DOI: [10.1093/nar/gku1057](https://doi.org/10.1093/nar/gku1057)
187. Biotechnology Information (NCBI) NC for. Expressed Sequence Tags (EST) from UniGene. 2019
188. Hanke N, Frechen S, Moj D, Britz H, Eissing T, Wendl T, and Lehr T. PBPK models for CYP<sub>3</sub>A<sub>4</sub> and P-gp DDI prediction: a modeling network of rifampicin, itraconazole, clarithromycin, midazolam, alfentanil, and digoxin. *CPT: Pharmacometrics & Systems Pharmacology*. 2018;7(1):647–59. DOI: [10.1002/psp4.12343](https://doi.org/10.1002/psp4.12343)
189. Zhou M, Xia L, and Wang J. Metformin transport by a newly cloned proton-stimulated organic cation transporter (plasma membrane monoamine transporter) expressed in human intestine. *Drug Metabolism & Disposition*. 2007;35(10):1956–62. DOI: [10.1124/dmd.107.015495](https://doi.org/10.1124/dmd.107.015495)
190. Han TK, Everett RS, Proctor WR, Ng CM, Costales CL, Brouwer KLR, and Thakker DR. Organic cation transporter 1 (OCT<sub>1</sub>/mOct<sub>1</sub>) is localized in the apical membrane of Caco-2 cell monolayers and enterocytes. *Molecular Pharmacology*. 2013;84(2):182–9. DOI: [10.1124/mol.112.084517](https://doi.org/10.1124/mol.112.084517)

191. Han TK, Proctor WR, Costales CL, Cai H, Everett RS, and Thakker DR. Four cation-selective transporters contribute to apical uptake and accumulation of metformin in Caco-2 cell monolayers. *Journal of Pharmacology and Experimental Therapeutics*. 2015;352(3):519–28. DOI: [10.1124/jpet.114.220350](https://doi.org/10.1124/jpet.114.220350)
192. U.S. Food and Drug Administration. Drug development and drug interactions. Possible models for decision-making. Using a PBPK model to explore drug-drug interaction potential between a substrate drug and an interacting drug. 2015. Available from: <https://web.archive.org/web/20130702211539/http://www.fda.gov/downloads/Drugs/DevelopmentApprovalProcess/DevelopmentResources/DrugInteractionsLabeling/UCM269210.pdf> [Internet] [cited 14 Jan 2022]
193. Mitchell M, Muftakhidinov B, and Winchen T. Engauge Digitizer Software. Available from: <https://markumitchell.github.io/engauge-digitizer> [Internet] [cited 01 Mar 2022]
194. Wojtyniak JG, Britz H, Selzer D, Schwab M, and Lehr T. Data digitizing: accurate and precise data extraction for quantitative systems pharmacology and physiologically-based pharmacokinetic modeling. *CPT: Pharmacometrics & Systems Pharmacology*. 2020;9(6):322–31. DOI: [10.1002/psp4.12511](https://doi.org/10.1002/psp4.12511)
195. Gormsen LC, Sundelin EI, Jensen JB, Vendelbo MH, Jakobsen S, Munk OL, Hougaard Christensen MM, Brøsen K, Frøkiær J, and Jessen N. In vivo imaging of human <sup>11</sup>C-metformin in peripheral organs: dosimetry, biodistribution, and kinetic analyses. *Journal of Nuclear Medicine*. 2016;57(12):1920–6. DOI: [10.2967/jnumed.116.177774](https://doi.org/10.2967/jnumed.116.177774)
196. Prasad B, Achour B, Artursson P, et al. Toward a consensus on applying quantitative liquid chromatography-tandem mass spectrometry proteomics in translational pharmacology research: a white paper. *Clinical Pharmacology & Therapeutics*. 2019;106(3):525–43. DOI: [10.1002/cpt.1537](https://doi.org/10.1002/cpt.1537)
197. Chu X, Chan G, and Evers R. Identification of endogenous biomarkers to predict the propensity of drug candidates to cause hepatic or renal transporter-mediated drug-drug interactions. *Journal of Pharmaceutical Sciences*. 2017;106(9):2357–67. DOI: [10.1016/j.xphs.2017.04.007](https://doi.org/10.1016/j.xphs.2017.04.007)
198. Arya V, Reynolds KS, and Yang X. Using endogenous biomarkers to derisk assessment of transporter-mediated drug-drug interactions: a scientific perspective. *Journal of Clinical Pharmacology*. 2022. Online ahead of print. DOI: [10.1002/jcph.2119](https://doi.org/10.1002/jcph.2119)

199. Yoshida K, Guo C, and Sane R. Quantitative prediction of OATP-mediated drug-drug interactions with model-based analysis of endogenous biomarker kinetics. *CPT: Pharmacometrics & Systems Pharmacology*. 2018;7(8):517–24. DOI: [10.1002/psp4.12315](https://doi.org/10.1002/psp4.12315)
200. Emami Riedmaier A, Burt H, Abduljalil K, and Neuhoff S. More power to OATP<sub>1B1</sub>: an evaluation of sample size in pharmacogenetic studies using a rosuvastatin PBPK model for intestinal, hepatic, and renal transporter-mediated clearances. *Journal of Clinical Pharmacology*. 2016;56(Suppl 7):S132–42. DOI: [10.1002/jcph.669](https://doi.org/10.1002/jcph.669)
201. Bricker NS. On the meaning of the intact nephron hypothesis. *The American Journal of Medicine*. 1969;46(1):1–11. DOI: [10.1016/0002-9343\(69\)90053-9](https://doi.org/10.1016/0002-9343(69)90053-9)
202. Li J, Guo HF, Liu C, Zhong Z, Liu L, and Liu XD. Prediction of drug disposition in diabetic patients by means of a physiologically based pharmacokinetic model. *Clinical Pharmacokinetics*. 2015;54(2):179–93. DOI: [10.1007/s40262-014-0192-8](https://doi.org/10.1007/s40262-014-0192-8)
203. Hsueh CH, Hsu V, Pan Y, and Zhao P. Predictive performance of physiologically-based pharmacokinetic models in predicting drug-drug interactions involving enzyme modulation. *Clinical Pharmacokinetics*. 2018;57(10):1337–46. DOI: [10.1007/s40262-018-0635-8](https://doi.org/10.1007/s40262-018-0635-8)
204. Li GF, Wang K, Chen R, Zhao HR, Yang J, and Zheng QS. Simulation of the pharmacokinetics of bisoprolol in healthy adults and patients with impaired renal function using whole-body physiologically based pharmacokinetic modeling. *Acta Pharmacologica Sinica*. 2012;33(11):1359–71. DOI: [10.1038/aps.2012.103](https://doi.org/10.1038/aps.2012.103)
205. Posada MM, Bacon JA, Schneck KB, Tirona RG, Kim RB, Higgins JW, Pak YA, Hall SD, and Hillgren KM. Prediction of renal transporter mediated drug-drug interactions for pemetrexed using physiologically based pharmacokinetic modeling. *Drug Metabolism & Disposition*. 2015;43(3):325–34. DOI: [10.1124/dmd.114.059618](https://doi.org/10.1124/dmd.114.059618)
206. Zhao P, Vieira MdLT, Grillo J, et al. Evaluation of exposure change of nonrenally eliminated drugs in patients with chronic kidney disease using physiologically based pharmacokinetic modeling and simulation. *Journal of Clinical Pharmacology*. 2012;52(1 Suppl):91S–108S. DOI: [10.1177/0091270011415528](https://doi.org/10.1177/0091270011415528)
207. Takita H, Scotcher D, Chinnadurai R, Kalra P, and Galetin A. Physiologically-based pharmacokinetic modelling of creatinine-drug interactions in the chronic kidney disease popu-

- lation. *CPT: Pharmacometrics & Systems Pharmacology*. 2020;9(12):695–706. DOI: [10.1002/psp4.12566](https://doi.org/10.1002/psp4.12566)
208. Chu X, Prasad B, Neuhoff S, et al. Clinical implications of altered drug transporter abundance/function and PBPK modeling in specific populations: an ITC perspective. *Clinical Pharmacology & Therapeutics*. 2022. Online ahead of print. DOI: [10.1002/cpt.2643](https://doi.org/10.1002/cpt.2643)
209. Duong JK, Roberts DM, Furlong TJ, Kumar SS, Greenfield JR, Kirkpatrick CM, Graham GG, Williams KM, and Day RO. Metformin therapy in patients with chronic kidney disease. *Diabetes, Obesity and Metabolism*. 2012;14(10):963–5. DOI: [10.1111/j.1463-1326.2012.01617.x](https://doi.org/10.1111/j.1463-1326.2012.01617.x)
210. Lalau JD, Kajbaf F, Bennis Y, Hurtel-Lemaire AS, Belpaire F, and De Broe ME. Metformin treatment in patients with type 2 diabetes and chronic kidney disease stages 3A, 3B, or 4. *Diabetes Care*. 2018;41(3):547–53. DOI: [10.2337/dc17-2231](https://doi.org/10.2337/dc17-2231)
211. Wallace A, Chinn D, and Rubin G. Taking simvastatin in the morning compared with in the evening: randomised controlled trial. *BMJ*. 2003;327(7418):788. DOI: [10.1136/bmj.327.7418.788](https://doi.org/10.1136/bmj.327.7418.788)
212. Lee Y. Roles of circadian clocks in cancer pathogenesis and treatment. *Experimental & Molecular Medicine*. 2021;53(10):1529–38. DOI: [10.1038/s12276-021-00681-0](https://doi.org/10.1038/s12276-021-00681-0)
213. Kelly RM, Healy U, Sreenan S, McDermott JH, and Coogan AN. Clocks in the clinic: circadian rhythms in health and disease. *Postgraduate Medical Journal*. 2018;94(1117):653–8. DOI: [10.1136/postgradmedj-2018-135719](https://doi.org/10.1136/postgradmedj-2018-135719)
214. European Medicines Agency. Guideline on the use of pharmacogenetic methodologies in the pharmacokinetic evaluation of medicinal products (Draft). 2011. Available from: [https://www.ema.europa.eu/en/documents/scientific-guideline/guideline-use-pharmacogenetic-methodologies-pharmacokinetic-evaluation-medicinal-products\\_en.pdf](https://www.ema.europa.eu/en/documents/scientific-guideline/guideline-use-pharmacogenetic-methodologies-pharmacokinetic-evaluation-medicinal-products_en.pdf) [Internet] [cited 06 Feb 2022]
215. Frechen S and Rostami-Hodjegan A. Quality assurance of PBPK modeling platforms and guidance on building, evaluating, verifying and applying PBPK models prudently under the umbrella of qualification: why, when, what, how and by whom? *Pharmaceutical Research*. 2022;39(8):1733–48. DOI: [10.1007/s11095-022-03250-w](https://doi.org/10.1007/s11095-022-03250-w)
216. Kanacher T, Lindauer A, Mezzalana E, Michon I, Veau C, Gómez-Mantilla JD, Nock V, and Fleury A. A physiologically-based pharmacokinetic (PBPK) model network for the prediction of CYP1A2 and CYP2C19 drug–drug–gene interactions with fluvoxamine, omeprazole, S-mephenytoin, mo-

- clobemide, tizanidine, mexiletine, ethinylestradiol, and caffeine. *Pharmaceutics*. 2020;12(12):1191. DOI: [10 . 3390 / pharmaceutics12121191](https://doi.org/10.3390/pharmaceutics12121191)
217. Frechen S, Solodenko J, Wendl T, Dallmann A, Ince I, Lehr T, Lippert J, and Burghaus R. A generic framework for the physiologically-based pharmacokinetic platform qualification of PK-Sim and its application to predicting cytochrome P450 3A4-mediated drug-drug interactions. *CPT: Pharmacometrics & Systems Pharmacology*. 2021;10(6):633-44. DOI: [10 . 1002 / psp4.12636](https://doi.org/10.1002/psp4.12636)
218. Wendl T, Frechen S, Gerisch M, Heinig R, and Eissing T. Physiologically-based pharmacokinetic modeling to predict CYP3A4-mediated drug-drug interactions of finerenone. *CPT: Pharmacometrics & Systems Pharmacology*. 2022;11(2):199-211. DOI: [10.1002/psp4.12746](https://doi.org/10.1002/psp4.12746)
219. Bayer HealthCare Pharmaceuticals Inc. KERENDIA (finerenone) tablets, for oral use. Highlights of prescribing information. 2021. Available from: [https://www.accessdata.fda.gov/drugsatfda\\_docs/label/2021/215341s000lbl.pdf](https://www.accessdata.fda.gov/drugsatfda_docs/label/2021/215341s000lbl.pdf) [Internet] [cited 18 Jul 2022]
220. Darwich AS, Ogungbenro K, Vinks AA, et al. Why has model-informed precision dosing not yet become common clinical reality? Lessons from the past and a roadmap for the future. *Clinical Pharmacology & Therapeutics*. 2017;101(5):646-56. DOI: [10.1002/cpt.659](https://doi.org/10.1002/cpt.659)





## APPENDIX

## A.1 PUBLICATIONS

A.1.1 *Original Publications*

- I Türk D, Müller F, Fromm MF, Selzer D, Dallmann R, and Lehr T. Renal transporter-mediated drug-biomarker interactions of the endogenous substrates creatinine and N<sup>1</sup>-methylnicotinamide: a PBPK modeling approach. *Clinical Pharmacology & Therapeutics*. 2022. Online ahead of print. DOI: [10.1002/cpt.2636](https://doi.org/10.1002/cpt.2636)
- II Loer HLH, Türk D, Gómez-Mantilla JD, Selzer D, and Lehr T. Physiologically based pharmacokinetic (PBPK) modeling of clopidogrel and its four relevant metabolites for CYP2B6, CYP2C8, CYP2C19, and CYP3A4 drug-drug-gene interaction predictions. *Pharmaceutics*. 2022;14(5):915. DOI: [10.3390/pharmaceutics14050915](https://doi.org/10.3390/pharmaceutics14050915)
- III Türk D, Hanke N, Lehr T. A physiologically-based pharmacokinetic model of trimethoprim for MATE<sub>1</sub>, OCT<sub>1</sub>, OCT<sub>2</sub>, and CYP2C8 drug-drug-gene interaction predictions. *Pharmaceutics*. 2020;12(11):1074. DOI: [10.3390/pharmaceutics12111074](https://doi.org/10.3390/pharmaceutics12111074)
- IV Hanke N, Türk D, Selzer D, Ishiguro N, Ebner T, Wiebe S, Müller F, Stopfer P, Nock V, Lehr T. A comprehensive whole-body physiologically based pharmacokinetic drug-drug-gene interaction model of metformin and cimetidine in healthy adults and renally impaired individuals. *Clinical Pharmacokinetics*. 2020;59(11):1419-31. DOI: [10.1007/s40262-020-00896-w](https://doi.org/10.1007/s40262-020-00896-w)
- V Hanke N, Türk D, Selzer D, Wiebe S, Fernandez É, Stopfer P, Nock V, Lehr T. A mechanistic, enantioselective, physiologically based pharmacokinetic model of verapamil and norverapamil, built and evaluated for drug-drug interaction studies. *Pharmaceutics*. 2020;12(6):556. DOI: [10.3390/pharmaceutics12060556](https://doi.org/10.3390/pharmaceutics12060556)
- VI Türk D, Hanke N, Wolf S, Frechen S, Eissing T, Wendl T, Schwab M, Lehr T. Physiologically based pharmacokinetic models for prediction of complex CYP2C8 and OATP1B1 (*SLCO1B1*) drug-drug-gene interactions: a modeling network of gemfibrozil, repaglinide, pioglitazone, rifampicin, clarithromycin and itraconazole. *Clinical Pharmacokinetics*. 2019;58(12):1595-1607. DOI: [10.1007/s40262-019-00777-x](https://doi.org/10.1007/s40262-019-00777-x)

A.1.2 *Review Articles*

I Türk D, Fuhr LM, Marok FZ, Rüdeshheim S, Kühn A, Selzer D, Schwab M, and Lehr T. Novel models for the prediction of drug-gene interactions. *Expert Opinion on Drug Metabolism & Toxicology*. 2021;17(11):1293-1310. DOI: [10.1080/17425255.2021.1998455](https://doi.org/10.1080/17425255.2021.1998455)

A.1.3 *Conference Abstracts and Posters*

I Türk D, Müller F, Fromm MF, Selzer D, Dallmann R, and Lehr T. PBPK models for OCT2 and MATE interaction predictions: a drug-biomarker interaction network of creatinine, N<sup>1</sup>-methylnicotinamide, trimethoprim, pyrimethamine and cimetidine. *American Conference on Pharmacometrics (ACoP) 13*. 2022. Aurora, United States. Accepted abstract.

II Loer HLH, Türk D, Selzer D, and Lehr T. Dose adaptations for drug-gene and drug-drug interactions involving clopidogrel – a physiologically based pharmacokinetic (PBPK) modeling approach. 30th Population Approach Group Europe (PAGE) meeting. 2022. Ljubljana, Slovenia.

III Türk D, Hanke N, and Lehr T. Physiologically-based pharmacokinetic models to predict CYP2C8 drug-drug interactions: a modeling network of trimethoprim, repaglinide, pioglitazone and rifampicin. *International PhD Student & Postdoc Meeting of the German Pharmaceutical Society (DPhG)*. 2021. Virtual Meeting, Germany. **Winner of Poster Award**

IV Türk D, Hanke N, and Lehr T. Physiologically-based pharmacokinetic modeling of trimethoprim drug-drug interactions with the CYP2C8 victim drugs repaglinide and pioglitazone. *Annual Meeting of the German Pharmaceutical Society (DPhG)*. 2019. Heidelberg, Germany.

V Türk D, Hanke N, and Lehr T. Physiologically-based pharmacokinetic modeling of the CYP2C8 perpetrator trimethoprim. 28th Population Approach Group Europe (PAGE) meeting. 2019. Stockholm, Sweden.

VI Türk D, Hanke N, and Lehr T. Physiologically-based pharmacokinetic modeling of gemfibrozil drug-drug interactions with the CYP2C8 victim drugs repaglinide and pioglitazone. 27th Population Approach Group Europe (PAGE) meeting. 2018. Montreux, Switzerland.

## ACKNOWLEDGMENTS

---

Ich möchte auf diese Weise die Möglichkeit nutzen, denjenigen zu danken, die zur Realisierung meiner Promotion beigetragen und mich währenddessen unterstützt haben.

Daher möchte ich mich als erstes bei Prof. Dr. Thorsten Lehr bedanken, durch ihn im Rahmen meines Studiums und meiner anschließenden Diplomarbeit mein Interesse an PBPK Modellierung geweckt wurde, sodass ich mich mit dieser auch gerne im Rahmen meiner Promotion beschäftigen wollte. Daher danke ihm für die Möglichkeit, meine Doktorarbeit unter seiner Betreuung anzufertigen und an diesem spannenden Thema arbeiten zu können sowie für seinen wertvollen Input in unseren Gesprächen. Außerdem danke ich ihm dafür, dass ich meine Fortschritte bei wissenschaftlichen Konferenzen wie dem PAGE Meeting oder der DPhG Jahrestagung präsentieren und so Kontakte knüpfen konnte. Ich möchte mich außerdem bei Prof. Dr. Markus R. Meyer bedanken, meinem wissenschaftlichen Begleiter der Promotion sowie der gesamten Prüfungskommission.

Ich möchte mich bei all meinen Kolleginnen und Kollegen der Klinischen Pharmazie in Saarbrücken bedanken, dass ich so herzlich in der Gruppe aufgenommen wurde. Ich erinnere mich gerne an alle gemeinsamen Aktivitäten auch außerhalb der Büros. Ich möchte dem gesamten "Team PBPK" für die interessanten Diskussionen danken, insbesondere Hannah Britz, Laura Fuhr, Fatima Marok and Simeon Rüdesheim für den Austausch und die immer hilfreichen Ratschläge und Ideen. Ich bedanke mich herzlich bei Dr. Nina Hanke dafür, dass ich sehr viel von ihrem Wissen zu PBPK lernen durfte und sie immer ein offenes Ohr hatte. Außerdem danke ich Dr. Dominik Selzer für seinen wertvollen fachlichen Input. Ich bedanke mich zudem bei allen Partnern und Co-Autoren für die gute Zusammenarbeit.

Ich möchte mich auch bei meiner Familie und meinen Freunden bedanken. Ich danke meinen Eltern, die mich schon immer in meinen Entscheidungen unterstützt und mir den Rücken gestärkt haben. Von ganzem Herzen danke ich meinem Mann Martin für sein Verständnis und seine unermüdliche Unterstützung in allen Prüfungen und dieser Arbeit.

## COLOPHON

This document was typeset using the typographical look-and-feel `classicthesis` developed by André Miede and Ivo Pletikosić. The style was inspired by Robert Bringhurst's seminal book on typography "*The Elements of Typographic Style*". `classicthesis` is available for both  $\text{\LaTeX}$  and  $\text{\LyX}$ :

<https://bitbucket.org/amiede/classicthesis/>

Happy users of `classicthesis` usually send a real postcard to the author, a collection of postcards received so far is featured here:

<https://postcards.miede.de/>

Thank you very much for your feedback and contribution.